



Grant Agreement No.: 814956
Research and Innovation action
Call Topic: ICT-22-2018 EU-China 5G Collaboration



5G Harmonised Research and Trials for service Evolution between EU and China

D4.4: Final report of V2X trials

Version: v1.1

Deliverable type	R (Document, report)
Dissemination level	Public
Due date	30/06/2021
Submission date	08/07/2021
Lead editor	Xiaoyun Zhang, Dynniq; Vladimir Vorotovic, ERTICO
Authors	Matti Kutila, Kimmo Kauvo, VTT; Yinxiang Zheng, China Mobile; Abdelwahab Boualouache, Uni.lu; Jaime Ferragut, Jean-Marc Chareau, Philippe Viaud, Fausto Bonavitacola, Tiziano Pinato, James Bishop, JRC; Xiaoyun Zhang, Dynniq; Matti Lankinen, Lasse Nykänen Juha Karppinen, Vediafi; Huiling Zhu, UKent, Slawomir Kukliński, Lechosław Tomaszewski, Robert Kołakowski, Orange
Reviewers	Feng Li, China Mobile; Victor Garrido-Martinez, BMW Group; Dr. Johanna Tzanidaki, ERTICO; Maxime Flament and Ralf Weber, External Advisory Board members
Work package, Task	WP4, T4.1, T4.2, T4.3, T4.4, T4.5
Keywords	V2X, LTE-V2X PC5, ITS-G5, coexistence, joint EU-China V2X trials, use cases, joint framework

Abstract

This report presents the final results of the V2X trialling activities done by the 5G-DRIVE project. It presents the conclusions of a 34-month activity of building end-to-end testbeds, trialling and demonstrating the cellular V2X communication, and more specifically the LTE-V2X via PC5 interface in joint EU-China V2X trials use cases and in commercial LTE/5G networks through trials in Finland and Italy, Europe.

These activities were conducted in collaboration with the Chinese twinning project - 5G Large-scale trials project V2X team in Shanghai, China, in order to facilitate LTE-V2X development in Europe and to bridge the V2X development differences in China and in Europe.

The joint EU-China V2X trial framework created to describe and define the harmonised joint trial methodology of these tests and trials has been used as guidance throughout the joint EU-China trial process. By virtue of strong collaboration under the joint EU-China V2X trial framework, the analysis of the findings from both the European and the Chinese project teams, are presented in the final report.

Document revision history

Version	Date	Description of change	List of contributors
v0.1	22/01/2020	First draft with initial vision of table of content	Xiaoyun Zhang, Dynniq
v0.2	24/01/2020	Review and modification on of table of content	Jaime Ferragut, JRC
v0.3	24/04/2020	Draft section 3.2, reviewing and modification	Xiaoyun Zhang, Dynniq
v0.4	30/04/2020	Further content added	Xiaoyun Zhang, Dynniq
v0.5	02/06/2020	Appendix A updated	Xiaoyun Zhang, Dynniq
v0.6	10/03/2021	Table of Content finalised	Xiaoyun Zhang, Jaime Ferragut, Abdelwahab Boualouache et al.
v0.7	29/03/2021	Inputs to section 2.2.2 and section 2.4 from Uni.lu	Abdelwahab Boualouache, UniLu
v0.8	08/04/2021	Draft D4.4 prepared for EAB members. Identification of input source.	Xiaoyun Zhang, Dynniq
v0.9	27/04/2021	Inputs to section 4.1.1 and 4.1.3	Kimmo Kauvo, VTT Matti Lankinen, Lasse Nykänen, Juha Karppinen, Vediafi
v0.90	29/04/2021	First polishing of the submission ready draft report	Vladimir Vorotovic, ERTICO
v0.91	07/05/2021	Polishing the test results	Matti Kutila, VTT
v0.92	12/05/2021	Analysis tool description added	Matti Kutila, VTT
v0.93	14/05/2021	Explanations to remarks, inputs to section 4.1.3.2	Matti Kutila, VTT Huiling Zhu, UKent
v0.94	18/05/2021	Inputs to section 4.1.3.3	Sławomir Kukliński, Robert Kołakowski, Lechosław Tomaszewski, Orange
v0.95	18/05/2021	Results review section 4.1 and inputs to section 5 and section 6, Inputs/re-writing section 3 and section 4.2	Matti Kutila, VTT Xiaoyun Zhang, Dynniq Yinxiang Zheng, China Mobile
v0.96	20/05/2021	Test tool description added to section 3.4.3, Categorising different test scenarios	Matti Kutila, Pasi Pyykönen, VTT
v0.97	21/05/2021	Added contributions from JRC	Jaime Ferragut, JRC
v0.98	21/05/2021	Complete section 3 and section 4.2, build figure, table citations	Xiaoyun Zhang, Dynniq
v0.981	25/05/2021	Optimised file size	Vladimir Vorotovic, ERTICO
v0.982	26/05/2021	Section number, comments	Vladimir Vorotovic, ERTICO

		addressing and polishing	
v0.983	27/05/2021	Final draft ready for 5GAA	Xiaoyun Zhang, Dynniq
v0.984	30/05/2021	Integration and modification to Dr. Johanna Tzanidaki's comments	Vladimir Vorotovic, ERTICO Xiaoyun Zhang, Dynniq
v0.985	31/05/2021	Modification to review comments from EAB members	Abdelwahab Boualouache, UniLu Jaime Ferragut, JRC Lechosław Tomaszewski, Orange Matti Kutila, VTT Xiaoyun Zhang, Dynniq
v0.986	04/06/2021	Integration of modification to review comments from the reviewers	Xiaoyun Zhang, Dynniq Abdelwahab Boualouache, UniLu Jaime Ferragut, JRC
V0.991	14/06/2021	Polishing: figures, tables and equations referencing. Full quality images	Xiaoyun Zhang, Dynniq
V0.992	21/06/2021	Final document ready for submission	Xiaoyun Zhang, Dynniq, Vladimir Vorotovic, ERTICO
V1.0	23/06/2021	Final editing	Anja Köhler, EURESCOM
V1.1	08/07/2021	Editorial changes and final checks	Jaime Ferragut, JRC, Uwe Herzog, EURESCOM

Disclaimer

This report contains material which is the copyright of certain 5G-DRIVE Consortium Parties and may not be reproduced or copied without permission.

All 5G-DRIVE Consortium Parties have agreed to publication of this report, the content of which is licensed under a Creative Commons Attribution-NonCommercial-NoDerivs 3.0 Unported License¹.

Neither the 5G-DRIVE Consortium Parties nor the European Commission warrant that the information contained in the Deliverable is capable of use, or that use of the information is free from risk, and accept no liability for loss or damage suffered by any person using the information.



CC BY-NC-ND 3.0 License – 2018-2021 5G-DRIVE Consortium Parties

¹ http://creativecommons.org/licenses/by-nc-nd/3.0/deed.en_US

Executive Summary

The project consortium of 17 partners from 11 countries, worked together in testing and demonstrating the latest 5G key technologies in Mobile Broadband (eMBB) and Vehicle-to-Everything (V2X) scenarios in pre-commercial 5G networks through trials in Finland, Italy and the UK. Several project activities were conducted in parallel with a Chinese twinning project so as to assess cross-regional interoperability. Researching key innovation in networking slicing, network virtualization, 5G transport network, edge computing and New Radio features to fill gaps between standards and real-world deployment was tested in trials in both Europe and China.

5G-DRIVE assessed the validation of standards and the roll-out of real 5G networks and innovative V2X solutions that will help drive new business opportunities, new jobs and business models.

During the project, 5G trials addressed two of the most promising 5G deployment scenarios: enhanced Mobile Broadband and Vehicle-to-Everything communications. By conducting trials in parallel with China, the project succeeded to develop and validate Key 5G technology functionalities and services as well as pre-commercial testbeds for eMBB and V2X services. The results of joint trials and research activities take an important step towards facilitating technology convergence, spectrum harmonisation and business innovation before the large-scale commercial deployment of 5G networks occurs.

This report explains the project 3-year work towards building end-to-end pilot sites in two cities with sufficient coverage to perform Internet of Vehicles (IoV) trials using V2V, V2I and V2N technologies, namely LTE-V2X PC5 at 5.9 GHz and commercial LTE/5G cellular network at 3.5 GHz. It also demonstrates the methodology and results of the joint EU-China V2X trial harmonised plan that were defined through the collaborative agreement with the Chinese twinning project: 5G Large-scale trials. The joint EU-China V2X trial framework, specifically created to describe and define the harmonised methodology and plan of these tests and trials has been used as guidance on the analysis of the findings from both the European and the Chinese project teams.

As far as experimental activities in vehicular communications are concerned, laboratory and field tests in 5G-DRIVE yielded the following key technical results:

1. For the experimental evaluation of co-channel coexistence method C (defined in ETSI Technical Report 103 766), laboratory results showed that this method contributed to reducing Packet Error Rate (PER) in a commercial ITS-G5 receiver compared to PER values obtained in the absence of co-channel coexistence methods, but not entirely. Similarly, laboratory experiments using commercial C-ITS devices showed a robust performance of the LTE-V2X PHY and MAC layers in the presence of interfering signals – with and without the use of co-channel coexistence methods.
2. Laboratory experiments of frequency jamming on ITS-G5 (near commercial equipment) using OpenC2X showed the impact of the jamming source power and its placement on performance while considering the distance between communicating devices.
3. The Ispra field trial illustrated the various trade-offs between key performance metrics of commercial ITS-G5 and LTE-V2X devices in a real-life deployment of C-ITS services. Overall, field tests results suggest a robust performance of the LTE-V2X PHY and MAC layers in terms of Packet Error Rate. As to end-to-end packet latency, ITS-G5 devices attained lower packet latency than LTE-V2X devices under clean channel and low load conditions. This is due to (a) the opportunistic nature of the CSMA/CA channel access mechanism of ITS-G5 and (b) the Packet Delay Budget of C-ITS messages being set to 100 ms in the factory-default configuration of the commercial LTE-V2X devices used in the Ispra field trial (packet latencies of up to 100 ms are in line with the service requirements for day-1 C-ITS services).
4. The field trial results of the joint EU–China trials performed in Espoo/Tampere, Finland, and

in Shanghai, China, under the joint EU-China V2X trial harmonised framework of the 5G-DRIVE and 5G Large-scale trial projects, showed that parallel comparison of findings in many ways, such as trial use cases, trial specifications and assessment methodology (i.e., jointly defined KPIs: end-to-end latency and Packet Error Rate (PER)) were encouraged and operable in field trials. The KPIs of latency (mean) and the PER showed from both China and Europe's trial sites, met the preliminary targeted KPIs when LTE-V2X devices are within communication range.

5. The importance of accurate and reliable hybrid positioning messaging for C-V2X, particularly in challenging satellite visibility environments, was validated through the hybrid navigation tests. These tests also showed the benefits of multi-sensor positioning systems using C-V2X communication to complement the positioning quality. The link budget model studies facilitated the field trial designs of the joint EU-China V2X trial in Tampere, respecting the vehicle speed and antenna height variation as impact factors. The Mobile Edge Computing (MEC) simulation studies verified the promise of low delay communication and effective traffic steering.

Table of Contents

Executive Summary	5
Table of Contents	7
List of Figures	9
List of Tables	13
Abbreviations.....	15
1 Introduction	19
2 V2X communication testbeds	20
2.1 Rationale and scope	20
2.1.1 Coexistence of ITS-G5 and LTE-V2X in the 5.9 GHz band	20
2.1.2 Frequency jamming and misbehaviour detection.....	21
2.2 Laboratory tests at the Joint Research Centre	23
2.2.1 Preparatory tests	23
2.2.2 Co-channel coexistence tests	25
2.3 Laboratory tests at the University of Luxembourg.....	43
2.3.1 Jamming tests on ITS-G5 using OpenC2X equipment	43
2.3.2 Misbehaviour detection system tests.....	51
3 Joint EU-China V2X trial framework.....	57
3.1 Joint EU-China trials introduction	57
3.2 V2X trials background and objectives	57
3.3 Joint V2X trials harmonised methodology.....	59
3.3.1 Trial spectrum comparison	59
3.3.2 V2X technologies paths comparison	60
3.3.3 Joint trial schematic	62
3.4 Joint trial harmonised plan	65
3.4.1 Joint V2X trials use cases	66
3.4.2 Joint V2X trials specification	70
3.4.3 Assessment methodology.....	77
4 Results	82
4.1 Joint V2X trials in Europe.....	82
4.1.1 Tampere trial results.....	82
4.1.2 Ispra trial results	98
4.1.3 Enhancement trials and studies results.....	109
4.2 Joint V2X trials in China	129

4.2.1	Interoperability tests among different vendors	129
4.2.2	V2I/V2V (LTE-V2X technology) coverage tests	129
4.2.3	LTE-V2X (PC5) performance tests	131
5	Conclusions.....	132
	References	135
Appendix A	Joint EU-China V2X trial campaign schematic	137
Appendix B	EU (CAM) and China (BSM) message comparison	138
Appendix C	Examples of test reports from the preparatory tests conducted in the JRC Radio Spectrum Laboratory	145
Appendix D	Laboratory setups for experimental evaluation of co-channel coexistence method C in ETSI TR 103 766.....	162

List of Figures

Figure 1: Harmonised safety-related ITS band in the European Union (5.9 GHz)	20
Figure 2: A scenario of the grey hole attack	22
Figure 3: Misbehaviour detection system deployment	23
Figure 4: Example of laboratory setup for conducting a preparatory test at the JRC Radio Spectrum Laboratory with a commercial LTE-V2X RSU	25
Figure 5: Block diagram of the generation of the LTE-V2X synthetic signal using a commercial LTE-V2X RSU, an external GNSS time/frequency reference and a Vector Signal Transceiver	28
Figure 6: Time series of an LTE-V2X packet in the synthetic signal with a prepended ITS-G5 PHY header	28
Figure 7: Spectrogram of an LTE-V2X packet (green box) in the synthetic signal with a prepended ITS-G5 PHY header (red box)	29
Figure 8: Laboratory setup for the experimental evaluation of co-channel coexistence method C (ITS-G5 header insertion) in the JRC Radio Spectrum Laboratory	30
Figure 9: Packet Error Rate vs. interferer power at the transmitter for all interfering signals (ITS-G5 as victim technology)	32
Figure 10: Busy channel notifications at the ITS-G5 transmitter vs. interfering power at the transmitter for all interfering signals	33
Figure 11: Packet decoding counters in the ITS-G5 transmitter when exposed to an LTE-V2X interfering signal (without header insertion)	34
Figure 12: Definition of the inter-packet gap for received packets	35
Figure 13: Time series of inter-packet gaps in the ITS-G5 receiver when the transmitter is exposed to ITS-G5 and LTE-V2X interfering signals	36
Figure 14: Empirical Cumulative Distribution Function of inter-packet gaps in the ITS-G5 receiver when the transmitter is exposed to ITS-G5 and LTE-V2X interfering signals	36
Figure 15: Time series of inter-packet gaps in the ITS-G5 receiver when the transmitter is exposed to ITS-G5 and LTE-V2X (with header insertion) interfering signals	37
Figure 16: Empirical Cumulative Distribution Function of inter-packet gaps in the ITS-G5 receiver when the transmitter is exposed to ITS-G5 and LTE-V2X (with header insertion) interfering signals	37
Figure 17: Packet Error Rate vs. interferer power in the transmitter for all interfering signals (LTE-V2X as a victim technology)	39
Figure 18: Inter-packet gap statistics of received LTE-V2X packets as a function of the interferer power at the receiver for different interfering signals	40
Figure 19: Average packet latency as a function of the interferer power at the transmitter for different interfering signals	41
Figure 20: End-to-end packet latency (LTE-V2X)	41
Figure 21: Experimental setup of jamming attacks on ITS-G5	45
Figure 22: The first test scenario for the jamming attack on ITS-G5	45
Figure 23: The second test scenario for the jamming attack on ITS-G5	46
Figure 24: The PDR versus the attacker gain considering different distances between the OpenC2X equipment	48

Figure 25: The PDR versus the distance between OpenC2X equipment	48
Figure 26: Comparison between one source of jamming and two sources of jamming scenarios (distance between the equipment = 2m).....	49
Figure 27: The impact of USRP2 jamming source in the second scenario	50
Figure 28: The impact of USRP1 jamming source in the second scenario	50
Figure 29: Laboratory experiments on the accuracy of the misbehaviour detect system	51
Figure 30: Scenario 1 of misbehaviour detection system tests	52
Figure 31: Scenario 2 of misbehaviour detection system tests	52
Figure 32: Scenario 3 of misbehaviour detection system tests	53
Figure 33: Direct Trust calculated analytically	54
Figure 34: Direct trust values for the first scenario	54
Figure 35: Direct trust values for the first scenario 2	55
Figure 36: Packet loss ratio vs. SNR.....	56
Figure 37: Direct trust values for scenario 3	56
Figure 38: The project timeline of 5G-DRIVE in EU (above) and 5G Large-scale trial in China (below) ..	59
Figure 39: Joint trial harmonised methodology design	65
Figure 40: The system architecture of joint V2X use case 2 - GLOSA, 5G-DRIVE V2X team	70
Figure 41: The system architecture of joint V2X use case 2 - GLOSA, 5G Large-scale trial V2X team ..	70
Figure 42: The intersection safety and GLOSA use cases architecture in Espoo/Tampere sites	71
Figure 43: The test site for automated driving in Shanghai, China.....	73
Figure 44: The RSUs from different vendors are deployed on a light pole at the intersection No. 51 ..	73
Figure 45: The OBU is placed on the top of the test car. The height of the antenna is about 1.5 m ...	74
Figure 46: User interface for the measurement tool.....	78
Figure 47: The test data transmission/receiver interface.....	78
Figure 48: The in-vehicle display of assessment tool during the trials in Tampere, Finland	79
Figure 49: The test intersection for trials in Tampere, Finland. 1 cm in the picture represents about 100 m.....	84
Figure 50: Antenna installations in the LTE-V2X trials. Left: antenna installations on the trailer; Right: the 5G and LTE-V2X antennas of the test vehicle "Martti" located on the roof.	84
Figure 51: Histograms of latency (mean) for LTE -V2X from RSU to OBU, various message intervals. ..	86
Figure 52: Latency contour plot (LTE-V2X): msg interval 20 ms, tx RSU at blue location (green < 26ms, red > 36ms). The driving speed in this case is 15-25 km/h	87
Figure 53: Histograms of latency (mean) for 5G from IP network to Vehicle, DENM message, various message intervals (1ms, 5ms, 10ms and 20ms).....	88
Figure 54: Latency contour plot (5G): msg interval 20ms, tx RSU in blue location (green < 51.6ms, red > 78.0ms).....	89
Figure 55: Histograms of latency (mean) for LTE -V2X from RSU to OBU, different driving speeds (message interval 50 ms).	90
Figure 56: Latency contour plot (LTE-V2X): msg interval 50ms, driving speed 5km/h, tx RSU in blue location (green < 26ms, red > 36ms).	91

Figure 57: Latency contour plot (5G): msg interval 50 ms, driving speed 5km/h, tx RSU in blue location (green < 51.6 ms, red > 78.0ms).....	91
Figure 58: Latency: LTE-V2X, antenna height 1.4m, tx RSU in blue location (green < 26ms, red > 36ms).	93
Figure 59: Latency: LTE-V2X, antenna height 3.8m, tx RSU in blue location (green < 26ms, red > 36ms).	93
Figure 60: Latency: Automated driving V2X, msg size 250B, tx RSU in blue location (green < 26ms, red > 36ms).....	95
Figure 61: Latency: Automated driving 5G, msg size 250B, cell mast in green location (green < 26ms, red > 36 ms).....	95
Figure 62: Test route for GLOSA measurements (start position on the right).....	96
Figure 63: 5G-DRIVE GLOSA speed advice application by Dynniq.	96
Figure 64: Sequence diagram of the SPaT message transmission.	97
Figure 65: Boxplot of the SPaT message jitter.	98
Figure 66: Protocol stack architecture of the ITS-G5 and LTE-V2X commercial devices used in the Ispra trial	99
Figure 67: Internal road track of the Ispra field trial (one lap ~ 1.7 km).....	100
Figure 68: Example of standard-compliant C-ITS messages sent by the commercial C-ITS RSU in the Ispra trial	100
Figure 69: Height of the commercial C-ITS RSU deployed in the Ispra trial.....	101
Figure 70: Line-of-sight road section (points B-A-C, length ~ 650 m) in the Ispra trial (ITS-G5 field test)	101
Figure 71: On-board equipment deployed in the test vehicle (ITS-G5 test drive).....	102
Figure 72: Physical architecture of the ITS-G5 field test trial.....	102
Figure 73: Line-of-sight road section (points B-A-C, length ~ 650 m) in the Ispra trial (LTE-V2X field test)	103
Figure 74: On-board equipment deployed in the test vehicle (LTE-V2X test drive)	103
Figure 75: Physical architecture of the LTE-V2X field test trial.....	104
Figure 76: Geolocated Packet Error Rate values in the ITS-G5 (a) and LTE-V2X (b) test drives of the Ispra trial	105
Figure 77: Cumulative Distribution Function of PER values for the ITS-G5 and LTE-V2X test drives..	106
Figure 78: End-to-end packet latency (ITS-G5)	107
Figure 79: End-to-end packet latency (LTE-V2X).....	107
Figure 80: Geolocated packet latency values in the ITS-G5 (a) and LTE-V2X (b) test drives of the Ispra trial	108
Figure 81: Empirical CDF of end-to-end packet latency for ITS-G5 and LTE-V2X in the Ispra trial	109
Figure 82: Hybrid navigation test vehicles	110
Figure 83: Comparison of good positioning accuracy and weak signal (green 0,02-0,5m and red >2m, on open-road (left side) and underground measurements (right side).)	111
Figure 84: GNSS positioning with IMU's support enabling weakening positioning accuracy when entering an underground parking area with a weak GNSS signal (green >2m and red <0.5m).	112

Figure 85: The test setup for hybrid navigation testing.....	112
Figure 86: Vediafi's test vehicle and RSU.	113
Figure 87: Positioning with RSU network.....	114
Figure 88: V2I communication model	115
Figure 89: Bit error rate under different number of paths when LOS exists	117
Figure 90: MEC App UTC procedure with the delay induced by each phase of the procedure.....	122
Figure 91: The area used for simulations (left) and its representation in SUMO simulator (right)....	124
Figure 92: A proposal of sharing UC for application controlled UCT.	127
Figure 93: Workflow of the application controlled UCT with UC sharing.	128
Figure 94: The PER and OBU–RSU distance relationship in an NLOS test environment.....	130
Figure 95: Test setup #002	146
Figure 96: Power sensor software used to measure duty cycle and output power	148
Figure 97: Test setup #001	151
Figure 98: Spectrum trace measured with 100 kHz RBW	153
Figure 99: Transmission spectrum mask for nominal carrier frequency $f_c=5860$ MHz	154
Figure 100: Transmission spectrum mask for nominal carrier frequency $f_c=5870$ MHz	154
Figure 101: Transmission spectrum mask for nominal carrier frequency $f_c=5880$ MHz	155
Figure 102: Transmission spectrum mask for nominal carrier frequency $f_c=5890$ MHz	155
Figure 103: Transmission spectrum mask for nominal carrier frequency $f_c=5900$ MHz	156
Figure 104: Transmission spectrum mask for nominal carrier frequency $f_c=5910$ MHz	156
Figure 105: Transmission spectrum mask for nominal carrier frequency $f_c=5920$ MHz	157
Figure 106: Test setup #001	158
Figure 107: Power spectral density measurement with R&S FSV7 spectrum analyser	160
Figure 108: Power spectral density measurement with 10 RBs allocated.....	161
Figure 109: Laboratory setup for experiment 1.1.....	163
Figure 110: Laboratory setup for experiment 1.2.....	164
Figure 111: Laboratory setup for experiment 1.3.....	165
Figure 112: Laboratory setup for experiment 2.1.....	166
Figure 113: Laboratory setup for experiment 2.2.....	167
Figure 114: Laboratory setup for experiment 2.3.....	168

List of Tables

Table 1: Summary of test setups for the experimental evaluation of co-channel coexistence method C (ETSI TR 103 766).....	30
Table 2: Summary of performance metrics captured for each combination of C-ITS transmitter and receiver.....	31
Table 3: The configuration of OpenC2X equipment.....	44
Table 4: Test procedure of jamming attack on ITS-G5 using OpenC2X	47
Table 5: Misbehaviour detection system test procedure	53
Table 6: The ITS 5.9 GHz spectrum allocation in Europe	60
Table 7: The ITS 5.9 GHz spectrum allocation in China	60
Table 8: A comparison of V2X technology path in different regions from OSI Model perspective	61
Table 9: A message type comparison of the intersection safety use case in china and in Europe.....	62
Table 10: Joint V2X trial use cases description overview.....	69
Table 11: Test conditions for V2V/V2I (PC5) and V2I (Uu) communication.....	74
Table 12: Joint EU-China V2X trials categorisation in Europe and in China	75
Table 13: Intersection safety (intelligent intersection with VRU crossing) use case trial procedure, in Europe	76
Table 14: Intersection safety (intersection collision warning) use case trial procedure, in China	77
Table 15: The preliminary targeted KPIs for the joint EU-China V2X use cases in Europe	80
Table 16: The preliminary targeted KPIs for the joint EU-China V2X use cases in China	80
Table 17: Calculated values: 5G from IP network to Connected Vehicle, MAP message. The number of samples used calculations is around 600 - 900.....	85
Table 18: Calculated values: LTE-V2X from OBU (Connected Vehicle) to RSU. The number of samples used for calculations is around 600 - 900.	85
Table 19: Calculated values: LTE-V2X from OBU (Connected Vehicle) to RSU, various message intervals.....	86
Table 20: Calculated values: 5G from IP network to Connected Vehicle, DENM message, various message intervals (1 ms, 5 ms, 10 ms, 20 ms, 50 ms and 150 ms).....	88
Table 21: Calculated values for LTE-V2X, different driving speeds (message interval 50 ms).....	90
Table 22: Calculated values for 5G, different driving speeds (message interval 50 ms).	91
Table 23: Calculated values for LTE-V2X with antenna height (on LTE-V2X RSU) variation (1.4m, 2.8m and 3.8m) and message size of 250 B and 750B. Vehicle driving speed 30km/h and msg. interval 100 ms. The number of samples used for calculations varied from 400 - 1000.....	92
Table 24: Calculated values for 5G antenna height variation, 250 B/msg (left) 750 B/msg (right), 30km/h, msg. interval 100 ms.....	94
Table 25: Calculated values for AUTOMATED DRIVING, fixed speed 30 km/h, message interval 100 ms, C-V2X (left) 5G (right).....	94
Table 26: The measured values (ellipse confidence and C-V2X improvement) FOR different GNSS Methods	113

Table 27: V2X use cases groups with exemplary use cases and associated latency and throughput requirements.....	119
Table 28: General service requirements for C-V2X as stated by the 3GPP [18]	120
Table 29: Delay factors present during the UCT procedure with the estimated delay induced by each factor.	124
Table 30: The configuration of RAN and MEC environment considered in the simulations.	124
Table 31: Parameters of simulations performed in SUMO	125
Table 32: Hosts deployment scenarios	125
Table 33: The estimation of the time duration of the UCT procedure	126
Table 34: The mean latency of varying OBU–OBU distance	130
Table 35: The mean latency of fixed OBU–OBU distances.....	131
Table 36: Results transmit power control measurement	149
Table 37: Configuration files used for each nominal carrier frequency.....	151
Table 38: Configuration files used for each nominal carrier frequency.....	158
Table 39: Results of RF output power measurement for all nominal carrier frequencies.....	160
Table 40: Laboratory setups for experimental evaluation of co-channel coexistence method C	162

Abbreviations

3GPP	3rd Generation Partnership Project
4G	The Fourth Generation of Mobile Communications
5G	The Fifth Generation of Mobile Communications
ADAS	Advanced driver-assistance systems
API	Application Programming Interface
AWGN	Additive White Gaussian Noise
BS	Base Station
BSM	Basic Safety Message
CAM	Cooperative Awareness Message
CAICV	China Industry Innovation Alliance for the Intelligent and Connected Vehicles
CAPEX	Capital Expenditures
CAV	Connected and Automated Vehicle
CCAM	Connected, Cooperative and Automated Mobility
CCSA	China Communication Standards Association
CCSP	Connected and Cooperative Services Platform
CDA	Clock Distribution Accessory
CDF	Cumulative Distribution Function
CEN	Comité Européen de Normalisation (European Committee for Standardisation)
C-ITS	Cooperative Intelligent Transport System
C-V2X	Cellular V2X referring to all forms of cellular V2X communications, i.e. LTE-V2X and 5G-V2X
CP	Control plane in LTE network to handle network operation
CPM	Collaborative Perception Message
CSAE	China Society of Automotive Engineers
CSMA/CA	Carrier Sense Multiple Access with Collision Avoidance
DENM	Decentralized Environmental Notification Basic Service as specified in ETSI EN 302 637
DP	Data plane in the LTE network
DSRC	Dedicated Short-Range Communications
EC	European Commission
EU	European Union
ECU	Embedded Control Unit
EIRP	Effective Isotropic Radiated Power
eMBB	enhanced Mobile Broadband
FESTA	Field opErational teSt supportT Action
ETSI	European Telecommunications Standards Institute

GLOSA	Green Light Optimized Speed Advisory
GNSS	Global Navigation Satellite System
GN-PDU	GeoNetworking-layer Protocol Data Unit
GPS	Global Positioning System
HARQ	Hybrid Automatic Repeat reQuest
HMI	Human-Machine Interface
HO	Handover
IMU	Inertial Measurement Unit
IoT	Internet of Things
IoV	Internet of Vehicles
IPG	Inter-Packet Gap
ITS	Intelligent Transport System
ITS-G5	Acronym defined in EN 302 663 (ITS access layer specification) and standing for the Physical and Data layers for the ITS ad hoc network, as defined in ETSI EN 302 665 (ITS communication architecture)
ISI	Inter-Symbol-Interference
IVIM	Infrastructure to Vehicle Information Message
JRC	Joint Research Centre in Ispra (see: https://ec.europa.eu/jrc/en/about/jrc-site/ispra)
KPI	Key Performance Indicator
LOS/NLOS	Line Of Sight/Non Line Of Sight
LTE	Long Term Evolution as standardised by 3GPP from release 8 onwards (see: http://www.3gpp.org/technologies/keywords-acronyms/98-lte)
LTE-V2X	LTE-V2X is a specific utilisation of LTE for vehicle to “everything” communications, including V2V, V2I, V2N, introduced first in 3GPP Release 14 (see: ETSI TR 121 914 V14.0.0 section 7)
MAC	Medium Access Control
MAP	Map Data Message
MAVEN	Managing Automated Vehicles Enhances Network
MCM	Manoeuvre Coordination Message
MCS	Modulation and Coding Scheme
MDS	Misbehaviour Detection System
MEC	Multi-access Edge Computing (formerly: Mobile Edge Computing)
MEO	MEC Orchestrator
MEP	MEC Platform
MEPM	MEC Platform Manager
MIIT	Ministry of Industry and Information Techno
MMSE	Minimum Mean Square Error
MOT	Ministry of Transport
MPS	Ministry of Public Security

MQTT	Message Queuing Telemetry Transport
NFV	Network Functions Virtualization
NTCAS	National Technical Committee of Auto Standardization
OBU	On-Board Unit
ODD	Operation Design Domain
OPEX	Operating Expenditures
PDB	Packet Delay Budget
PDCP	Packet Data Convergence Protocol
PDR	Packet Delivery Ratio
PC5	Direct V2V, V2I, and V2P link without base-station
PCAP	Packet Capture format
PDU	Protocol Data Unit
PER	Packet Error Rate
PHY	Physical layer
QoS	Quality of Service
RACH	Random Access Channel
RAN	Radio Access Network
RF	Radio Frequency
RGT	Remaining Green Time
RMS	Root Mean Square
RRC	Radio Resource Control
RSRP	Reference Signal Received Power
RSU	Road Side Unit
RTT	Round Trip Time
RTTT	Road Transport and Traffic Telematics
SAE	Society of Automotive Engineers
SINR	Signal to Interference plus Noise Ratio
SLR	Service Level Requirement
SINR	interference plus noise ratio
SNR	Signal-to-noise ratio
SPaT	Signal Phase and Timing
SPS	Semi-Persistent Scheduling
SR	Success Rate
SRVCC	Single Radio Voice Call Continuity
TB	Transport Block
TC	Technical Committee

TPC	Transmit Power Control
TTG	Time To Green
UC	User Context
UCT	User Context Transfer
UE	User Equipment
UPS	Uninterruptible Power Supply
URLLC	Ultra-Reliable Low-Latency Communication
USRPTM	Universal Software Radio Peripheral
V2I	Vehicle to Infrastructure
V2N	Vehicle to Network
V2V	Vehicle to Vehicle communication
V2X	Vehicle to Everything
VoLTE	Voice over LTE
VRU	Vulnerable Road User
WP	Work Package

1 Introduction

You are reading a report that summarises the main contributions to the 5G-DRIVE project which spans over 34 months. The future Connected, Cooperative and Automated Mobility (CCAM) in Europe can't be delivered without the work undergone in this and other research and innovation projects exploring the 5G connectivity, security and possibility to implement very complex technological solutions in urban and rural environments. The 5G-DRIVE project specifically tested and validated the interoperability between European Union's (EU) and People's Republic of China (in further text: China) 5G networks operating at 3.5 GHz bands for enhanced Mobile Broadband (eMBB) and 3.5 & 5.9 GHz bands for V2X scenarios. In Europe, 17 partners from 11 countries, including industry, mobile operators, a car manufacturer, SMEs, research institutes, academia and consulting partners, worked on Horizon 2020 funded project. The focus of the document is on V2X trials conducted in Europe, including all necessary actions conducted in preparing both the laboratory experiments and on-site tests, as well as reporting the key results of these activities. Furthermore, the European Commission funded project had its twin project partner, led by the China Mobile Research Institute, which overlap to a certain degree in both time and content of the trials conducted in China. The joint EU-China V2X trial framework has been specifically created to describe and define the methodology and analyse the findings from both project teams. Results from experiments in China are also presented and analysed in the report.

One of the 5G-DRIVE project main objectives has been the development of key 5G technologies at pre-commercial testbeds V2X services and then demonstrate IoV services using Vehicle-to-Infrastructure (V2I) and Vehicle-to-Vehicle (V2V) communications. The 5G trials have been conducted in the two principal use cases, GLOSA and intersection safety (intelligent intersection with VRU crossing). The cases have been selected as the ones which can bring the biggest benefit in up taking of the connected and automated driving on our roads under the CCAM framework. Special attention is paid in automated driving challenges. In Europe, on-site V2X trials have been executed in two different locations, Espoo/Tampere in Finland and at the EC's Joint Research Centre in Ispra, Italy and are presented respectively.

Since the project aim was to investigate and analyse the 5G cellular and LTE-V2X PC5 benefits between Europe and China, the common test scenarios were planned so they can be realised both in China and the European trial sites. The common KPIs and assessment methods are defined to investigate the performance and analyse the similar trends through results comparison. This document is focusing on LTE-V2X PC5, considering more precisely the existing standards and requirements for operation in C-ITS systems.

2 V2X communication testbeds

The 5G-DRIVE V2X communication testbeds are a research instrument to study and validate some of the key technical and policy-related issues in road ITS technologies. Analysing these issues through experimental means helps to build a detailed understanding of the communication technologies implemented in commercial/prototyping road ITS equipment and enables the possibility to spot specific behaviours not previously detected in analytical or simulation studies. To this end, the experimental work conducted in the framework of 5G-DRIVE constitutes an added-value proposition to existing analytical and simulation studies on V2X-related topics, such as co-channel coexistence of road ITS technologies in the 5.9 GHz band, disruption of C-ITS services through jamming, attack detection using a misbehaviour detection system, or improvements to passenger safety via the deployment of basic C-ITS safety services.

2.1 Rationale and scope

The following sections describe the rationale and scope of the experimental work carried out by 5G-DRIVE on two key policy and technical topics, namely the coexistence of road ITS technologies in the 5.9 GHz band and the frequency jamming and misbehaviour detection of road ITS services.

2.1.1 Coexistence of ITS-G5 and LTE-V2X in the 5.9 GHz band

Commission Implementing Decision (EU) 2020/1426 of 7 October 2020 [1] harmonises the conditions for the availability and efficient use of frequency band 5875-5935 MHz (the so-called “5.9 GHz band”) for safety-related applications of Intelligent Transport Systems in the European Union. As a result of this Decision, the 5.9 GHz band is organised as follows:

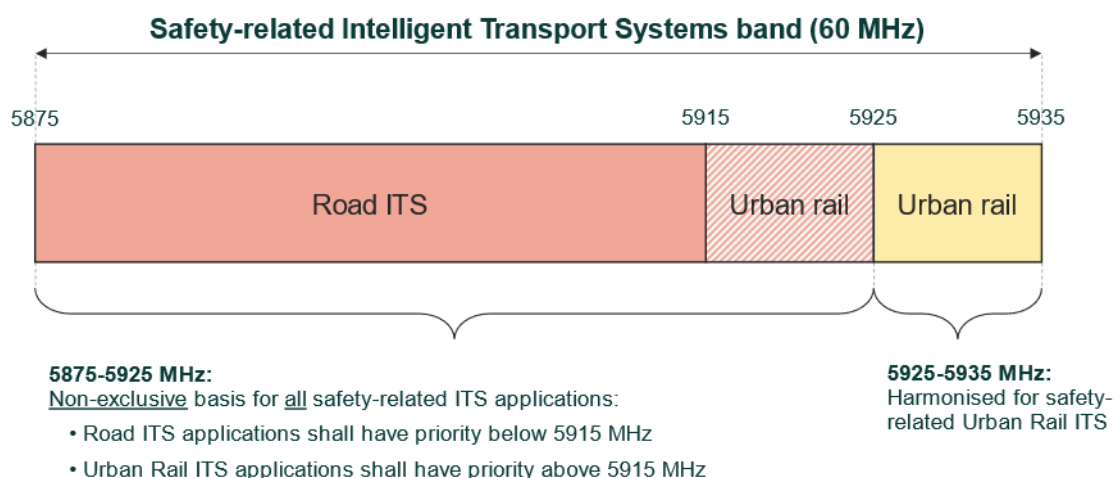


Figure 1: Harmonised safety-related ITS band in the European Union (5.9 GHz)

As shown in Figure 1, the 5875-5925 band is allocated to safety-related road ITS and urban rail ITS technologies on a non-exclusive basis – i.e. road ITS shall have priority below 5915 MHz whereas urban rail ITS shall have priority above 5915 MHz. Consequently, *any* road ITS technology (such as ITS-G5 or LTE-V2X) is allowed to operate in the 5875-5915 MHz band provided that it conforms to the EU Radio Equipment Directive (e.g., by complying with the technical requirements defined in Harmonised European Standard ETSI EN 302 571 [2] as well as national regulations in Member States).

Notwithstanding the EU legislative framework for granting ITS equipment access to the 5.9 GHz radio spectrum band, ITS-G5 and LTE-V2X can potentially cause harmful interference to each other when deployed in a co-channel fashion in the same geographical region, as neither of the two technologies has been designed to operate simultaneously with each other. Harmful interference could potentially

lead to service degradation, which is an undesired outcome for a safety-critical application such as Intelligent Transport Systems. In view of the above, coexistence of road ITS technologies in the 5875-5915 MHz band is a relevant policy- and technology-related topic that must be studied in detail.

At the time of drafting this Report, Technical Group 37 of the ETSI Technical Committee on Electromagnetic Compatibility and Radio Spectrum Matters (ETSI TC ERM TG37) is developing two Technical Reports (TRs) to study the issues of co-channel and adjacent-channel coexistence of road ITS technologies in the 5.9 GHz band. In particular:

- Technical Report 103 766 (**ETSI TR 103 766**) [3] is focusing on a pre-standardisation study on co-channel coexistence methods for ITS-G5 and LTE-V2X in the 5.9 GHz band;
- Technical Report 103 667 (**ETSI TR 103 667**) [4] is conducting a study on spectrum sharing techniques between ITS-G5 and LTE-V2X technologies in the 5.9 GHz band.

ETSI TC ERM TG37 is expected to release TR 103 766 and TR 103 667 to the public by the end of August 2021.

5G-DRIVE aims at complementing the simulation studies carried out in ETSI TR 103 766 by experimentally evaluating the impact of one of the two leading co-channel coexistence methods on ITS-G5 and LTE-V2X proposed by ETSI. To do so, 5G-DRIVE has conducted an experimental campaign with commercial ITS-G5 and LTE-V2X devices in the JRC Radio Spectrum Laboratory in Ispra (Italy). This work does not aim to replace/supersede the work carried out by ETSI, nor to be used to make general statements about the overall performance of road ITS technologies. Furthermore, 5G-DRIVE's decision to experimentally evaluate a particular co-channel coexistence method from ETSI TR 103 766 is motivated solely by the technical feasibility of emulating such method in a laboratory environment and does not respond to any particular preference over the choice of co-channel coexistence methods proposed in ETSI TR 103 766.

Section 2.2.2 presents an experimental evaluation of the impact of ETSI co-channel coexistence method C (ITS-G5 header insertion) on commercial ITS-G5 and LTE-V2X devices. The experimental evaluation of other co-channel coexistence methods proposed in ETSI TR 103 766 (such as method A: Time-Division Multiplexing) is currently under implementation assessment at the Joint Research Centre and, consequently, is beyond the scope of this deliverable.

2.1.2 Frequency jamming and misbehaviour detection

Testing is an important stage in the development of V2X technology. It should be carried out to ensure the maturity and reliability of this technology. Road safety and information security V2X services must be rigorously verified and tested before their real deployment [5]. As described in deliverable D4.3, penetration testing is one of the methods considered to validate V2X security solutions. This method consists of simulating an attacker's behaviours and testing the performance of the target system.

In the context of 5G-DRIVE, we have performed security tests covering various security requirements. Specifically, jamming attack laboratory tests were conducted assessing the power of attackers to make V2X communications and services unavailable. Frequency jamming is a dangerous physical level attack that drastically decreases the performance of the V2X communication system. It consists of the intentional transmission of a signal to disrupt the transmission channel. This signal significantly reduces the signal-to-noise ratio (SNR) for the receiver. However, interference is an unintentional signal that occurs when the signal is transmitted in an already used and operational frequency band. It is important to study the impact of jamming in the vehicular communications; therefore we carried out a set of in-lab experiments to assess such impact.

We have also performed tests on a developed misbehaviour detection system to detect internal attacks, which threaten confidentiality, authenticity, and integrity security requirements. Generally, solutions for secure and reliable V2X communications are classified into two categories: cryptography-based solutions and misbehaviour detection systems (MDSs). The latter mainly

addresses internal attackers where cryptography-based solutions may completely fail. In addition, MDSs are more suitable for delay-sensitive applications since the processing time is shorter. Existing MDSs for V2X communication systems are classified into three categories: entity-oriented, data-oriented, and hybrid trust models [6]. While entity-oriented MDSs are primarily interested in nodes (vehicles, RSUs, ...etc), data-oriented MDSs are primarily interested in data rather than nodes. However, most proposed MDSs adopt hybrid trust models where an entity-oriented mechanism is used to evaluate nodes according to the correctness of the exchanged data, while the correctness of data is verified using a data-oriented mechanism. However, the accuracy of hybrid trust-based MDSs depends on direct and indirect parameters. The direct parameters are only related to how trust values are calculated. On the other hand, the indirect parameters are related to the V2X environment such as the physical layer characteristics, radio interferences, and obstacles. In this vein, it is thus important to assess the efficiency of our MDS developed in the scope of WP5 to detect internal attacks. More specifically, we have investigated the accuracy of our MDS to detect grey hole internal attacks under radio interferences and how to make it more resilient to radio interferences. In the following, we give some background on grey hole attacks and our developed MDS.

2.1.2.1 Grey hole attack

Grey hole attack is a serious internal attack for V2X applications/services, which requires disseminating data from a source to a destination. In this attack, a malicious node advertises itself as having the shortest route to a source node requesting a network route to its destination. Then, after the source selects this route for use, the malicious node selectively drops some data packets it receives with a dropping ratio, instead of relaying these to the next hop [7]. Figure 2 illustrates an example of the grey hole attack. In this example, a source vehicle (**S**) disseminates a set of data packets to a destination vehicle (**D**). The attacker vehicle (**A**) is selected as part of the dissemination route. The attacker can then selectively drop a set of data packet received from (**S**) according to a dropping ratio. To detect grey hole attacks the deployment of a misbehaviour detection system is required.

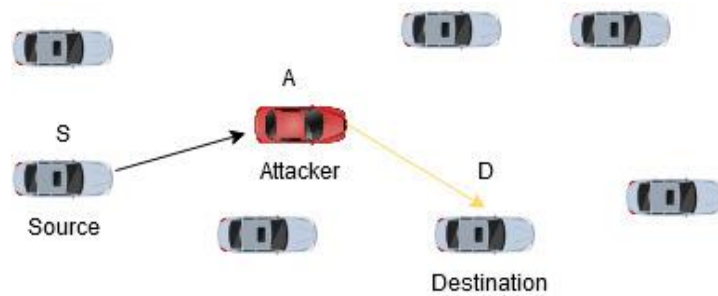


Figure 2: A scenario of the grey hole attack

2.1.2.2 Misbehaviour Detection System

In a MDS previously developed in the scope of 5G-DRIVE Task 5.4 (see subsections 3.4.3.1 and 3.4.3.3 of D5.3 [8]), we propose to deploy watchdogs that monitor the behaviour of connected vehicles and report the misbehaving vehicles. To evaluate the misbehaviour of connected vehicles, watchdogs periodically calculate their trust level based on their actions. Equation 1 gives how the direct trust of a given vehicle is calculated:

$$DT_v = \frac{A_v^h}{A_v} * \frac{1}{\gamma * A_v^m + 1}$$

$$\text{where } A_v = A_v^h + A_v^m$$

Equation 1

A_v is the number of actions performed by the vehicles during the evaluation period, which is the sum of the honest actions (A_v^h) and the malicious actions (A_v^m). The proposed trusted-based misbehaviour detection system is generic, for example, malicious actions can represent any attack performed by vehicles. γ is the attack sensitivity parameter, which characterizes the severity of the attack.

In the context grey hole attacks, malicious actions are the actions of dropping data packets. In our proposed MDS, a vehicle is detected as malicious if its trust value is below a fixed threshold. For example, in Figure 3 the source vehicle (**S**) disseminates a set of data packets to a destination vehicle (**D**). These data packets are disseminated through a network route consists of two vehicles (**H**) and (**A**) to reach its destination (**D**). However, the vehicle (**A**) is a grey hole attacker that selectively drops a set of data packets received from (**H**). To detect the grey hole attacks the watchdog (**W**) should control the receiving and disseminating packets of vehicles (**H**) and (**A**) during the evaluation period. After the end of this period, the watchdog then can calculate the trust level using the Equation 1. In our laboratory experiments, we evaluated the accuracy of the MDS not only to distinguish between honest vehicles and attackers, but also to detect the dropping ratio of the attackers.

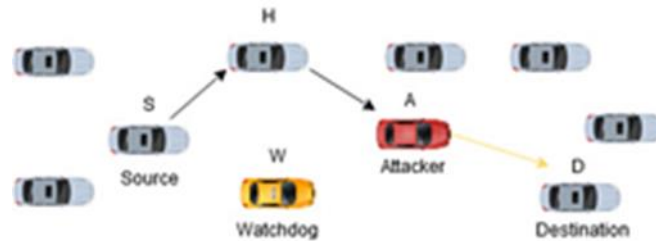


Figure 3: Misbehaviour detection system deployment

2.2 Laboratory tests at the Joint Research Centre

In the framework of 5G-DRIVE, the Joint Research Centre has conducted laboratory tests with commercial ITS-G5 and LTE-V2X devices in its Radio Spectrum Laboratory in Ispra (Italy). The aim of these tests is to study some of the RF/PHY/MAC phenomena stemming from co-channel coexistence of road ITS technologies through experimental means.

The test plan was structured in two sequential stages, namely:

- **Preparatory tests:** the objective of these tests was to build technical competences and hands-on expertise on the operation of commercial road ITS equipment and the implementation of ETSI conformance testing procedures. These tests did not aim at assessing whether such commercial ITS-G5/LTE-V2X devices conformed to the technical requirements laid down in EN 302 571 (e.g., market surveillance activities).
- **Co-channel coexistence tests:** the purpose of these tests was to study some of the RF/PHY/MAC phenomena stemming from co-channel coexistence of road ITS technologies in the 5.9 GHz band. JRC co-channel coexistence tests were not intended to replace/supersede the simulation studies conducted in ETSI TR 103 766 and ETSI TR 103 667; instead, they aim at analysing some of the practical implementation aspects of a particular co-channel coexistence method proposed in ETSI TR 103 766 (method C: ITS-G5 header insertion) from an experimental point of view.

2.2.1 Preparatory tests

This section describes the preparatory tests carried out with commercial ITS-G5 and LTE-V2X devices in the JRC Radio Spectrum Laboratory.

2.2.1.1 Objectives

The objective of the preparatory tests was to build technical competences and hands-on expertise with commercial ITS-G5 and LTE-V2X devices, as well as with the testing procedures described in the Harmonised European Standard for radio communications equipment for Intelligent Transport Systems in the 5.9 GHz band (ETSI EN 302 571). Furthermore, the preparatory tests also paved the way for the implementation of co-channel coexistence experiments using commercial ITS-G5 and LTE-V2X equipment.

2.2.1.2 Summary of tests

The following tests from ETSI EN 302 571 were implemented using commercial ITS-G5 and LTE-V2X (Rel.14) RSUs from two world leading device manufacturers:

Transmitter frequency stability (section 5.3.2 in ETSI EN 302 571 V2.1.1):

The purpose of this test is to ensure that an ITS device operates on the applicable specific carrier centre frequencies that correspond to the nominal ITS carrier frequencies.

RF output power (section 5.3.3 in ETSI EN 302 571 V2.1.1)

The purpose of this test is to ensure that an ITS device does not exceed the maximum RF output power of 33 dBm EIRP.

Power spectral density (test 5.3.3 in ETSI EN 302 571 V2.1.1)

The purpose of this test is to ensure that an ITS device does not exceed the maximum power spectral density of 23 dBm/MHz EIRP.

Transmit power control (test 5.3.3 in ETSI EN 302 571 V2.1.1)

The purpose of this test is to ensure that an ITS device implements a mandatory Transmit Power Control (TPC) mechanism to coexist with the CEN DSRC protocol at toll plazas.

Transmitter unwanted emissions outside the 5 GHz ITS frequency band (section 5.3.4 in ETSI EN 302 571 V2.1.1)

The purpose of this test is to ensure that an ITS device complies with the transmitter unwanted emission limits in the spurious domain below and above 1 GHz, as well as in the out-of-band domain of the 5 GHz ITS frequency band.

Transmitter spectrum mask within the 5 GHz ITS frequency band for 10 MHz channels (section 5.3.5 in ETSI EN 302 571 V2.1.1)

The purpose of this test is to ensure that an ITS device does not exceed the limits of the transmitter spectrum mask for 10 MHz channel bandwidth.

Decentralised Congestion Control (section 5.3.11 in ETSI EN 302 571 V2.1.1)

The purpose of this test is to ensure that an ITS-G5 device implements a mandatory mechanism to ensure that the radio channel is not congested by too many transmissions within a certain geographical range. Note that this test is only applicable to ITS-G5, thus not technology agnostic².

Duty cycle (new testing procedure proposed to ETSI EN 302 571)

² During the implementation of the preparatory tests, the JRC submitted several technical contributions to ETSI TC ERM TG37. These contributions aimed at improving the overall quality of Harmonised European Standard ETSI EN 302 571, as well as at replacing non-technology agnostic test requirements and procedures with technology-agnostic provisions. This work has been summarised in Deliverable D6.4.

The purpose of this proposal is to replace the ITS-G5 specific testing procedure for Decentralised Congestion Control defined in section 5.3.11 of ETSI EN 302 571 with a technology-agnostic version that can also be applicable to other ITS technologies, such as LTE-V2X.

2.2.1.3 Results

The JRC conducted an experimental campaign in its JRC Radio Spectrum Laboratory to implement the tests described in Section 2.2.1.2 using commercial ITS-G5 and LTE-V2X RSUs. This work allowed JRC staff to build technical competences and hands-on expertise on commercial road ITS devices and conformance testing, such as:

- Setting the commercial ITS-G5 and LTE-V2X devices up;
- Operating the devices in a laboratory vs. an operational (field) deployment;
- Generating application-layer payloads for different configurations of packet rate, packet length and Modulation and Coding Scheme (MCS);
- Generating standard-compliant application-layer messages using the C-ITS protocol stack;
- Collecting performance metrics by polling the hardware drivers of the radio chipset;
- Collecting performance metrics by analysing packet captures via tcpdump/Wireshark.

Figure 4 shows an example of a laboratory setup to carry out some of the preparatory tests listed above with a commercial LTE-V2X RSU.

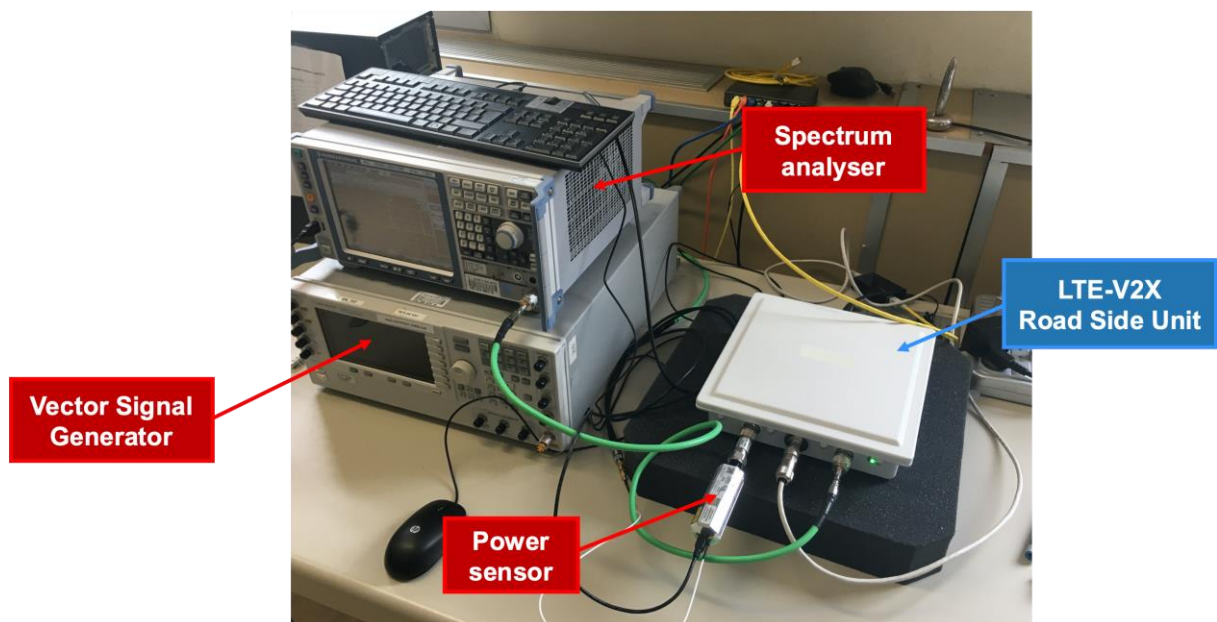


Figure 4: Example of laboratory setup for conducting a preparatory test at the JRC Radio Spectrum Laboratory with a commercial LTE-V2X RSU

For illustrative purposes, a selection of three test reports from the preparatory tests listed in section 2.2.1.2 has been included in Appendix C. Full reports for all preparatory tests are available upon request.

2.2.2 Co-channel coexistence tests

This section describes the objectives, experimental setup, results and conclusions from the co-channel coexistence experiments carried out in the JRC Radio Spectrum Laboratory in the framework of the 5G-DRIVE project. In addition, it provides a brief overview of the ITS-G5 PHY header insertion method proposed in ETSI TR 103 766 (also known as ETSI co-channel coexistence method C). For a detailed description of ETSI method C, the reader is referred to [3] and [9].

2.2.2.1 Objectives

The objectives of the co-channel coexistence tests are as follows:

- To complement the co-channel coexistence simulation studies carried out in ETSI TR 103 766;
- To analyse the impact of co-channel coexistence method C on commercial ITS-G5 and LTE-V2X devices;
- To study low-level PHY/MAC phenomena that might not have been detected in simulations.

The following technical disclaimers are made in relation to the above objectives:

- **JRC experiments do not aim at replacing simulation studies in ETSI TR 103 766:** JRC experiments in the framework of the 5G-DRIVE project aim at studying PHY/MAC phenomena not covered in detail by system-level simulations. ETSI is expected to publish full simulation results of co-channel coexistence methods by end of August 2021 in ETSI TR 103 766 and ETSI TR 103 667.
- **Experimental results from JRC tests may be specific of a particular ITS-G5/LTE-V2X radio chipset implementation:** this is a natural consequence of conducting experimental work with a subset of commercial devices, as some of the observed PHY/MAC phenomena might be due to SW/HW design and implementation choices from chipset manufacturers. Consequently, readers are advised to exercise caution when extrapolating concrete experiment observations to ITS-G5 and LTE-V2X as a whole.
- **JRC experiments do not address the entire set of co-channel coexistence methods proposed in ETSI TR 103 766:** the choice of ETSI method C as a candidate method for the experimental evaluation in the framework of 5G-DRIVE responds to its ease of implementation in a laboratory setup and is not driven by any preference in terms of performance or efficiency in relation to other ETSI co-channel coexistence methods.

2.2.2.2 A brief overview of ETSI co-channel coexistence methods

ETSI TR 103 766 defines 6 methods for the co-channel coexistence of ITS-G5 and LTE-V2X in the 5.9 GHz band. A detailed description of each one of these methods is beyond the scope of this deliverable; however, a comprehensive summary is provided in [9].

A summary of the 6 co-channel coexistence methods proposed in ETSI TR 103 766 is shown below:

Method A: Classic Time-Division Multiplexing

This method advocates for creating a so-called “superframe” time structure to split the shared medium into disjoint timeslots such that each slot is allocated to a C-ITS technology in a mutually exclusive fashion. This way, each C-ITS technology can use the shared medium during its allocated timeslot without the risk of causing harmful interference to the other technology. This method assumes that the superframe length, with deterministic start and end times, is known by both technologies.

Method B: Energy signals

In this method, LTE-V2X follows a superframe time structure like that of method A and uses energy signals to prevent ITS-G5 from transmitting during specific periods of time. During the LTE-V2X transmission periods, the ITS-G5 devices refrain from accessing the channel by sensing the energy signals sent by the LTE-V2X devices, as per the listen-before-talk mechanism in the ITS-G5 MAC layer.

Method C: ITS-G5 PHY header insertion

This method advocates for inserting the ITS-G5 PHY header in all LTE-V2X packets to help ITS-G5 stations detect LTE-V2X transmissions and defer access to the shared medium. Method C also relies on the superframe structure described in methods A and B; however, detailed knowledge of the

superframe time boundaries is not required for ITS-G5 stations since they can infer the start of the LTE-V2X slots by detecting the inserted ITS-G5 PHY headers in the LTE-V2X transmissions.

Method D: Reservation messages

Method D relies on the transmission of ITS-G5 frames by LTE-V2X devices. These ITS-G5 frames do not contain user data; instead, they are broadcast to enable ITS-G5 and LTE-V2X stations to reserve resources. Each reservation message announces the time instant at which a single or multiple LTE-V2X transmissions will start, together with their duration. To enforce this reservation, all C-ITS stations (ITS-G5 and LTE-V2X) must be able to decode the reservation messages.

Method E: Combination of ITS-G5 PHY header insertion and reservation messages

This method combines methods C (ITS-G5 PHY header insertion) and D (reservation messages). By combining these two methods, legacy ITS-G5 stations can also decode the reservation messages described in method D.

Method F: LTE-V2X applying IEEE 802.11 NAV setting

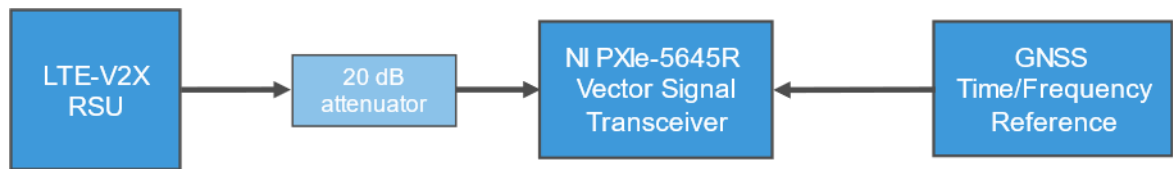
This method assumes that LTE-V2X devices will take over the timing management of all C-ITS technologies deployed in the 5.9 GHz band. To do so, LTE-V2X devices can set the IEEE 802.11 Network Allocation Vector (NAV) – a virtual carrier-sensing mechanism that limits the need for physical carrier-sensing in the air interface to improve power efficiency. The MAC frame headers contain a duration field that specifies the transmission time required for the frame (i.e., indicating the time during which the shared medium will be busy). Other stations will listen on the shared medium to read the duration field and, in turn, they will set their NAV accordingly during such interval.

2.2.2.3 Emulation of ETSI TR 103 766 method C with commercial LTE-V2X equipment

All co-channel coexistence methods proposed in ETSI TR 103 766 require modifications to the PHY and/or MAC layers of the ITS-G5 and LTE-V2X radio protocol stacks. This poses some practical challenges to the experimental evaluation of such methods using commercial equipment, as modifying the radio protocol stack of commercial C-ITS devices might not be feasible. Under such constraints, one of the main technical challenges is how to emulate a particular coexistence method using commercial equipment whilst avoiding the need for implementing software/hardware artefacts in the experimental setup that might compromise the experiment results.

In the context of 5G-DRIVE, the JRC conducted an experimental evaluation of ETSI TR 103 766 method C using commercial LTE-V2X and ITS-G5 equipment without modifying the LTE-V2X radio protocol stack. To do so, the JRC recorded live signals from a commercial LTE-V2X device transmitting LTE-V2X packets using a Vector Signal Transceiver (VST). Then, IQ samples from the recorded signals were post-processed using Matlab to add a standard-compliant ITS-G5 PHY header to each LTE-V2X transmission in the signal recording. The resulting signal was denoted as a “synthetic LTE-V2X signal”, as it contained real LTE-V2X packets to which a standard-compliant ITS-G5 header had been prepended. Overall, 4 different synthetic signals with *duty cycle* = $\frac{t_{ON}}{t_{ON}+t_{OFF}}$ equal to 1.86%, 5.57%, 13.3% and 38.7% were generated.

The ITS-G5 PHY header was generated using Matlab’s WLAN (802.11) toolbox such that the encoded RATE and LENGTH values in the ITS-G5 PHY header would indicate a transmission of 1 ms of duration for each LTE-V2X packet (LTE-V2X transmissions last slightly less than 1 ms, approximately 930 µs). The process of generating the LTE-V2X synthetic signal is illustrated in Figure 5, Figure 6 and Figure 7.



Waveform #	Duty cycle	Duration
1	1.86 %	60 s
2	5.57 %	60 s
3	13.3 %	60 s
4	38.7 %	60 s

Figure 5: Block diagram of the generation of the LTE-V2X synthetic signal using a commercial LTE-V2X RSU, an external GNSS time/frequency reference and a Vector Signal Transceiver

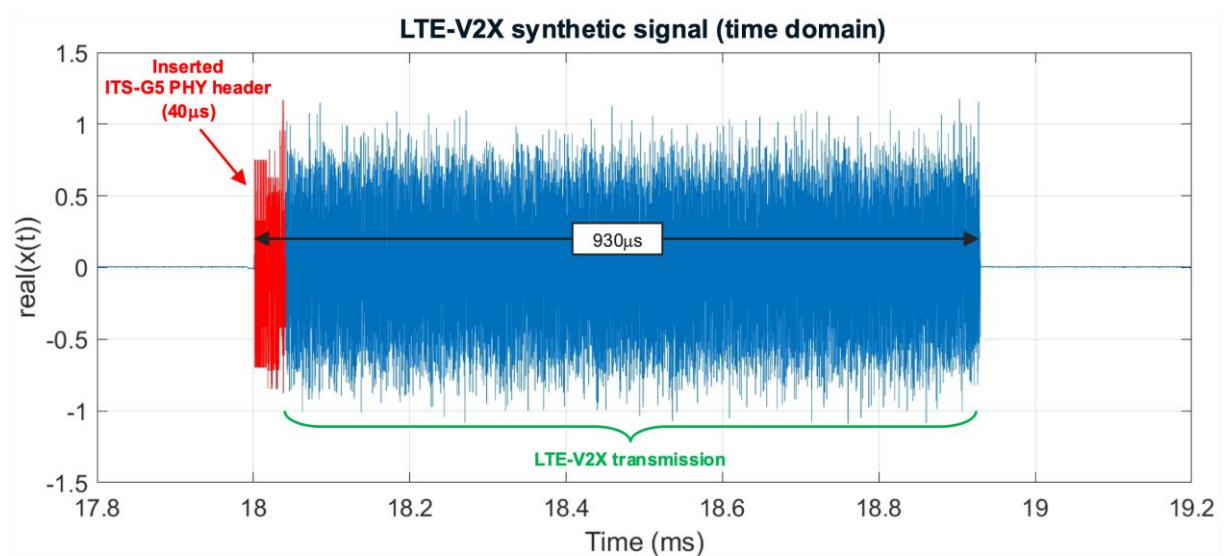


Figure 6: Time series of an LTE-V2X packet in the synthetic signal with a prepended ITS-G5 PHY header

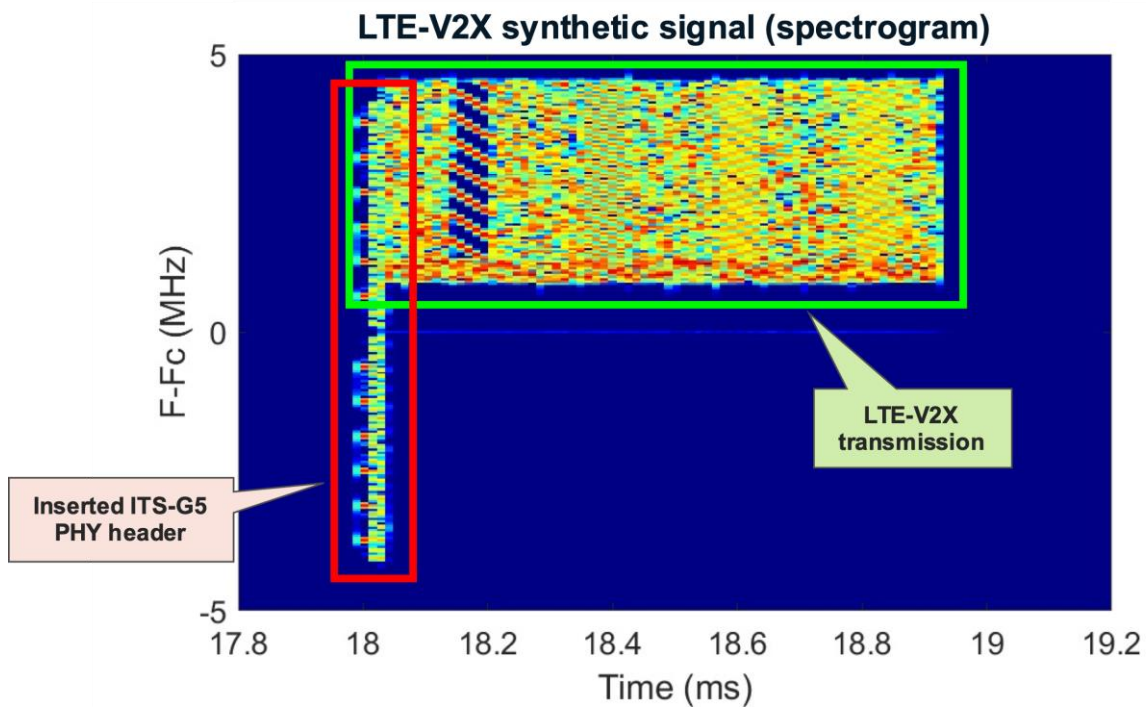


Figure 7: Spectrogram of an LTE-V2X packet (green box) in the synthetic signal with a prepended ITS-G5 PHY header (red box)

The objective of generating the LTE-V2X synthetic signal was to evaluate the performance co-channel coexistence method C on commercial devices without the need to modify the PHY/MAC layers in the LTE-V2X radio protocol stack. Once generated, the LTE-V2X synthetic signal could be replayed to commercial ITS-G5 and LTE-V2X devices with the same Vector Signal Transceiver used to build it. This procedure is described in more detail in the next section.

2.2.2.4 Experimental setup

Table 1 provides a high-level summary of the co-channel coexistence experiments carried out in the JRC Radio Spectrum Laboratory. Each experiment features a different test setup depending on the transmitting, receiving and interfering technologies, as well as on how the interfering signal is being generated (i.e. live ITS-G5/LTE-V2X signals from commercial devices vs. replayed synthetic signal from a Vector Signal Transceiver). Detailed diagrams for each test setup in Table 1 can be found in Appendix D.

C-ITS Transmitter	C-ITS Receiver	Interfering signal	Observations
ITS-G5	ITS-G5	None	
ITS-G5	ITS-G5	ITS-G5	Interferer is a commercial device
ITS-G5	ITS-G5	LTE-V2X	Interferer is a commercial device
ITS-G5	ITS-G5	LTE-V2X (with ITS-G5 header)	Interferer is a VST replaying the synthetic signal

C-ITS Transmitter	C-ITS Receiver	Interfering signal	Observations
LTE-V2X	LTE-V2X	None	
LTE-V2X	LTE-V2X	ITS-G5	Interferer is a commercial device
LTE-V2X	LTE-V2X	LTE-V2X	Interferer is a commercial device
LTE-V2X	LTE-V2X	LTE-V2X (with ITS-G5 header)	Interferer is a VST replaying the synthetic signal

Table 1: Summary of test setups for the experimental evaluation of co-channel coexistence method C (ETSI TR 103 766)

Figure 8 shows a simplified test setup for all laboratory experiments in Table 1. For all co-channel coexistence experiments, an ongoing communication link between a C-ITS transmitter (ITS-G5 or LTE-V2X) and a C-ITS receiver (ITS-G5 or LTE-V2X) is disrupted by a C-ITS interfering signal (ITS-G5, LTE-V2X or LTE-V2X with ITS-G5 PHY header insertion).

The goal of the co-channel coexistence experiments is to evaluate the impact of the different interfering signals on the transmitter and receiver devices, as well as to explore some potential implementation-specific PHY/MAC phenomena not detected in simulation studies. To do so, a power scan of the interferer signal at point B was conducted whilst evaluating a suite of performance metrics at points A and C.

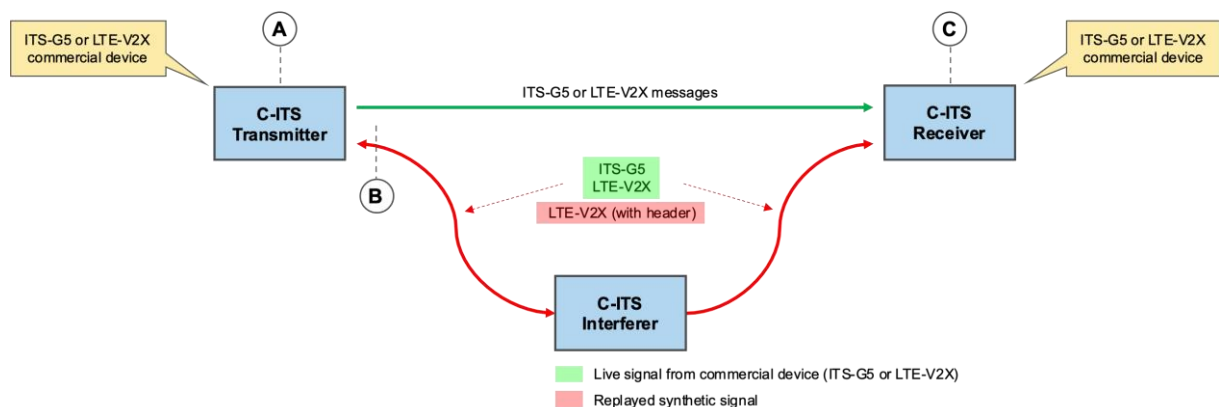


Figure 8: Laboratory setup for the experimental evaluation of co-channel coexistence method C (ITS-G5 header insertion) in the JRC Radio Spectrum Laboratory

2.2.2.5 Performance metrics

All co-channel coexistence experiments were conducted using commercial ITS-G5 and LTE-V2X devices (Rel.14) featuring radio chipsets from two different world leading chipset manufacturers. The set of performance metrics exposed by the ITS-G5 and LTE-V2X radio chipsets to the operating system running in the commercial ITS-G5/LTE-V2X devices is chipset-specific. Consequently, for each victim technology (ITS-G5 or LTE-V2X) the set of performance metrics is different.

Table 2 shows a summary of the performance metrics captured for each combination of C-ITS transmitter and receiver.

C-ITS Transmitter	C-ITS Receiver	Performance metrics
ITS-G5	ITS-G5	PER ³ , PHY/MAC hardware counters ⁴ , inter-packet gap
LTE-V2X	LTE-V2X	PER, IPG, latency

Table 2: Summary of performance metrics captured for each combination of C-ITS transmitter and receiver

2.2.2.6 Results

This section presents the results of the co-channel coexistence experiments for each victim technology (ITS-G5 and LTE-V2X).

ITS-G5 as victim technology

In this setup, an ITS-G5 communication link between an ITS-G5 RSU and an ITS-G5 OBU was disrupted by three different interfering signals (one signal at a time) – namely, ITS-G5, LTE-V2X and LTE-V2X with header insertion. For each interferer signal, the received interferer power at the transmitter varied between -100 and -50 dBm. A detailed description of the three laboratory setups for these experiments can be found in Appendix D.

Figure 9 shows the Packet Error Rate at the ITS-G5 receiver as a function of the interference power at the ITS-G5 transmitter for each interfering signal. In this experiment, the Signal-to-Interference Ratio (SIR) at the ITS-G5 receiver was fixed to 10 dB.

³ Packet Error Rate is the ratio (in percentage) of the number of packets not successfully received by a C-ITS receiver to the number of packets sent by a C-ITS transmitter.

⁴ PHY/MAC hardware counters are an instrumentation mechanism of the ITS-G5 radio chipset. Upon user request, the hardware driver of the ITS-G5 radio chipset can expose PHY and MAC statistics (such as number of Active Firings, RX PHY Acquisitions, RX PHY Valid SIGNAL Field Frames, etc.) to userspace applications. These statistics can be read periodically to monitor the performance of the PHY and MAC layers throughout an experiment run.

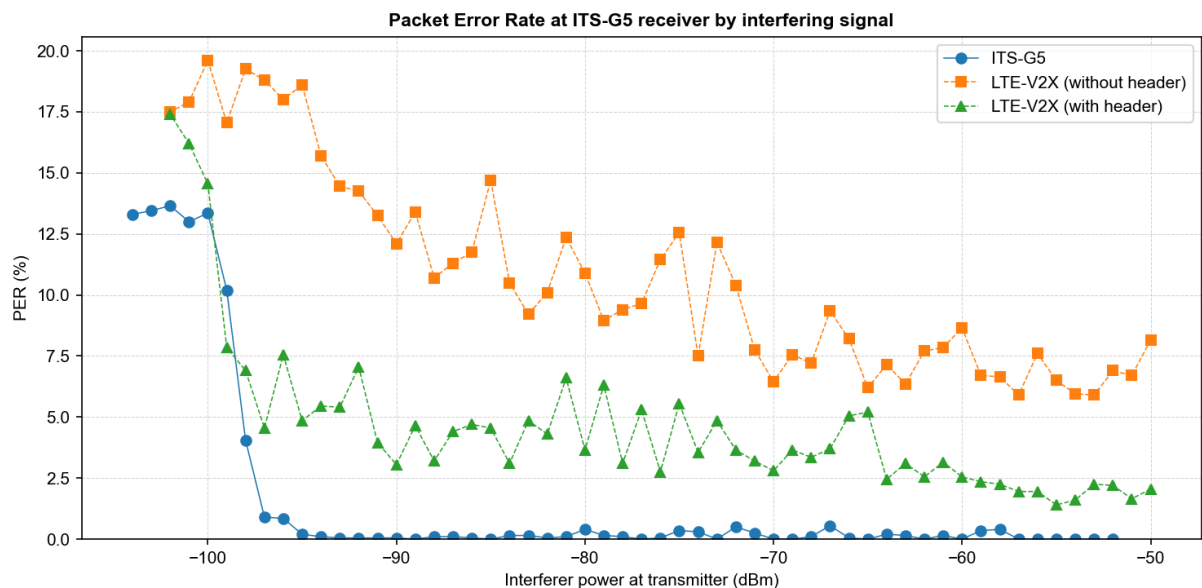


Figure 9: Packet Error Rate vs. interferer power at the transmitter for all interfering signals (ITS-G5 as victim technology)

As shown in the figure, the MAC layer of the ITS-G5 transmitter reacts differently to each interfering signal:

- For an ITS-G5 interference (**blue datapoints**), as soon as the transmitter starts detecting the interfering signal (at around 100 dBm), the MAC layer starts predicting the duration of the interfering transmissions by decoding the RATE and LENGTH fields in the ITS-G5 PHY header of the interfering packets. This enables the CSMA/CA mechanism in the MAC layer of the transmitter to schedule future transmissions at times in which the channel is expected to be idle, thus avoiding collisions at the receiver. This behaviour is illustrated in Figure 9 by the sharp decrease of PER in the receiver at around -100 dBm.
- For an LTE-V2X interference without header insertion (**orange datapoints**), the ITS-G5 transmitter is unable to decode the RATE and LENGTH fields in the ITS-G5 PHY headers, as LTE-V2X transmissions do not include such header. Consequently, the ITS-G5 transmitter cannot predict the duration of the interfering packets and can only attempt future transmissions after sensing the channel using energy detection (instead of preamble detection) mechanisms. This results in a higher PER for all power levels of the interfering signal at the transmitter.
- Lastly, for an LTE-V2X interference with ITS-G5 PHY header insertion (**green datapoints**), the ITS-G5 transmitter can predict the duration of interfering packets by decoding the RATE and LENGTH fields in the inserted ITS-G5 PHY headers of the synthetic signal. This enables the ITS-G5 transmitter to schedule future transmissions at times in which the channel is expected to be idle, thus reducing the PER at the receiver. In this case, however, PER is not reduced completely to 0% as with an ITS-G5 interference. Since both interfering signals (ITS-G5 and LTE-V2X with header insertion) contain ITS-G5 PHY headers to help predict the duration of the interfering packets, the difference in PER levels might be due to (a) collisions caused by overlapping ITS-G5 and LTE-V2X packets in the receiver or (b) dropped ITS-G5 packets in the transmitter as a result of PHY/MAC phenomena caused by the interfering signal. A further analysis of these PHY/MAC phenomena in the transmitter is illustrated in Figure 10.

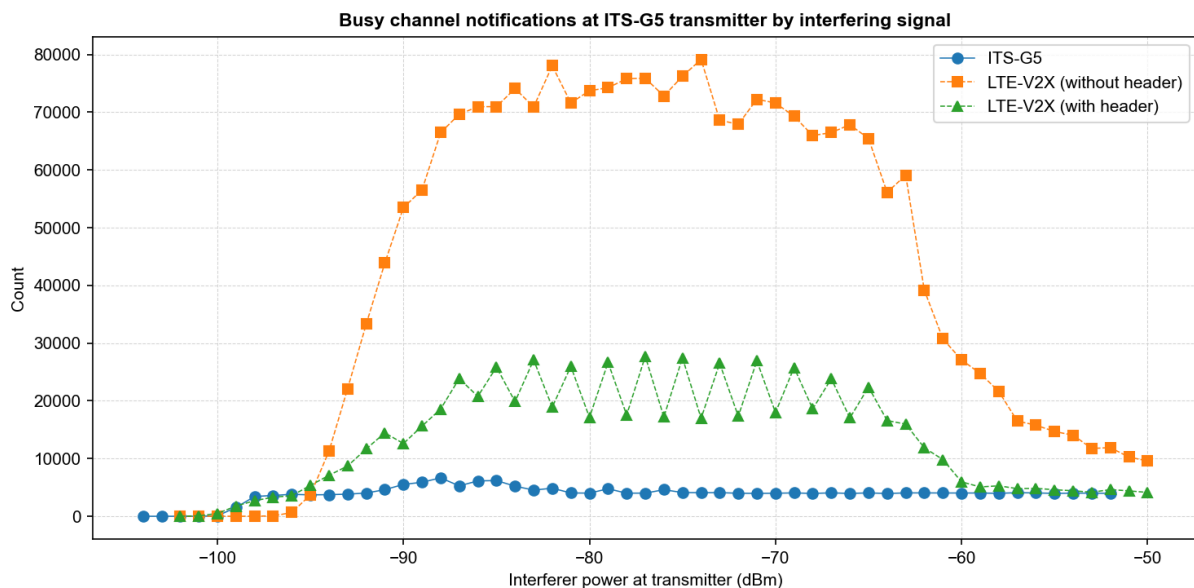


Figure 10: Busy channel notifications at the ITS-G5 transmitter vs. interfering power at the transmitter for all interfering signals

Figure 10 shows the number of busy channel notifications at the ITS-G5 transmitter for different power levels of the three interfering signals at the transmitter. A busy channel notification event is generated by the PHY layer in the ITS-G5 transmitter each time the channel is sensed busy – either by energy detection or preamble detection mechanisms. For each busy channel event, the ITS-G5 PHY layer issues a busy channel notification to the ITS-G5 MAC, and the MAC reacts to this notification by resetting ongoing CSMA/CA timers to prevent upcoming transmissions from causing collisions in the receiver.

In terms of busy channel notifications, the PHY layer in the ITS-G5 transmitter reacts different to each interfering signal (ITS-G5, LTE-V2X and LTE-V2X with header insertion). In particular, Figure 10 seems to suggest the following behaviour:

- For an ITS-G5 interference (**blue datapoints**), the ITS-G5 PHY layer in the transmitter starts issuing busy channel notifications to the MAC layer at approximately -99 dBm. These notifications are triggered by ITS-G5 packets from the interferer being detected at the ITS-G5 transmitter by both energy and preamble detection mechanisms. The number of busy channel notifications issued by the ITS-G5 PHY layer is in line with the number of interfering packets received at the transmitter.
- For an LTE-V2X interference without header insertion (**orange datapoints**), the ITS-G5 PHY layer in the transmitter starts issuing busy channel notifications to the MAC layer at approximately -96 dBm. These notifications are triggered by LTE-V2X transmissions being detected by the ITS-G5 PHY layer in the transmitter by both energy and preamble detection mechanisms. An interesting phenomenon is that the number of busy channel notifications triggered by the LTE-V2X interfering signal is significantly higher than the number of LTE-V2X packets⁵ received in the transmitter. In addition, the number of busy channel notifications for LTE-V2X is higher than for any other interfering signal (on average, 11 times higher than ITS-G5). This seems to suggest that the specific implementation of the channel sensing mechanism in the PHY layer of the ITS-G5 transmitter is being disrupted by LTE-V2X signals. This could be due to various reasons (the LTE-V2X waveform structure, implementation-specific issues in the energy detection/preamble detection mechanisms in the ITS-G5 PHY

⁵ For simplicity purposes, the term “LTE-V2X packet” is used interchangeably with “LTE-V2X Transport Block”.

layer, etc.). In all these cases, the main consequence of such high number of busy channel notifications issued by the ITS-G5 PHY layer of the transmitter is a significant degradation of the ITS-G5 MAC layer performance caused by the constant resetting of the CSMA/CA counters to prevent collisions in the receiver. This impairment of the CSMA/CA mechanism could also lead to dropped packets in the MAC queues, thus resulting in increased PER values in the receiver, as illustrated in Figure 9.

- Lastly, for an LTE-V2X interference with ITS-G5 PHY header insertion (**green datapoints**), the number of busy channel notifications issued by the ITS-G5 PHY layer to the MAC layer in the transmitter is higher than for an ITS-G5 interference (on average, 3.5 times higher), but significantly lower than that of a 'pure' LTE-V2X interference. This behaviour seems to suggest that the header insertion method helps the ITS-G5 transmitter to detect ongoing transmissions over the shared medium; however, the number of busy channel notifications is still higher than that of an ITS-G5 interfering signal. Since both signals (ITS-G5 and LTE-V2X with header insertion) contain the same standard-compliant ITS-G5 PHY headers, the difference in the number of busy channel notifications issued to the MAC layer seems to be caused by how the chipset-specific implementation of the channel sensing mechanism in the ITS-G5 transmitter reacts to the dynamics of the LTE-V2X synthetic signal.

In addition to the above observations, laboratory experiments also revealed a phenomenon caused by the impact of LTE-V2X signals (without header insertion) on the MAC layer of the ITS-G5 transmitter. This is illustrated in Figure 11.

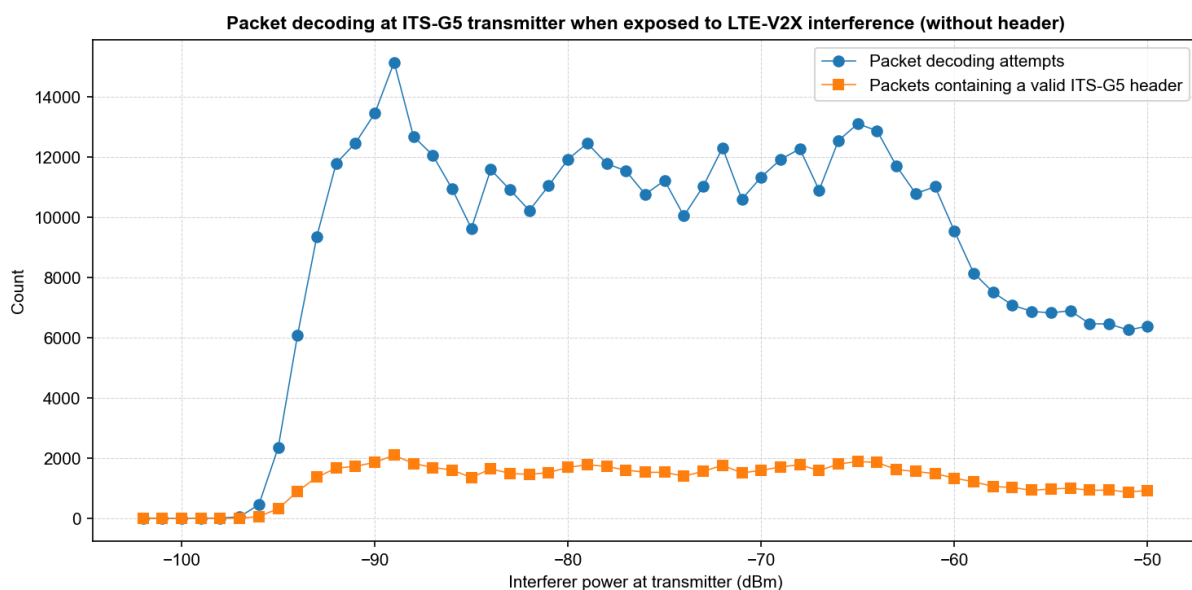


Figure 11: Packet decoding counters in the ITS-G5 transmitter when exposed to an LTE-V2X interfering signal (without header insertion)

Figure 11 shows two performance metrics (hardware counters) from the ITS-G5 PHY layer in the transmitter when it is exposed to a 'pure' LTE-V2X interfering signal (without ITS-G5 header insertion). In particular, the figure shows the number of packet decoding attempts (**blue datapoints**) and the number of packets containing a valid ITS-G5 header (**orange datapoints**) for various power levels of the LTE-V2X interferer in the ITS-G5 transmitter.

A *packet decoding attempt* is an event triggered by the PHY layer of the ITS-G5 transmitter each time that a PHY frame acquisition occurs – i.e., each time the PHY layer starts decoding an incoming frame. All ITS-G5 frames contain a SIGNAL field – i.e., a 24-bit field in the ITS-G5 PHY header that contains the RATE and LENGTH fields for this transmission. As previously discussed, the ITS-G5 MAC layer uses the RATE and LENGTH values to predict the duration of an ongoing transmission and to defer future transmissions to instants in which the shared medium is expected to be idle.

Figure 11 illustrates a PHY/MAC phenomenon in which the ITS-G5 PHY layer in the transmitter reports to the MAC that a valid SIGNAL field (thus containing valid RATE and LENGTH values) has been decoded from an LTE-V2X interfering signal without header insertion (note that LTE-V2X signals do not contain a SIGNAL field). In practice, this means that the ITS-G5 PHY layer reacts to an LTE-V2X interfering signal by issuing wrong RATE and LENGTH values to the MAC. In turn, the MAC reacts to these indications by deferring upcoming transmissions to random, non-optimal instants in time, thus increasing the number of collisions in the receiver and degrading the overall performance of the MAC layer. Experiment results seem to suggest that this *transmitter disruption* phenomenon is due to a chipset-specific implementation of the signal detection and decoding functions in the ITS-G5 radio. Consequently, this observation may not be generalised to the ITS-G5 technology as a whole. To confirm this hypothesis, additional laboratory experiments with commercial ITS-G5 devices featuring ITS-G5 radio chipsets from different manufacturers (thus containing different firmware implementations of the ITS-G5 PHY layer) should be conducted. These experiments are beyond the scope of this deliverable and, therefore, left for future research.

The effects of exposing the ITS-G5 transmitter to different interfering signals can also be measured in the ITS-G5 receiver by analysing the inter-packet gap statistics of received ITS-G5 packets. *Inter-Packet Gap* (IPG) is a performance metric defined as the time difference between successfully decoded packets in the receiver with consecutive frame sequence numbers (12 bits in the case of ITS-G5). This definition is illustrated in Figure 12.

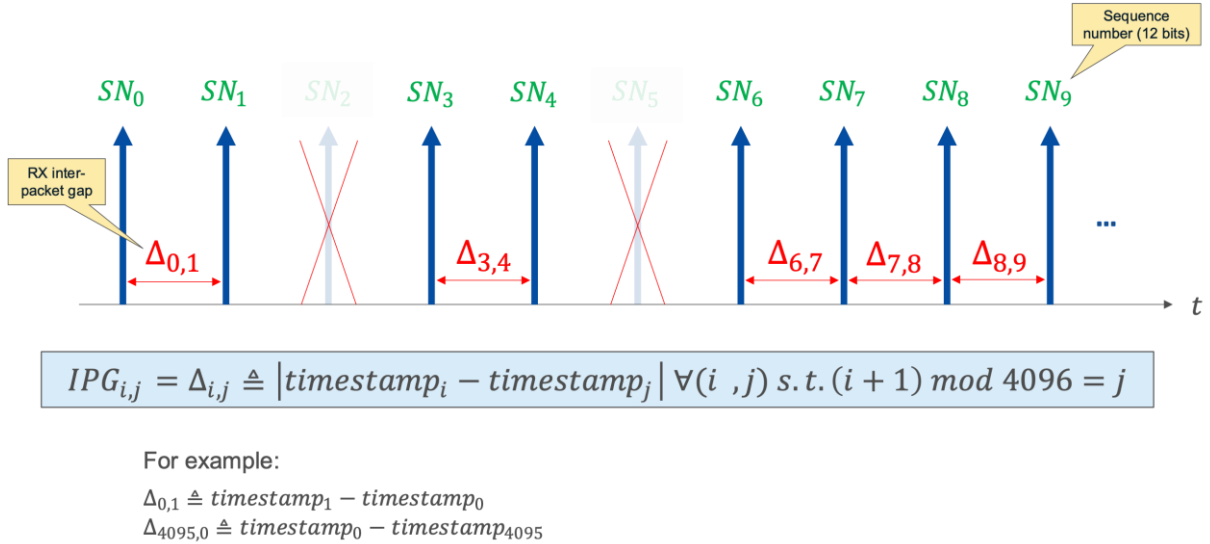


Figure 12: Definition of the inter-packet gap for received packets

Figure 13 shows a time series of IPG gaps in the ITS-G5 receiver when the ITS-G5 transmitter is exposed to ITS-G5 and LTE-V2X interfering signals at around -90 dBm. Figure 14 shows the Cumulative Distribution Function of the IPG values in the receiver when the transmitter is exposed to ITS-G5 and LTE-V2X. Both figures show a higher spread of the IPG values at the ITS-G5 receiver when the ITS-G5 transmitter is exposed to an LTE-V2X interfering signal.

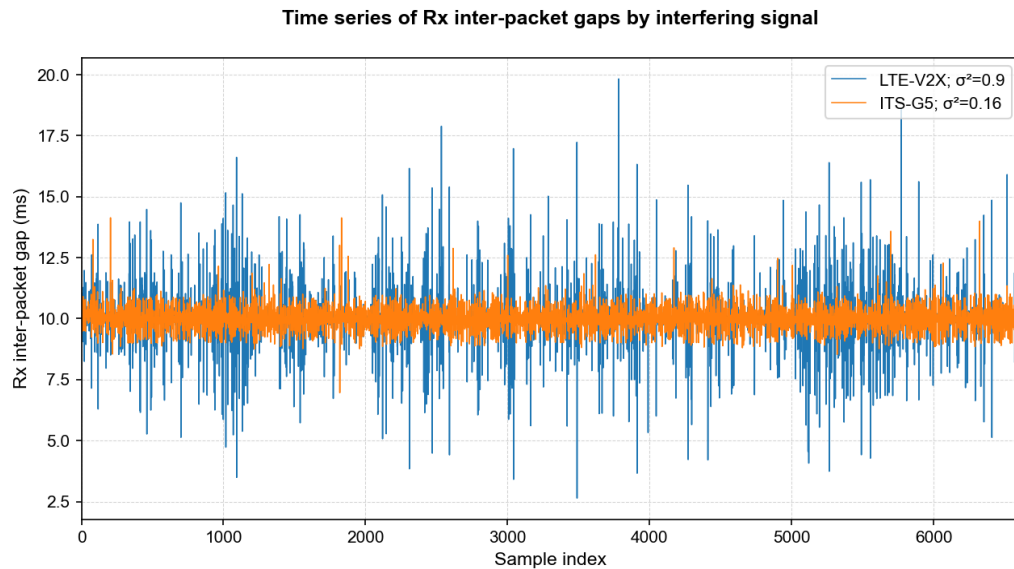


Figure 13: Time series of inter-packet gaps in the ITS-G5 receiver when the transmitter is exposed to ITS-G5 and LTE-V2X interfering signals

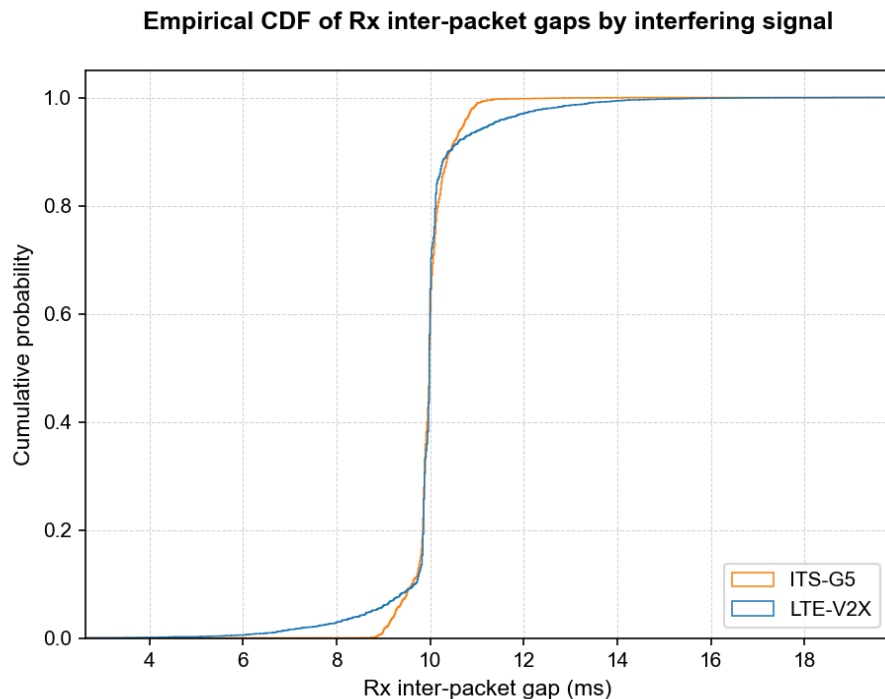


Figure 14: Empirical Cumulative Distribution Function of inter-packet gaps in the ITS-G5 receiver when the transmitter is exposed to ITS-G5 and LTE-V2X interfering signals

For the ITS-G5 interfering signal (**orange datapoints** in both figures), the IPG values concentrate around 10 ms with a relatively low variance. Note that IPG=10 ms is the expected IPG value for the signal sent by the ITS-G5 transmitter (packet rate of 100 packets/s). In this case, transmitted packets do not experience significant queueing delays due to the correct operation of channel sensing mechanism in the ITS-G5 PHY layer and the channel access mechanism in the ITS-G5 MAC layer.

By contrast, for the LTE-V2X interfering signal (**blue datapoints** in both figures), the higher spread of IPG values reflects the impact of the higher number of busy channel notifications issued by the ITS-G5 PHY layer on the channel access mechanism – in particular, on the longer channel access delay experienced by ITS-G5 transmitted packets. Also, deferring transmissions to random, non-optimal instants in time (due to the decoding of wrong RATE and LENGTH values in the ITS-G5 PHY header)

contributes to increasing IPG values, as the shared medium might be busy when the ITS-G5 transmitter attempts to transmit a deferred packet, thus incurring in further delays.

Figure 15 and Figure 16 show a time series of IPG gaps and its corresponding empirical Cumulative Distribution Functions (CDF) in the ITS-G5 receiver when the ITS-G5 transmitter is exposed to ITS-G5 and LTE-V2X (with header insertion) interfering signals.

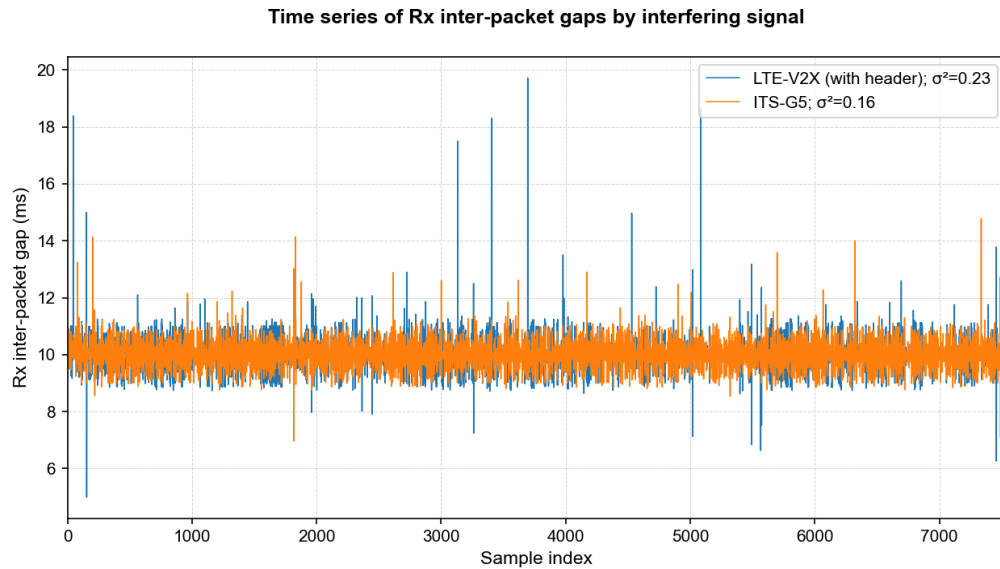


Figure 15: Time series of inter-packet gaps in the ITS-G5 receiver when the transmitter is exposed to ITS-G5 and LTE-V2X (with header insertion) interfering signals

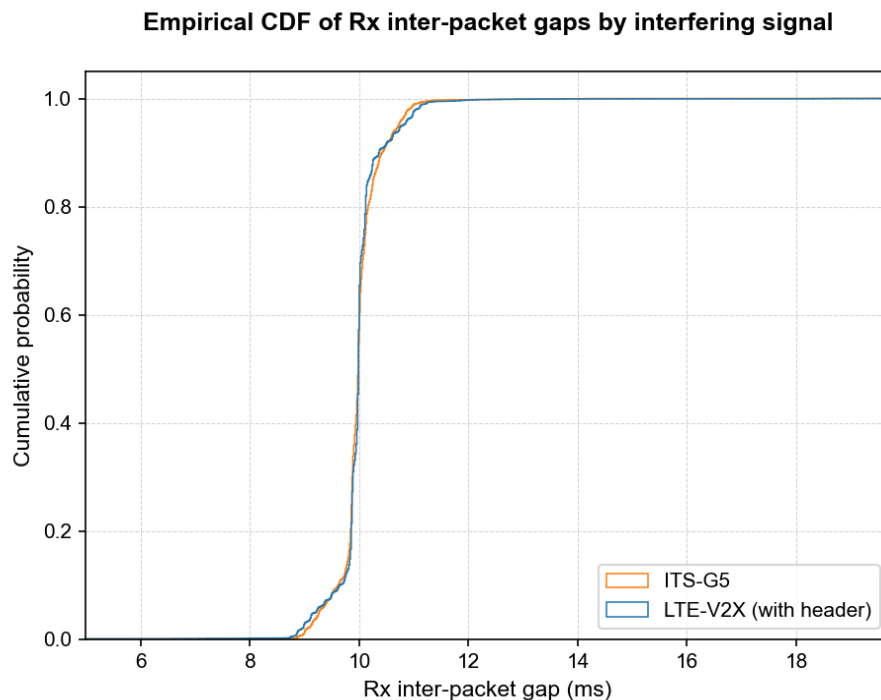


Figure 16: Empirical Cumulative Distribution Function of inter-packet gaps in the ITS-G5 receiver when the transmitter is exposed to ITS-G5 and LTE-V2X (with header insertion) interfering signals

In contrast to the behaviour illustrated in Figure 13 and Figure 14, for both interfering signals the IPG values of received ITS-G5 packets concentrate around 10 ms with a relatively low variance (orange and blue datapoints in both figures). This is due to transmitted packets not experiencing additional

channel access delays due to the correct operation of the channel sensing and channel access mechanisms in the PHY and MAC layers of the ITS-G5 transmitter, respectively.

For the LTE-V2X interfering signal with header insertion, the lower number of busy channel notifications issued by the PHY layer in the ITS-G5 transmitter leads to fewer interruptions of the CSMA/CA counters in the MAC layer, thus reducing the channel access delay of transmitted packets. In general, the IPG dynamics of the transmitted packets exposed to ITS-G5 and LTE-V2X (with header insertion) interfering signals is very similar. Since all LTE-V2X packets with header insertion contain a standard-compliant SIGNAL field, no random, non-optimal predictions of ongoing packet durations are issued to MAC layer of the ITS-G5 transmitter, thus not disrupting the operation of the MAC scheduler.

LTE-V2X as victim technology

In these experiments, an ongoing communication between an LTE-V2X transmitter and an LTE-V2X receiver was disrupted by three different interfering signals (one signal at a time): ITS-G5, LTE-V2X and LTE-V2X with header insertion. An additional experiment in which there was no interfering signal was also conducted as a benchmark baseline. The purpose of these experiments was to evaluate the impact of different interfering signals on an LTE-V2X receiver and transmitter (LTE-V2X as victim technology).

As described in section 2.2.2.5, the set of performance metrics exposed by each C-ITS radio chipset to the operating system varies across chipset manufacturers. For example, the radio chipset in the commercial LTE-V2X devices used in the co-channel coexistence experiments does not directly expose PHY/MAC performance metrics to the operating system; instead, a proprietary application from the chipset manufacturer is required to gain access to a subset of performance metrics. This adds some practical challenges to evaluating the impact of different interfering signals on the PHY/MAC performance of the LTE-V2X transmitter.

To overcome this challenge, the performance of the PHY/MAC layers in the LTE-V2X transmitter was evaluated indirectly by observing performance metrics in the LTE-V2X receiver, such as PER, average packet latency, and inter-packet gap. Note that observing these metrics does not require any instrumentation mechanism in the LTE-V2X radio chipset, as they can be calculated by inspecting the packet captures generated in the transmitting and receiving devices using a conventional protocol analyser, such as Wireshark or tcpdump.

Figure 17 shows the PER at the LTE-V2X receiver as a function of the interferer power at the transmitter for all different interfering signals (including the case of no interference). The scale of the Y-axis has been set to 10% to illustrate the threshold above which PER might start causing performance degradation to C-ITS services.

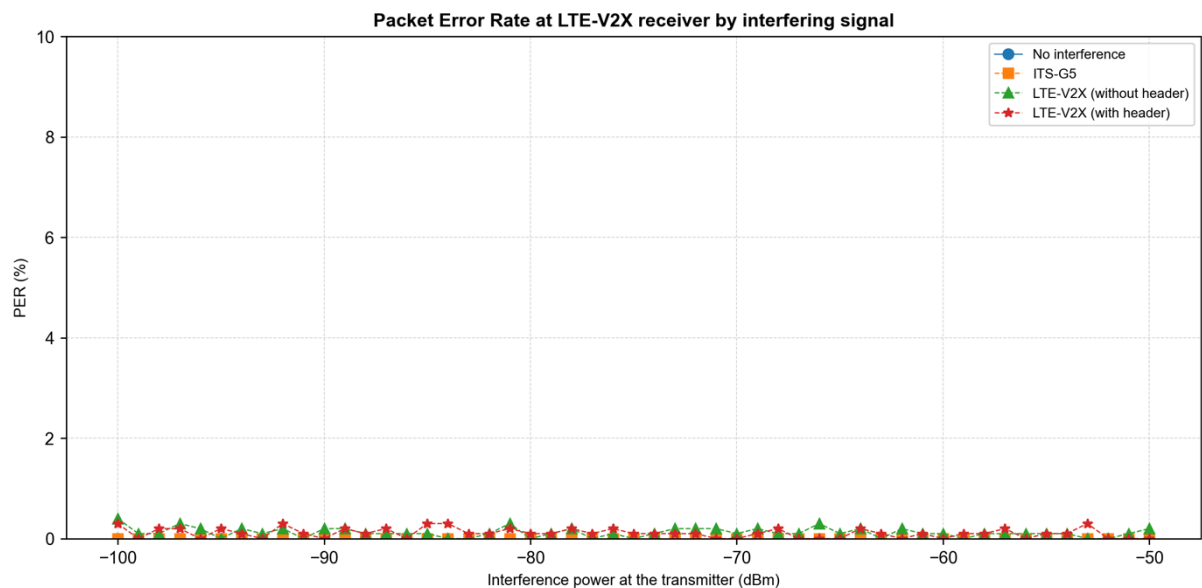


Figure 17: Packet Error Rate vs. interferer power in the transmitter for all interfering signals (LTE-V2X as a victim technology)

Results from laboratory experiments show that PER values in the LTE-V2X receiver fluctuate between 0% and 0.3% for all interfering signals, with negligible differences amongst them. This is due to the Semi-Persistent Scheduling (SPS) algorithm in the MAC layer of the LTE-V2X transmitter detecting transmissions opportunities (i.e., time-frequency resources in the shared medium) not currently used by the interfering signal or –alternatively– with an acceptable level of interfering energy. By targeting these opportunities, SPS increases the probability that the majority of LTE-V2X packets will successfully reach the receiver, thus leading to PER values close to 0%. In addition, blind HARQ retransmissions sent by the LTE-V2X transmitter also increase the probability that (at least) one out of two LTE-V2X transmissions will successfully reach the receiver – particularly when a collision between one of the two LTE-V2X transmissions and an interfering packet occurs. For a detailed description of the Semi-Persistent Scheduling algorithm in the LTE-V2X MAC layer, the reader is referred to [10].

Figure 18 shows two IPG plots for received LTE-V2X packets as a function of the interferer power in the LTE-V2X transmitter for different interfering signals. In particular, the figure shows the average IPG and its standard deviation to illustrate how the SPS algorithm in the MAC layer of the LTE-V2X transmitter reacts to different interfering signals.

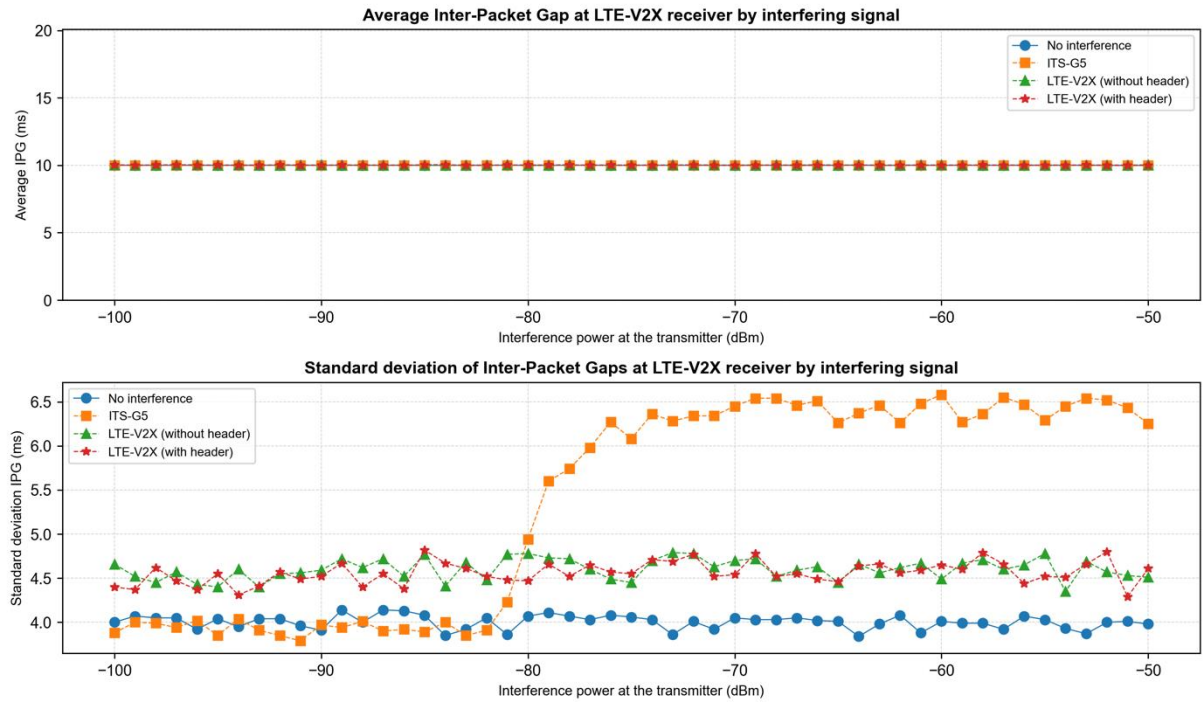


Figure 18: Inter-packet gap statistics of received LTE-V2X packets as a function of the interferer power at the receiver for different interfering signals

Overall, the SPS algorithm in the LTE-V2X transmitter keeps the average IPG of received packets consistently around 10 ms (thus honouring the packet rate of 100 packets/s of the requested data flow – see experimental setups in Appendix D). In terms of IPG spread (standard deviation), Figure 18 reveals some small differences depending on the interfering signal. In the absence of an interfering signal (**blue datapoints**), experiment results suggest a baseline IPG spread of approximately 4 ms. This spread increases to approximately 4.5 ms for the LTE-V2X and LTE-V2X (with header insertion) interferences (**green** and **red** datapoints). For an ITS-G5 interfering signal (**orange datapoints**), the spread of IPG values in the receiver increases to approximately 6.5 ms – particularly once the LTE-V2X transmitter starts detecting the interfering signal at around -81 dBm. Overall, the spread of IPG values for different interfering signals does not cause a significant impact to the performance of the LTE-V2X PHY and MAC in the receiver and does not necessarily lead to performance degradation in the receiving device.

Figure 19 shows the average packet latency at the LTE-V2X receiver as a function of the interferer power in the transmitter for different interfering signals. For an LTE-V2X system, *average packet latency* is defined as the average end-to-end delay experienced by upper-layer packets from the moment they are delivered to the PDCP layer in the LTE-V2X transmitter until the moment the PDCP layer in the LTE-V2X receiver delivers them to the upper layers. One contribution to the average packet latency is the channel access delay caused the SPS algorithm in the LTE-V2X transmitter's MAC layer. This is shown in Figure 20.

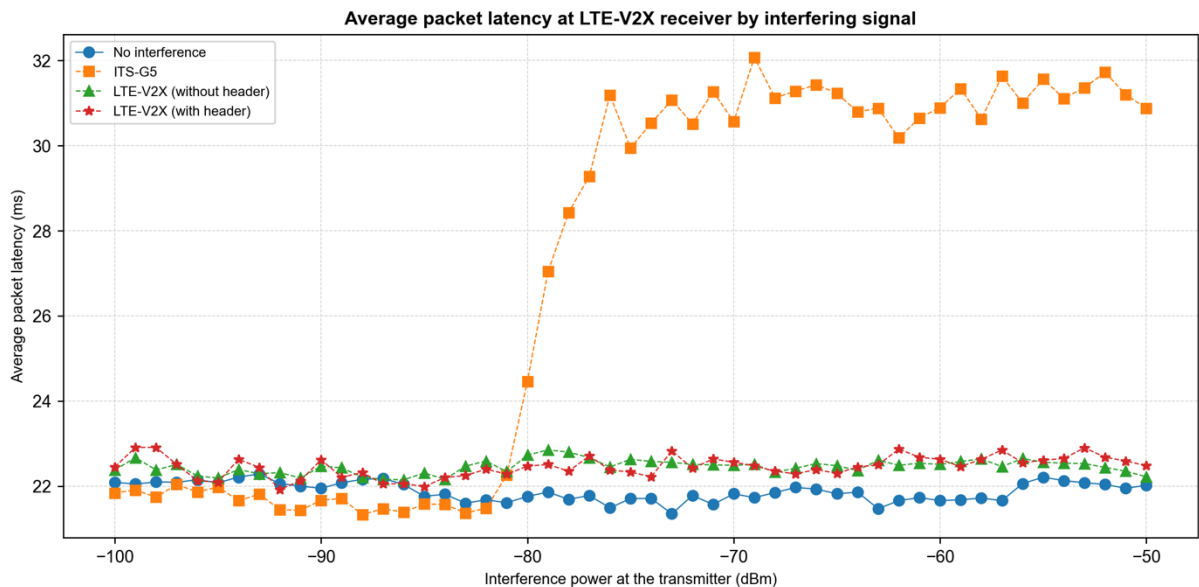


Figure 19: Average packet latency as a function of the interferer power at the transmitter for different interfering signals

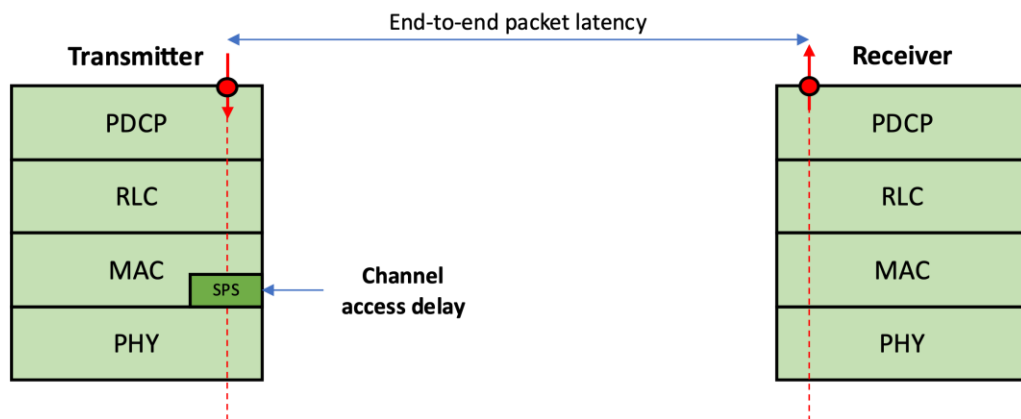


Figure 20: End-to-end packet latency (LTE-V2X)

As shown in Figure 19, in the absence of an interfering signal (**blue datapoints**), the SPS algorithm incurs in a baseline average packet latency of around 22 ms. Similarly, the average packet latency for both LTE-V2X interfering signals (with and without header insertion – **red** and **green** datapoints, respectively) is very similar, at approximately 23 ms. By contrast, the average packet latency of LTE-V2X packets exposed to an ITS-G5 interfering signal (**orange datapoints**) increases up to approximately 31 ms – particularly once the LTE-V2X transmitter starts detecting the interfering signal at approximately -80 dBm. This behaviour seems to suggest that the SPS algorithm in the LTE-V2X transmitter is robust in keeping PER low and IPG constant in the receiver whilst keeping the average packet latency within a user-configurable Packet Delay Budget (PDB).

The collision avoidance mechanism of the SPS algorithm is based on the knowledge of upcoming transmission reservations. These reservations are indicated in the Sidelink Control Information transmitted (and decoded) by LTE-V2X stations. To this extent, collision avoidance in SPS does not necessarily depend on the transmission pattern of an interfering signal being stable over time, but instead on the fact that transmission reservations are known to LTE-V2X stations. Since ITS-G5 signals do not contain LTE-V2X Sidelink Control Information, the SPS algorithm of an LTE-V2X transmitter is likely to experience performance degradation when exposed to an ITS-G5 interfering signal.

2.2.2.7 Conclusions

This section summarises the main findings from the co-channel coexistence experiments conducted with commercial ITS-G5 and LTE-V2X devices in the JRC Radio Spectrum Laboratory:

ETSI method C helps reduce the Packet Error Rate in the ITS-G5 receiver, but not entirely:

- Inserting an ITS-G5 PHY header at the beginning of each LTE-V2X packet helps ITS-G5 devices detect LTE-V2X transmissions. By decoding the RATE and LENGTH values in the inserted ITS-G5 PHY headers, ITS-G5 devices can predict the duration of ongoing LTE-V2X transmissions, thus deferring upcoming transmissions to instants in which the shared medium is more likely to be found idle. This helps reduce PER in the ITS-G5 receiver, although not completely to 0%.

Co-channel coexistence is not only a matter of RF interference in the receiver:

- Co-channel coexistence is generally associated with RF interference in the receiver (e.g., packet collisions). Experiment results suggest that interfering signals may also disrupt PHY and MAC functions in the transmitter (i.e. the *transmitter disruption* effect), thus causing further performance degradation in the receiver.

Transmitter disruption is difficult to detect in system-level simulations:

- Generally, system-level simulators do not model all PHY and MAC functions in detail. Therefore, spotting chipset-specific PHY/MAC phenomena (such as transmitter disruption) using system-level simulators is unusual. This reinforces the added value of conducting experimental analysis with commercial ITS-G5 and LTE-V2X devices.

Transmitter disruption is an implementation-specific phenomenon and cannot be extrapolated to an entire C-ITS technology:

- Since transmitter disruption may be specific of certain ITS-G5 chipset implementations (hardware and firmware), it should not be extrapolated to ITS-G5 as a whole. To gauge the extent of the transmitter disruption effect on the ITS-G5 chipset market, additional experiments with ITS-G5 devices featuring radio chipsets (and firmware) from different manufacturers need to be carried out.

The SPS algorithm in the LTE-V2X MAC layer shows a robust performance against all three interfering signals (ITS-G5, LTE-V2X and LTE-V2X with header insertion):

- For an LTE-V2X interference (with and without header insertion), SPS keeps PER low and a stable IPG and latency. Instead, for an ITS-G5 interference, SPS keeps PER low and IPG stable

at the expense of increasing the average packet latency. Further experiments with different levels of Carrier-to-Interference ratios in the LTE-V2X receiver are left for future research.

From the SPS perspective, there are no significant differences between LTE-V2X interfering signals with or without header insertion:

- The dynamics of an LTE-V2X interfering signal with and without header insertion are very similar. In general, the rate at which the LTE-V2X packets are generated (including the blind HARQ retransmissions) is the same in both cases. This also applies to transmission duration, which is kept at 930 μ s regardless of whether LTE-V2X packets carry an inserted ITS-G5 header or not. One of the main differences between LTE-V2X and LTE-V2X (with header insertion) signals, is that during the first 40 μ s of an LTE-V2X transmission with header insertion, the ITS-G5 PHY header occupies a larger number of frequency resources in the C-ITS channel bandwidth, as illustrated in Figure 7. Although this might result in SPS marking some of these time-frequency resources as ineligible, experiment results have not shown at this stage any significant performance degradation of the SPS algorithm caused by header insertion.

Co-channel coexistence methods may lead to some degree of performance degradation of upper-layer C-ITS services:

- ITS-G5 and LTE-V2X are very different technologies at the PHY and MAC levels. ITS-G5 is a fully distributed asynchronous technology based on an opportunistic CSMA/CA channel access mechanism. By contrast, LTE-V2X is a fully distributed synchronous technology based on a Semi-Persistent Scheduling channel access mechanism. Any co-channel coexistence method that attempts to prescribe a synchronous behaviour on an asynchronous technology (or a contention-based channel access mechanism on a Semi Persistent Scheduling-based channel access technology) may result in some degree of performance degradation to upper-layer C-ITS services. In addition, from the implementation perspective, co-channel coexistence methods described in ETSI TR 103 766 require modifications to the PHY and MAC technical specifications of LTE-V2X and/or ITS-G5. A detailed analysis of the impact of co-channel coexistence methods on the performance of upper-layer C-ITS services and the ITS-G5/LTE-V2X technical specifications is beyond the scope of this deliverable.

2.3 Laboratory tests at the University of Luxembourg

In the framework of 5G-DRIVE, the University of Luxembourg has conducted laboratory tests with prototyping equipment that supports ETSI ITS-G5. These tests aim to evaluate the impact of different levels of jamming attacks on the ITS-G5 technology and evaluate the impact of radio interferences on the accuracy of a misbehaviour detection system to detect grey hole attacks, and then enhance its resilience to radio interferences. The following sections describe the objectives, experimental setup, results, and conclusions for both the jamming tests on ITS-G5 and misbehaviour detection system tests carried out.

2.3.1 Jamming tests on ITS-G5 using OpenC2X equipment

This section describes the jamming tests on ITS-G5 using OpenC2X equipment carried out at the University of Luxembourg.

2.3.1.1 Objectives

As we have already mentioned in D4.3, in these in-lab experiments have performed jamming tests on ITS-G5 using OpenC2X. The goal is to evaluate the impact of different levels of jamming attacks on the ITS-G5 technology. These experiments consider different distances between ITS-G5-enabled equipment and the position of jamming source relative to the receiving equipment. We have performed these in-lab experiments using OpenC2X, which is an open-source experimental and

prototyping platform that supports ETSI ITS-G5 [11]. Although it is not commercial grade equipment, It enables real-world tests and validations of new protocol options and standards. OpenC2X supports most of the ETSI ITS-G5 features and runs on the IEEE standard.

2.3.1.2 Experimental setup

Figure 21 Figure 21 shows the experimental setup used to carry out these experiments, which consists of the following hardware and software tools:

- **2 x OpenC2X equipment:** As shown in Figure 21, in our experiments, one of the OpenC2X equipment is set up as a sender and the other equipment is set up as a receiver. Table 3 shows the default configuration of OpenC2X equipment.

Parameter	Value	
Frequency band	5.9 GHz	
Transmission Power	100mW/20 dBm	
Frequency channel	10 MHz	
Distance between the sender equipment and the receiving equipment (D)	{1,2,3,4,5} m	
Distance between jamming source(s) and receiving equipment	One-source of jamming scenario	D/2
	Two-sources of jamming scenario	(2*D)/3 for the first jamming source (USRP1) D/3 for the second jamming source (USRP 2)

Table 3: The configuration of OpenC2X equipment

- **2 x USRP B205mini-i equipment:** are used to perform the jamming attacks on the control channel in the frequency band 5.9 GHz. The maximum gain setting of USRP B205mini is 89 dB. Depending on the scenario, we used one or two USRPs as illustrated in Figure 21 (c) and Figure 21 (d). In addition, as shown in Table 3, the distance from the receiving equipment to the jamming source depends on the distance (**D**) between the sender equipment and the receiving equipment. Specifically, in the one-source of jamming scenario, the jamming source was installed on **D/2** far from the receiving equipment. On the other hand, in the two-source of jamming scenario, the first jamming source (**USRP 1**) is installed on **(2*D)/3** far from the receiving equipment, while the second jamming source (**USRP 2**) was installed on **D/2** far from the receiving equipment.
- **2 x laptop** equipped with GnuRadio and HyperTerminal software (shown in Figure 21 (b), and Figure 21 (c)): GnuRadio is a free & open-source software development toolkit that provides signal processing blocks to implement software radios. We have used GnuRadio to create blocks to generate the jamming signal and send it using USRP equipment. In addition, one of the two laptops is also connected to OpenC2X through a serial cable to retrieve information about the number of received packets using TCPDump command executed on HyperTerminal software.

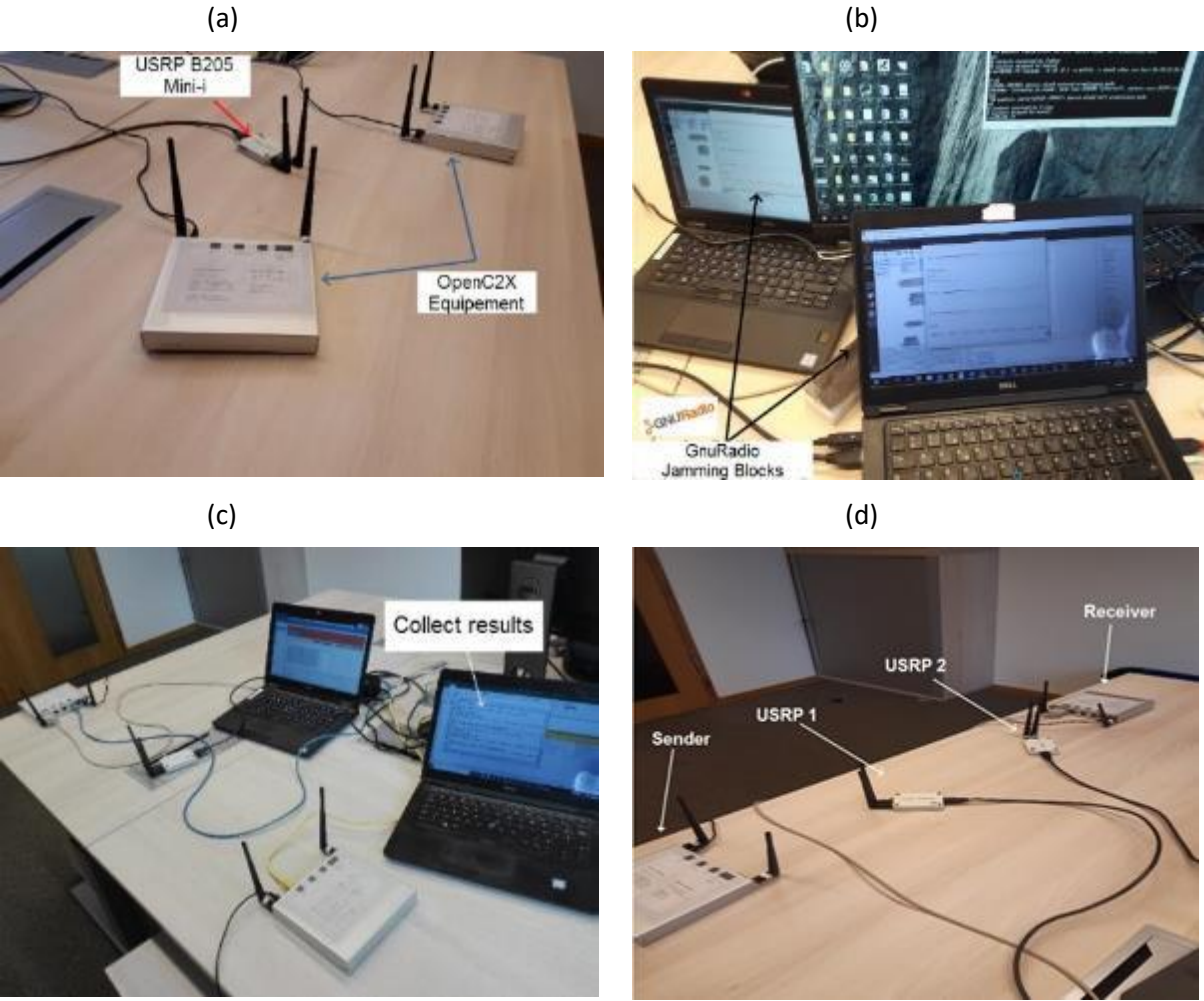


Figure 21: Experimental setup of jamming attacks on ITS-G5

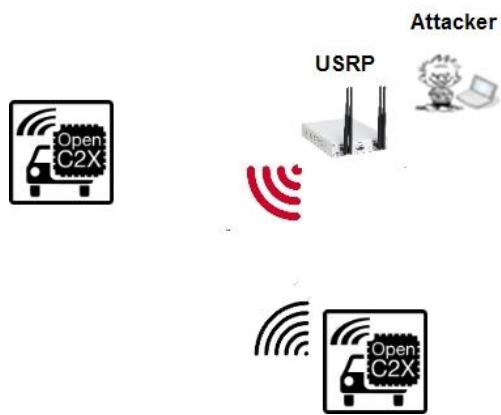


Figure 22: The first test scenario for the jamming attack on ITS-G5

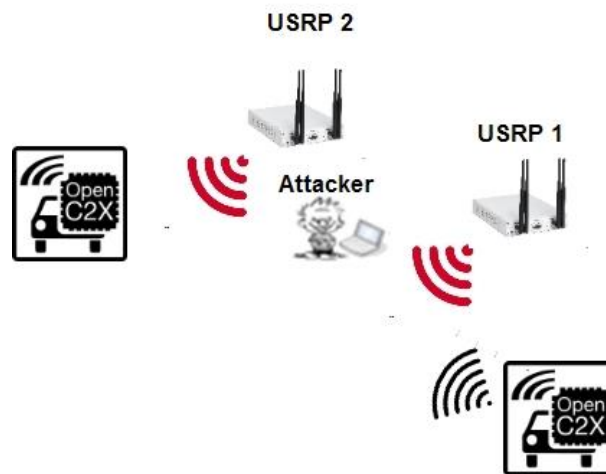


Figure 23: The second test scenario for the jamming attack on ITS-G5

We considered two test scenarios. The first one, illustrated in Figure 22, consists of a OpenC2X equipment sending messages to a second OpenC2X equipment, and USRP equipment controlled by an attacker performing a jamming attack. Unlike the first scenario, the second scenario, illustrated in Figure 23 considers two USRP equipment controlled by the attacker instead of one. We have carried out several experiments. In each experiment, the sender OpenC2X equipment sends 100 messages to the receiving OpenC2X equipment. The power of jamming source (s) is (are) varied by changing the gain value of the USRP(s) equipment on GnuRadio software. The sampling rate of the jamming source (s) is 5MHz. Each experiment with the same configuration is repeated several times. The average of Packet Delivery Ratio (PDR) values obtained in the experiment instances was taken as the result of this experiment. Table 4 defines the test procedure for the two scenarios.

Name	Jamming attack test	
Preconditions:	<ul style="list-style-type: none"> OpenC2X equipment are able to communicate between them. USRP(s) is(are) able to generate jamming signals in the 5.9 GHz frequency band. 	
Test step	Description	Success criterion
1.	<ul style="list-style-type: none"> OpenC2X equipment are communicating between them. The distance between OpenC2X equipment is relatively short. The USRP(s) equipment is off. 	Messages are delivered to the receiver.
2.	<ul style="list-style-type: none"> The USRP(s) equipment is(are) switched on. USRP(s) equipment generate(s) a strong jamming signal 	Messages could not be delivered to receivers.
3.	<ul style="list-style-type: none"> Fix the distance between OpenC2X equipment Gradually decreases the 	Some messages could be delivered to receivers.

	gain of jamming signals generated by the USRP(s).	
4.	<ul style="list-style-type: none"> Fix the gain of jamming signals. Gradually increases the distance between the OpenC2X equipment. 	Less messages could be delivered to receivers.
Success criteria	<ul style="list-style-type: none"> The delivery ratio is equal (or close) to 0 in step 2 The delivery ratio increases with the decrease of the gain of jamming in step 3. The delivery ratio decreases with the increase of distance between the equipment in step 4 The delivery ratio in step 3 is greater than the delivery ratio in step 4 (considering the same gain of jamming signal) 	

Table 4: Test procedure of jamming attack on ITS-G5 using OpenC2X

2.3.1.3 Results and conclusions

Impact of one source of jamming

Figure 24 and Figure 25 show the results of scenario 1, which considers one source of jamming. Figure 24 shows the PDR variation to the power of the jamming source in terms of gain (dB), and under different distances between OpenC2X equipment ranging from 1 meter to 5 meters. The results show that the jamming source starts to interfere with the communication between OpenC2X equipment when the gain at the jamming source is set to 75 dB. At the maximum gain (89 dB) the jamming source was able to completely jam the communication between the equipment. At 89 dB, we noticed that the PDR is 0 if the distance between the equipment is greater or equal to 4 meters. Figure 25 evaluates the influence of the distance between the equipment on the jamming attack. The gain of the attacker was fixed to 80 dB, whilst the distance between the equipment varied from 1m to 5m. The result shows that there is a direct and proportional relation between the position of the equipment (specifically, the distance between) and the impact of the source's jamming.

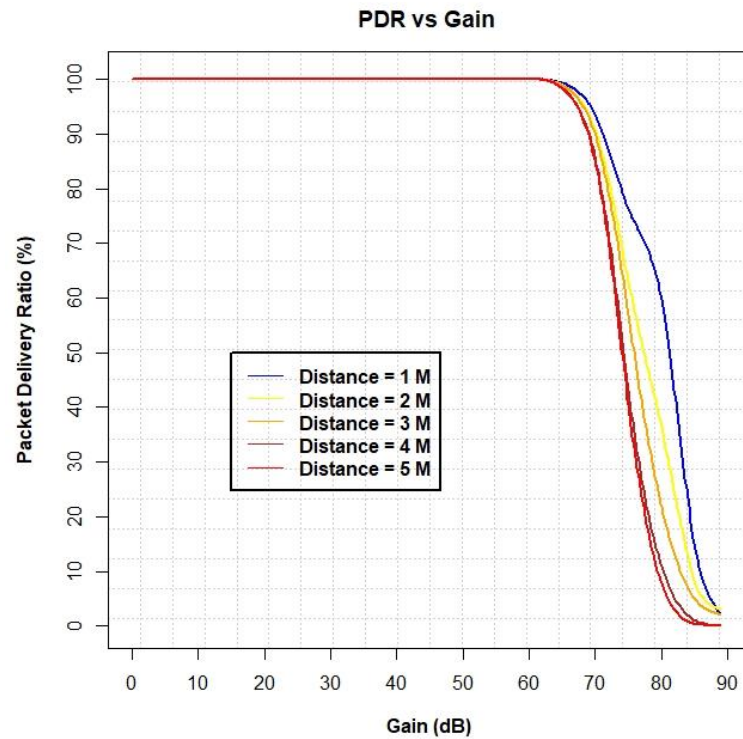


Figure 24: The PDR versus the attacker gain considering different distances between the OpenC2X equipment

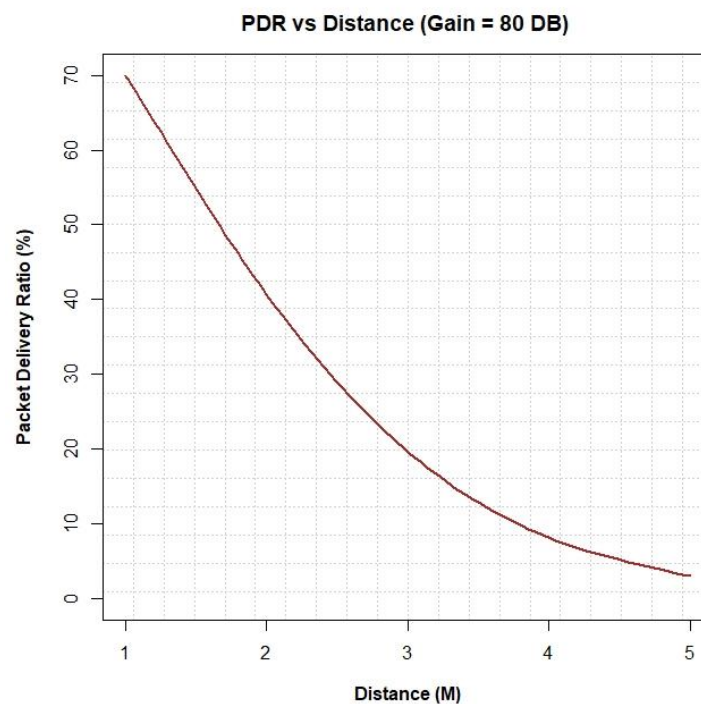


Figure 25: The PDR versus the distance between OpenC2X equipment (Jamming source gain =80 dB)

Impact of two sources of jamming

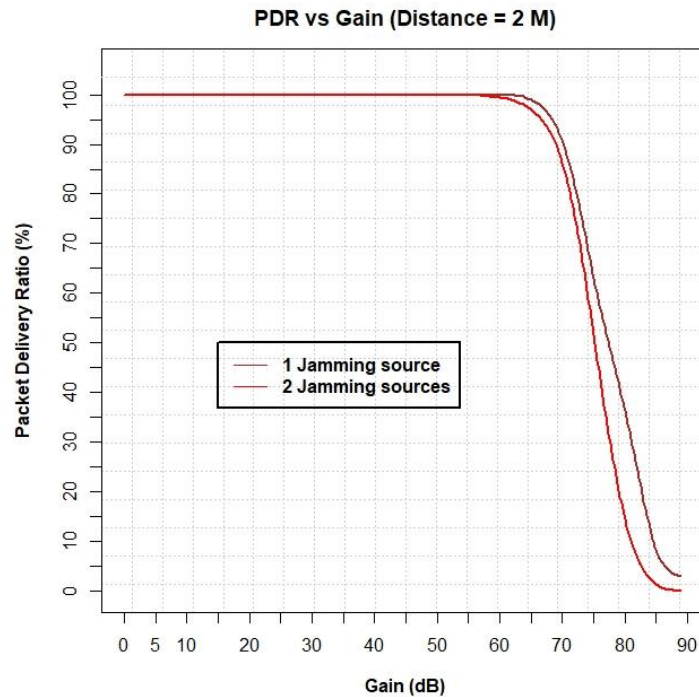


Figure 26: Comparison between one source of jamming and two sources of jamming scenarios (distance between the equipment = 2m)

Figure 26 compares the PDR values between one-source of jamming and two-sources of jamming scenarios. The distance between the two OpenC2X equipment was set to 2 meters. In scenario 2, the power (the gain) of the USRPs equipment was varied at the same time. As expected, the impact of two sources of jamming on the PDR values is more significant than one source of jamming. However, we observe that the difference in the PDR values between the two scenarios is small. To investigate this point further, we assessed the impact of each jamming source separately in scenario 2. Therefore, we fixed the transmission gain of the jamming source **USRP1** to 75 dB and varied the power of the jamming source **USRP2**. Figure 27 shows the impact of the power of **USRP2** in this experiment. As we can see, when the attack power of **USRP2** is weak, the observed PDR is approximately 90%. However, the real influence of **USRP2** can be observed when its gain is equal or greater to 70 dB. Indeed, the PDR is 0 when the transmission gain of **USRP2** achieves its maximum value (89 dB). In the second experiment, we have fixed the transmission gain of the jamming source **USRP2** to 75 dB and varied the gain of the jamming source at the sender side (**USRP1**). Figure 28 shows the impact of the power of **USRP1** in this experiment. Compared to the first experiment, we observe that when the power of **USRP1** is weak, the PDR is around 59%. We also observe that the PDR values don't change a lot when the gain is varied. Indeed, we still have around 43% of PDR even though the gain of **USRP1** is set to its maximum value (89 dB). Thus, the nearest jamming source to the receiver (**USRP2**) had more impact than the jamming source (**USRP1**). This is because the closer to the receiver the jamming source is, the more powerful the jamming is.

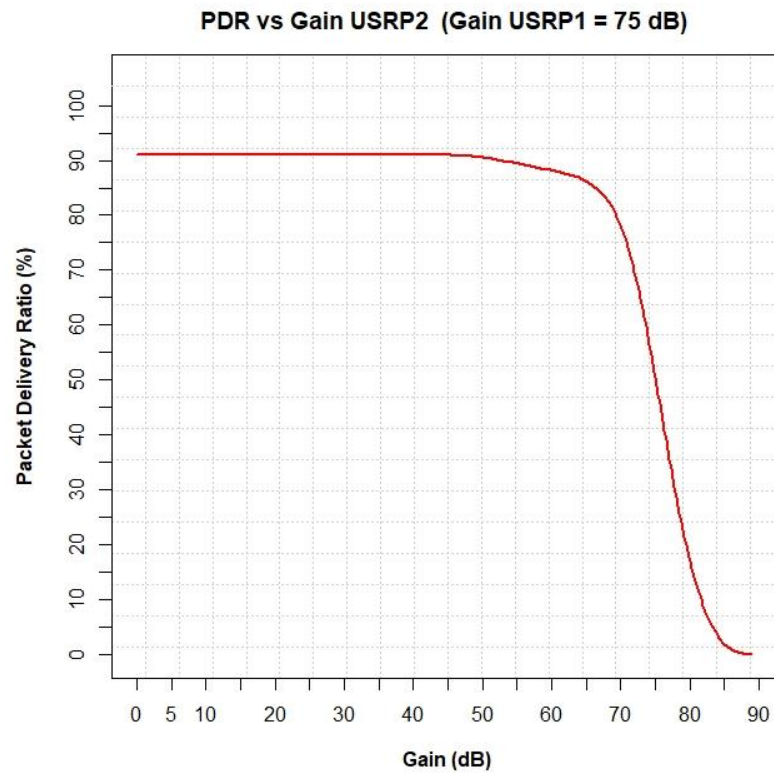


Figure 27: The impact of USRP2 jamming source in the second scenario

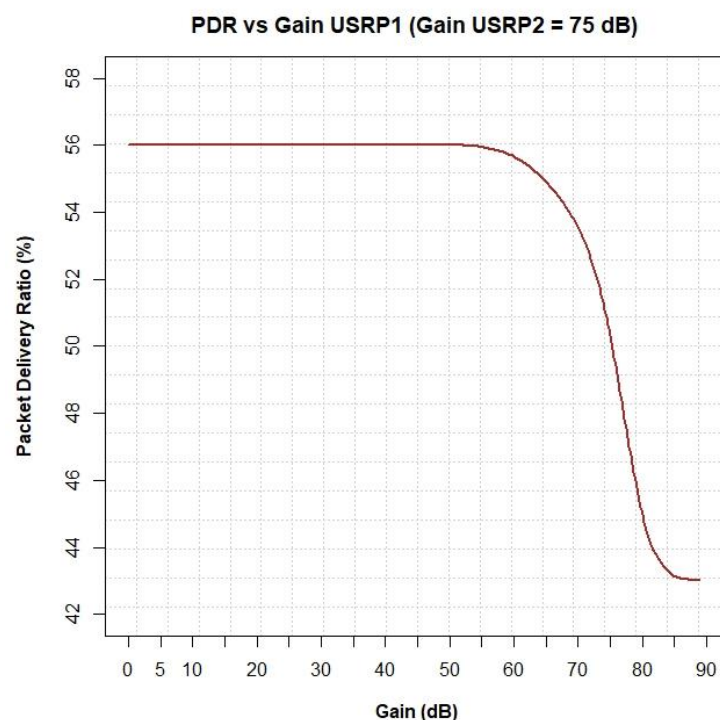


Figure 28: The impact of USRP1 jamming source in the second scenario

To summarize, our experiments have achieved the success criteria defined in Table 4. They also gave some insights on the impact of the distance between the communicating ITS-G5 enabled equipment and the placement of the jamming source on the severity of the jamming attack on ITS-G5. The results show that the larger the distance between the ITS-G5 devices, the higher the jamming efficiency. It also shows the impact of different transmission gain values of the jamming sources(s),

considering its/their distance to the receiver, on the communications between the OpenC2X equipment.

2.3.2 Misbehaviour detection system tests

This section describes the misbehaviour detection system tests carried out at the University of Luxembourg.

2.3.2.1 Objectives

In these in-lab experiments, we have performed tests on a misbehaviour detection system already developed in the scope of 5G-DRIVE Task 5.4. The objectives of these tests are (i) to evaluate the impact of radio interferences on the accuracy of MDS to detect grey hole attacks, and (ii) to use the results of the experiments for enhancing the resilience of the developed MDS by taking the radio interferences into the account.

2.3.2.2 Experimental setup

Figure 29 shows the experimental setup used to carry out these experiments, which consists of the following hardware and software tools:

- **2 x OpenC2X equipment:** As shown in Figure 29, the first OpenC2X equipment **(1)** is considered as a Watchdog. Depending on the scenario the second OpenC2X equipment **(2)** can be considered either honest or attacker. In our scenarios, we have assumed that the second OpenC2X equipment **(2)** received 30 messages that need to be forwarded to another OpenC2X equipment. The first equipment (the watchdog) is monitoring the second OpenC2X equipment **(2)** to detect the grey hole attack.
- **1 x USRP B205mini-i:** marked in Figure 29 with the number (3), it is used to generate interference signals. The USRP is connected to the PC.
- **1 x Laptop:** is used to produce and send the interference signal using GnuRadio. It is also connected to the first OpenC2X via Ethernet cable to collect the statistics about the received packets and the Signal-to-Noise Ratio (SNR) values.

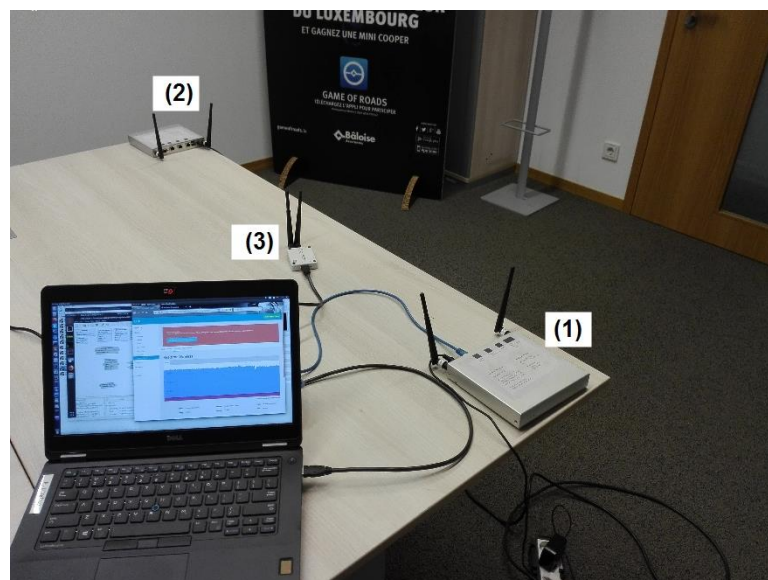


Figure 29: Laboratory experiments on the accuracy of the misbehaviour detect system

We have considered three scenarios for these experiments:

- In the first scenario, we considered that the equipment (2) is controlled by an attacker and the equipment (1) is the watchdog that monitors the behaviour of the equipment (2) to

calculate its trust level using Equation 1. In this scenario (Figure 30), we have considered three message dropping ratios: 10%, 20%, and 30%. The objective of this experiment to test the ability of the proposed MDS to detect the grey hole attack under a non-interference environment.



Figure 30: Scenario 1 of misbehaviour detection system tests

- The second scenario aims to test the ability of our proposed MDS to detect grey hole attacks under radio interferences. The results of this test were used to improve the detection capabilities of the proposed MDS. In this scenario (Figure 31), we use USRP equipment (3) to generate different levels of interferences. In the first case of this scenario, honest equipment (2) is sending messages while watchdog equipment (1) equipped with the MDS to detect the grey hole attacks under radio interferences. The second case is similar to the first scenario (Figure 30) but under radio interferences. In this case we used the equipment (2) controlled by the attacker with different message dropping ratios (10%, 20%, and 30%).

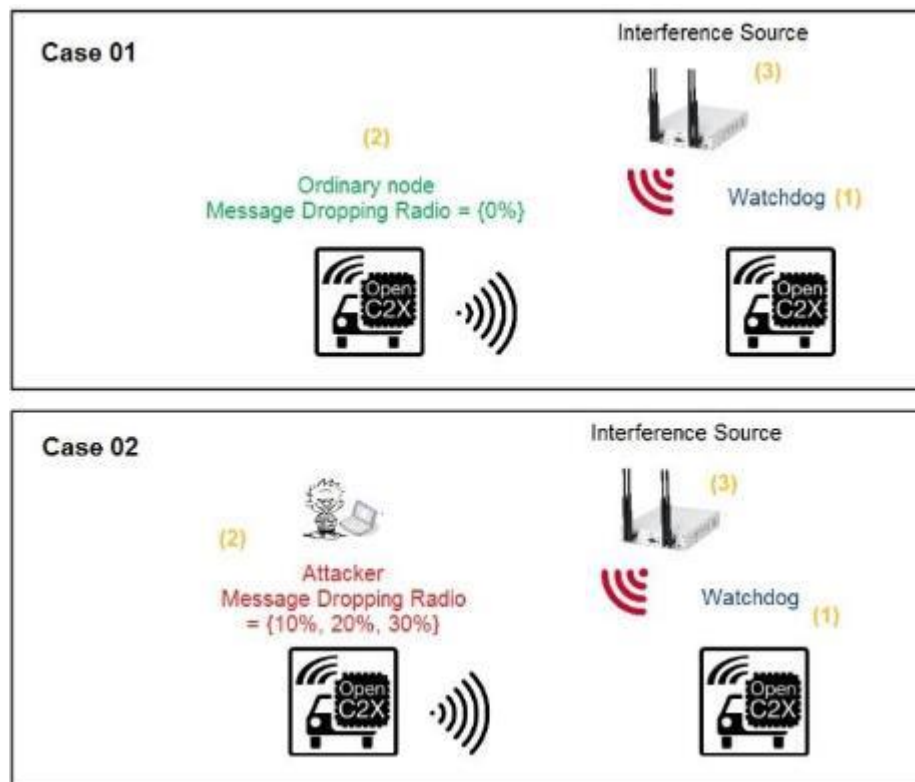


Figure 31: Scenario 2 of misbehaviour detection system tests

- The third scenario:** based on the test results of scenario 2, we have carried out some improvements on the proposed MDS. Thus, the goal of this scenario is to assess the impact of these improvements on the detection capabilities of our MDS. This scenario (Figure 32) consists of four cases. The first two cases are to test if the improved MDS can still accurately detect the attack in the non-interference environment. Cases 3 and 4 are similar to the ones considered in scenario 2. The procedure of these tests is defined in Table 5:

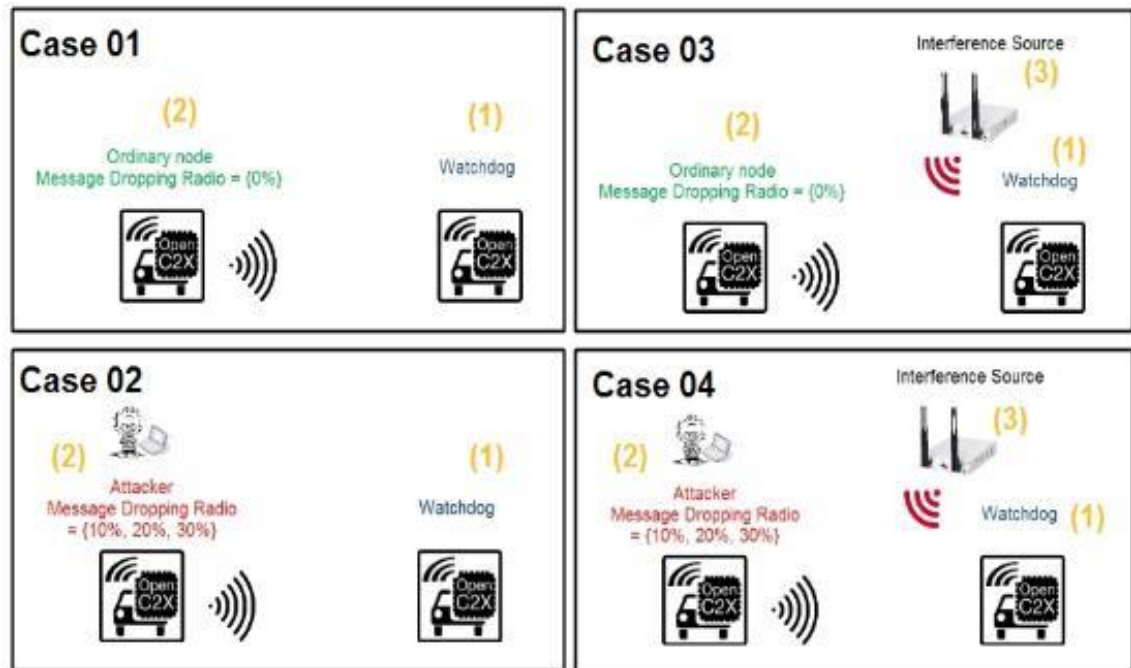


Figure 32: Scenario 3 of misbehaviour detection system tests

Name	Trust-based solutions reliability	
Preconditions:	OpenC2X equipment are able to send/receive messages. MDS is implemented in the equipment (1). USRP is able to generate radio interferences in the 5.9 GHz frequency band.	
Test step	Description	Success criterion
1.	The USRP equipment is off. OpenC2X equipment are sending messages	Messages are delivered to receivers.
2.	Case 1: (1) calculates the direct-trust values of (2). Case 2: (1) calculates the direct-trust values of (2).	Case 1: (2) is not detected as an attacker. Case 2: (2) is detected as an attacker with an accurate estimation of messages dropping ratio.
3.	The USRP equipment is switched on. OpenC2X equipment are sending messages	Messages are delivered to receivers.
4.	Case 3: (1) calculates the direct-trust values of (2). Case 4: (1) calculates the direct-trust values of (2).	Case 4: (2) is not detected as an attacker. Case 3: (2) is detected as an attacker with an accurate estimation of messages dropping ratio.
Success criteria	100% detection rate and no false positive in steps 2 and 4 The dropping ratio is accurately detected in steps 2 and 4	

Table 5: Misbehaviour detection system test procedure

2.3.2.3 Results and conclusions

Before presenting the experimental results, we present in Figure 33 expected values of direct trust calculated analytically using Equation 1. In our experiments, we have considered that the sensitivity of grey hole attack $\gamma = 0.5$. Figure 33 shows expected trust values versus the messages dropping ratio. Specifically, the Figure highlights the expected directed trust values for the 10%, 20%, and 30% dropping ratios used in our experiments.

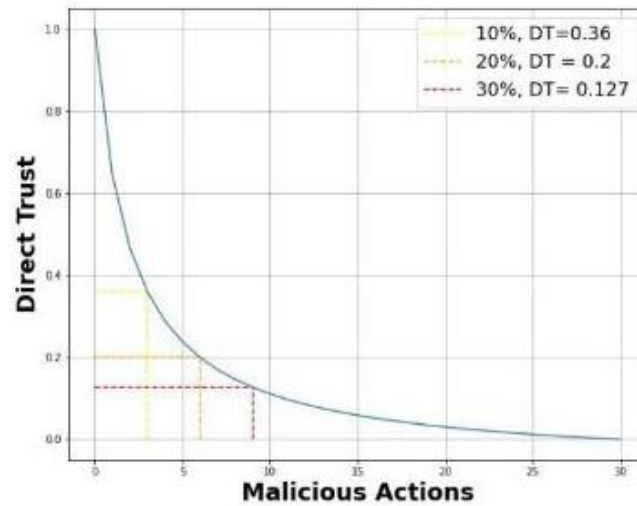


Figure 33: Direct Trust calculated analytically

Scenario 1

Figure 34 shows direct trust values for different message dropping ratios obtained from the experiment of scenario 1. The obtained results show that under no-interference the proposed MDS can accurately detect the grey hole attack. From the obtained trust value, the proposed MDS can also detect the dropping rate of the attacker.

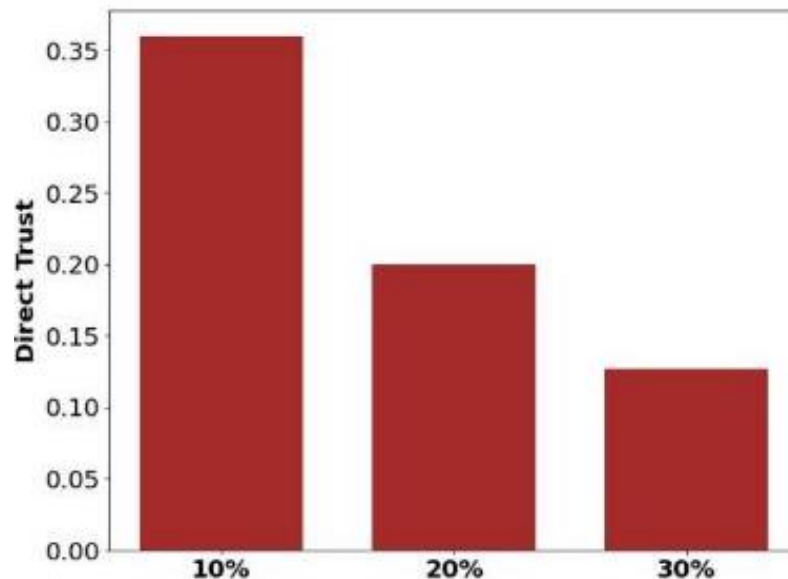


Figure 34: Direct trust values for the first scenario

Scenario 2

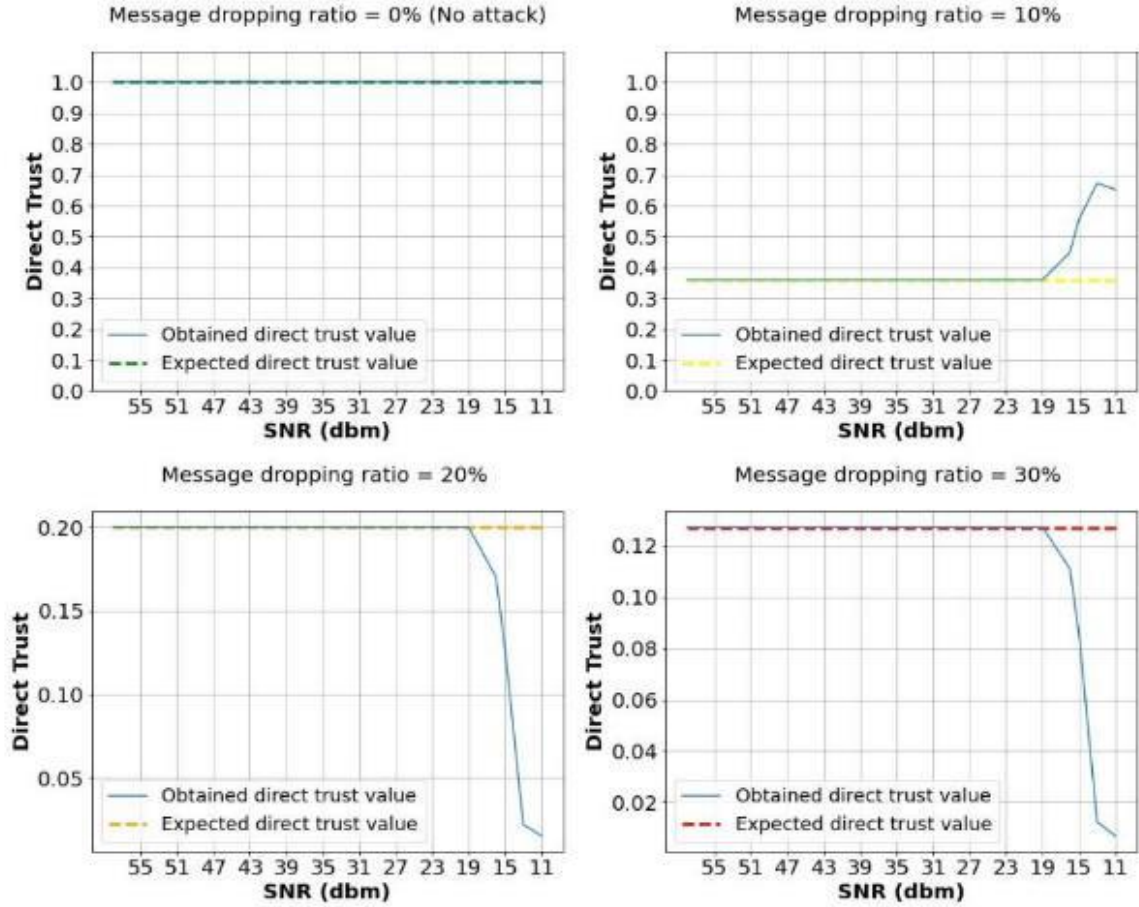


Figure 35: Direct trust values for the first scenario 2

Figure 35 shows the direct trust values obtained for scenario 2 under different levels of radio interferences quantified using the SNR as a metric. The results show that under SNR value = 19 dBm, the obtained direct value is below the expected trust value. As a result, for case 1 (message dropping ratio = 0%), the ordinary equipment is mistakenly considered as an attacker, which increases the false-positive ratio. In addition, for case 2 (message dropping ratio = 10%, 20%, and 30%), the direct trust values don't accurately reflect the (real) message dropping ratio of the attacker. The reason for these results is that Equation 1 used by the proposed MDS (the watchdog) cannot distinguish between the action of dropping a data packet and the packet loss due to the radio interference. To take the interference into the account, we have modified Equation 1 to consider the interferences by adding the packet loss ratio (ρ), which should be adjusted as a function of interference level (SNR). The modified formula is given as follows:

$$DT_v = \frac{A_v * (1-\rho) - A_v^m}{A_v} * \frac{1}{\gamma * (A_v^m - (A_v * \rho)) + 1}$$

Equation 2

To calculate the different values of ρ corresponding to different SNR values, we have considered honest equipment sending its messages under different levels of radio interference. We have then calculated the number of packet loss messages as a function of the SNR values. Figure 36 shows the packet loss ratio as a function of SNR values. As we can see, below SNR= 19 dBm, the packet loss increases. We noticed that no message is received if the SNR is below 11dbm.

Figure 36 shows the direct trust values obtained for **scenario 3** under different levels of radio interferences quantified using SNR. In this scenario, the trust values are calculated using Equation 2. The results show the MDS was able to distinguish between the honest vehicles and attackers under

non-interference and interference conditions. In addition, the proposed MDS can detect direct trust as analytically expected. The reason for this is that using Equation 2 the MDS can adapt the calculation of the direct trust according to the packet loss that occurs in low SNR values.

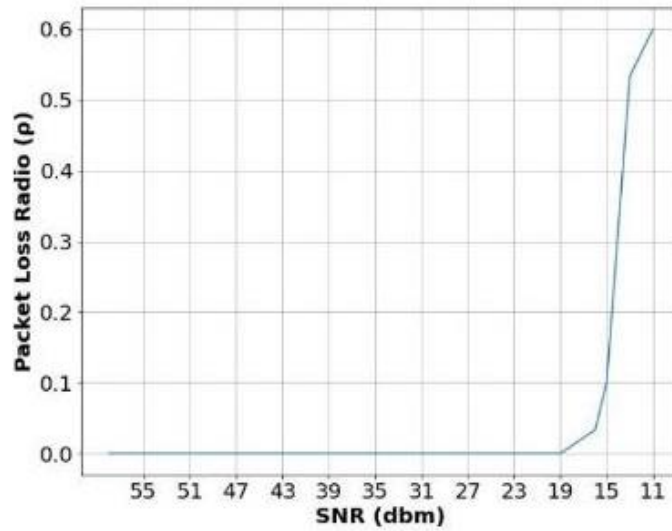


Figure 36: Packet loss ratio vs. SNR

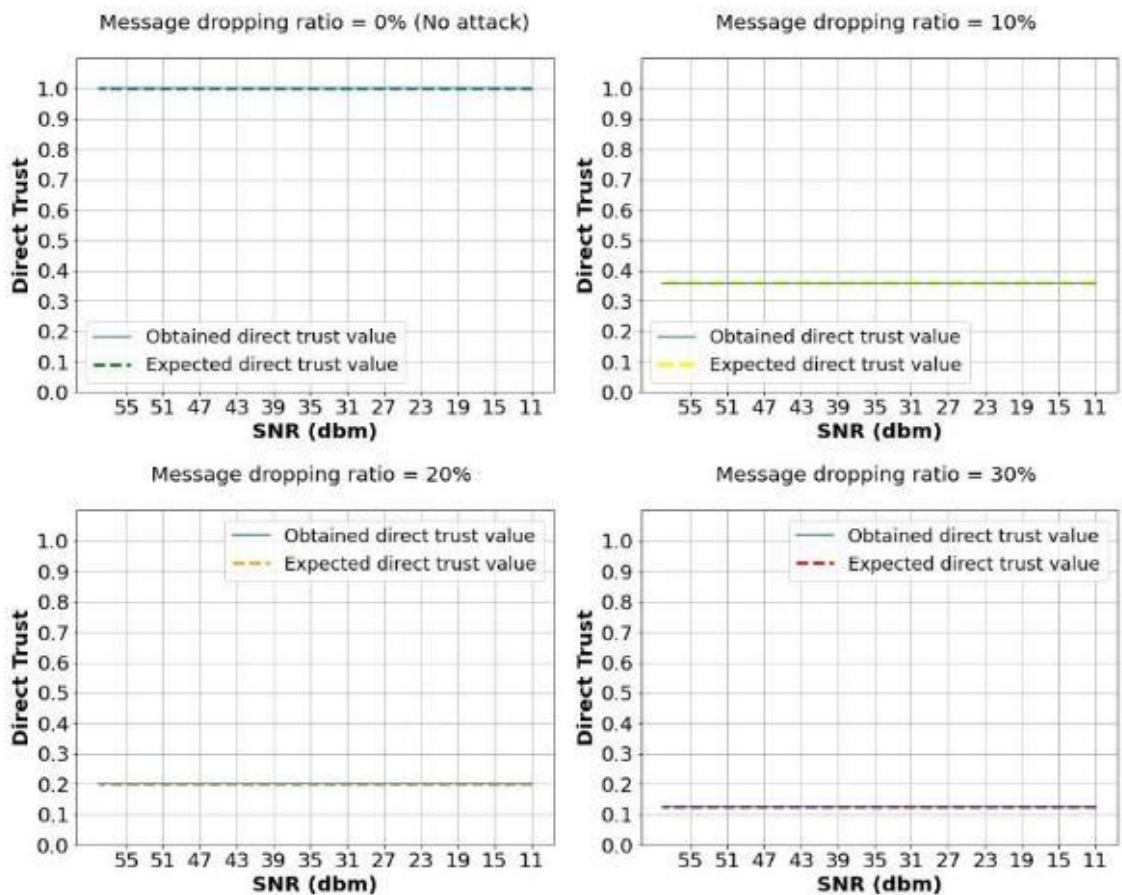


Figure 37: Direct trust values for scenario 3

To summarize, these results demonstrated that our in-lab experiments have improved the resilience of our developed MDS. Indeed, using Equation 2 to adapt to radio interference, our MDS satisfies the success criteria defined in Table 5.

3 Joint EU-China V2X trial framework

This section will introduce the joint EU-China V2X trial framework by defining and clarifying the joint EU-China V2X trials, to allow the feasibility and performance of C-V2X to be evaluated, and a parallel comparison to be obtained.

This section analyses the background, identifies the objectives, and propose the harmonised methodology of the joint EU-China trials. Based on these discussions, the joint trial harmonised plan is drafted collaboratively on joint V2X use cases, trial specifications and unified assessment methodology, which leads to performing the joint EU-China V2X trial in Europe and in China's trial sites and collecting comparable measurement results by adopting the same assessment approaches.

3.1 Joint EU-China trials introduction

At 5G-DRIVE project kick-off (September 2018), 5G-DRIVE and its twinning project: 5G Large-scale trial project (led by China Mobile) have envisioned collaboration on Cellular Vehicle to everything (C-V2X) joint V2X trial in China and in Europe. To clear a path for the joint EU-China trials, a Collaboration Agreement between these twin projects was signed in Nov 2018. To strengthen and enhance the synergies between the trials, the two projects initially agreed on a common timeline for the cooperation from November 2018 to June 2020 considering practicality and effectivity. Due to the COVID-19 crisis, a request for timeline extension to June 2021 was done by the 5G-DRIVE project to ensure the fulfilment of all the project goals. The request was agreed with the full support of the 5G Large-scale trial project V2X team, although the 5G Large-scale trial project was then officially finished.

Already recognized by the development of mobile communication, it is strategically important to harmonize the technology evolution path in an early phase. There are two technical evolution paths for short-range V2X technologies: LTE-V2X (direct communication mode of C-V2X) and IEEE 802.11p based ITS-G5. Europe and US have adopted both C-V2X and ITS-G5, while China selects C-V2X from the beginning, which includes LTE-V2X (currently in industry development stage in China) and NR-V2X (strategy and research stage). Work Package 4 (WP4) of 5G-DRIVE aims to develop and perform C-V2X trials under the collaboration of joint EU-China trials, to test the feasibility and performance of C-V2X, to bridge V2X trial activities based on C-V2X state-of-the-play in China and in Europe, and to harmonize the technology convergence in Europe.

3.2 V2X trials background and objectives

China

The 5G Large-scale trial project in China is funded in the Ministry of Industry and Information Technology (MIIT)⁶ of the Chinese government and is vested in National Major Project program. The project consists of eight partners, with China Mobile as the leader and seven participants coming from network vendors, industry and research institutes and trial sites providers, such as Huawei, Beijing University of Posts and Telecommunications (BUPT), Ericsson, Datang, Shanghai Automobile City etc. As the name suggests, the scope of the project is large-scale covering five cities and more than 100 trial sites per city.

⁶ In China, three ministries have defined the V2X test specification. The V2X development is regulated by the Ministry of Industry and Information Technology (MIIT), Ministry of Public Security (MPS), and Ministry of Transport (MOT). The MIIT specifies the spectrum for V2V and V2I operation and coordinates the C-V2X trial activities in China. The MPS takes charge of the standard revision on traffic light and regulations on traffic information access. The MOT is responsible for regulating the road infrastructure for V2X services.

C-V2X trials in 5G Large-scale trial are conducted on LTE-V2X to complement the current industry development stage. So far, the LTE-V2X trials have been done in Wuxi, Shanghai, and other pilot areas. The trials deploy multiple V2X services on large-scale basis. The definition of these V2X services is mostly comparable to the Day 1 C-ITS⁷ services defined in Europe. Some of these V2X services (comparable to Day 1.5 services in Europe), such as VRU protection have also been tested. The C-V2X trials were concluded in end of December 2020.

Europe

The 5G-DRIVE project in Europe is a 34-month (September 2018 – June 2021) Research and Innovation Action project, funded under the Horizon 2020 Framework programme by European Commission⁷. There are seventeen partners from ten European countries (Germany, Finland, Belgium, Italy, Switzerland, Poland, Greece, Portugal, United Kingdom and Luxembourg).

One of the main objectives of 5G-DRIVE WP4 is to develop and trial V2X services at pre-commercial testbeds. To this end, V2X communication was set up using automated vehicles and open-road intersections at these trial sites. Keeping in mind the different characteristics of the V2X services definition in China and in Europe, WP4 plans to perform two use cases on a single intersection each of the two trial sites (in Finland and in Italy), respective to the large scale (multiple intersections) characteristic of 5G Large-scale trial in China,

Based on above V2X trials descriptions in China and in Europe, both 5G-DRIVE V2X and 5G Large-scale V2X have defined and summarized the followings objectives for the joint EU-China V2X trial:

- Objective 1: Strengthen collaboration of the current V2X developments in China and in Europe through joint trials, aiming to create a harmonised joint trial methodology.
- Objective 2: Bridge the current differences in V2X developments in China and in Europe through comparison of V2X use cases and technical details such as system architectures, communication requirements and specifications, and benchmarking KPIs, to facilitate the cooperation and interoperability between the future V2X development in China and in Europe.

To achieve these objectives, a joint trial project timeline has been coordinated among partners of 5G Large-scale trial and 5G-DRIVE projects, see Figure 38. The light blue block timeline (above) shows the 5G-DRIVE project timeline, and the dark blue block timeline (below) shows the 5G Large-scale trial project timeline. Milestone 7 and Milestone 8 indicate the beginning of joint trial phase I and Phase II. The black curly bracketed period shows the coordinated time interval when the collaboration work between both projects intensifies to reach the goal of Milestone 7 and Milestone 8 completion (red diamond).

Both projects have made project plans and progress expectations at the beginning of each project. On top of the trial plans from each side, joint EU-China V2X trial planned to collaborate on a physical joint trial and to demonstrate V2X use case scenarios together in China's trial sites. Regarding the finalization dates for each project, there are 6-month project time-frame discrepancy between 5G-DRIVE (34-month in timeline) and 5G Large-scale trial (30-month in timeline)⁸. To gain advantage on collaboration time and achieve this goal most effectively, the physical joint V2X trial was planned to

⁷ In Europe, the V2X development is driven by European Commission under the Cooperative Intelligent Transport Systems (C-ITS) framework. On the policy and regulatory level, the Commission coordinates the V2X development in different member states of the European Union. In November 2016, the European Commission approved the C-ITS strategy for Europe Union. It provides the legal framework to facilitate the convergence of investments and regulatory frameworks across the EU.

⁸ The 5G Large-scale trial project in China started in June 2018 (3-month earlier the 5G-Drive project in EU) and therefore should have ended in June 2020, 9-month earlier than the ending time of the 5G-Drive in EU. Due to the COVID-19 pandemic impact, the 5G Large-scale trial project in China is extended until December 2020 and the 5G-Drive in EU is extended until end June 2021.

happen in China in June 2020 before 5G Large-scale trial project in China reaches the end. But this plan could not be carried out due to COVID-19 and it was adjusted into an online Joint EU-China V2X trial.

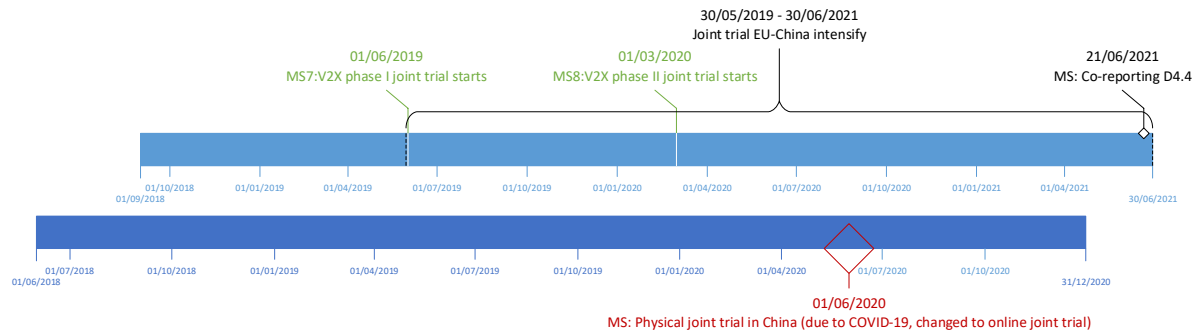


Figure 38: The project timeline of 5G-DRIVE in EU (above) and 5G Large-scale trial in China (below)

3.3 Joint V2X trials harmonised methodology

This section describes the joint V2X trials harmonised methodology from three perspectives: the spectrum comparison in Europe and in China, the short range V2X communication technology path selection, and the campaign schematic of joint V2X trial that fostered the joint trial harmonized plan.

3.3.1 Trial spectrum comparison

In general, the ITS 5.9 GHz spectrum has been issued for ITS usage both for China and Europe. Spectrum allocation is of great importance to the V2X technology spectrum harmonization and business model. Many efforts have been devoted to issues related to the carrier frequency being allocated on 5.9 GHz, especially signal propagation. The usage of 5.9 GHz band for ITS services applications such as short-range vehicle-to-vehicle (V2V) and vehicle-to-infrastructure (V2I) communication is harmonized in many regions of the world. There are several regulatory decisions especially focused on the usage of ITS 5.9 GHz spectrum [12], [13].

Europe

In 2008, the Electronic Communications Committee (ECC) issued a recommendation (ECC/REC/(08)01) and a decision (ECC/DEC/(08)01) regarding intelligent transport systems (ITS) in the 5.9 GHz band. The very same year the European Commission designated a 30 MHz frequency band (5 875-5 905 MHz) for ITS through Commission Decision 2008/671/EC for safety related ITS applications. In addition, the ECC decision (ECC/DEC/(08)01) addresses other ITS uses in the 5 905-5 925 MHz band, where there are usage restrictions which may limit usability in the near future. Vehicle devices are licence-exempt because of safety aspects, whilst licensing for roadside devices is defined at national level.

On 7 October 2020, the European Commission published Commission Implementing Decision (EU) 2020/1426 [12], effectively repealing Commission Decision 2008/671/EC. Commission Implementing Decision (EU) 2020/1426 harmonises the conditions for the availability and efficient use of frequency band 5875-5935 MHz for safety-related applications of Intelligent Transport Systems in the European Union. The allocation of the ITS spectrum at the time of writing this deliverable is summarised in Table 6.

Spectrum band	5855 - 5875 MHz	5875 - 5915 MHz	5915 - 5925 MHz	5925 - 5935 MHz
EU	20 MHz	40 MHz	10 MHz	10 MHz
	Allocated to non-safety road ITS applications	Priority for road ITS applications	Priority for urban rail ITS applications	Harmonised for safety-related urban rail ITS applications

Table 6: The ITS 5.9 GHz spectrum allocation in Europe

In May 2018 the EU commission published the strategy for mobility of the future outlining the direction for Connected, Cooperative and Automated Mobility (CCAM). An integrated approach between automation and connectivity in vehicles is considered and by 2020, all new vehicles will be connected to the internet. The ITS Directive 2010/40/EU provides the legal framework for the deployment of Intelligent Transport Systems in the field of road transport and for interfaces with other modes of transport. In July 2019, the Council of the European Union rejected a proposal from the European Commission for an ITS-G5 based connected car standard. The aim is to allow technology neutrality and co-existence of C-ITS technologies (ITS G5 and C-V2X) [14]. The availability of radio spectrum for ITS in Europe is on a technology neutral basis.

China

Tests conducted in various areas of China have already been using the 20 MHz in the 5.9 GHz spectrum. In October 2018, Ministry of Industry and Information Technology (MIIT) allocated the 5905-5925MHz band as the Internet of Vehicles (Intelligent & Connected Vehicle) direct link frequency band which is used in the LTE-V2X/C-V2X based connectivity. Any organization that intends to build and/or use roadside wireless equipment in the 5905-5925MHz frequency band shall apply for a radio frequency license from the national radio regulatory administration. After obtaining the frequency license, the organization that will use the roadside wireless equipment shall apply for a radio station license from the local regions or municipalities' radio regulatory administration. The current 20 MHz allocation is sufficient to support initial use cases, especially safety related ones. As the roll-out of C-V2X in China progresses, additional spectrum needs to be considered.

Table 7 presents the overview of current specific ITS spectrum allocation and in China. In the current allocation of 20 MHz, the lower 10 MHz in the 5905-5915MHz frequency band is used in V2V communications and the upper 10 MHz in the 5915-5925MHz frequency band is used in V2I communications. The trial conditions of the joint EU-China V2X trials in China (see section 3.4.2.2) is an exemplary spectrum usage in the field trials.

Spectrum band	5905 MHz – 5925 MHz	
China	20 MHz	
	Lower 10 MHz V2V communications	Upper 10 MHz V2I communications

Table 7: The ITS 5.9 GHz spectrum allocation in China

3.3.2 V2X technologies paths comparison

In recent years, different regions in the world have intensively conducted V2X trials [15]. There are two V2X technical paths followed by the automotive industry. One is the IEEE 802.11p-based ITS-G5 technology; the other is the 3GPP-based LTE-V2X access layer. Both ITS-G5 and LTE-V2X access layers are ETSI standards defined in EN 302 663 and EN 303 613, respectively.

Different regions show their own preference on the technologies. Chinese industry selects LTE-V2X Uu and PC5 as the large-scale roll-out currently because of China' envision of C-V2X technology with

NR-V2X in the future. The IMT-2020 (5G) promotion group in China is a major platform to promote 5G research, organizing discussions together with China Communication Standards Association (CCSA), China ITS Industry Alliance (C-ITS), China Society of Automotive Engineers (CSAE), China Industry Innovation Alliance for the Intelligent and Connected Vehicles (CAICV), National Technical Committee of Auto Standardization (NTCAS). Market rollout of LTE-V2X is ongoing at the time of this report.

In Europe, the debate is ongoing on how to adopt the technologies, and a technology-neutral approach has been taken. Since the ETSI ITS-G5 based on IEEE 802.11p technology is prior to LTE-V2X technology and it was already present in its market, Europe is presented with coexistence of these two technologies. Considering the life cycle of road infrastructure is normally 30 years, and the life cycle of a car is 10-15 years, the selection the V2X technology will be critical for the future evolution of technologies. For compatibility reasons it is crucial that the various regions cooperate to ensure harmonization of technologies.

From the technology perspective, the situations in the world tend to a common, single global standard: 3GPP radio access layer, see Table 8. The common goal based on the fundamental standard is to increase road traffic safety, traffic efficiency and comfort at user perspective. On top of the 3GPP standard, specifics of different application protocol layers for each region, such as China, Europe, United States etc., is derived. For this, the messages differ slightly in terms of message sizes, message types, and message profiles.

Application	Safety US	Safety EU	Safety China
	BSM	CAM/DENM	BSM
Transport	WSMP	BTP	DSMP
Network		GeoNet	ADLayer
MAC	Packet Data Convergence		
	Radio Link Control		
	Medium Access Control		
PHY	SC-FDMA		
	USA	EU	China

Note: WSMP – Wave Short Message Protocol; ADLayer – Adaptation Layer; DSMP – DSRC Short Message Protocol.

Table 8. A comparison of V2X technology path in different regions from OSI Model perspective

Upon deeper discussion on V2X technology harmonization between both sides, one noticeable difference is the message types and format used in Day 1 safety use cases. This difference directly affects and joint V2X trials plan (see section 3.4). Table 9 presents a comparison on different message types used for Day 1 safety use cases in China and in Europe. Although only relevant messages used in the joint V2X use cases are listed, the differences lay in Application Identity Division of different messages under corresponding use case. In addition, the message format and message profile comparison were made by using a BSM and CAM message as example in Appendix B.

Message Types	China	EU
BSM	V2V basic safety-regular vehicle status	-
BSM	V2V basic safety-regular vehicle incident	-
BSM	V2V basic safety-emergency vehicle status	-

BSM	V2V basic safety- emergency vehicle status incident	-
BSM	V2V basic safety- post-installed vehicle UE	-
DENM		Informing Hazardous event and other information relevant for safety
CAM		Vehicle (OBU) status and Infrastructure (RSU) status

Table 9: A message type comparison of the intersection safety use case in china and in Europe

3.3.3 Joint trial schematic

According to the 5G-DRIVE project organisation, the work of joint EU-China V2X trials is being carried out in Task 4.5 of work package 4. Following the joint V2X trial harmonised methodology in previous section, the joint EU-China V2X trial campaign schematic is conceptualized to mapping and facilitating the activities of joint EU-China V2X trial, see Appendix A.

The schematic begins with the main task: Two projects from Europe and China jointly demonstrate and trial the C-V2X use case scenarios. To start the main task, two milestones have been planned: Milestone 7 - V2X phase I joint trial starts (due month 10 June 2019) and Milestone 8 - V2X phase II joint trial starts (due month 19 March 2020).

The joint EU-China V2X trial is an ambitious plan with multiple layers of complexities, such complexities include use case designing, technical specifications, execution, and collaboration differences. First and foremost, the joint trials schematic identifies these issues and branches out according to the priorities (in terms of technical importance and time urgency) and to the categories of these complications. In terms of priority, two branches are formed as 5G-DRIVE project timeline evolves: before COVID-19 (M1-M16) and on-going COVID-19 (M16 onwards). It is noticeable between M16 (December 2019) and M17 (January 2020) the division in time due to the COVID-19 outbreak in China in January 2020 and the COVID-19 outbreak in EU a month later. Therefore, the strategies of joint trial China-EU have transformed considerably, which guide the joint trial plan to divert from a physical joint trial plan to an online joint trial plan.

Physical joint trial

In the description of work of 5G-DRIVE project, it is explained that WP4 V2X development and trials aims to define the IoV scenarios together with Chinese partners, to jointly trial and demonstrate the 5G-based IoV scenarios, and to ensure interoperability between Chinese and European IoV technology choices. While these objectives are listed in the beginning of the project in 2018, 5G-DRIVE partners and 5G Large-scale trial partners realized gradually through cooperation that these objectives shall be elaborated and shall capture the essence of fast development of V2X. Therefore, the interpretation of these objectives is elaborated in section 3.2.

To recapitulate, objective 1 aims to create a cross-region joint trial harmonised methodology, to consolidate the creation of joint trial schematic and to guide collaboration of the current V2X developments in China and in Europe through joint trials and research activities. Led by the joint EU-China V2X trial framework, objective 2 aims to bridge the current differences in V2X developments in China and in Europe through the following manners: compare V2X use cases and define joint EU-China V2X use cases; design initial trials separately and align technical details such as system architectures, communication requirements, trial specifications, and benchmarking KPIs, in order to facilitate the cooperation of joint EU-China V2X trials and the interoperability between the future V2X development in China and in Europe.

The execution of objective 2 is mapped on the left and in the middle of Appendix A. These two

different approaches were generated and followed from the beginning of collaboration until April 2020 (month 20 of 5G-DRIVE project timeline).

On the left of the schematic, the joint EU-China V2X trial plans to test the interoperability of the C-V2X trial between China and Europe on the physical layer, where LTE-V2X technology based UEs (user equipment) with different chipsets are compared and implemented in the joint trials, to study how they function and communicate with each other upon data packet transmitting and receiving. Since 5G-DRIVE project and 5G Large-scale trial project are using different chipset-based hardware development platforms, the functionalities of these hardware that play major role in the joint EU-China V2X trials shall be tested. In this phase, most of the tests are performed in the laboratory in Europe (conformance tests) and in the laboratory in China (interoperability of equipment from different vendors).

In the middle of the schematic, the joint EU-China V2X trial plans to test the interoperability of the V2X trial between China and Europe on the application and ultimately the system layer. In this case, there are many sub-tasks that need to be performed. With the same starting point of defining the joint EU-China V2X trials use case scenarios, China and Europe partners need to set up their own V2X trials for 5G Large-scale trial and 5G-DRIVE respectively, exchange the binary data of the messages which will be used in the joint trials, decode and re-encode according to the ASN.1 encoding rules and specific encoding scheme of each side. This process shall be then made automatically with a message converter, to convert messages at real-time that are able to be transmitted and received via local LTE-V2X technology based UEs. If the UEs are from both sides which are based on different chipsets, with the expected success of the physical layer interoperability (shown on the left approach), the entire system interoperability can be achieved and demonstrated during the joint EU-China V2X trial.

Aiming for the interoperability across all layers, the joint trials EU-China have been working on extensive preparation for the physical joint EU-China V2X trials in Shanghai/Wuxi in June 2020. The efforts made for the physical trials include sharing resources, such as documents and knowledge of V2X trials at each side, sharing technical details, development progress, periodic results, and analysing up-to-date trial results.

Due to the mismatch of V2X trials planning in timeline (see Figure 38), the work of joint trial EU-China has encountered quite a few challenges. As shown in the 5G-DRIVE Periodic Report RP1-Part-B document [16], the workflow has been spread out through the timeline with intensive collaboration from May 2019 to June 2021.⁹

Online joint trial

Since COVID-19 outbreak in China and in Europe, the joint trial EU-China activities above were greatly affected. On the right of the schematic (see Appendix A), a new approach was needed urgently since the physical form joint EU-China V2X trial was not anymore possible under the circumstances. For Task 4.5 Joint trial and reporting, due to severe consequences induced by COVID-19, it has been under discussion between China and Europe partners as the pandemic progresses. Upon intensive discussion between China and EU partners, we agreed that physical V2X joint trial was not anymore feasible. Therefore, the EU partners proposed a pandemic resilience plan of online version joint trial. We focused on activities that were independent from equipment and trial sites. The joint trial work will then be transferred completely online. The pandemic resilience plan includes transfer all joint trial work to online version; performing iteration for data gathering; exchange results measurements and data analysis; write joint articles, papers, and reports on the topics of joint EU-China V2X trials.

⁹ The delays of C-V2X equipment for EU partners and the COVID-19 situation led to the intensive collaboration from May 2019 to June 2021. COVID-19 was first onset in China where movement restriction and lockdown were approximately 3-month long while later, it was spread across European countries where movement restriction and lockdown are ongoing and continuously extending. The impact and repercussion are hard to estimate but affect physical joint EU-China V2X trials greatly.

The results of online collaboration have generated the co-authoring, co-reviewing of this final deliverable 4.4, multiple publications and events collaboration that are summarized in work package 6.

3.4 Joint trial harmonised plan

Since the start of the joint trial phase I with the Milestone 7, the joint EU-China V2X trial collaboration has been carried out in parallel with other task activities in 5G-DRIVE and in 5G Large-scale trial projects. The collaborative activities started to progress since communication circle of Europe and Chinese partners in these two projects were well established.

As this early stage, we realized the level of complexity of joint EU-China V2X trial. Therefore, we started to design a harmonised methodology to identify the issues of difference and harmonise the trial set-up and specifications, such as test conditions, test procedures and KPIs.

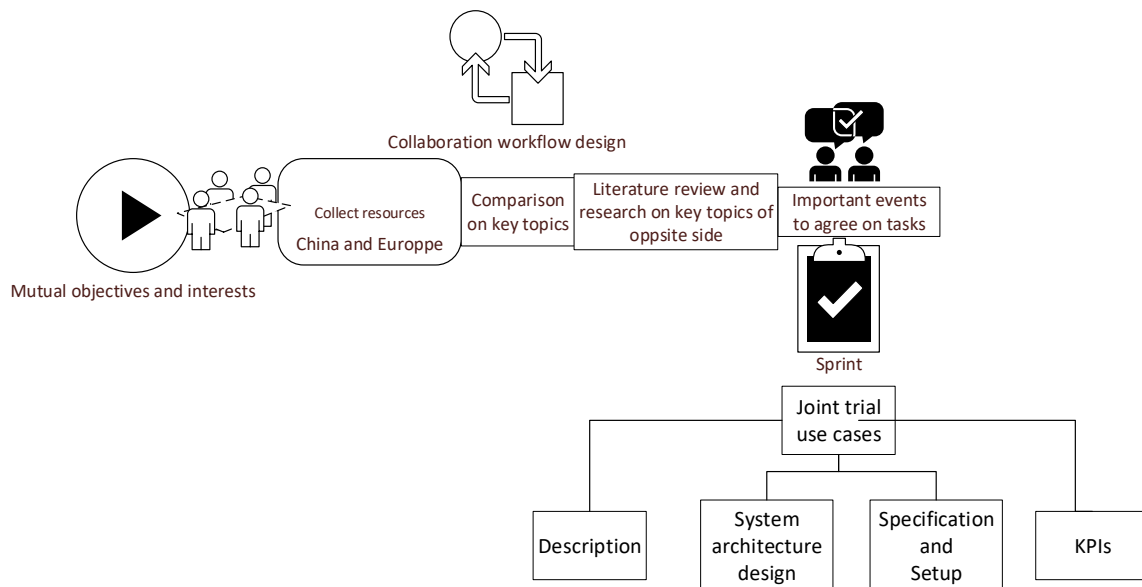


Figure 39: Joint trial harmonised methodology design

The results of the early-stage issue identification show the following similarities and differences between China and Europe in terms of trial methodology:

- 1) LTE-V2X PC5 mode 4 serves the same fundamental communication purpose in the V2X trials in both projects. Therefore, both 5G-DRIVE and 5G Large-scale trial face the same challenges in their V2X trials, to name a few, high security, low latency, and high reliability while the electromagnetic interference is complex in specific trial sites environment.
- 2) 5G Large-scale trial is, as the name suggests, a cross-province, large-scale project for eMBB trials. For C-V2X, the scale of the C-V2X trial is also large, since it covers several areas across 20 square kilometres, including at least 5 intersections and 15 intersections' units.

5G-DRIVE V2X trial is focused on the system and services development of chosen key use cases, located in trial sites mainly in Espoo, Tampere, Finland and Ispra, Italy. Focusing on system, services and application development, these trials are relatively small-scale with 1-2 intersections involved. They cover open-road trial sites of Nokia research centre, Tampere city and the JRC campus.

From the trial set-up perspective, the intersection size of LTE-V2X trials in 5G Large-scale trial and 5G-DRIVE are similar. However, 5G Large-scale trial covers a much bigger magnitude including more intersections and more User Equipment (UEs) and terminal devices.

- 3) The services and scenarios are categorized differently. On the one hand, C-V2X scenarios in 5G Large-scale trial are categorized in V2V (such as Emergency braking warning), V2I (such as traffic light optimization) and V2N (such as traffic information broadcasting). On the other hand, C-ITS in Europe are categorized according to services: Day 1 services, Day 1.5 services and Day 2 services. Nonetheless, 5G Large-scale trial (as well as other C-V2X trials in China) is

also acquainted with the service terms of C-ITS Europe. Therefore, only merely minor cross-category differences need to be clarified.

- 4) The featured joint V2X use cases in both projects are comparable regarding Service Level Requirement (SLR). From this perspective, the joint use cases and trial plans are tailor made to test the validity of the harmonised methodology, and to ensure comparability of GLOSA use case and Intersection Safety use case (collision warning of vehicle to Vehicles, VRU¹⁰ crossing or incident warning).

3.4.1 Joint V2X trials use cases

5G Large-scale trial V2X team and 5G-DRIVE V2X team have been identifying mutual use cases together since the joint EU-China trial starts. Following the joint trial harmonised methodology in section 3.3, first, both 5G-DRIVE and 5G Large-scale trial identify the services and scenarios that are of great importance to reach the goals of their projects. Then, both sides exchange trial description and seek for key use cases according to service priorities, common interests, and operational practicality. In this section, the use case description and harmonised system architecture are explained.


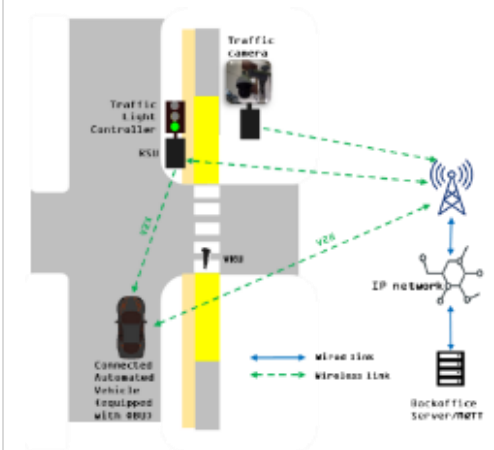
3.4.1.1 Use case description

In this section, the joint trial use cases are described in parallel with equivalent use case details, such as user story steps, background/rationality, and service level requirement of each side. Among the multiple use cases and multiple use cases overlay scenarios of 5G Large-scale trial, two key use cases: use case 1- intersection safety and use case 2 - GLOSA, are acknowledged and designed by both 5G-DRIVE and 5G Large-scale trial projects.

Table 10 presents an overview of use case 1 and 2 on both sides under the following items: general description, trial sites road environment, actors and their roles in the use cases, main event flows during use cases trialling, and the event diagram illustrating the use cases visually (looking from above).

	5G Large-scale trial V2X team	5G-DRIVE V2X team
Use case 1	Joint EU-China V2X trial use case 1	
Intersection Safety	Intersection collision warning	Intelligent intersection with VRU crossing
General description	At an unsignalized intersection that is prone to intersection collision, intersection collision warning is given to avoid vehicles colliding, whose potential conflicted trajectories can cause the collisions.	At a signalized/unsignalized intersection, an intersection perception/detection system (camera, pedestrian pushbutton, etc.) detects the pedestrian. An approaching Connected Automated Vehicle (CAV) is given broadcasted DENM message to prevent potential collision and protect the pedestrian crossing.
Road environment	Semi-Open/Closed intersection at trial sites	Open intersection at trial sites

¹⁰ VRU stands for vulnerable road user. They are “non-motorised road users”, such as pedestrian and cyclists as well as motorcyclists and persons with disabilities or reduced mobility and orientation. This category is described in detail in the technical report of ETSI TR 103 300-1 V2.1.1 (2019-09).

Actors and Roles	Host Vehicle (HV), equipped with OBU (LTE-V2X).	HV approaches intersection, on a conflicted trajectory with RV-1.	Pedestrian (VRU)	VRU is crossing the intersection using the pedestrian walk (zebra line).
	Remote Vehicle 1 (RV-1), equipped with OBU (LTE-V2X).	RV-1 approaches intersection, on a conflicted trajectory with HV.	Traffic camera connected with RSU (LTE-V2X)	Traffic camera detects the walking pedestrian, triggers RSU to broadcast DENM messages.
	Remote Vehicle 2(RV-2)	RV-2 arrives at or is approaching the intersection, creating obscured view to the HV.	CAV, equipped with OBU (LTE-V2X).	CAV approaches the intersection; has an obscured view of the pedestrian; receives DENM messages from intersection RSU.
User story – Main event flows	<div>1. HV approaches intersection, on a conflicted trajectory with RV-1.</div> <div>2. RV-1 approaches intersection, on a conflicted trajectory with HV.</div> <div>3. BSM messages are sent out from the OBU on RV-1 and broadcasted over the air in the vicinity.</div> <div>4. HV receives the BSM and brakes to avoid possible collision.</div>		<div>1. A pedestrian is crossing the intersection using the pedestrian walk (zebra line).</div> <div>2. A CAV approaches the intersection and intended to turn (pass over the zebra line); this vehicle has an obscured view of the pedestrian.</div> <div>3. Traffic camera detects the walking pedestrian, triggers RSU to broadcast DENM messages.</div> <div>4. The CAV receives DENM messages from intersection RSU; this vehicle decelerates to stop and wait for the pedestrian to cross over; it accelerates and keep on driving.</div>	
Event diagram (Bird view illustration)				
Use case 2	Joint EU-China V2X trial use case 2			
GLOSA	GLOSA		GLOSA with individual speed advice	
General description	At a signalized intersection, SPaT messages are sent from the intersection RSU (LTE-V2X) to approaching vehicles (equipped with LTE-V2X OBU) to inform about the intersection traffic signal (coming) status.		At a signalized intersection, SPaT messages are sent from the intersection RSU (LTE-V2X) to approaching CAV (equipped with LTE-V2X OBU) to inform it about the intersection traffic signal (coming) status. An GLOSA application inside the CAV calculates the speed advice and displays it	

			on the in-vehicle display, to prevent the CAV from stopping for red light.	
Road environment	Semi-Open/Closed intersection at trial sites		Open intersection at trial sites	
Actors and Roles	Vehicle(s), equipped with OBUs (LTE-V2X).	Vehicle(s) approach the signalized intersection.	CAV, equipped with OBU (LTE-V2X) and GLOSA application.	<ul style="list-style-type: none"> - CAV approaches the signalized intersection. - OBU inside the CAV gives the real-time position and speed of the CAV. -GLOSA application calculate speed advice and display it on the in-vehicle display
	Traffic light controller (TLC) connected with intersection RSU (LTE-V2X)		Virtual traffic light controller (vTLC), is running on Dynniq's server in the Netherlands.	vTLC publishing SPaT messages via MQTT broker.
			RSU (LTE-V2X), residing inside the MEC system at the intersection	RSU subscribing SPaT messages from MQTT broker; send it to the OBU, then to the GLOSA app.
User story – Main event flows	<ol style="list-style-type: none"> 1. Vehicle(s) approaches a signalized intersection. 2. TLC sends SPaT messages to RSU. 3. RSU broadcasts SPaT to the vehicle(s) via PC5 interface. 4. Vehicle(s) display the traffic light states on in-vehicle display. 		<ol style="list-style-type: none"> 1. Virtual traffic light is running remotely, and publishing SPaT messages via MQTT broker. 2. RSU at trial site intersection is subscribing SPaT messages from the above broker. 3. A CAV is approaching the intersection and it follows the virtual traffic light state without violation (the CAV also strictly follows trial site intersection traffic rule since the intersection is with dense public traffic and unsignalized for all other traffic). 4. RSU sends SPaT to the OBU inside CAV. 5. OBU relays the SPaT to GLOSA application. OBU sends the real-time CAV position and speed to GLOSA application. 6. GLOSA application decodes SPaT to get TTG, calculate speed advice based on TTG and CAV position. 	

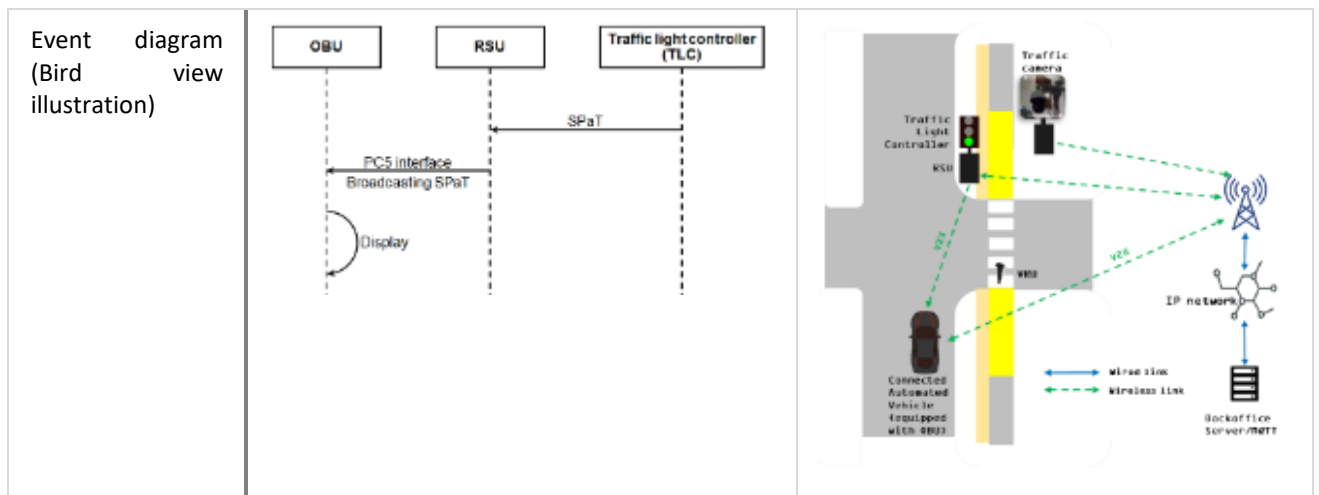


Table 10: Joint V2X trial use cases description overview

3.4.1.2 Harmonised system architecture

This section discusses on the harmonised system architecture. Based on the joint V2X use cases described in Table 10, the system architectures of the two featured joint V2X use cases on both sides are quite similar in principle, thanks to the harmonised methodology (see section 3.3) developed beforehand.

For joint V2X use case 1: intersection safety, there are different elements on the data flow stream. On 5G Large-scale trial side, the BSM messages that contain the vehicle's real-time basic information are sent from vehicle to vehicle (LTE-V2X OBU to LTE-V2X OBU), since multiple vehicles are involved in trials; on 5G-DRIVE side, the DENM messages that contain the warning of camera detected pedestrian crossing zebra lines, are sent from infrastructure to vehicle (LTE-V2X RSU to LTE-V2X OBU). Regardless of different elements in the data flow stream, the joint V2X trials harmonised plans are not affected on each side because the channel and interface of data flow are fundamentally unified on both sides: in the 5.9 GHz and via PC5 interface (LTE-V2X Mode 4).

For joint V2X use case 2: GLOSA, there are variations on two aspects: whether a real-life traffic light controller or a virtual traffic light controller is used; and whether individual speed advice is provided to the vehicle to prevent it from stopping for red lights. Once again, these differences won't affect the harmonised plan. The following system architectures of joint V2X use case 2: GLOSA from each side are shown as example. Figure 40 shows the architecture of the sub-system implemented for the V2X trials in Espoo/Tampere and Figure 41 does it for the trials in Shanghai.

For the Espoo/Tampere trial, the LTE-V2X RSU resides inside the MEC system (The mobile system is in a trailer named "Marsu") on the intersection. Traffic camera and physical traffic light are also on this MEC system. The antenna of the LTE-V2X RSU is on the mast on top of the MEC system. In the GLOSA trial, the physical traffic light is not in use, but a virtual traffic light is running and maintained in the Backoffice in the Netherlands. The virtual traffic light software is also publishing SPaT messages (contains the traffic light data) on a Dynniq server in The Netherlands. The SPaT messages are subscribed by the LTE-RSU via the MQTT interface and sent to the Connected and Automated Vehicle (CAV, with the LTE-OBU). The in-vehicle GLOSA application (shown on in-vehicle display from the in-vehicle view photo in Figure 40) reads the current position/speed and the received SPaT messages from the LTE-OBU in the vehicle. The GLOSA application decodes these traffic data and calculates the speed advice for the CAV, which is displayed to the driver to follow and avoid stopping for red traffic light.

For the Shanghai trial, the architecture of the sub-system implementation is similar, see Figure 41. At a signalized intersection, the LTE-RSU is installed on intersection light pole. The LTE-RSU is connected to the physical traffic light, see purple line ① from LTE-RSU to traffic controller. SPaT messages that contain traffic light information are sent from the traffic controller to the LTE-RSU. Like the previous

architecture description on Espoo/Tampere sites, the SPaT messages are broadcasted to vehicles (equipped with LTE-OBUs) approaching the intersection, see red lines ②. The traffic data are displayed to the drivers in a vehicle fleet.

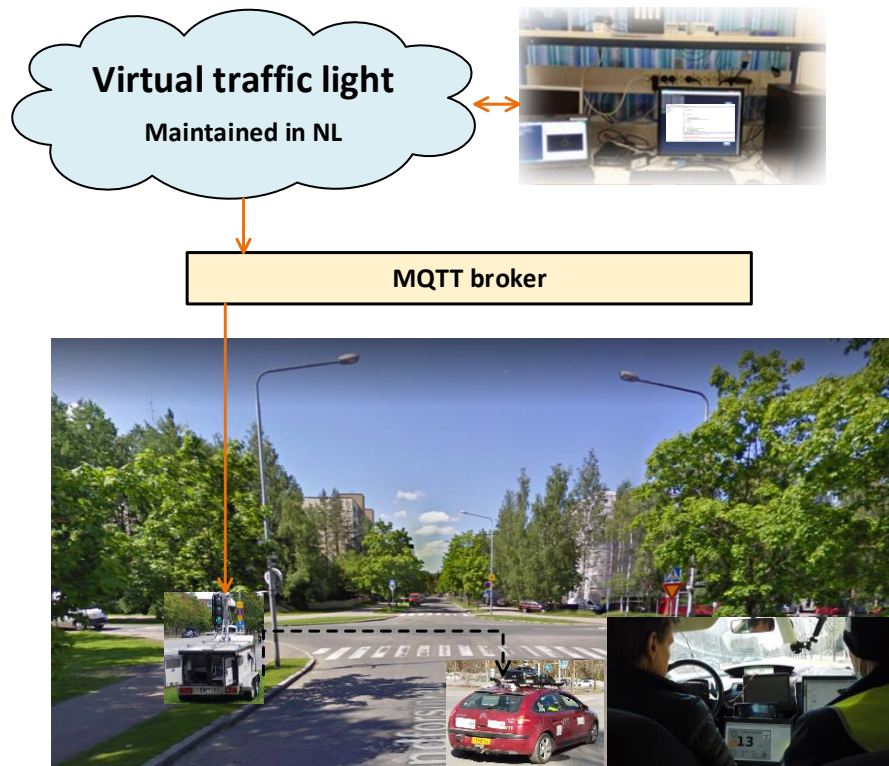


Figure 40: The system architecture of joint V2X use case 2 - GLOSA, 5G-DRIVE V2X team

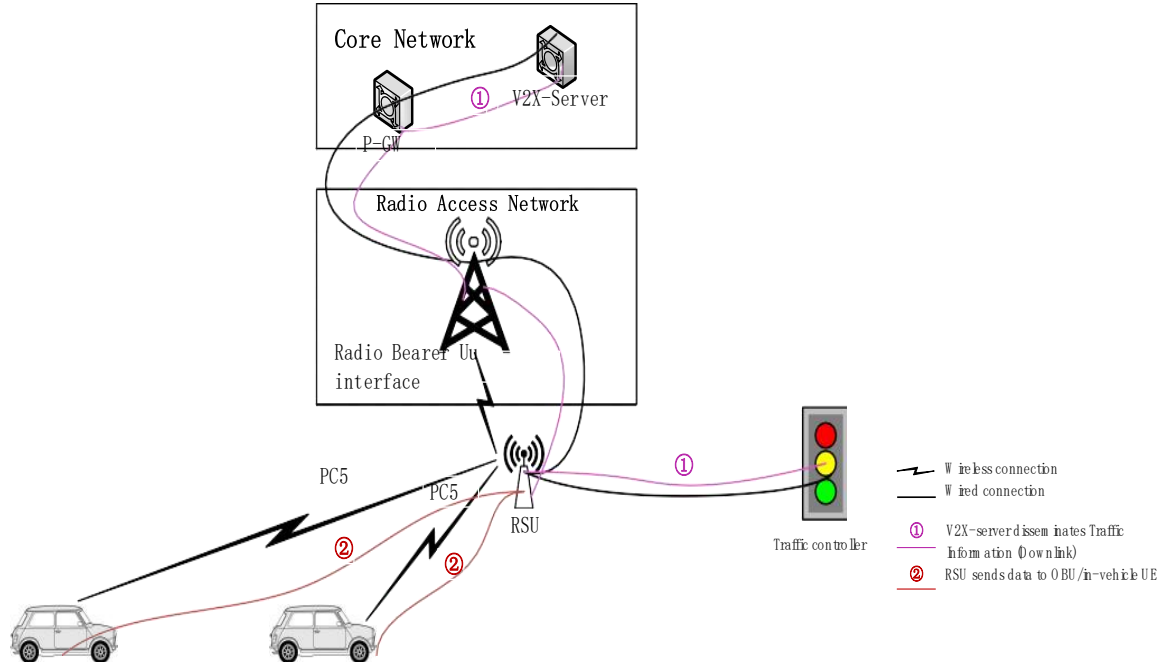


Figure 41: The system architecture of joint V2X use case 2 - GLOSA, 5G Large-scale trial V2X team

3.4.2 Joint V2X trials specification

Guided by the joint trial harmonised methodology, the joint trial specifications including trial setup, trial conditions, and trial procedures are described in this section.

3.4.2.1 Joint V2X trials setup

The joint EU-China V2X trials setup in Europe (Espoo/Tampere) and in China (Shanghai) are described in this section. Since the joint EU-China V2X trials are transferred from face-to-face joint trialling at one site (Shanghai, China) to remote (online streaming) jointly trialling in Europe and in China separately, the joint harmonised framework guides the operation and execution of the joint trial harmonised plan in the aspects of use case definitions, trials specification and finally assessment methodology. This section explains the joint EU-China V2X trials setup in Europe and in China.

In Europe, the two joint EU-China V2X trial use cases: intersection safety and GLOSA use cases, are deployed at Espoo and Tampere sites, Finland. With the use case architecture previously used in the event diagram of Table 10 (originally designed in deliverable D4.2 Joint specification for V2X trials), Figure 42 shows the use case architecture with the components and their setup explained in detail.

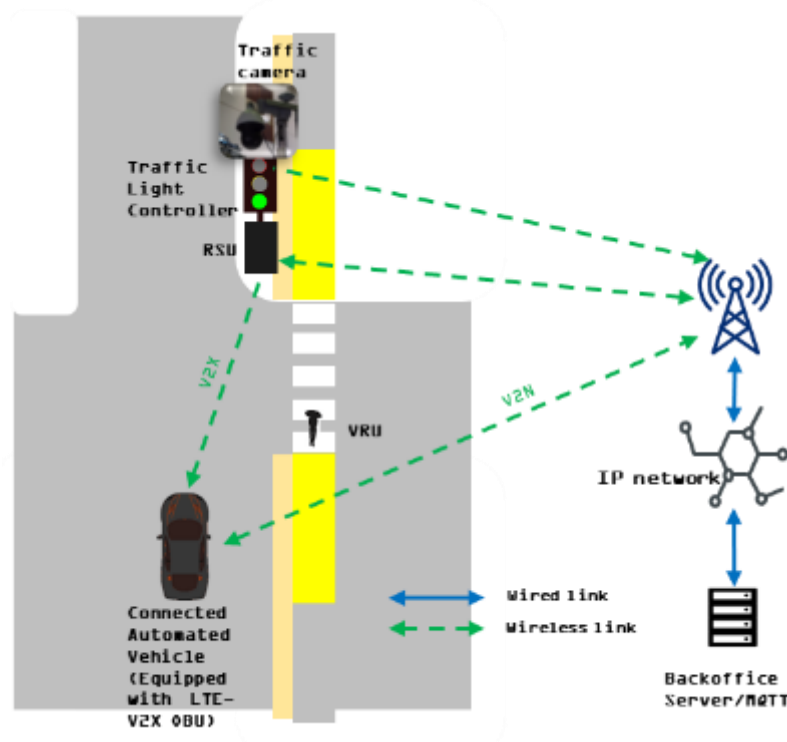


Figure 42: The intersection safety and GLOSA use cases architecture in Espoo/Tampere sites, Finland

The key components and their setups in the two joint EU-China V2X use cases are as follows:

- A **physical and a virtual traffic light** in static control mode to implement the transitions between the “red”, “amber” and “green” states (fixed phases). The traffic light data is only required for the GLOSA use case and the content of the SPaT message must be retrieved from it. The intersection safety (intelligent intersection with VRU crossing) does not require a traffic light, but a traffic camera is mandatory. For the GLOSA use case without speed advice, the physical traffic light is used. For the enhanced GLOSA use case with individual speed advice, a virtual traffic light is used.
- A **virtual traffic light server (MQTT)** in Dynniq data centre running needed supporting services to publish SPaT messages and MAP messages for the intersection in Espoo/Tampere.
- An **LTE-V2X RSU** (build in trailer “Marsu”; antenna is the mast on top of “Marsu”) co-located with the physical traffic light and traffic camera, communicating with the traffic light and traffic camera implementation. Two scenarios (4G-LTE/5G and LTE-V2X PC5 interface) are tested in each use case. The LTE-V2X RSU is used in the scenario of LTE-V2X Sidelink communication by sending SPaT and DENM messages to LTE-V2X OBU. The LTE-V2X RSU used here are deployed with the factory default configurations.

- A **VTT Traffic camera** detecting and tracking VRUs on the intersection.
- A **VTT Backoffice server** in the VTT data centre running all the needed supporting services. It will provide connectivity between the “Marsu” (traffic camera, physical traffic light, local computing units and power) and various supporting services/servers running in the VTT data centre. The intersection safety use case will be used here to illustrate: In the LTE-V2X Sidelink scenario, when a pedestrian is detected on the zebra lines, a Decentralized Environmental Notification Message (DENM) should be broadcasted by the LTE-V2X RSU, and the LTE-V2X OBU equipped test vehicle in communication range will receive these messages. In the 4G-LTE scenario, the VTT RSU Backoffice server geocast these messages to the test vehicle when it is in the vicinity of the intersection.
- One **LTE-V2X OBU** deployed in the test vehicle. The LTE-V2X OBU will send CAM messages to present the position, speed and headings of test vehicle, and it receives and processes the MAP, SPaT, and DENM messages. The LTE-V2X OBU used here are deployed with the factory default configurations.
- A **VTT connected and automated vehicle with on-board sensors**. This vehicle is a VTT research phase automated vehicle. It is equipped with the above LTE-V2X OBU. The LTE-V2X OBU and LTE-V2X RSU are essentially the same LTE-V2X development platforms using the same chipset.

To execute the tests, the following tools will be used:

- **ACME application**. This is default tool that comes with the LTE-V2X Development Platform (OBU/RSU) to interface with LTE-V2X RSU/OBU. It enables sending and receiving of raw application layer byte arrays.
- **Encoding/Decoding software**. The virtual traffic software has the encoder/decoder module to encode and decode SPaT. The messages used for the two joint EU-China V2X use cases are defined using the ASN.1 standard.
- **Virtual traffic light software**. It simulates a static traffic light controller, generates SPaT and MAP messages, and publish these messages on the MQTT server.
- **Message generator**. With the inputs (such as VRU crossing) of cooperative perception system, it generates needed messages for the two joint EU-China V2X use cases, such as CAM, DENM and MAP messages.
- **GLOSA application**. First, it decodes the virtual traffic light information. Second, it retrieves the vehicle GPS location and speed data, and it decodes the SPaT messages to get the time-to-green (remaining green time). Finally, it calculates the individual speed advice for the test vehicle to follow and avoid stopping for red light at the intersection.
- **In-vehicle GUI for GLOSA application**. It shows the virtual traffic light and its status on the in-vehicle display screen. It also shows the speed and distance to the intersection stopline of the test vehicle. Lastly, it shows the speed advice in the middle of the screen for the driver to follow.

In China, the two joint EU-China V2X trial use cases: intersection safety and GLOSA use cases, are deployed at Shanghai sites, China. The tests are performed in the National Intelligent Connected Vehicle, Shanghai, where a semi-open/enclosed test zone is dedicated for V2X trials. Traffic lights are deployed running at each intersection. Roadside units (LTE-V2X RSUs) from different vendors are deployed at the intersection No. 51 (see, red circle in Figure 22).



Figure 43: The test site for automated driving in Shanghai, China

The equipment in the Chinese field trials consists of the following network and onboard unit (OBU) devices (see Figure 44 and Figure 45):

- The LTE network (2.6 GHz)
- 5.9 GHz RSU and OBU
- 5.9 GHz NEBULA OBU

Similar to the trial setup in Europe, it should be pointed out the devices such as OBU and RSU used in the Chinese field trials are deployed with the factory default configurations.

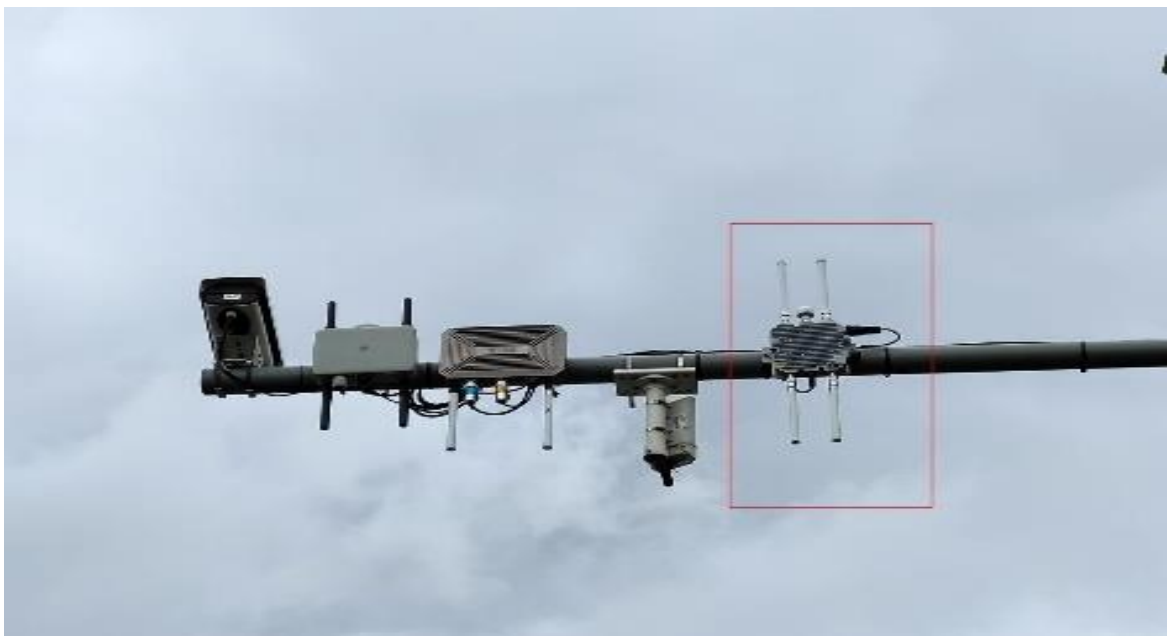


Figure 44: The RSUs from different vendors are deployed on a light pole at the intersection No. 51



Figure 45: The OBU is placed on the top of the test car. The height of the antenna is about 1.5 m

3.4.2.2 Trial conditions

The frequency bands used in 5G Large-scale trial and 5G-DRIVE projects are listed below in Table 11. The joint EU-China V2X trials in Europe were performed mostly with connected and automated vehicles. Each test is executed under two scenarios: 5G communication measurement and LTE-V2X short range communication measurements using LTE-V2X devices. C-V2X devices were not available during the trial implementation phase. Therefore, for the LTE-V2X measurements, the equipment used at the EU site are two 5.9 GHz Qualcomm® Cellular Vehicle-to-Everything (C-V2X) Development Platforms supplied by Intrinsync, which are using the 5,9 GHz band. The devices are operating in 5875-5905 MHz frequencies. The C-V2X antennas used were NMO4E5350B antennas by LARSEN. For the 5G measurements, Huawei CPE Pro router and commercial 5G Elisa network are used. These trial sites in Espoo/Tampere, Finland are specific public areas dedicated for the development and validation of automated driving systems. The test route length is in total about 950 metres. The test vehicle drives from southeast approaching the four-way intersection (Linforsinkatu - Ahvenisjärventie) where RSU, MEC, physical traffic light and camera are deployed. Assuming the communication range is about 400 metre upstream to the intersection, the measurement test route includes a hill, buildings and heavy greenery along the road that can influence the V2X communication performance, as it does in the real situation.

Parameters	Channel used in China trials		Channel used in Europe trials
PC5	5905MHz-5925MHz		5900MHz-5910MHz
	5905MHz-5915MHz	5915MHz-5925MHz	
	Sending (OBU sends)	Sending (RSU sends)	
	Receiving		
Uu	2.6GHz		3.5GHz

Table 11: Test conditions for V2V/V2I (PC5) and V2I (Uu) communication

The joint EU-China V2X trials in China are performed with a crew of connected vehicles and several consecutive intersections (all equipped with LTE-V2X devices, shown in Figure 44 and Figure 45) from different vendors. The devices are operating in 5905MHz-5925MHz frequencies. The two joint EU-

China V2X trial use cases are tested as the featured use cases, along with multiple use cases defined and tested in the scope of 5G Large-scale trial. The test site has full coverage of 2.6GHz 5G commercial network. For each test, only LTE-V2X short range communication measurements using LTE-V2X devices are performed.

3.4.2.3 Trial categorisation and procedures

Per trial performance order and per objectives, the joint EU-China V2X trials in Europe and in China can be both characterized into three major categories. Table 12 shows the overview of trial categorisation in Europe and in China.

Category number	Joint EU-China V2X trials in Europe 5G-DRIVE	Joint EU-China V2X trials in China 5G Large-scale trial
1	Initial quality testing (reliability)	Interoperability tests (different vendors devices)
2	Performance of LTE-V2X:	V2I/V2V coverage tests:
	Impact Factor 1 - Number of LTE-V2X stations (emulated)	Two sub-categories
	Impact Factor 2 - Vehicle speed	V2I (OBU-RSU) coverage test under NLOS
	Impact Factor 3 - Antenna height	V2V (OBU-OBU) coverage test under LOS/NLOS ¹¹ : 1) Driving 2) Fixed locations
3	Two featured joint EU-China use cases: LTE-V2X Feasibility and Performance	Two featured joint EU-China use cases among 17 day-1 C-ITS services: LTE-V2X Performance
	Intersection safety (intelligent intersection with VRU crossing)	Intersection safety (intersection collision warning)
	GLOSA (individual speed advice to C(A)V utilising LTE-V2X communication)	GLOSA

Table 12: Joint EU-China V2X trials categorisation in Europe and in China

For the joint EU-China V2X trials in Europe, the first category is to set up initial quality test and determine reliability of LTE-V2X communications with moderate activity on the channel. With inputs from link budget model study (see section 4.1.3.2) and inputs from 5G Large-scale trial practice, the second category is designed according to three impact factors. By variation the impact factors of emulated stations, vehicle speed and antenna height, we aim to test the performance of LTE-V2X. The goal of the third category is to perform the two joint EU-China use cases with slight variations compared to China. For intersection safety, the focus is on protecting the VRU with DENM message warning via low latency LTE-V2X communication; for GLOSA, the focus is on developing a GLOSA application to provide individual speed advice to assist (automated) driving, with the focus on improving traffic efficiency and environmental metrics (by decreasing the number of vehicles stopping and stopping times for red) and improving user perspective metrics in the future.

¹¹ LOS/NLOS: line of sight or none line of sight trial site conditions. The none line of sight can be caused by greenery, buildings, obstacles etc. Note that regarding the surrounding morphology of the test environment, the test areas are mostly LOS/NLOS, where NLOS are caused by stationary obstructions: greenery, infrastructure etc.

For the joint EU-China V2X trials in China, the LTE-V2X test are divided into three categories: interoperability tests among different vendors, V2I/V2V coverage tests, and finally, LTE-V2X (PC5) performance tests. The first category is to set up initial tests and determine the interoperability of different LTE-V2X devices. The second category is divided in driving mode and in fixed position mode, to determine the coverage range of LTE-V2X (PC5). The goal of the third category is to perform the two joint EU-China use cases with variations compared to Europe. For intersection safety, the focus is on preventing intersection collision with BSM message warning via low latency LTE-V2X communication; for GLOSA, the focus is to traffic light status to connected (equipped with LTE-V2X OBU) vehicles to assist (automated) driving, to the end of avoiding intersection traffic light violation and improving traffic efficiency.

The trial procedure for joint EU-China V2X trial - GLOSA use case is similar in the two twinning projects, except for the variation on a GLOSA application providing individual speed advice in Europe. Therefore, the trial procedure is based on the User story – Main event flows as shown in Table 10. The following Table 13 and Table 14 demonstrate the trial procedure of the joint EU-China V2X trial - intersection safety use case in Europe and in China respectively. Note that for the joint EU-China V2X trial in Europe, the same trial procedure is reused with variation on precondition 4 in Table 13 for 5G measurements on latency and Packet Error Rate (PER). In the 5G measurement scenario, the camera detection data is sent to the VTT Backoffice then to the vehicle, and the 5G latency is measured from Backoffice server to the connected (automated) vehicle.

Name	Intersection safety (intelligent intersection with VRU crossing)	
Preconditions	<ol style="list-style-type: none"> 1. Traffic camera is on 2. Traffic camera is detecting and tracking VRUs 3. In-vehicle OBU is switched on, transmitting CAM and ready to receive messages from RSU. 4. RSU is connected to camera system tracking VRUs and transmitting DENM when a VRU is on the zebra lines. 	
Test step	Description	Success criterion
1.	Vehicle starts approaching from (southeast ingress) 350 m upstream to the intersection.	NA
2.	VRU enters the zebra lines	VRU detected and DENM transmission triggered.
3.	Vehicle receives DENM messages	DENM received
4.	Repeat 5 test runs of step 1-3, collect latency and Packet Error Rate data along test route	Raw data points collected without abnormality, sufficient for post-trial data analysis
KPI criteria	<ul style="list-style-type: none"> - Packet error rate < 10% - Latency (end-to-end mean latency from RSU to OBU) < 100 ms 	

Table 13: Intersection safety (intelligent intersection with VRU crossing) use case trial procedure, in Europe

Name	Intersection safety (intersection collision warning)	
Preconditions	<ol style="list-style-type: none"> 1. RSU, V2X platform, OBU switched on and functioning 2. RSU, V2X platform, OBU communication on 3. RSU broadcasts RSI messages (incident) every 1 second. 4. OBU broadcasts BSM messages every 0.1 second. 	
Test step	Description	Success criterion
1.	Vehicles start approaching the intersection.	NA
2.	1/5/10 OBU(s) in the coverage of intersection RSU.	NA
3.	Transmit and receive duration more than 10 minutes.	BSM received and warning is received by vehicles.
KPI criteria	<ul style="list-style-type: none"> - Packet error rate < 10% - Latency (end-to-end mean latency from OBU to OBU) < 100 ms 	

Table 14: Intersection safety (intersection collision warning) use case trial procedure, in China

3.4.3 Assessment methodology

3.4.3.1 Assessment tools

A proprietary data analytic application was developed and used in the joint EU-China V2X trial in Europe. During the trial, the data gathering in vehicles was automated and special tools were implemented and integrated in the vehicles. The used data gathering application enabled parallel 5G and C-V2X measurements which is not available in the market today. The tool (see Figure 46 and Figure 47) can adjust 1) payload, 2) interval 3) communication method (4G, 5G, V2X), 4) different location and 5) dedicated only for current measurement. This has been tailored for the needs to benchmark the new build 5G network performance between inside network (MEC Mobile Edge Computing unit) to outside test server. The tool provides possibility to install measurement unit inside a moving vehicle with GNSS antenna and mobile 5G unit. Between different test runs, the software allows change of benchmark variables and stores results to files. The novelty here is that it combines performance measures between different networks, enabling a measurement method for hybrid communication. Some of the connected driving cases are dedicated to send the cellular channels when payload and latency requirements are met.

Network latency can be calculated in two ways. For 5G-measurement, MQTT-broker (server) could be used inside or outside the measurement network. When the server is outside the network shell, total latency is the combination of the internal latency in the network and the global internet latency. As an inside server (MEC), only the measured network internal delays are affecting the latency. Also, V2X latency can be calculated as device-to-device measurement. In this case the measurement software is in both ends of the V2X device network (for example, in two vehicles or RSU). In such V2X latency measurement, latency is defined as the time difference between the sending and receiving time of a packet between two nodes (vehicle to vehicle or vehicle to RSU).

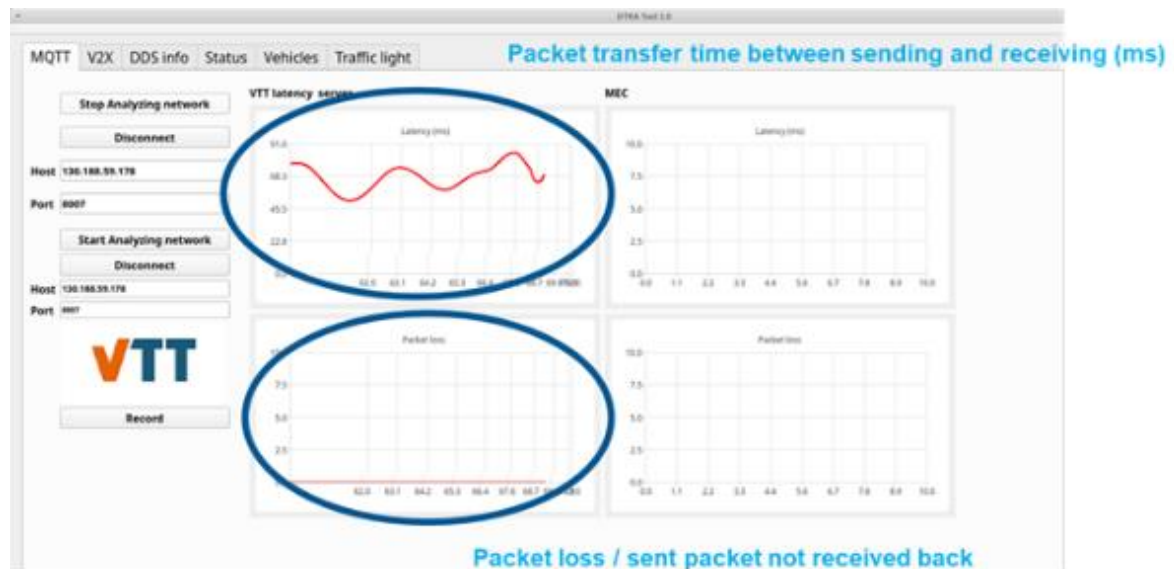


Figure 46: User interface for the measurement tool

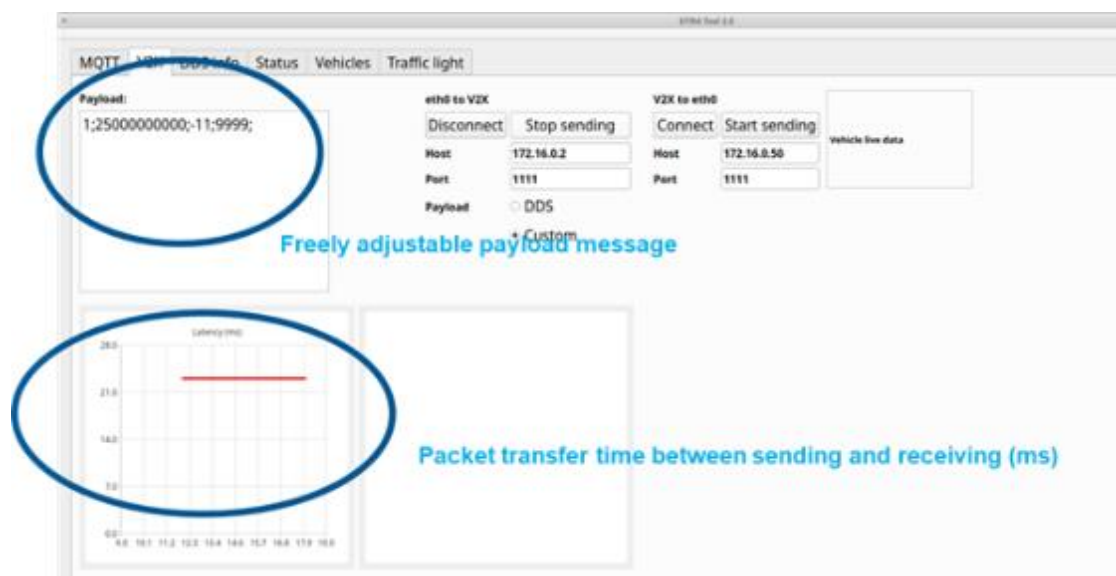


Figure 47: The test data transmission/receiver interface

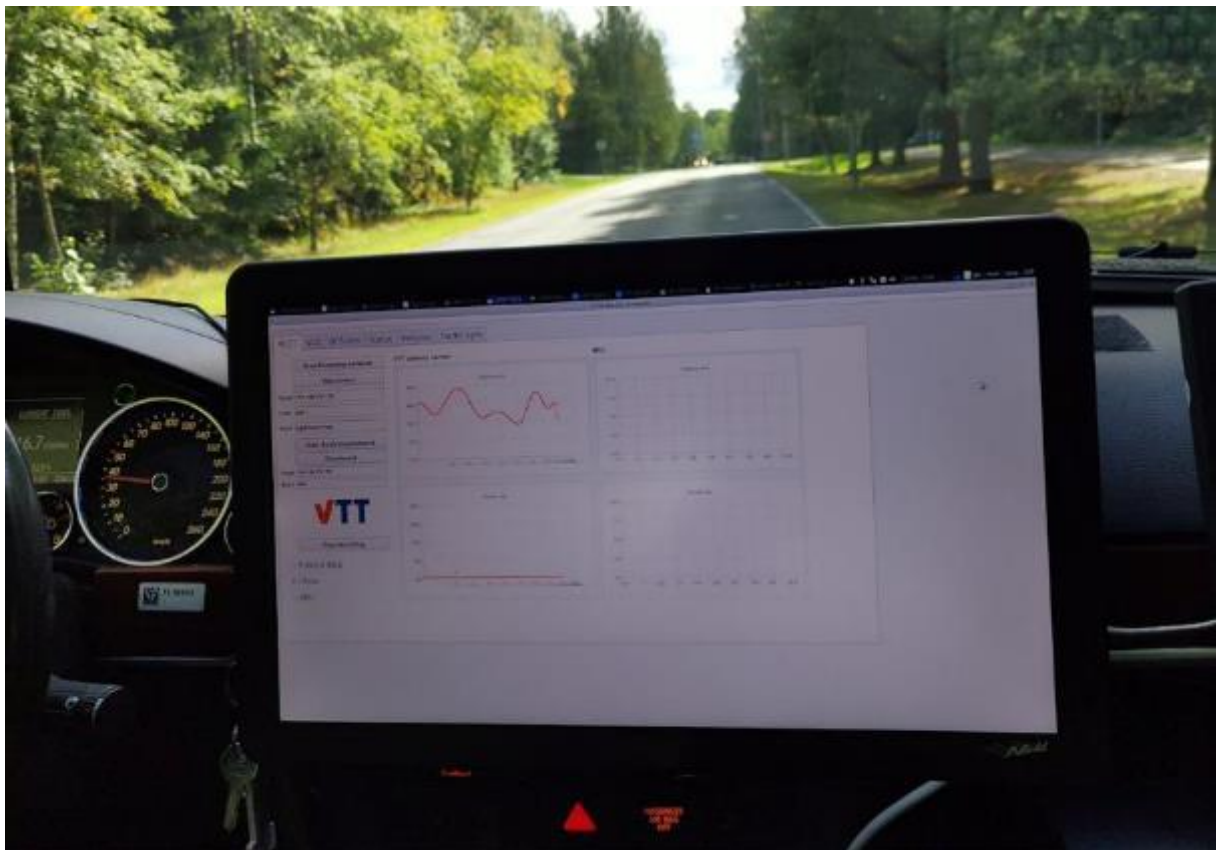


Figure 48: The in-vehicle display of assessment tool during the trials in Tampere, Finland

3.4.3.2 Assessment KPIs

5G-DRIVE and 5G Large-scale trial intend to measure the main KPIs (see Table 15 and Table 16) and generate conclusions how they support V2X future automated driving scenarios.

Table 15 and Table 16 show the use cases and its preliminary targeted KPIs on latency (mean) and Packet Error Rate (PER) for joint EU-China V2X trials on both sides. The objectives for the listed preliminary targeted KPI are two-fold: 1) They set the criteria for the feasibility of V2X trials in real-life condition. 2) They provide an overview of the main KPIs that will be measured and compared between the joint EU-China V2X trials in Europe and in China.

Since the safety-critical Day 1 messages should arrive with minimal latency and packet loss. The KPI criteria are very strict and challenging due to the safety nature of the use cases. In the joint EU-China V2X trials, we adopted the general service level requirements from 3GPP, see Table 15 and Table 16. Comparing the KPIs of the messages used in the intersection safety use case, although they are different (DENM in Europe and BSM in China), they are equal. For example, the DENM PER target in Europe is less than 10 % and the BSM PER target in China is the same. Also, the DENM latency target in Europe is less than 100 ms and so is the BSM latency China.

Scenario	KPI title	Metrics
GLOSA use case with GLOSA application		
5G - MAP		
	Latency	< 5 s
	Packet Error Rate	< 10 %
5G - SPaT		
	Latency	< 2 s
	Packet Error Rate	< 10 %
LTE-V2X - MAP		

	Latency	< 100 ms
	Packet Error Rate	< 10 %
LTE-V2X - SPaT		
	Latency	< 100 ms
	Packet Error Rate	< 10 %
Intersection Safety (intelligent intersection with VRU crossing) use case		
5G - DENM		
	Latency	< 1 s
	Packet Error Rate	< 10 %
5G - CAM		
	Latency	< 1 s
	Packet Error Rate	< 10 %
LTE-V2X - DENM		
	Latency	< 100 ms
	Packet Error Rate	< 10 %
LTE-V2X - CAM		
	Latency	< 100 ms
	Packet Error Rate	< 10 %

Table 15: The preliminary targeted KPIs for the joint EU-China V2X use cases in Europe

Scenario	KPI title	Metrics
GLOSA use case		
BSM		
	Latency	< 100 ms
	Packet Error Rate	< 10 %
SPaT		
	Latency	< 100 ms
	Packet Error Rate	< 10 %
MAP		
	Latency	< 100 ms
	Packet Error Rate	< 10 %
Intersection Safety (intersection collision warning) use case		
BSM		
	Latency	< 100 ms
	Packet Error Rate	< 10 %
MAP		
	Latency	< 100 ms
	Packet Error Rate	< 10 %

Table 16: The preliminary targeted KPIs for the joint EU-China V2X use cases in China

3.4.3.3 Assessment methods

In the joint EU-China V2X trials, the main assessment methods adopted are aiming for measuring, analysing, and displaying the KPIs by using proprietary tools from VTT (5G-DRIVE partner) and China Mobile (5G Large-scale trial partner). Although with different tools, the assessment methods are harmonised at both sides.

To begin with, the end-to-end latency (mean), latency jitter and Packet Error Rate (PER) are automatically collected using these proprietary tools.

Firstly, the end-to-end latency is measured as the elapsed time from the moment a data packet is transmitted by the source UEs (OBUs/RSUs)/ application server to the moment it is received by the destination UEs (OBUs/RSUs)/ application server [17]. In joint EU-China V2X trials in Europe, the end-to-end latency of LTE-V2X communication is measured by sending a use case message (CAM, SPaT, MAP and DENM) from a RSU end to an OBU end. In joint EU-China V2X trials in China, the end-to-end latency of LTE-V2X communication is measured by sending a use case message (BSM, SPaT and MAP) from a RSU to an OBU end or from an OBU to another OBU end. The control plane and user plane latency are not distinguished in the scope of joint EU-China V2X trials.

Secondly, the method of latency jitter calculation is only used in the joint EU-China V2X trials in Europe. The detailed explanation of the jitter calculation method can be found in section 4.1.2.1.

The last but not the least, the assessment method of Packet Error Rate (PER) is used to test the performance of a C-ITS terminal's receiver. PER is the ratio, in percent, of the number of packets not successfully received by a C-ITS receiver to the number of packets sent by a C-ITS transmitter. The PER measuring method is harmonised for the joint EU-China V2X trials on both Europe and China trials. For each LTE-V2X trials, the PER of packets transmitting and receiving is being collected along the test route once the connectivity establishment is successful. The preliminary PER requirement target is jointly defined in Table 15 and Table 16.

Upon successful setup and configuration of the assessment tools, they automatically collect KPIs during the trial runs, providing preliminary performance estimation online and storing data to the files for offline analysis. Simultaneously, KPIs such as latency and PER are measured during the trial runs. The process is repeated for all trials runs.

Afterwards, the evaluation and assessment of the data was performed using several tools. Excel and QGIS tools are used for visualising network coverage and jitters. The results are then displayed in a graphic and linked to a map thanks to the GNSS data in order to facilitate the analysis of the influence of surrounding elements (buildings, hills, greenery etc.) in the connectivity establishments and the final performance of V2X.

4 Results

This section presents the trial findings and results in the following aspects:

- The LTE-V2X field trial findings and results of joint EU-China V2X trials in Finland and Italy in Europe and in Shanghai in China
- The LTE/5G cellular field trials findings and results of joint EU-China V2X trials in Finland of Europe
- The results of three enhancement trials and studies on vehicle positioning, key V2X link budget parameters study and on interruption of communication in MEC-based V2X services from Finland, UK and Poland.

4.1 Joint V2X trials in Europe

Section 4.1 presents the field trials findings of joint EU-China V2X trials in Espoo/Tampere, Finland and in Ispra, Italy. These sections aim to show the outcomes and findings retrieved under the joint EU-China V2X trial framework in section 3. Since these trials were performed under the joint EU-China V2X trials framework with different trial experimental setup, instead of benchmarking the LTE-V2X performance with assessment KPIs, we aim to provide a snapshot of trial results during the demonstration and execution of the trials. Please note that the trials results are subjective to the specific trial environment with experimental devices and factory default settings, which shall not be used as performance and comparison of technologies.

4.1.1 Tampere trial results

This section shows the field trial outcomes and findings of joint EU-China V2X trials in Espoo/Tampere in Finland, Europe. Based on the joint trial harmonised plan in section 3.4, this section shows the outcomes of the two joint EU-China V2X use cases under LTE/5G cellular network scenarios and under LTE-V2X PC5 scenarios.

4.1.1.1 Objectives

The main test objectives for the Tampere test sessions were the followings:

- To set up initial test environment, and to test the feasibility and reliability of C-V2X trials in Espoo and Tampere, Finland. The reliability is tested under various message sizes over the 5G and LTE-V2X communications.
- To execute performance of LTE-V2X trials: to measure latency (mean), jitter of latency, number of lost messages (Packet Error Rate) according to number of emulated LTE-V2X stations, vehicle driving speed and antenna height variations. The same trial procedure is reused for 5G communication to lay the benchmarks.
- To set up, configure and perform the joint EU-China V2X trials – intersection safety and GLOSA use cases in Tampere, Finland, and to measure latency (mean), jitter of latency, number of lost messages (Packet Error Rate) during the performance of these use cases.
- To explore the impact of environmental factors on the performance of LTE-V2X.

To achieve these main objectives and to perform the joint EU-China V2X trial as much as possible to the equivalent of face-to-face trials with 5G Large-scale trial consortium, the following sub-objectives are defined:

- To test autonomous driving in real environment with different environmental factors.
- To facilitate automated driving when a VRU on the zebra lines (Intersection safety use case).
- To test virtual traffic light communication from the NL Backoffice server.

- To test SPaT message subscribing from NL Backoffice server and transmitting via LTE-V2X devices (RSU to OBU) in the GLOSA use case.
- To assist automated driving with individual speed advice from GLOSA speed advice application (developed under the scope of 5G-DRIVE) using virtual traffic light in the open-road field tests.
- Live video streaming of the Tampere test sessions part of the joint EU-China trial with twining project, 5G Large-scale trial project V2X team. Live video streaming was used to share the Tampere test sessions of the joint EU-China trial with twining project, 5G Large-scale trial V2X team.

4.1.1.2 Experimental setup

Figure 49 presents the test route in Hervanta area. The tests in Finland were carried out in a specific public area that is dedicated for the development and validation of automated driving sub-systems. The selected urban area intersection is a typical four approaches intersection with equal right on each approach and a low traffic density (see section 3.4.2.2 for the detailed trial conditions). Automated test vehicle “Martti” was approaching the intersection and mobile RSU trailer “Marsu” was located at the intersection (green spot in Figure 49).

Additionally, there was a virtual traffic light implemented for executing complementary test sessions of GLOSA speed advice application. Using the same intersection, the test route for this complementary test sessions was slightly different because the vehicle drives straight (or stop) if the virtual traffic light is green (or red and amber). After egressing the intersection, the vehicle makes a round-trip to the beginning of the test route for the next test run. The setup in Tampere followed the joint architecture presented in Figure 42.

In addition to the key component’s setups in the two joint EU-China V2X use cases explained in section 3.4.2, the equipment used at the Tampere site were the following: 5G-capable Huawei CPE Pro router for the 5G measurements and 5.9 GHz Qualcomm® Cellular Vehicle-to-Everything (C-V2X) Development Platform for the C-V2X measurements. Both the test vehicle and the trailer had this same hardware installation. The used LTE/5G network was the commercial 3.5 GHz network.

Figure 50 (right) shows the antenna installations on the test vehicle “Martti” at 1.4 m height. The RSU antenna was located on the roof of the trailer and it had three different height installations from the ground (1.4 m, 2.8 m and 3.8 m).

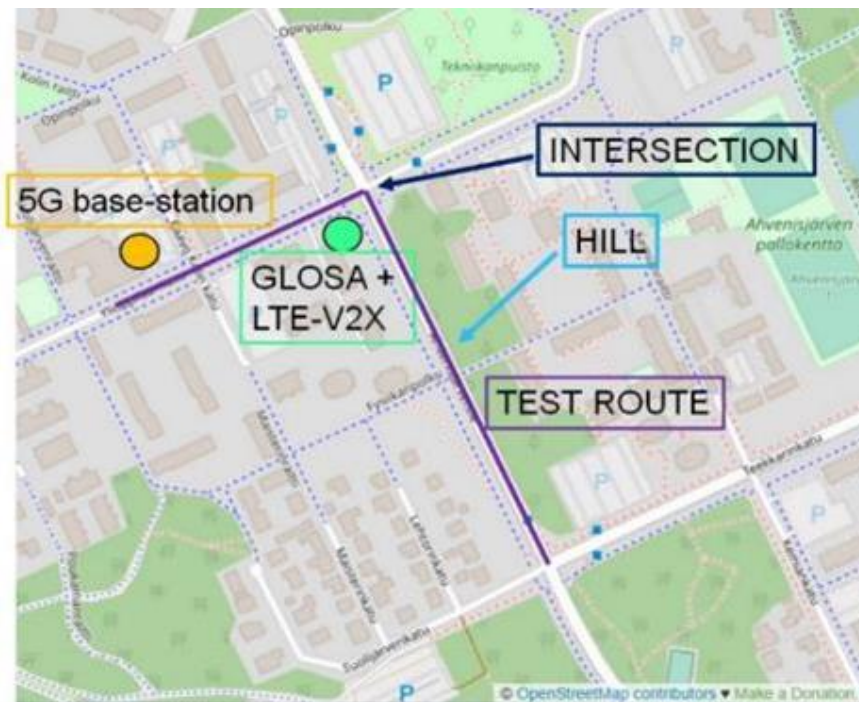


Figure 49: The test intersection for trials in Tampere, Finland. 1 cm in the picture represents about 100 m.



Figure 50: Antenna installations in the LTE-V2X trials. Left: antenna installations on the trailer; Right: the 5G and LTE-V2X antennas of the test vehicle "Marti" located on the roof.

The Tampere test session consisted of four different separate test sessions, between autumn 2020 and spring 2021 and they aim for the three categories listed in Table 12:

1. Initial quality testing (reliability) of LTE-V2X assisted connected and automated driving
2. Performance of LTE-V2X by varying three assumed impact factors:
 - a. Number of emulated LTE-V2X stations
 - b. Vehicle speed
 - c. Antenna height
3. Featured joint EU-China use cases:
 - a. Intersection safety (intelligent intersection with VRU crossing)
 - b. GLOSA (individual speed advice to C(A)V utilising LTE-V2X communication)

RELIABILITY OF LTE-V2X COMMUNICATIONS - Test session one: 24-25. August 2020

The first LTE-V2X communication test aimed to determine the reliability of communications with moderate activity on the channel. Specifically, the goal for this test session was to measure the latency, jitter, and packet loss measurements with different message sizes (200B, 400B, 800B and 1500B) and different maximum distances (50m and 300m). Jitter calculation was done by using 5 samples moving median window. The jitter is calculated using the sum of differences between two

consecutive measurements for five consecutive samples, then divided by 4 (number of samples - 1). The moving average is selected for analysing the changes in jitter when approaching areas where network signal is not strong.

One scenario was sending the messages from IP network to the test vehicle (connected and automated vehicle) using 5G network. The other scenario is setting up LTE-V2X communication and sending messages from the test vehicle to RSU using LTE-V2X short range communication.

Under established connection, the results in Table 17 and Table 18 showed that there is less jitter in LTE-V2X scenario than in the 5G connection scenario, where the network availability for both scenarios were established in the trial site area, especially the intersection where tests measurements have been taken. Packet error rate (shown as lost messages) where 0 lost message indicated good connection between devices. Thus, these initial reliability tests indicated that connectivity among vehicle, MEC (traffic light, camera and RSU), and network has been successfully established.

	200 B	400 B	800 B	1500 B
Latency (Mean)[ms]	37	44	46	36
Jitter [ms]	101	132	117	93
Lost messages	0	0	0	0

Table 17: Calculated values: 5G from IP network to Connected Vehicle, MAP message. The number of samples used calculations is around 600 - 900.

	200 B	399 B	799 B	1499 B
Latency (Mean)[ms]	37	40	42	36
Jitter [ms]	21	19	18	72
Lost messages	0	0	0	0

Table 18: Calculated values: LTE-V2X from OBU (Connected Vehicle) to RSU. The number of samples used for calculations is around 600 - 900.

Performance of LTE-V2X - Test session two + three, 9. & 24. September 2020 +22. October 2020

The second topic was broadening the latency, jitter, and packet error rate measurements by applying:

- 1) A bandwidth stress test by using different message intervals (1ms, 5ms, 10ms, 20ms, 50ms and 150ms).
- 2) Using different autonomous vehicle speeds (5km/h, 10 km/h, 15 km/h, 20 km/h, 30 km/h and 40 km/h¹²).
- 3) Different antenna heights on the LTE-V2X RSU.

The aim of the test was to measure the performance of LTE-V2X traffic and connectivity under different varying impact factors on the test site. Figure 51 - Figure 61 show LTE-V2X measurement conducted for the used LTE-V2X OBU and LTE-V2X RSU, and for 5G measurements from IP network to vehicle using the commercial network in Tampere, Finland.

Bandwidth stress test

¹² The speed variation assumption is originated from doppler effects in the V2X link budget and deployment optimisation, see section 4.1.3.2.

For impact factor 1), messages were sent from IP network to the connected vehicle using 5G network or LTE-V2X short range communication. In all cases, the message size was fixed on 277B and the antenna height was set at 1.4m (for LTE-V2X OBU and RSU). Figure 51, Figure 52, Figure 53, Figure 54, Table 19, and Table 20 show the results of these tests. One additional test was to send virtual traffic light SPaT message over LTE-V2X devices. This test was to examine whether the virtual traffic light Backoffice server in the Netherlands is accessible from Finland and whether the subscribing and receiving messages were functional.

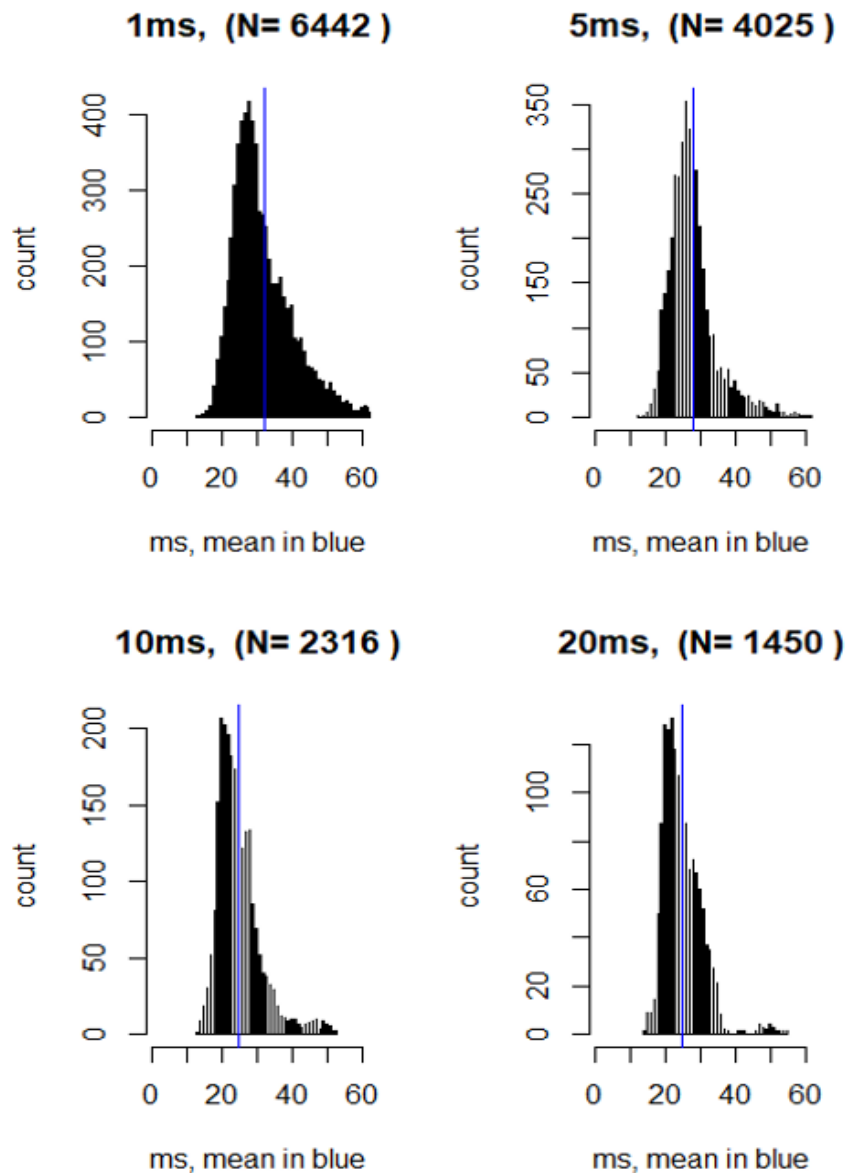


Figure 51: Histograms of latency (mean) for LTE -V2X from RSU to OBU, various message intervals.

Message Interval [ms]	1	5	10	20	50	150
Latency (Mean) [ms]	32	28	25	25	24	24
Jitter [ms]	68	50	40	41	39	34
# of sent messages	6442	4025	2316	1450	805	260

Table 19: Calculated values: LTE-V2X from OBU (Connected Vehicle) to RSU, various message intervals.



Figure 52: Latency contour plot (LTE-V2X): msg interval 20 ms, tx RSU at blue location (green < 26ms, red > 36ms). The driving speed in this case is 15-25 km/h

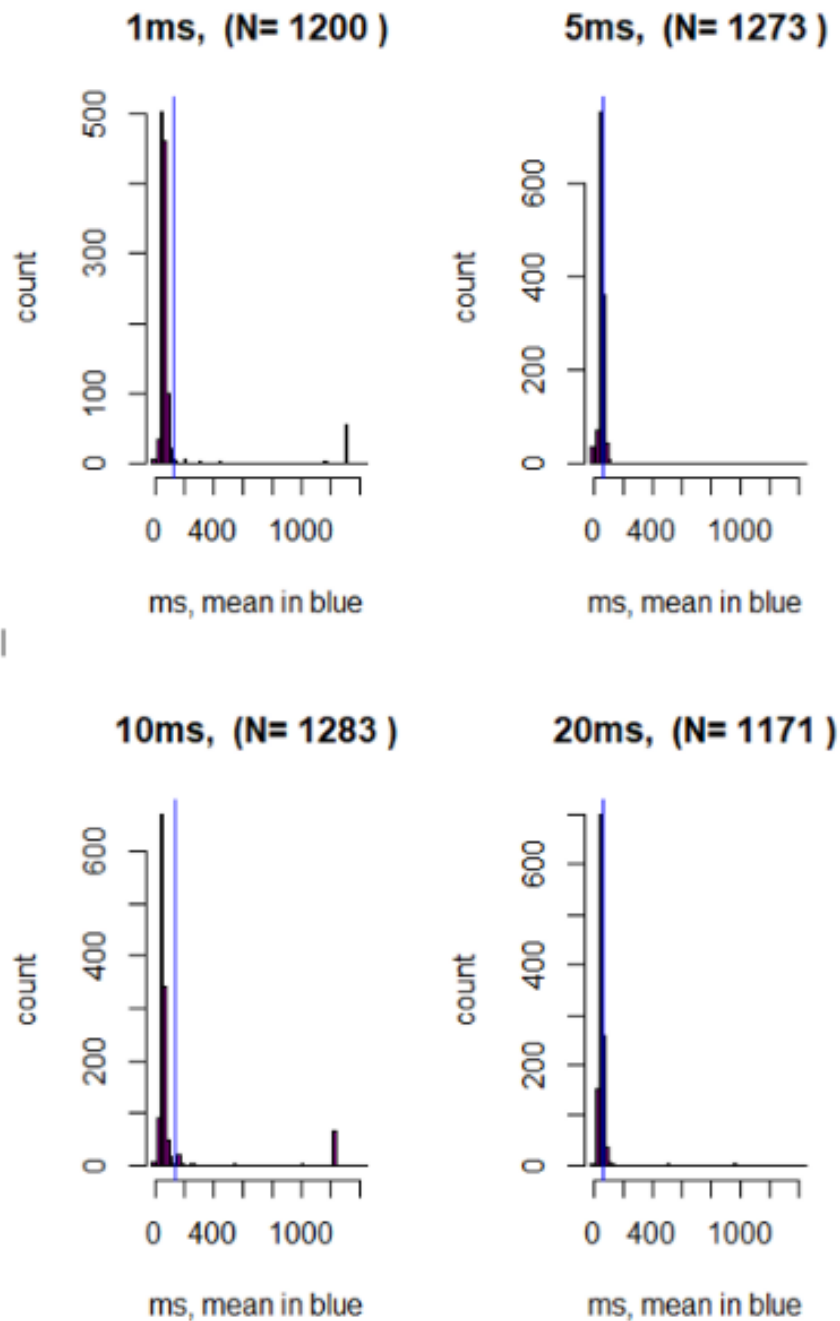


Figure 53: Histograms of latency (mean) for 5G from IP network to Vehicle, DENM message, various message intervals (1ms, 5ms, 10ms and 20ms).

Msg Interval [ms]	1	5	10	20	50	150
Latency (Mean) [ms]	133	62	137	69	61	64
Jitter [ms]	4902	4978	4783	4272	3683	3466
# of sent messages	1200	1273	1283	1171	1090	1037

Table 20: Calculated values: 5G from IP network to Connected Vehicle, DENM message, various message intervals (1 ms, 5 ms, 10 ms, 20 ms, 50 ms and 150 ms).

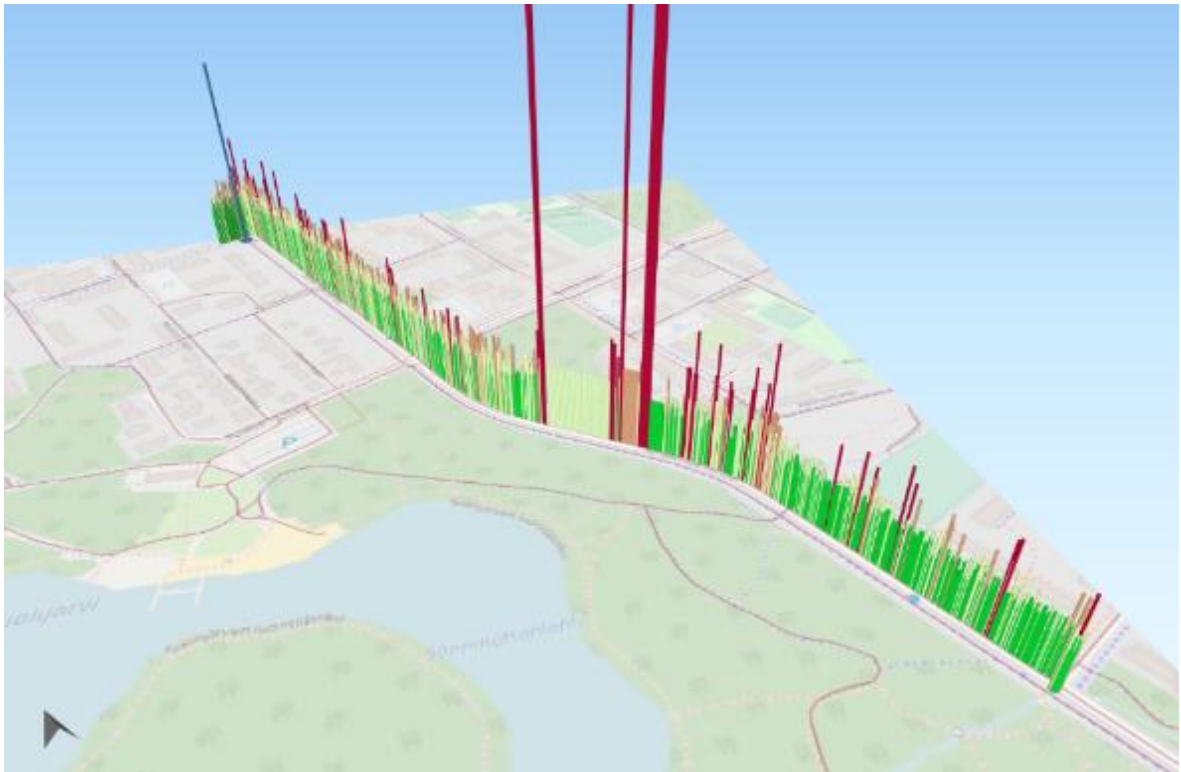


Figure 54: Latency contour plot (5G): msg interval 20ms, tx RSU in blue location (green < 51.6ms, red > 78.0ms).

Vehicle speeds variation

For impact factor 2), messages were sent from IP network to connect vehicle using 5G network or LTE-V2X short range communication. The message size was fixed to 277 B and message sending interval is fixed to 50 ms. The vehicle driving speed was varying from 5km/h to 40km/h. Figure 55, Figure 56, Figure 57, Table 21, and Table 22 show the results of these tests.

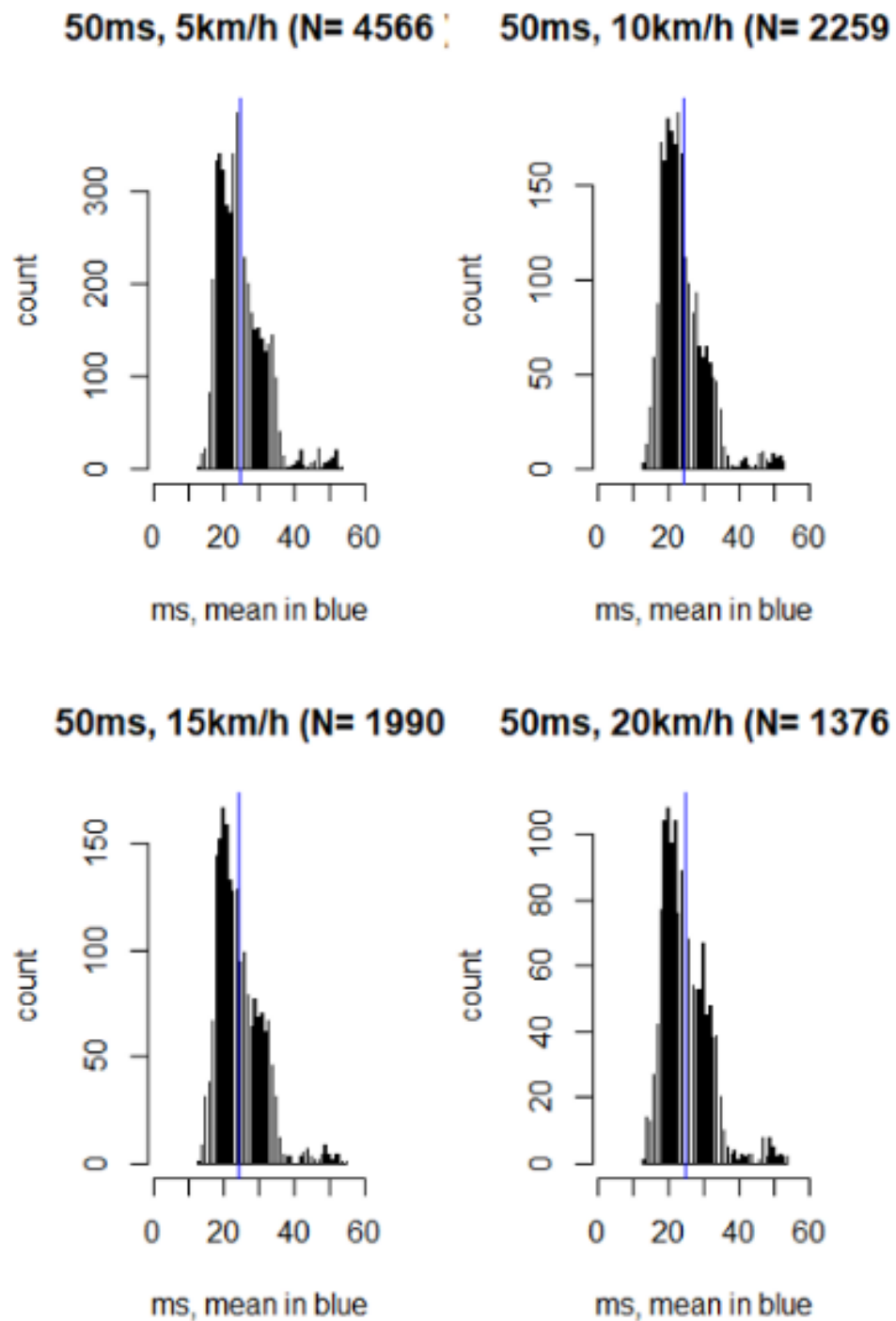


Figure 55: Histograms of latency (mean) for LTE -V2X from RSU to OBU, different driving speeds (message interval 50 ms).

km/h	5	10	15	20	30	40
Latency (Mean) [ms]	25	24	25	25	24	24
Jitter [ms]	41	40	42	41	40	39
# of sent messages	4566	2259	1990	1376	936	856

Table 21: Calculated values for LTE-V2X, different driving speeds (message interval 50 ms).

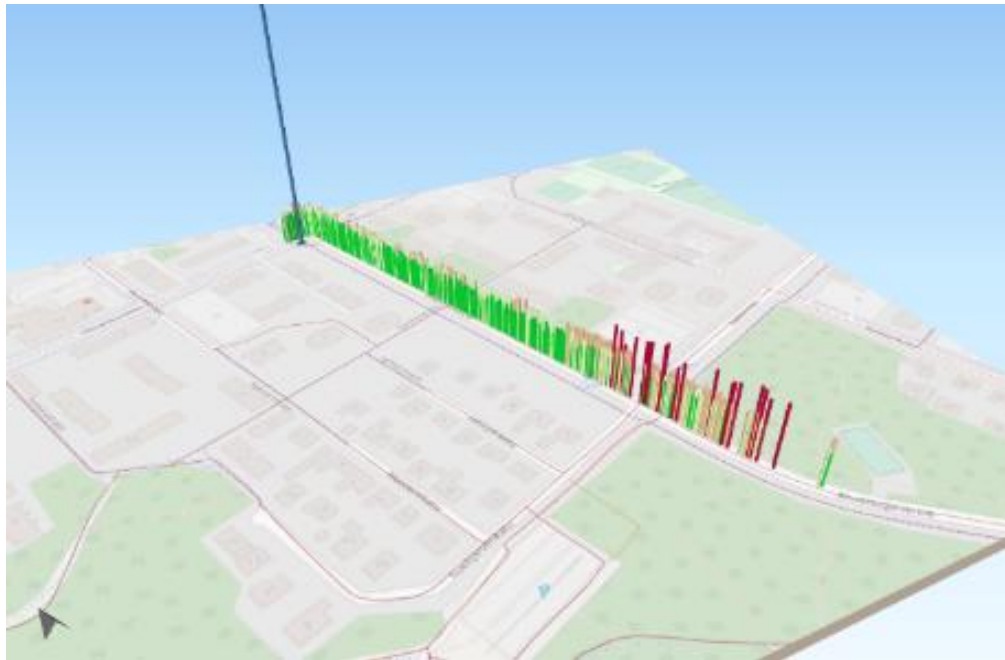


Figure 56: Latency contour plot (LTE-V2X): msg interval 50ms, driving speed 5km/h, tx RSU in blue location (green < 26ms, red > 36ms).

km/h	5	10	15	20	30	40
Latency (Mean) [ms]	91.1	65.9	103	130	72.5	94.1
Jitter [ms]	4347.0	4696.0	4833	3258	4799.0	944.0
# of sent messages	2887	5709	2656	1830	1264	951

Table 22: Calculated values for 5G, different driving speeds (message interval 50 ms).

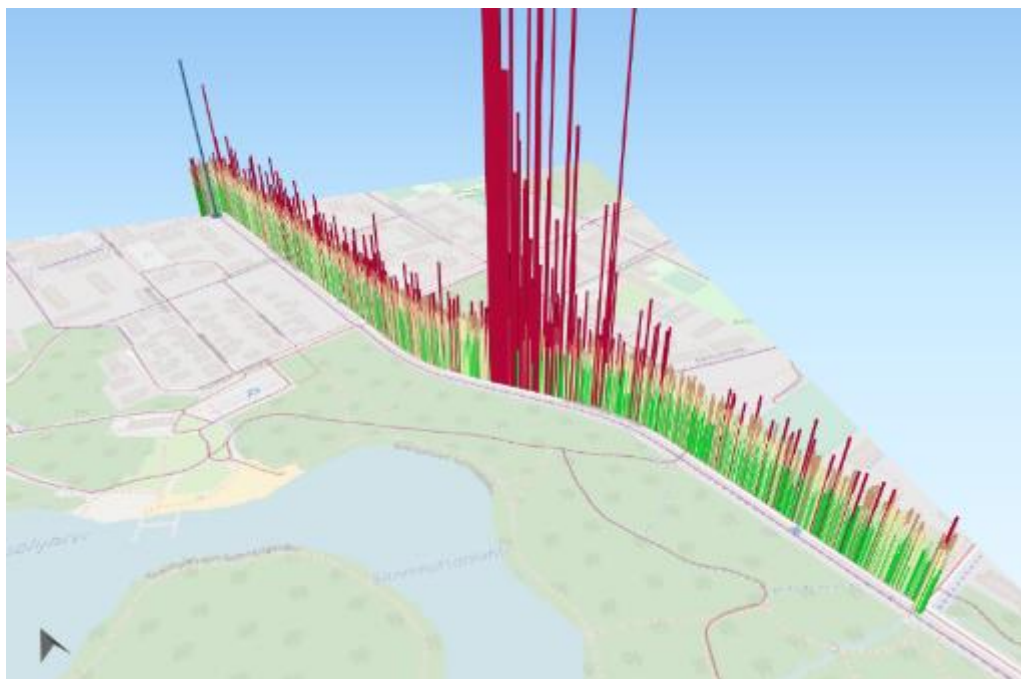


Figure 57: Latency contour plot (5G): msg interval 50 ms, driving speed 5km/h, tx RSU in blue location (green < 51.6 ms, red > 78.0ms).

Different antenna heights

For impact factor 3), messages were sent from IP network to connect vehicle using 5G network or LTE-V2X short range communication. The test was dedicated for checking the needs of automated driving and therefore, the vehicle was setup to drive in automated mode with support of V2X messages (CAM, DENM) in the intersection safety (intelligent intersection with VRU crossing use case).

The aims of the tests were twofold; using different antenna heights for the LTE-V2X (1.4m, 2.8m and 3.8m) and using different message sizes for automated driving (250B and 750B). In all cases connected and automated vehicle drives at constant speed: 30km/h.

For the LTE-V2X short range communication, “Martti” the connected and automated vehicle was used to perform the following sequences:

1. vehicle approaching intersection
2. green light (physical traffic light)
3. pedestrian is detected by camera
4. DENM message is sent from RSU to OBU (LTE-V2X)
5. vehicle stops the right turning/left turning movement and moves on after the pedestrian safely crossing over

This typical use case in the urban area where the automated vehicle sometimes failed to handle due to insufficiency of on-board sensor, is expected to be assisted with 5G or LTE-V2X (PC5) communication. This test scenario was also broadcasted to 5G Large-scale trial consortium member China Mobile for comparing the trial procedures.

	250 Bytes/message			750 Bytes/message		
Antenna height [m]	1.4	2.8	3.8	1.4	2.8	3.8
Latency (mean) [ms]	35	30	26	33	32	26
Jitter [ms]	9	9	8	12	9	7
Max. distance	385	368	373	311	288	305
Packet Error Rate [%]	32	19	9	12	11	7

Table 23: Calculated values for LTE-V2X with antenna height (on LTE-V2X RSU) variation (1.4m, 2.8m and 3.8m) and message size of 250 B and 750B. Vehicle driving speed 30km/h and msg. interval 100 ms. The number of samples used for calculations varied from 400 - 1000.

During the trial, the test vehicle was approaching the RSU at constant speed 30 km/h and was sending UDP messages with constant 100ms message interval. Total number of sent messages per measurement drive was around 400. Latency values are below 30ms with antenna height 3.8 meter. Jitter is calculated using 5-samples moving median window and almost all values are slightly below 10ms. When the antenna height was low (1.4-meter height), the test arrangement became non-line-of-sight due to the intersection topology. Heavy scattering due to trees on both sides of the road and climatic conditions such as rain fade also affected the latency and packet loss rate. However, packet loss values are remarkably low when the used antenna height was 3.8 meter. It seems that higher antenna installations show better performance results, specifically in this environmental test setup, where RSU was on top of a small hill and line-of-sight was only achieved with the antenna height 3.8 meter. The maximum distance between transmitting and receiving for 750B message is consistently (around 21%) shorter comparing to 250B. Since distance is a major contributor to the error in the transmission and data analysis shows that most of errors are located in the farther parts of the test route, which is a possible reason for the lower PER in 750B message cases. Figure 58 and Figure 59 show the results of these tests. The tests were carried partly in LOS and NLOS areas and therefore,

signal strength also varied in the tests. However, the signal level was not directly available via the device interfaces and synchronising the manual measures would be too time consuming and inaccurate compared to automatic analysis.

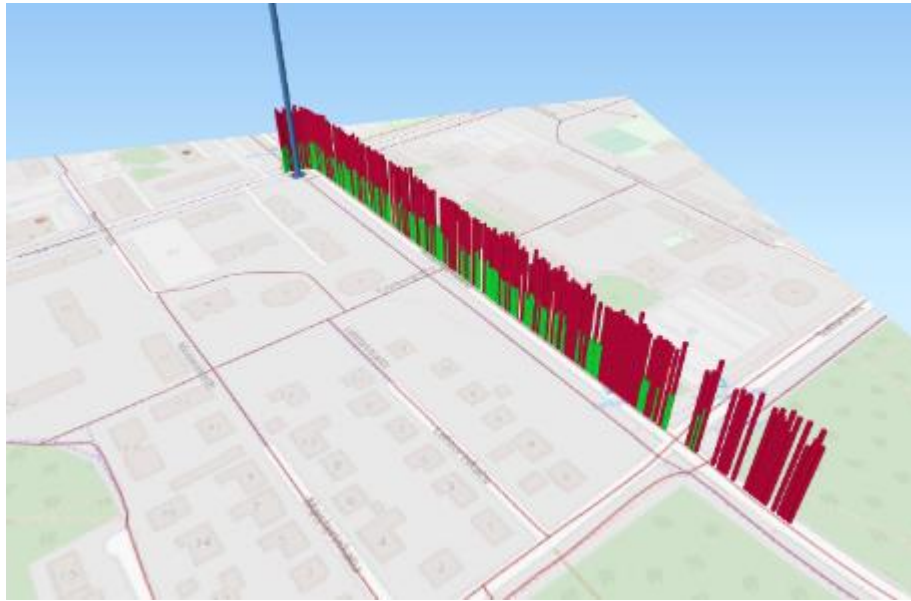


Figure 58: Latency: LTE-V2X, antenna height 1.4m, tx RSU in blue location (green < 26ms, red > 36ms).

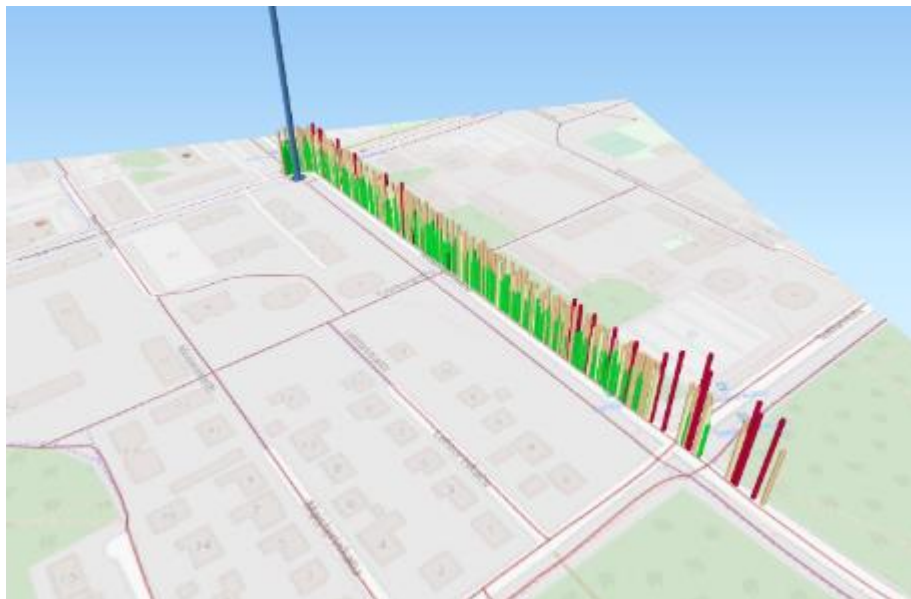


Figure 59: Latency: LTE-V2X, antenna height 3.8m, tx RSU in blue location (green < 26ms, red > 36ms).

Table 24 shows the measured values when antenna height of the cellular network (5G) antenna was varied. The antennas were installed to the pole in the road-side unit which was changed between 1.4 m and 2.8 m. The same measurements were conducted for two different package sizes (250 Bytes and 750 Bytes). The variations in terms of latency (mean) are observable under different antennas heights, which could be caused by many cellular network environmental conditions at the trial sites, such as cellular network quality, base stations handovers etc.

Further comparisons of latency (mean), jitter and packet error rate were made in Table 25 for automated driving mode. Mean latency values in LTE-V2X network is significantly better compared to the cellular network considering latency and jitter.

	250 Bytes/message		750 Bytes/message	
Antenna height [m]	1.4	2.8	1.4	2.8
Latency (mean) [ms]	208	444	203	149
Jitter [ms]	29	29	29	26
Number of msg	1072	983	1072	1122
Max. distance	876	717	909	887
Packet Error Rate [%]	0	0	0	0

Table 24: Calculated values for 5G antenna height variation, 250 B/msg (left) 750 B/msg (right), 30km/h, msg. interval 100 ms.

	LTE-V2X				5G			
Packet size [B]	250	500	750	1000	250	500	750	1000
Latency (mean) [ms]	15	15	13	13	43	58	61	50
Jitter [ms]	5	9	6	6	20	23	26	14
Number of msg	662	596	550	623	665	847	512	829
Max. distance	294	284	299	285	282	328	268	299
Packet Error Rate [%]	0	0	2	6	0	0	0	0

Table 25: Calculated values for AUTOMATED DRIVING, fixed speed 30 km/h, message interval 100 ms, C-V2X (left) 5G (right).

Figure 60 and Figure 61 show the LTE-V2X and 5G results in the graphical format how they are behaving over the test routes. An overall finding of LTE-V2X and 5G measurements, is the low variation in LTE-V2X scenarios. The performance of 5G results is dependent to the time of the day and the commercial LTE/5G cellular network on the trial sites, which may yield non-ideal results. The latency (mean) results of LTE-V2X are in overall better compared to the prior two test categories. The reason for improvement is not fully clear, which can only be investigated in the future studies.



Figure 60: Latency: Automated driving V2X, msg size 250B, tx RSU in blue location (green < 26ms, red > 36ms).

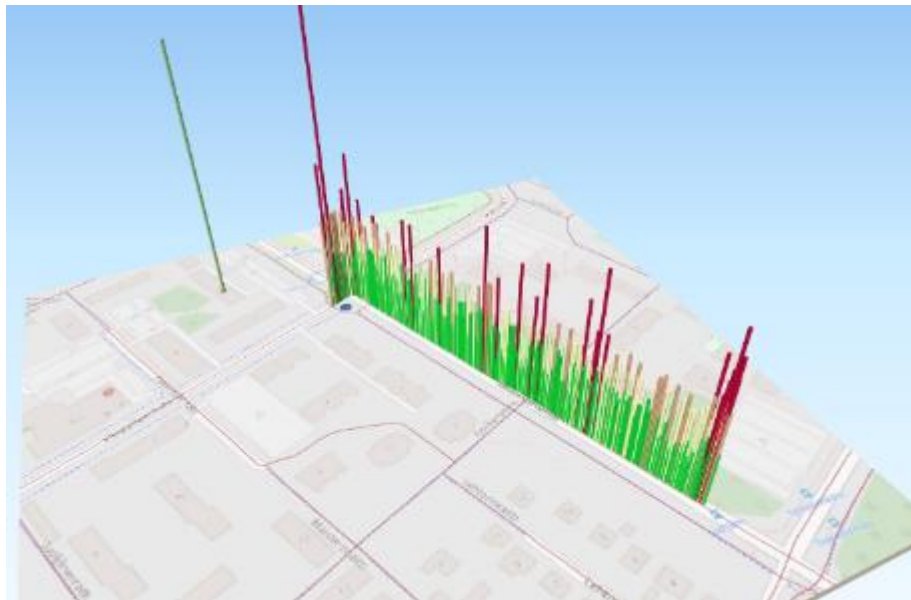


Figure 61: Latency: Automated driving 5G, msg size 250B, cell mast in green location (green < 26ms, red > 36 ms).

The joint EU-China use cases: GLOSA speed advice application - Test session three, 16. April 2021

This test session concentrated on 5G-DRIVE dedicated GLOSA speed advice application (in combination with virtual traffic light) utilising LTE-V2X short range communication. The measured KPIs were drive through success rate and SPaT messages latency jitter. Figure 62 depicts the test route, starting position was on the right side and RSU was located on the blue spot. For the baseline scenario, ten test runs were done without individual speed advice, only concentrating on the state of the virtual traffic light on the in-vehicle HMI. For the enhanced scenario (with individual speed advice), ten test runs were performed where the driver followed the speed advice displayed on the in-vehicle HMI of the connected vehicle (Figure 63) generated by the GLOSA speed advice application. The virtual traffic light Backoffice server was in the Netherlands.

The first aim was to reveal if the GLOSA speed advice application utilising LTE-V2X short range communication would improve user perspective performance metrics (such as smooth approaching

to the intersection, automated driving comfort level, less stop and go, etc.). The second aim was to investigate if the right speed advice reduces waiting times and increases the number of passes through the intersection at green phase without stopping, to improve traffic efficiency and to minimize carbon footprint in urban areas.

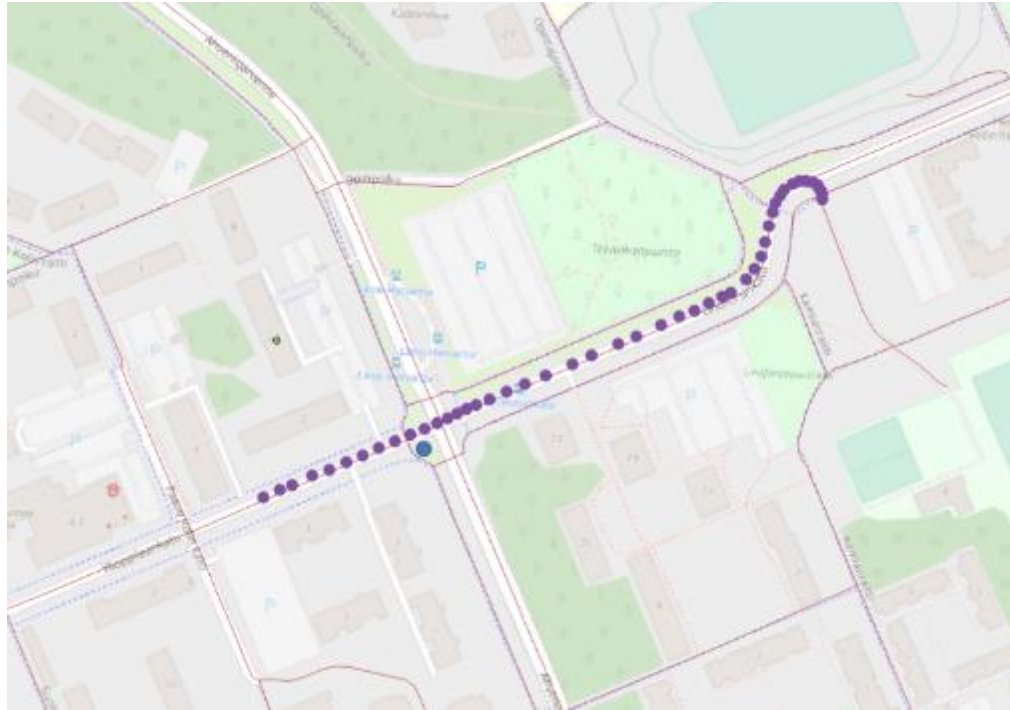


Figure 62: Test route for GLOSA measurements (start position on the right).



Figure 63: 5G-DRIVE GLOSA speed advice application by Dynniq.

The results show that the success rate (go through green phase of virtual traffic light without stopping) was 40% for baseline (without speed advice), and 90% for enhanced scenario (with GLOSA speed advice application). The result for lost messages was zero meaning none of the messages was lost.

The jitter was calculated as follows: SPaT messages were sent at 10Hz frequency. The end-to-end latency (LTE-V2X RSU to OBU) is measured on the receiving side (OBU side). The latency jitter is calculated using the same method previously described in the **RELIABILITY OF LTE-V2X COMMUNICATIONS** category. Figure 64 presents the SPaT message flow from the virtual traffic light Backoffice server. Note that, although the GLOSA speed advice application is not fully integrated in the automated vehicle, it is running inside the vehicle and displayed on the in-vehicle HMI.

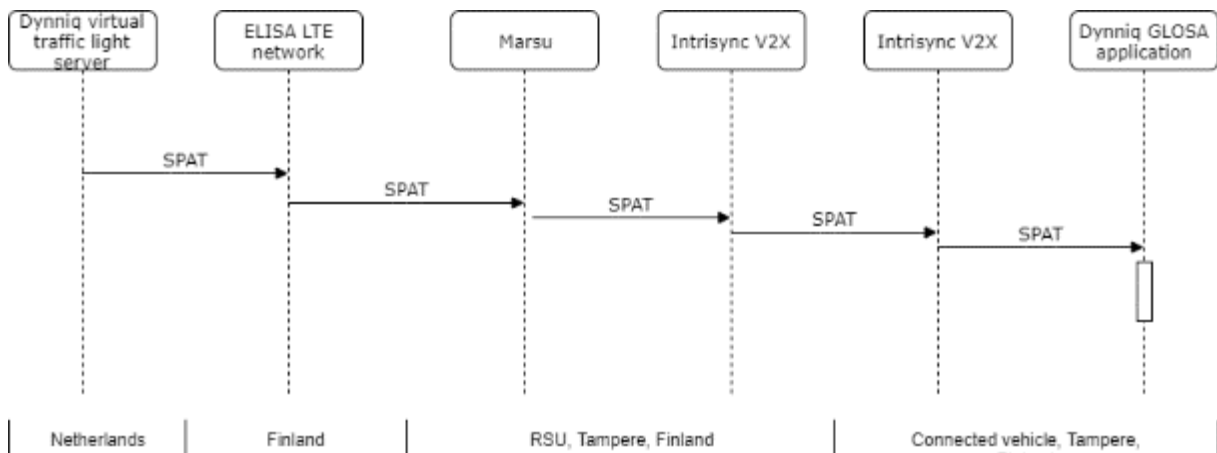


Figure 64: Sequence diagram of the SPaT message transmission.

Results of the jitter calculation are presented in Figure 65: 1st quartile is – 7 ms and 3rd quartile 14 ms. Low and high whiskers were: -37 ms and 45 ms. On this test route no mobile network handovers were detected.

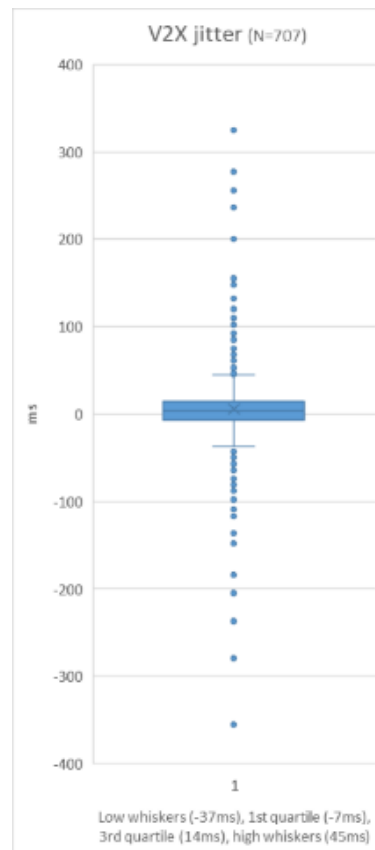


Figure 65: Boxplot of the SPaT message jitter.

4.1.1.3 Results and conclusions

The outcome of these test sessions indicates that LTE-V2X performance highly depends on antenna height and line of sight. The latencies for both 5G and V2X are stable, being 20 - 50 ms for 5G and below 30 ms for the V2X. This is the case when operating inside 5G mobile cell coverage and inside LTE-V2X coverage range. Packet error rate increases rapidly when going out of range. Virtual traffic light GLOSA concept seems to work surprisingly well even when the Backoffice server was in another country, one possible reason was that jitter values were below |10| ms value thanks to LTE-V2X (PC5) communication.

4.1.2 Ispra trial results

This section presents the findings of the operational deployment of day-1 C-ITS services in the JRC campus in Ispra (Italy) using ITS-G5 and LTE-V2X commercial devices in a non-coexistent fashion. The JRC campus is a 167-hectares research and experimentation facility with 40 km of internal roads and real-life traffic conditions (e.g., vehicles, pedestrians, and other vulnerable road users).

4.1.2.1 Objectives

The objective of the Ispra trial was to deploy a suite of day-1 C-ITS services in a real-life environment using commercial devices from the two C-ITS technologies currently available in the market (ITS-G5 and LTE-V2X). Field tests were conducted in a non-coexistent fashion – i.e., only one C-ITS technology was active at a time to avoid mutual harmful interference. The aim of the Ispra trial was to report the findings of such non-coexistent deployments and not to benchmark C-ITS technologies against each other.

To identify some of the trade-offs of key performance metrics in each standalone deployment, the Ispra trial evaluated the Packet Error Rate and average packet latency of commercial ITS-G5 and LTE-V2X devices running the entire C-ITS protocol stack (application to physical layer). To do so, ITS-G5

and LTE-V2X devices were configured and operated using the factory default settings provided by the device manufacturers¹³.

4.1.2.2 Experimental setup

Contrary to the laboratory tests described in section 2.2 (where test applications were used to generate user-defined traffic flows on top of the ITS-G5/LTE-V2X access layers), the C-ITS services deployed in the Ispra trial involved the operation of all layers in the C-ITS protocol stack. This is shown in Figure 66.

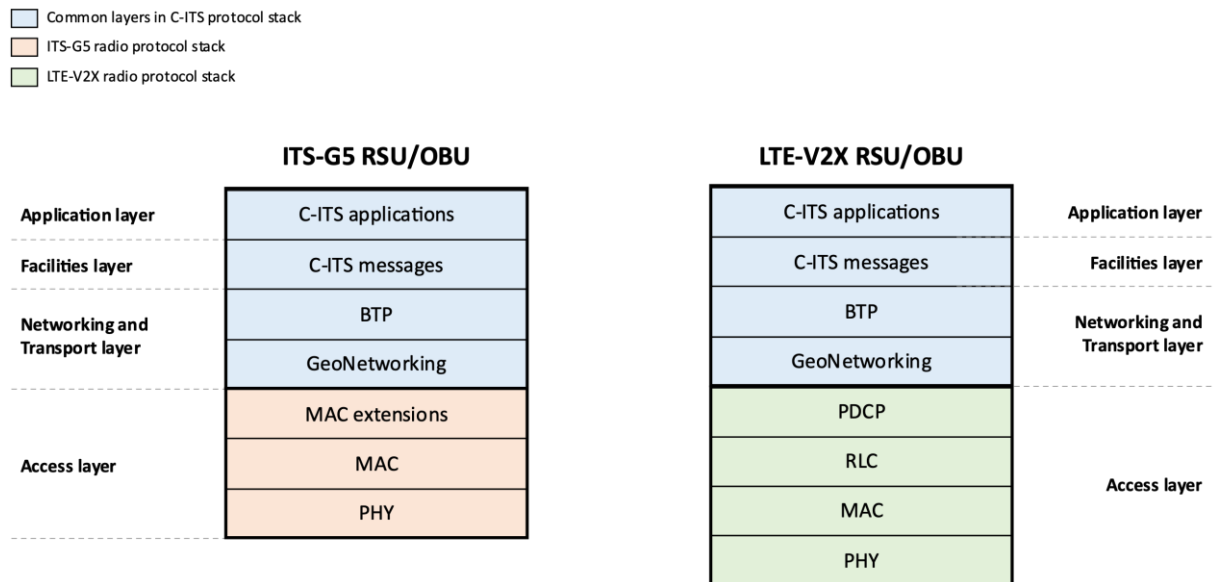


Figure 66: Protocol stack architecture of the ITS-G5 and LTE-V2X commercial devices used in the Ispra trial

For the field trial, a commercial C-ITS RSU was deployed on the rooftop of a JRC building (point A in Figure 67) at a height of approximately 7.5 metres from the road level. From point A, the RSU illuminated a 650-meter-long road section in line-of-sight conditions (determined by points B-A-C in Figure 67). The RSU was operated in field mode – i.e., it was configured to send periodic standard-compliant CAM, DENM, SPaT, MAP and IVIM messages as it would do in a real-life deployment. To emulate the information broadcast by commercial RSUs in an operational deployment, C-ITS messages contained dummy information elements, such as in-vehicle information messages, green/amber/red phase states for a virtual traffic light, GNSS coordinates for a protected DSRC tolling zone, GNSS coordinates and specific geometry of a road intersection, etc.

On the receiver side, a test vehicle was equipped with commercial C-ITS on-board units¹⁴, vehicular antennas, an Uninterruptible Power Supply (UPS) and a laptop. The test vehicle performed a test drive of several laps around an internal road track of approximately 1.7 kilometres at various speeds ranging from 30 to 60 km/h under normal traffic conditions (i.e., presence of other vehicles, pedestrians, and other vulnerable road users). For each C-ITS technology (ITS-G5 and LTE-V2X), the test vehicle performed a total of 10 laps along the internal track whilst capturing periodic C-ITS messages from the RSU. Field test results were aggregated over several test drives conducted on different days with similar weather conditions.

¹³ Device manufacturers and/or road operators might optimise the factory-default settings of C-ITS equipment depending on the specific use cases being targeted. Optimisation of factory-default settings for C-ITS devices is out of scope of this deliverable.

¹⁴ The C-ITS OBUs used in the Ispra field trial transmitted periodic CAM messages following the specific dynamics of the test vehicle.

All ITS-G5 and LTE-V2X commercial devices used in the Ispra trial were deployed out-of-the-box using the factory-default configuration provided by their respective device manufacturers.

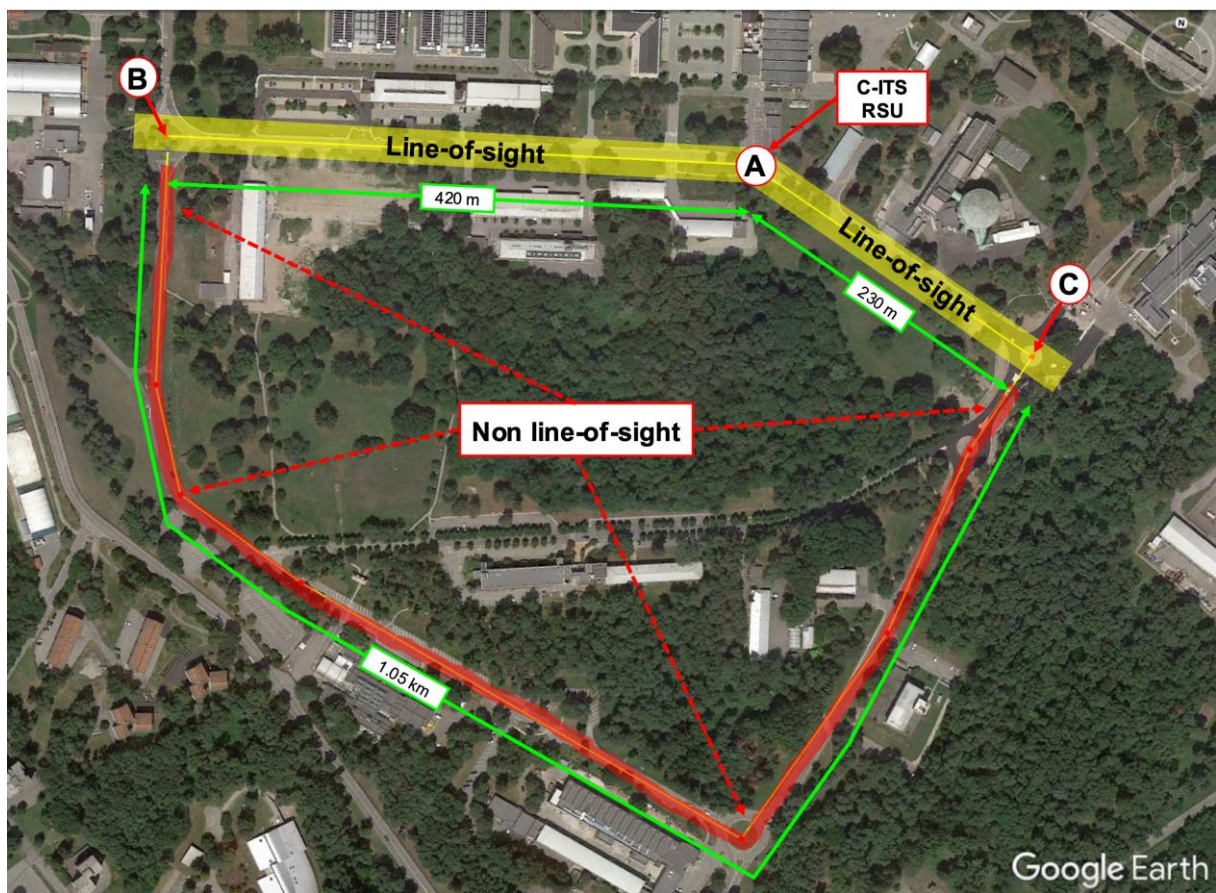


Figure 67: Internal road track of the Ispra field trial (one lap ~ 1.7 km)

No.	Time	Source	Destination	Protocol	Length	Info
58	7.781747		Broadcast	ITS	487	SPATEM(v2) [Secured (v3)]
59	8.029170		Broadcast	ITS	487	SPATEM(v2) [Secured (v3)]
60	8.038715		Broadcast	ITS	459	IVIM(v2) [Secured (v3)]
61	8.048214		Broadcast	ITS	459	IVIM(v2) [Secured (v3)]
62	8.122661		Broadcast	ITS	465	MAPEM(v2) [Secured (v3)]
63	8.132097		Broadcast	ITS	523	DENM(v2) [Secured (v3)]
64	8.141541		Broadcast	ITS	421	CAM(v2) [Secured (v3)]
65	8.281104		Broadcast	ITS	487	SPATEM(v2) [Secured (v3)]
66	8.531668		Broadcast	ITS	487	SPATEM(v2) [Secured (v3)]
67	8.781762		Broadcast	ITS	487	SPATEM(v2) [Secured (v3)]
68	9.031050		Broadcast	ITS	487	SPATEM(v2) [Secured (v3)]
69	9.122431		Broadcast	ITS	465	MAPEM(v2) [Secured (v3)]
70	9.132048		Broadcast	ITS	523	DENM(v2) [Secured (v3)]
71	9.141502		Broadcast	ITS	459	IVIM(v2) [Secured (v3)]
72	9.150810		Broadcast	ITS	459	IVIM(v2) [Secured (v3)]
73	9.160580		Broadcast	ITS	421	CAM(v2) [Secured (v3)]
74	9.281121		Broadcast	ITS	487	SPATEM(v2) [Secured (v3)]

Frame 73: 421 bytes on wire (3368 bits), 421 bytes captured (3368 bits)	
GeoNetworking_CW: Secured (TSB Single Hop)	
Basic Transport Protocol (Type B)	
ETSI ITS (CAM)	
CAM	
header	
cam	
generationDeltaTime: Unknown (60456) (0xec28, 60.456 sec)	
camParameters	

Figure 68: Example of standard-compliant C-ITS messages sent by the commercial C-ITS RSU in the Ispra trial

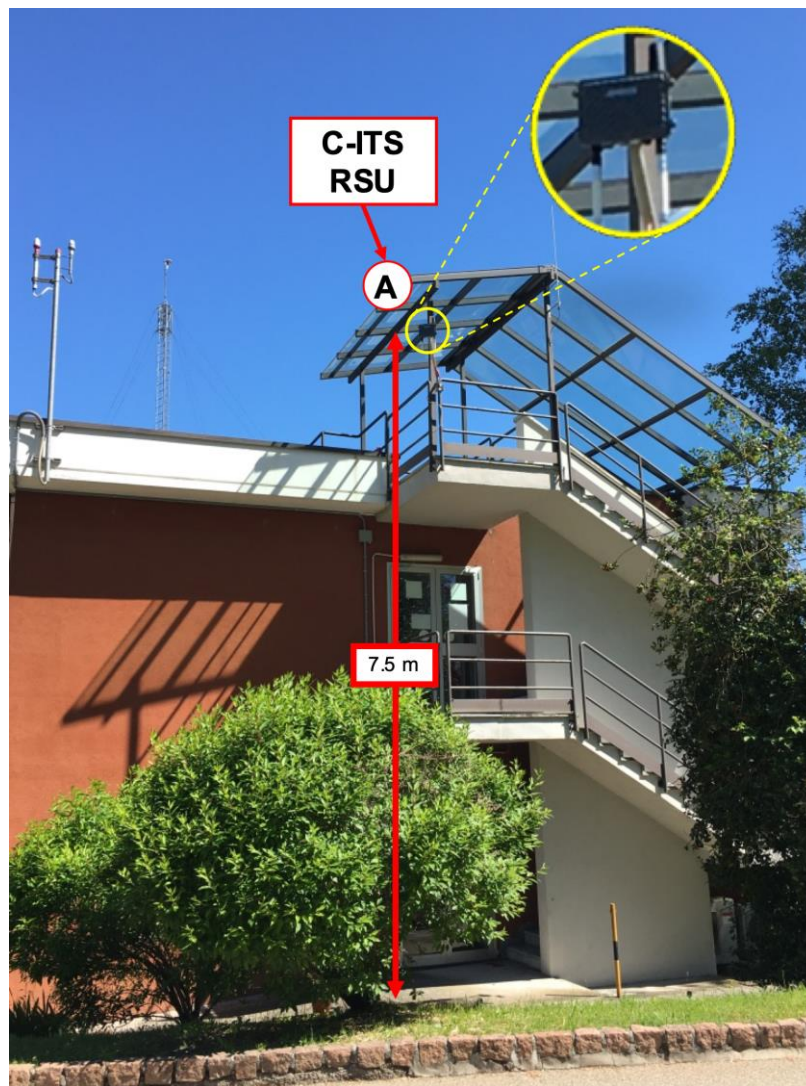


Figure 69: Height of the commercial C-ITS RSU deployed in the Ispra trial

Experimental setup of the ITS-G5 field test

For the ITS-G5 test drives, both the RSU deployed at point A in Figure 67 and the OBUs embedded in the test vehicle were commercial ITS-G5 devices operated in field mode using the factory-default settings provided by the device manufacturer.



Figure 70: Line-of-sight road section (points B-A-C, length ~ 650 m) in the Ispra trial (ITS-G5 field test)

Figure 71 shows the test setup in the field test vehicle for the ITS-G5 test drives. The on-board equipment comprised two commercial ITS-G5 OBUs connected to external vehicular antennas, an

Ethernet switch, a UPS, and a laptop for interacting with the ITS-G5 OBUs. One ITS-G5 OBU ran a live capture of ITS-G5 packets sent by the ITS-G5 RSU in monitor mode, whilst the second ITS-G5 OBU captured the GNSS coordinates of the field test vehicle to geolocate all captured metrics to a specific (latitude, longitude) tuple¹⁵. A physical architecture diagram of the experimental setup for the ITS-G5 field trial is shown in Figure 72.

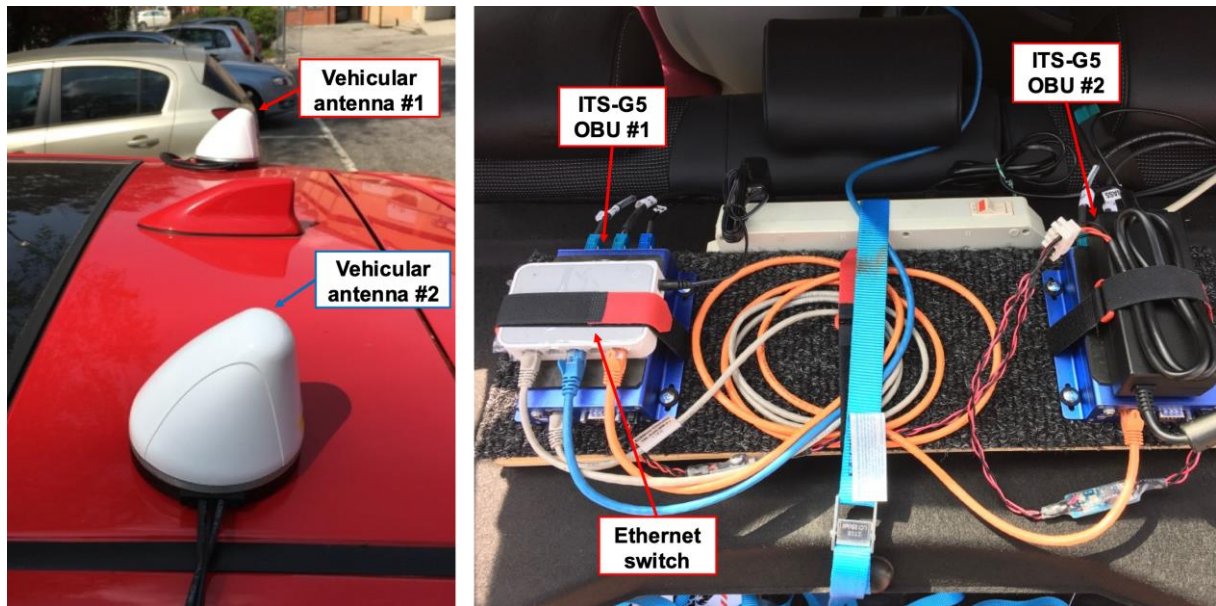


Figure 71: On-board equipment deployed in the test vehicle (ITS-G5 test drive)

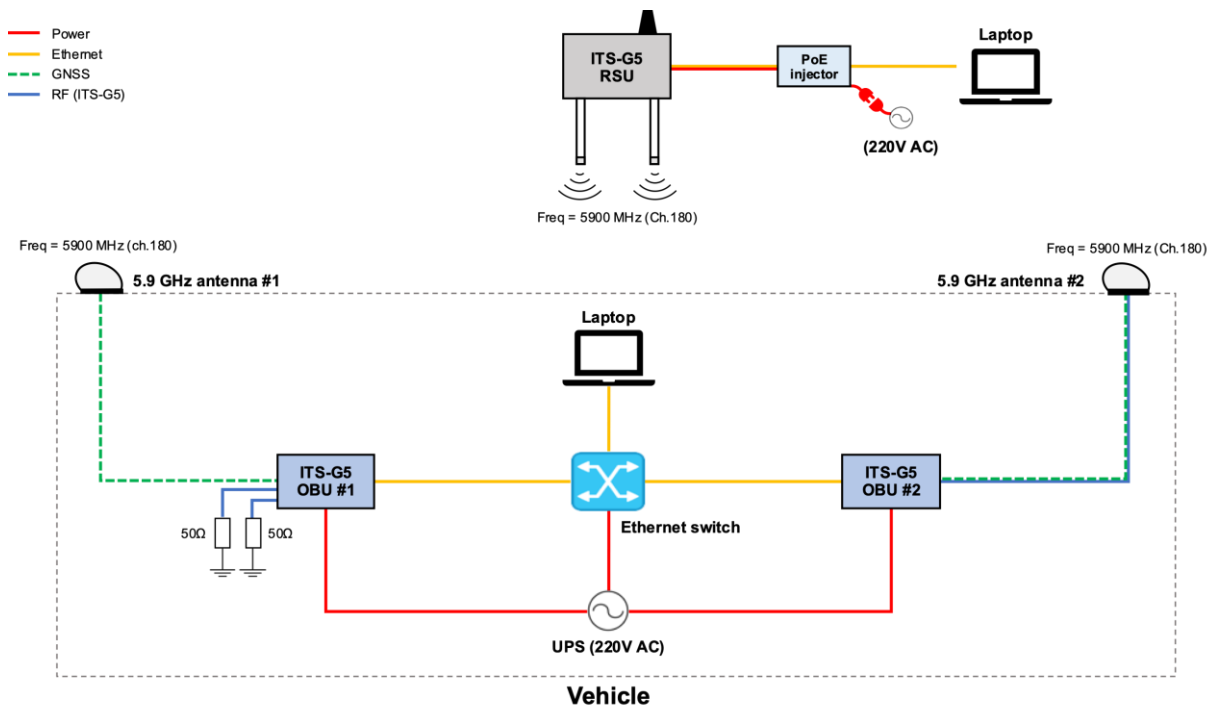


Figure 72: Physical architecture of the ITS-G5 field test trial

¹⁵ The commercial devices used in the ITS-G5 field trial support the capture of ITS-G5 packets in monitor mode. In this type of capture, the ITS-G5 radio chipset embeds PHY-layer parameters in the radiotap header of each captured packet. To isolate the capture of ITS-G5 packets sent by the ITS-G5 RSU from the GNSS coordinates generated by the ITS-G5 OBU, one OBU was dedicated entirely to capturing ITS-G5 packets, whilst the second one focused on logging GNSS data generated by its internal GNSS hardware module.

Experimental setup of the LTE-V2X field test

For the LTE-V2X test drives, both the RSU deployed at point A in Figure 67 and the OBU embedded in the test vehicle were commercial LTE-V2X devices operated in field mode using the factory-default settings provided by the device manufacturer.

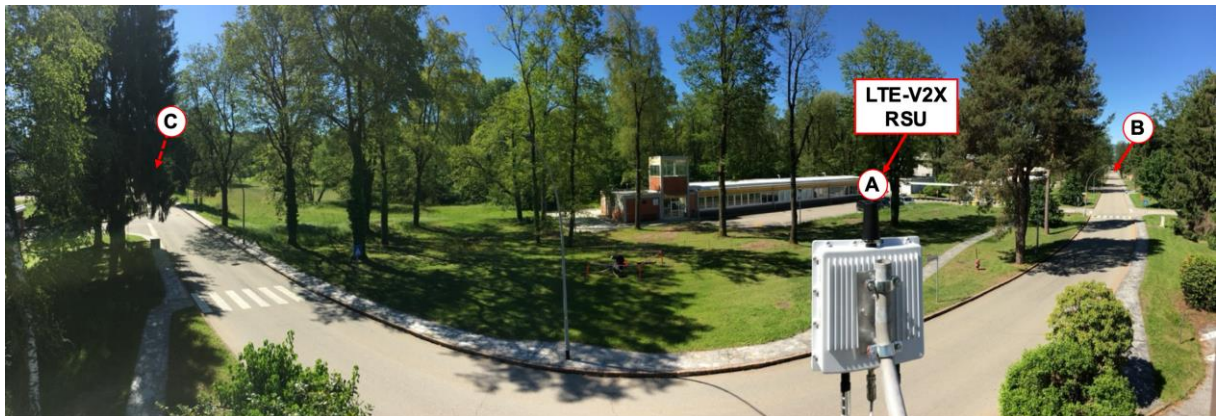


Figure 73: Line-of-sight road section (points B-A-C, length ~ 650 m) in the Ispra trial (LTE-V2X field test)

Figure 74 shows the test setup in the field test vehicle for the LTE-V2X test drives. The on-board equipment comprised a commercial LTE-V2X OBU connected to an external vehicular antenna, a UPS and a laptop for interacting with the LTE-V2X OBU. In contrast to the ITS-G5 field test setup, the LTE-V2X OBU ran a live capture of LTE-V2X frames sent by the LTE-V2X RSU in non-monitor mode¹⁶, as well as a capture of the GNSS coordinates of the field test vehicle to geolocate captured metrics to a specific (latitude, longitude) tuple. A physical architecture diagram of the experimental setup for the LTE-V2X field trial is shown in Figure 75.

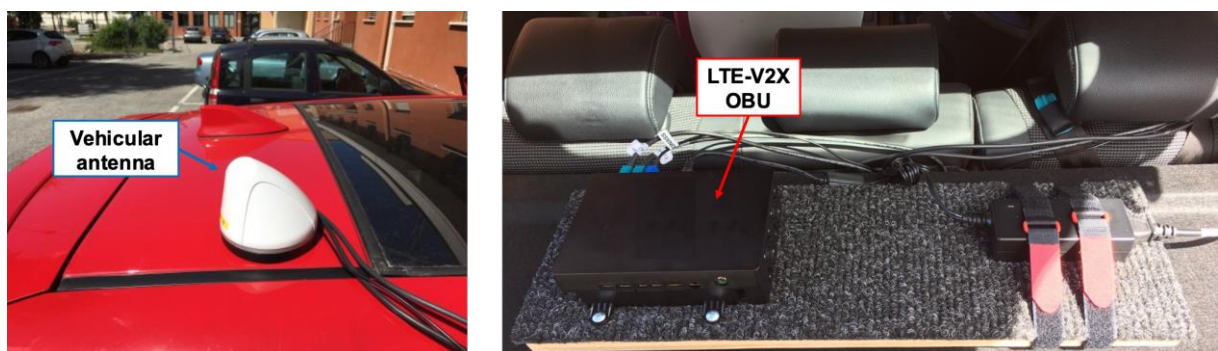


Figure 74: On-board equipment deployed in the test vehicle (LTE-V2X test drive)

¹⁶ The radio chipset in the commercial devices used in the LTE-V2X test drives does not support exposing PHY-layer parameters to upper layers via radiotap headers. In this case, a single LTE-V2X OBU was in charge of capturing both the LTE-V2X packets sent by the LTE-V2X RSU and the GNSS coordinates generated by the LTE-V2X OBU itself.

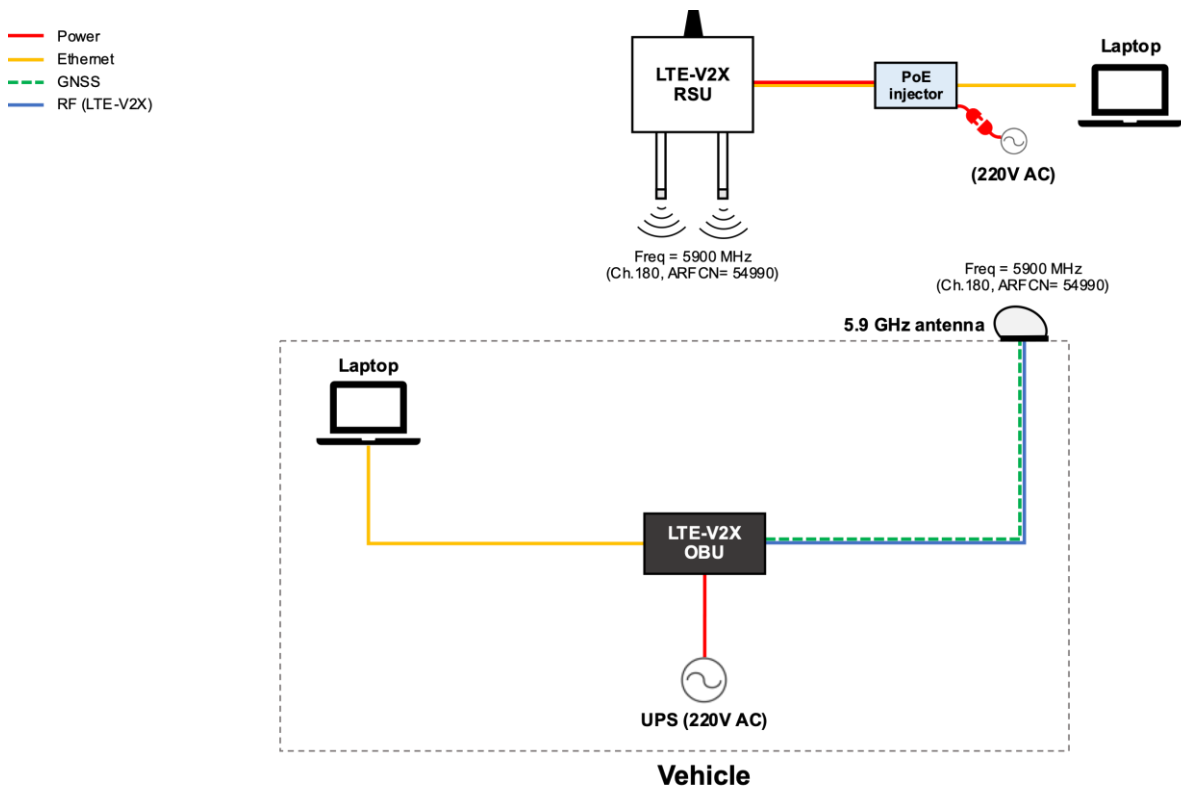


Figure 75: Physical architecture of the LTE-V2X field test trial

4.1.2.3 Results and conclusions

This section presents the observations of the Ispra field trial for both the ITS-G5 and LTE-V2X experiments. For each standalone experiment, the Packet Error Rate and end-to-end latency of C-ITS packets sent by the C-ITS RSU were evaluated. For plotting purposes, all performance metrics were geolocated to the position of the test vehicle at the exact time in which they were calculated.

Performance metric #1: Packet Error Rate

Figure 76 shows the geolocated values of PER in the C-ITS receiver for the ITS-G5 and LTE-V2X test drives carried out in the JRC Ispra site. In both cases, each PER value (coloured dot in Figure 76) was calculated over a 10-packet window of Infrastructure to Vehicle Information Message (IVIM) sent by the ITS-G5/LTE-V2X RSU¹⁷ throughout the duration of the test drive (10 laps). For both C-ITS technologies, IVIM messages were broadcast every 500 ms.

In general, PER values remained low ($\sim 0\%$) along the line-of-sight road section of the drive loop located between points B-A-C in Figure 76-a. In the ITS-G5 test drive (Figure 76-a), PER increases rapidly from 0% to 100% as the test vehicle starts driving southbound from point B into the non-line-of-sight road section of the drive loop (at approximately 420 metres from the ITS-G5 RSU). PER remains steadily at 100% throughout the entire non-line-of-sight road section of the drive loop (south of point B towards point D in Figure 76-a). As the vehicle starts heading north-east from point D towards point C, PER starts decreasing from 100% to 0% in the course of approximately 170 metres. Once the test vehicle re-enters the line-of-sight road section of the drive loop (in the vicinity of point C in Figure 76-a), PER stabilises again at 0%.

¹⁷ IVIM messages embed the Epoch timestamp at which they were generated by the C-ITS RSU in their application-layer payload. This timestamp can be used at the C-ITS receiver to calculate the PER by comparing the transmitted and received packet captures over a sliding window of user-defined length.

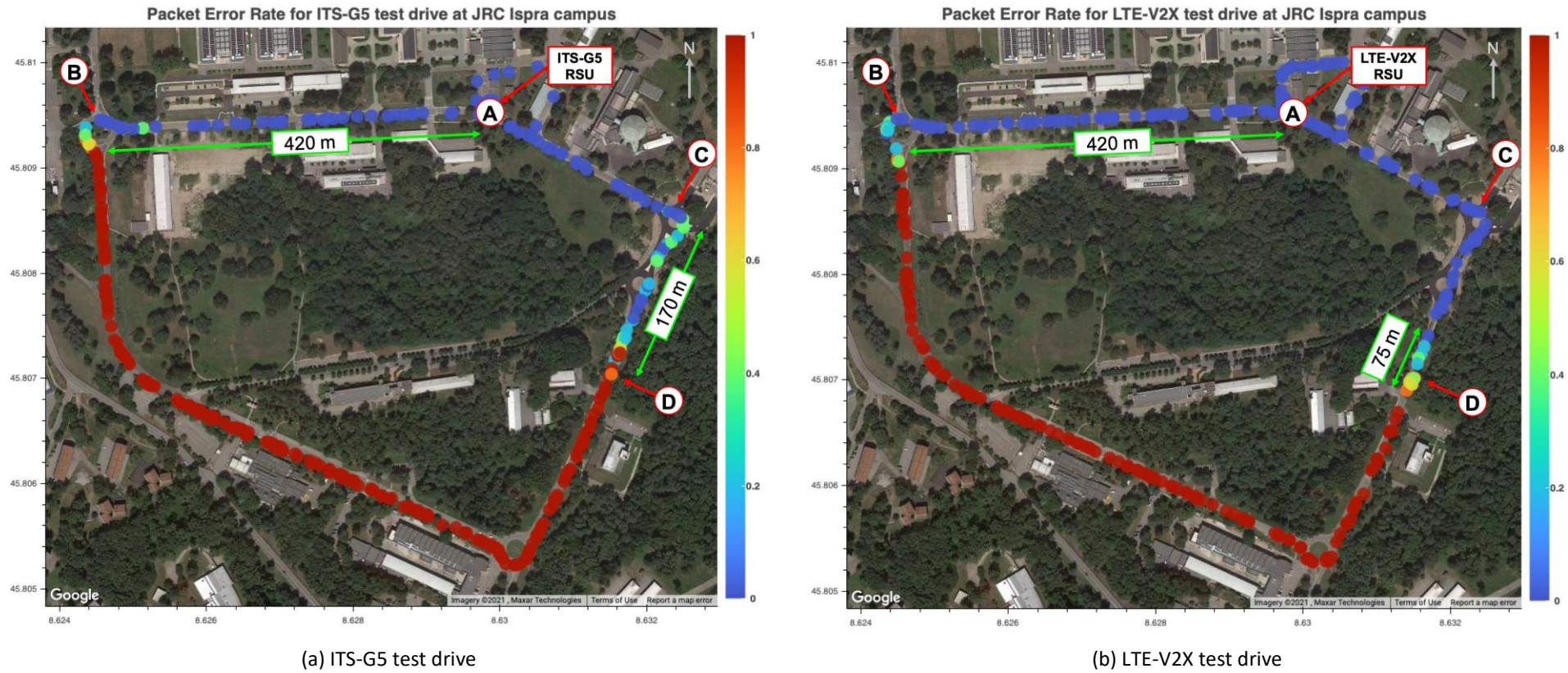


Figure 76: Geolocated Packet Error Rate values in the ITS-G5 (a) and LTE-V2X (b) test drives of the Ispra trial

In the LTE-V2X test drive (Figure 76-b), PER also increases rapidly from 0% to 100% in the vicinity of point B (i.e., at approximately 420 metres from the LTE-V2X RSU) as the test vehicle starts driving southbound from point B into the non-line-of-sight road section of the drive loop. PER remains consistently at 100% throughout the entire non-line-of-sight road section (south of point B towards point D in Figure 76-b). As the vehicle starts heading north-east from point D towards point C, PER starts decreasing from 100% to 0% in the course of approximately 75 metres. Once the test vehicle re-enters the line-of-sight road section of the drive loop (in the vicinity of point C in Figure 76-b), PER stabilises again at 0%.

Figure 77 shows the empirical Cumulative Distribution Functions of the PER values obtained in the ITS-G5 and LTE-V2X test drives. As shown in the figure, the LTE-V2X receiver showed more robustness against packet errors than the ITS-G5 receiver. This might be due to the use of blind HARQ retransmissions and turbocoding schemes, as well as to the higher energy per bit resulting from the longer transmission time of LTE-V2X transport blocks.

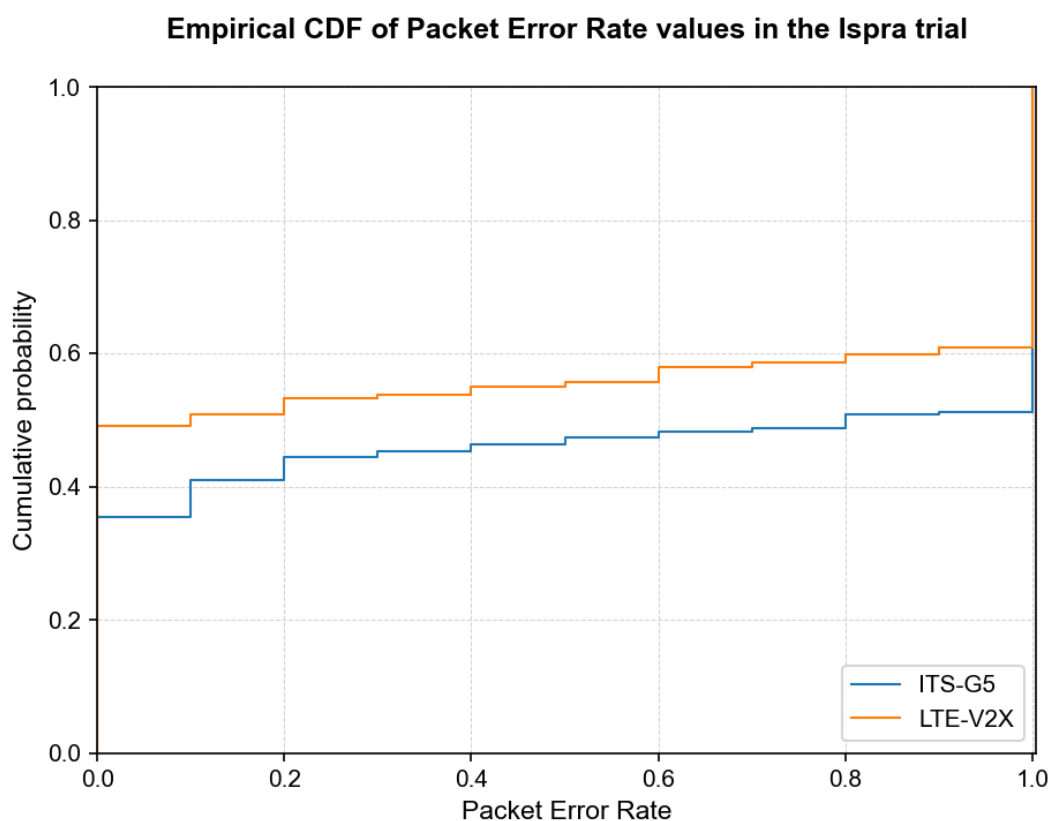


Figure 77: Cumulative Distribution Function of PER values for the ITS-G5 and LTE-V2X test drives

Performance metric #2: end-to-end packet latency

Figure 78 and Figure 79 show a graphical representation of how end-to-end packet latency has been calculated in the ITS-G5 and LTE-V2X test drives, respectively. As shown in the figures, end-to-end packet latency is defined as the delay experienced by a GeoNetworking Protocol Data Unit (GN-PDU) from the instant it is delivered to the C-ITS access layer in the transmitter until the instant the C-ITS access layer in the receiver delivers it to the GeoNetworking layer. One of the main contributions to end-to-end packet latency is the channel access delay incurred by the channel access mechanism in the C-ITS access layer (CSMA/CA in ITS-G5 and SPS in LTE-V2X).

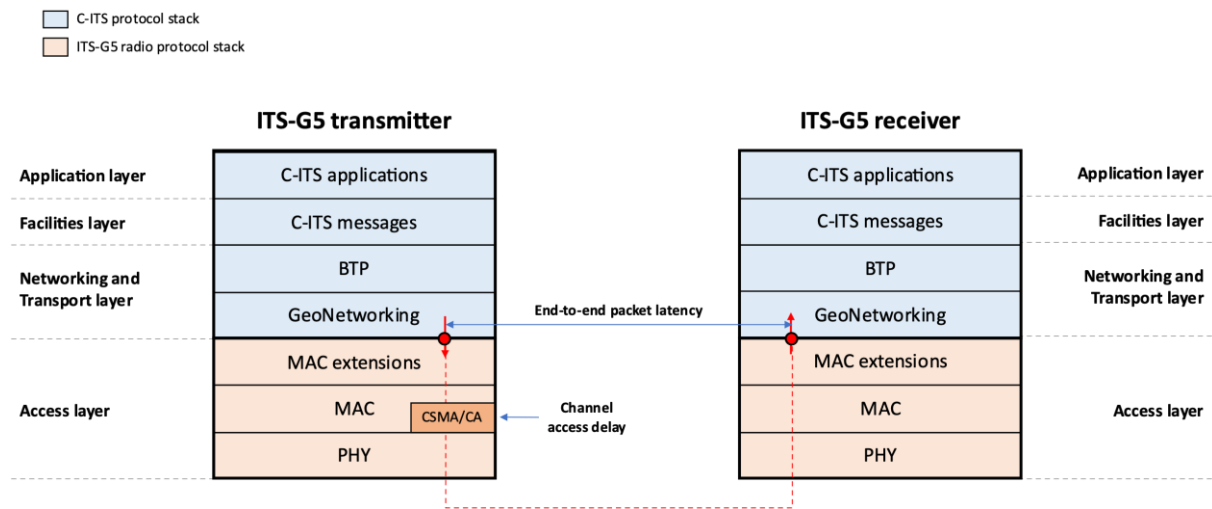


Figure 78: End-to-end packet latency (ITS-G5)

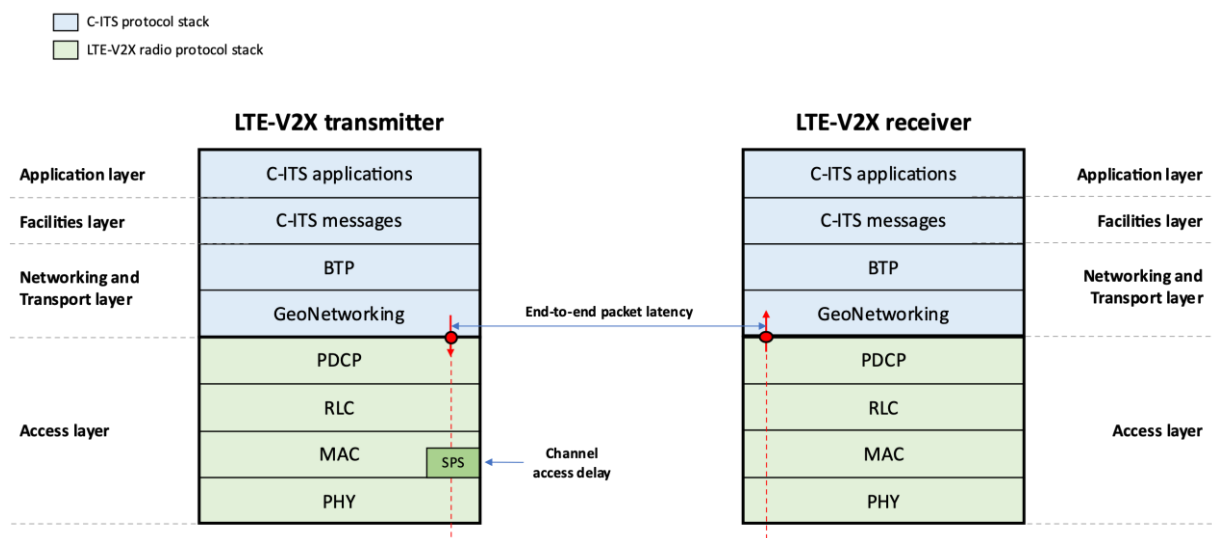
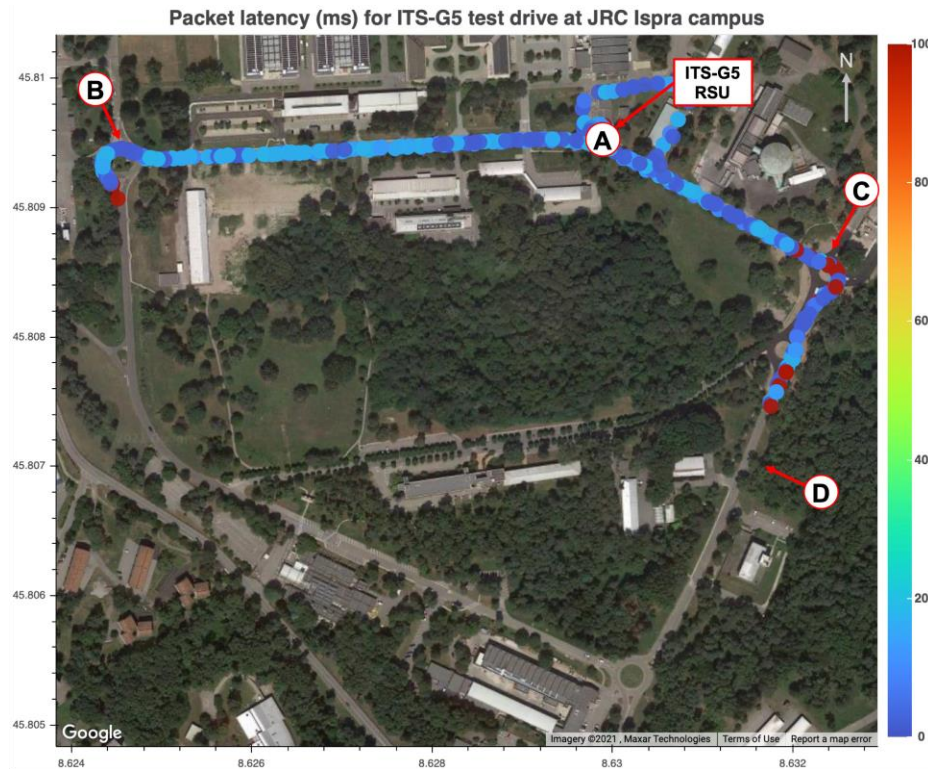


Figure 79: End-to-end packet latency (LTE-V2X)

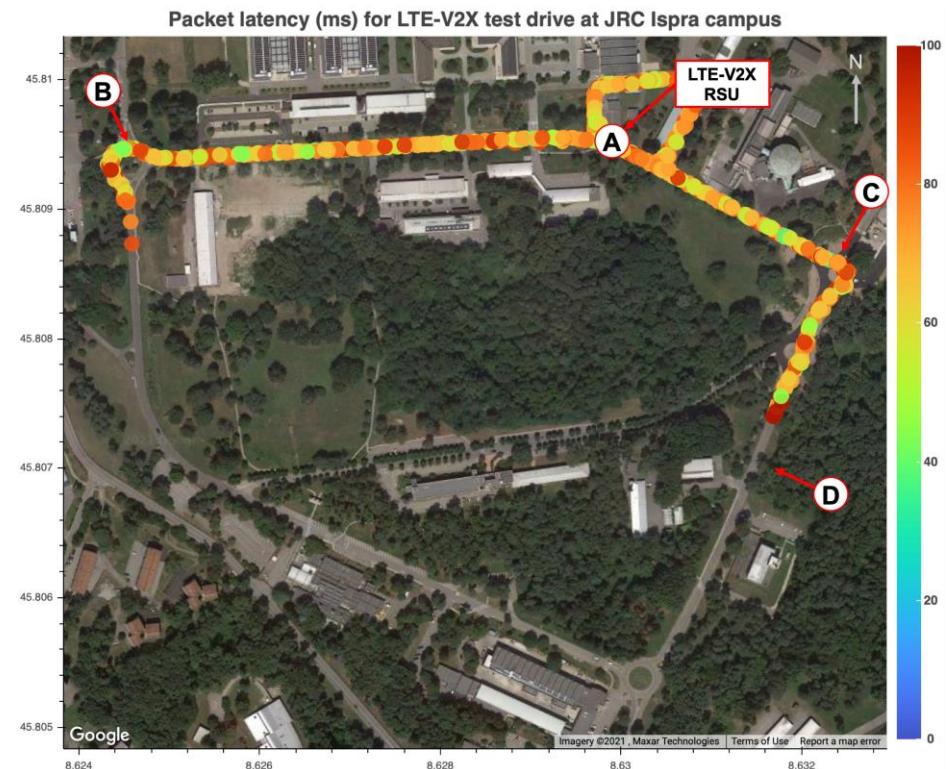
Figure 80 shows the geolocated values of packet latency for the ITS-G5 (a) and LTE-V2X (b) test drives in the Ispra trial. In both cases, latency was calculated for every IVIM packet successfully received in the ITS-G5/LTE-V2X OBU¹⁸. IVIM messages were broadcast every 500 ms. The lack of packet latency samples along the non-line-of-sight section of the drive loop (south of point B towards point D) is a consequence of the high PER (100%) experienced by both the ITS-G5 and LTE-V2X receivers in that road section.

In general, end-to-end packet latency values were lower in the ITS-G5 test drives than in the LTE-V2X test drives. This expected behaviour is due to the way in which the channel access mechanism of each C-ITS technology operates. ITS-G5 features an opportunistic CSMA/CA channel access mechanism, thus transmitting packets as soon as the shared medium is sensed idle for a certain period of time. LTE-V2X features a Semi-Persistent Scheduling mechanism that aims at keeping per-packet latency values within a user-configurable Packet Delay Budget (PDB) – e.g., 20 ms, 50 ms or 100 ms, depending on the specific C-ITS service requirements.

¹⁸ To keep the number of geolocated packet latency samples in the same order of magnitude of PER samples and to speed up post-processing of field test results, packet latency was calculated over IVIM packets successfully received in the ITS-G5/LTE-V2X OBU.



(a) ITS-G5 test drive



(b) LTE-V2X test drive

Figure 80: Geolocated packet latency values in the ITS-G5 (a) and LTE-V2X (b) test drives of the Ispra trial

Figure 81 shows the CDFs of packet latency values for the ITS-G5 test drive (**blue datapoints**) and LTE-V2X test drive (**orange datapoints**). As shown in the figure, packet latency in the ITS-G5 test drives was upper-bounded at approximately 24 ms (as per the opportunistic nature of the CSMA/CA channel access mechanism). On the other hand, packet latency in the LTE-V2X test drives was upper-bounded at approximately 108 ms (as per the ability of the SPS algorithm to keep per-packet latencies within a configurable Packet Delay Budget). These results suggest that the factory-default settings of the commercial LTE-V2X devices used in the Ispra trial assigned a PDB of 100 ms to IVIM messages. This PDB value is in line with the latency requirements defined in 3GPP TS 22.185 [18].

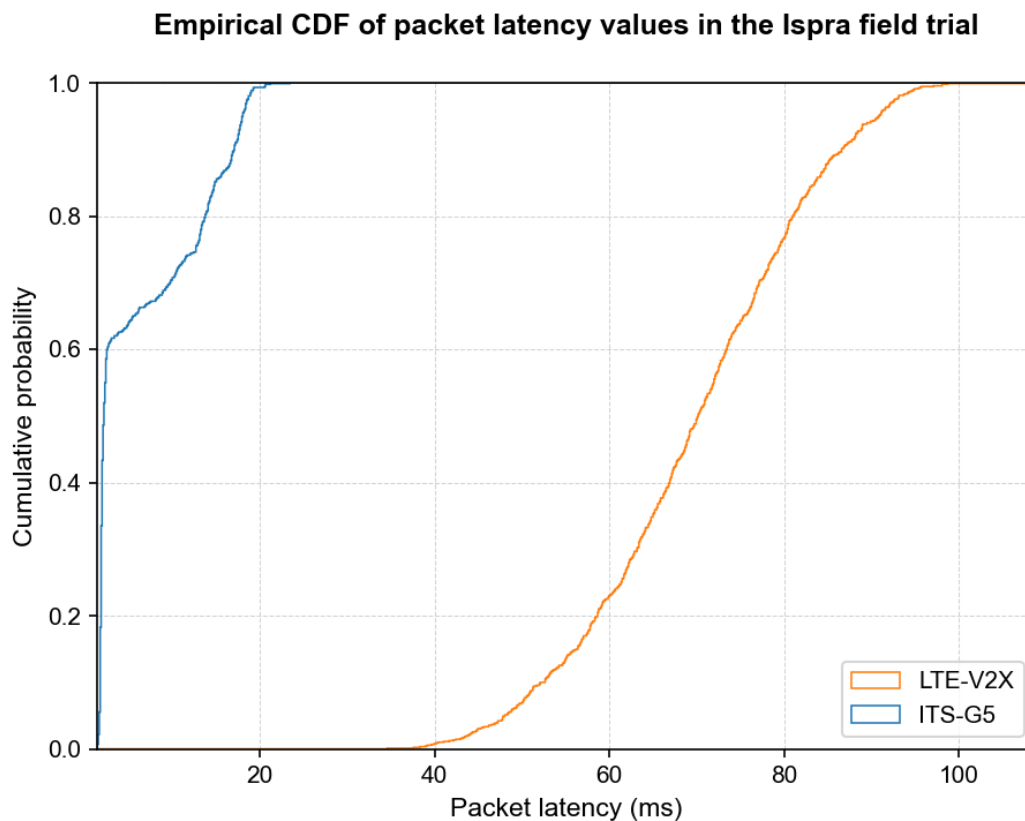


Figure 81: Empirical CDF of end-to-end packet latency for ITS-G5 and LTE-V2X in the Ispra trial

Summary of conclusions

In terms of **Packet Error Rate**, results show that the access layer in the LTE-V2X devices used in the field tests behaved more robustly than that of the ITS-G5 devices due to the performance gains of blind HARQ retransmissions and link-layer turbocoding schemes. A detailed analysis of the impact of PER on upper-layer C-ITS services is left for future research.

As far as **latency** is concerned, field tests results show that ITS-G5 packets experienced lower end-to-end delay than LTE-V2X packets in clean channel and low load conditions. In both test drives, end-to-end latency values complied with the service requirements for V2X services set out in 3GPP TS 22.185.

4.1.3 Enhancement trials and studies results

This section presents the findings from three enhancement trials and studies: vehicle hybrid positioning trials, study of key V2X link budget parameters and impact on Espoo/Tampere results, and study of communication interruption in MEC-based V2X services.

4.1.3.1 Hybrid positioning trials

The Vediafi hybrid navigation and accurate positioning tests were performed at Karaportti and Otaniemi test sites in Espoo together with VTT. The tests were done in an open-road environment with test cars from VTT and Vediafi (see Figure 82). Hybrid navigation tests aimed to study how multi-sensor navigation and C-V2X network location information can enhance the quality and the availability of positioning solutions. The RTK (Real-Time Kinematics, see 5G-DRIVE deliverable D4.1[19]) accurate positioning solution was used as the foundation for positioning as it can produce centimetre-level precise positioning. This base information was supported and complemented with additional positioning solutions and data sources in the hybrid navigation by utilizing data fusion.



Figure 82: Hybrid navigation test vehicles

Multi-channel radio and inertial navigation were used in the first phase tests to improve positioning quality (see Figure 83 top half). Afterwards, this study was complemented with the use of C-V2X C-ITS message stack and location information, which is part of official Day 1 messages. The aim was to share C-ITS message location information between RSU and OBU to get one additional location information source, which can also be used to enhance the positioning of the vehicle further. This kind of information could be used in full, if GNSS information is lost because of system interruption or lack of satellite connectivity. Such an unwanted situation might occur because of covered road sections or urban environments where buildings block the connection, for example.

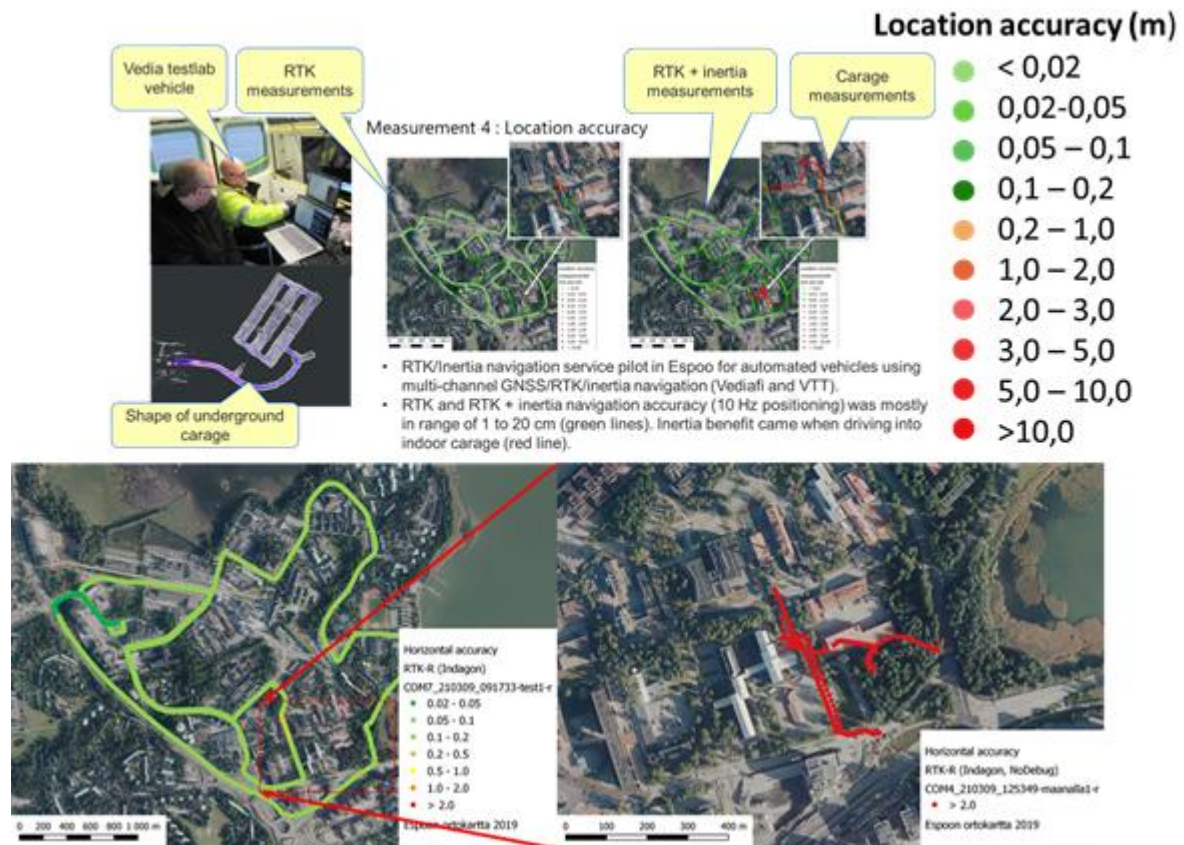


Figure 83: Comparison of good positioning accuracy and weak signal (green 0,02-0,5m and red >2m, on open-road (left side) and underground measurements (right side).)

However, with additional positioning data sources, some information can be provided to the system to maintain its location. These supplementing systems can be used as backup or supporting systems as an additional location data source, but they do not provide the same accuracy as primary systems, such as GNSS with RTK. For example, when RTK can provide 1-2 cm accuracy, GPS can provide meters' level accuracy, and additional data sources can tell which direction the vehicle is going or information that the vehicle is somewhere close to a certain RSU.

Maintaining continuous location and timing messaging information at least at some level is essential since without it, Day 1 messages cannot be sent between OBU and RSU. Before actual message exchange, RSU and OBU need to be synchronized to be able to open the message channel, which can be used to share location information between the devices. Location information is also part of GeoNetworking protocol which is part of V2X communication. Based on this information exchange, the RSU can process OBU's location information and maintain its capability for C-ITS messaging. Even if the location information is not very accurate, it would permit to establish a communication using Day-1 messages.

Hybrid navigation field tests

Based on Vediafi's field tests, vehicle positioning via GNSS is the most prevalent and lack of GNSS satellite signals is common in some areas. In underground parking halls, where satellite signals are blocked; road tunnels and building areas where signals are partially blocked, signals suffer multipath interference, causing lower positioning accuracy or even the lack of location information.

Out of GNSS signal, the Inertial Measurement Unit (IMU), combined with previous RTK accuracy, creates a temporary relief. Based on 5G-DRIVE project test results in 2020, IMU shows an advantage when GNSS signals are not available (see Figure 84 and Figure 85). During test planning phase, we recognized challenges with commercially available connected vehicles which were using North America continent frequency band and private certificates. Therefore, these field tests were done with one OEM RSU and OBU pair to avoid communication compatibility issues. Besides, C-V2X

communication could help support the inertial navigation system when inertial navigation accumulated errors in position increase over time. The position accuracy is weakened by distance, and the possible vehicle turning manoeuvres.

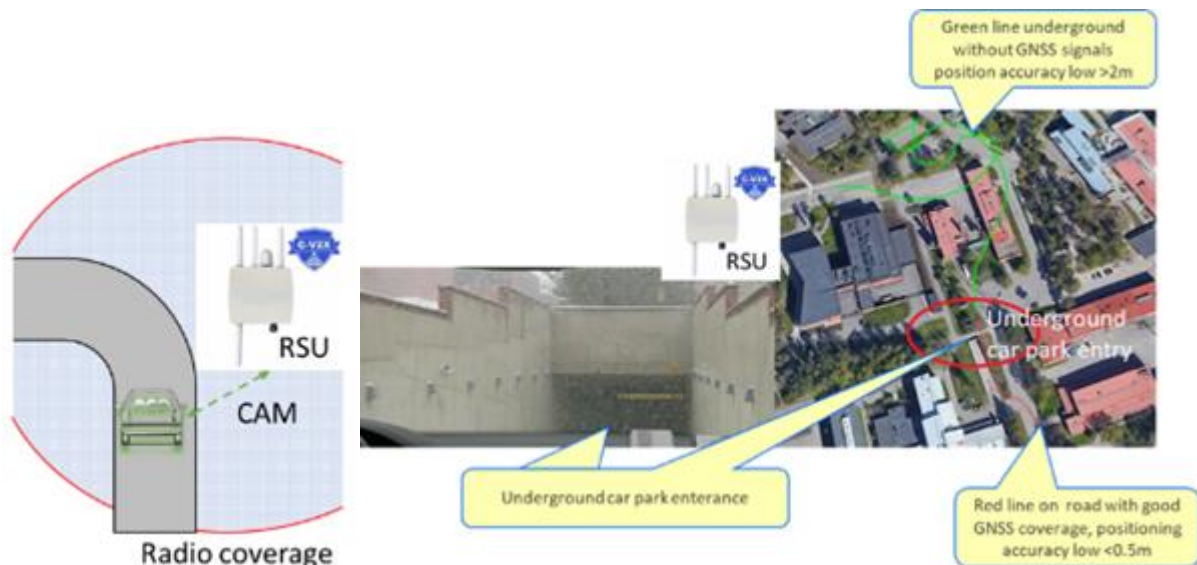


Figure 84: GNSS positioning with IMU's support enabling weakening positioning accuracy when entering an underground parking area (C-V2X RSU located on entry) with a weak GNSS signal (green $>2\text{m}$ and red $<0.5\text{m}$).

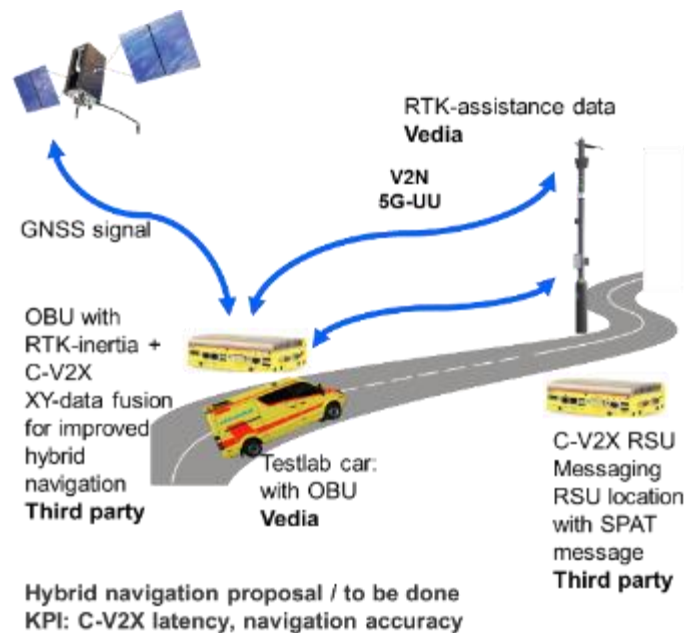


Figure 85: The test setup for hybrid navigation testing

However, the C-V2X enables a RSU and OBU to transmit and receive CAM messages with information such as current location, speed, etc., which is a potential solution to overcome the above challenge and provide a mean for error correction. The field trial findings indicate that GNSS satellite signals are utilized to ensure the C-V2X stack starting correctly and without GNSS signals devices are not fully operational, known relation with GNSS signals usage for communication links synchronization defined by 3GPP. GNSS-based location information (longitude and latitude) is part of GeoNetworking protocol-based messages routing. Although GNSS-based location can be overruled with a fixed location, missing GNSS satellite signals generate issues with C-V2X stack and limit possibilities to manage devices, as stack is not properly started without GNSS signals. Since GNSS signals do not exist underground and all radio connectivity will be a challenge inside, C-V2X positioning would be supported by utilizing synchronized RSU to keep the OBU-RSU messaging alive. Yet, the actual positioning would have accuracy limitations in practice.

The communication between the RSU and the OBU is extremely limited without GNSS coverage. Typical GPS positioning accuracy is not enough for lane level, especially inside densely built areas, indoors, and on surface parking halls. Furthermore, in underground parking areas without any visibility to satellite signals, an accurate position cannot be determined, and inertial (Dead Reckoning) accuracy fading with distance and manoeuvres.

The overview of the results from the field trials described above (mean values with three test runs) is shown in Table 26. It compares C-V2X improvement regarding each GNSS method and fix measured in trial tests. In densely built areas, the results show that C-V2X positioning improvement is limited when a single C-V2X-RSU and a moving vehicle equipped with RTK float accurate positioning and C-V2X OBU were used in the trials. Table 26 shows the complete list of trial combinations between C-V2X and each GNSS method.

GNSS method and fix in built areas	Position ellipse confidence (Major) (meter)	Position ellipse confidence (Minor) (meter)	C-V2X accuracy improvement (meter)
RTK fix	0.5	0.3	None
RTK float	10.21	7.27	None
GPS	27.62	5.36	None
Dead Reckoning (Inertial), after last known position fading	N.A. (Large)	N.A. (Large)	20-50 (position circle within narrow underground parking area driving lane)
No satellites signals, no base position	No position / N.A.	No position / N.A.	20-50 (position circle within narrow underground parking area driving lane)

Table 26: The measured values (ellipse confidence and C-V2X improvement) FOR different GNSS Methods

Hybrid navigation test setup

Vediafi's test lab vehicle was used for tests. The RTK device and LTE-V2X OBU were integrated to the vehicle, while the LTE-V2X RSU was installed at stationary position inside the parking hall and at the entry of parking hall. Figure 86 demonstrates trial setup and environment in Espoo Finland in spring 2021. All the results are described above in Table 26.



Figure 86: Vediafi's test vehicle and RSU.

Potential usage of GNSS repeater

With GNSS repeater comes the possibility to get satellites signal underground. Underground 5G network coverage is tested for the "synchronization" of RSU and OBU to keep communication working.

With multiple RSUs, the possibility of chaining GNSS information to an area without coverage and calculating a moving vehicle OBU location should theoretically increase the positioning accuracy by numerous connection points (triangulation of a signal). Lack of multiple test RSUs leads this to be a more theoretical approach (see Figure 87).

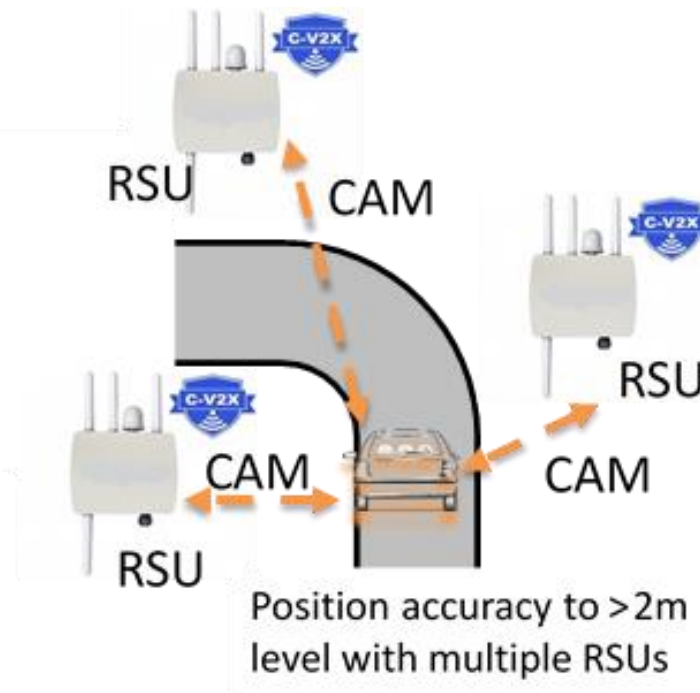


Figure 87: Positioning with RSU network.

Vehicle recognition via C-V2X

In Vediafi's pilots, we realized that C-V2X could also be used to combine, e.g., vehicle-specific CO₂ emissions data to passing OBU/vehicle when the vehicle's identification is part of the RSU-OBU-messaging. In the Vedia Clean Vehicles Wizard reporting solution [20], a vehicle ID is connected to vehicle-specific emissions. In such a case, the vehicle ID, with relevant data, needs to be implemented in the C-V2X messaging structure to enable such service. Protection of personal data is implemented with encryption and secure communication certificates. Practical testing with commercial vehicles would be needed to verify the vehicle's identification and relevant data sharing approach. Practical use cases are numerous, as cameras perform vehicle recognition at entries of paid parking areas and help restrict the usage of special designated lanes or areas to certain vehicles. Also, an opportunity to use V2X messages with vehicle identification to open wider data sharing or even software updates over the air.

Besides participation in joint EU-China trial planning and preparations together with WP4 partners, and in addition to the hybrid positioning trials, Vediafi has prepared EU-Russia-China test drive ion wider project collaboration together with VTT, Finnish authorities and Russian authorities. Aim of this test drive was to enable device testing with same devices in EU and China. Because of COVID-19 the actual pilot drive from Finland to China did not happen, but preliminary test drive was driven from Finland to East Russia close to the border of Russia and China in December 2020. There is still a plan to do the pilot drive on late summer 2021 but it is not yet confirmed due to the COVID-19 situation.

4.1.3.2 Key V2X link budget parameters and impact on Espoo/Tampere results

In 5G-DRIVE, one of the objectives for Tampere trial was to explore the factors which affect the performance of LTE-V2X. Based on Tampere trial results, the V2X link budget model is provided to analyse the impact of key parameters affecting the V2X communication performance. The trial results used for the following performance analyses mainly comes from the Tampere trials which have an LTE-V2X connection established between a single base station (BS) and a vehicle.

In Tampere trials, V2I communications was set up and can be illustrated as Figure 88. In the V2I communication system, considering the roadside environment around the BS and vehicle in the trials, a radio signal transmitted from the BS encounters multiple objects, such as the road kerbs, road median dividers and other vehicles. Therefore, the vehicle, as a receiver, will receive copies of the transmitted signal which are reflected, diffracted, and scattered from these objects, besides receiving the signal from the line-of-sight (LOS) transmission along the straight line between the BS and vehicle. Therefore, the V2I channel is considered as a multipath channel, including a potential LOS path and reflected, diffracted, or scattered path components. Based on the set-up of the trials, the following parameters are also considered in the link budget model:

- 1) The carrier frequency is 5.9 GHz and the channel bandwidth, B_s , is 10 MHz. The carrier signal's wavelength is 0.05 m.
- 2) The height difference between the BS antenna and vehicle antenna is denoted by d_h .
- 3) The speed of the vehicle is denoted by v .
- 4) the distance between the BS and vehicle is denoted by d_s .

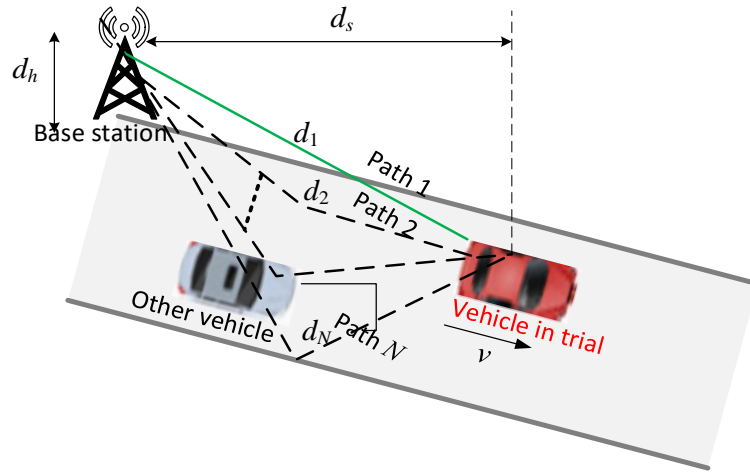


Figure 88: V2I communication model

For a multipath channel, its key characteristics include its nature of time-varying and delay spread caused by the delay difference between different paths. At an instantaneous time t , the impulse response of the time-varying multipath channel can be given by

$$h(t) = \sum_{n=1}^{N(t)} [\alpha_n(t) \cdot e^{-j(2\pi f_c(t-\tau_n(t)) + \varphi_{Dn}(t))} \delta(t - \tau_n(t))]$$

Equation 3

where at time t , $N(t)$ is the number of path, $\alpha_n(t)$ is fading amplitude of path n , f_c is the carrier frequency, $\tau_n(t)$ is the delay of path n , and $\varphi_{Dn}(t)$ is Doppler phase shift, given by $\varphi_{Dn}(t) = \int_t 2\pi f_{Dn}(x) dx$. $f_{Dn}(t)$ is the Doppler shift cause by the speed of the vehicle, v . Here, $f_{Dn}(t) = v \cos(\theta_n(t)) / \lambda$, where λ is the wavelength of the carrier signal and $\theta_n(t)$ is angle of arrival for path n .

Thus, due to the multipath effect, for a received signal, inter-symbol-interference (ISI) will be introduced from signals transmitted at previous symbol periods. The received signal at the vehicle can be given by

$$y(t) = x(t - \tau_1(t)) \otimes h(t) + \sum_{n=2}^{N_s(t)} x(t - \tau_n(t)) \otimes h(t) + \sum_{i=1}^{N_I(t)} [x(t - iT_s) \otimes h(t)] + n_0(t)$$

Equation 4

where \otimes indicates the convolution operator. $n_0(t)$ represents the additive white Gaussian noise (AWGN). $x(t)$ denotes the signal transmitted at time t . T_s is the symbol period. $N_s(t)$ indicates the number of paths from which the copies of the signal would be received at the symbol duration of the signal received from the first path. $N_I(t)$ represents the number of interfering symbols from the previous symbol periods. The maximum value of $N_I(t)$ is $N_I(t) = \lceil \tau_{max}(t)/T_s \rceil$, with $\tau_{max}(t)$ denoting the maximum multipath delay.

$\sum_{n=2}^{N_s(t)} x(t - \tau_n(t)) \otimes h(t)$ indicated the copies of the signal received within the symbol duration. Therefore, in Equation 4, the first two items are the desired signal to be received from different paths during a symbol duration. The $\sum_{i=1}^{N_I(t)} [x(t - iT_s) \otimes h(t)]$ is the sum of the interfering signals from the previous symbol periods.

It can be seen from Equation 4, that the received signal may experience intra-symbol interferences and inter-symbol interferences. Considering the bandwidth of the channel is 10MHz, the symbol duration of the signal, T_s , is 0.1us. Based on measurement, the Root Mean Square (RMS) delay spread in a typical urban environment is approximately to be 2.5us, and it could be larger in rural environment due to the attenuation of the ISI from multipath not being at the same degree as in cities [21]. Considering the trial environment in Tampere, the environment is between a busy urban area and a rural area. Therefore, it can be assumed that the interference is mainly coming from the inter-symbol interferences (ISIs). The received signal includes the signal received from the first path and ISIs, given by

$$y(t) = x(t - \tau_1(t)) \otimes h(t) + \sum_{i=1}^{N_I(t)} [x(t - iT_s) \otimes h(t)] + n_0(t)$$

Equation 5

Taking the effect of channel estimation error caused by Doppler shift and ISI, the received signal to interference plus noise ratio (SINR) is given by

$$\gamma(t) = \frac{p_t \cdot \alpha_1^2(t)}{\sigma_e^2(t) + \sigma_I^2(t) + \sigma_0^2}$$

Equation 6

where p_t is the transmit power. $\sigma_e^2(t)$ represents the channel estimation error caused by Doppler shift. $\sigma_I^2(t)$ is the power of the sum of ISIs. σ_0^2 is the power of AWGN noise.

A. Impact of Doppler Shift

In the V2I system, the Doppler shift can cause the channel estimation error, which will impair the system performance. According to [22] and [23], for the minimum mean square error (MMSE) associated optimal channel estimator, the channel estimation error for each subchannel can be assumed to be Gaussian distributed and its variance is related to the Doppler shift, which is given by

$$\sigma_e^2(t) = \frac{1}{1 + \frac{E(p_t \cdot \alpha_1^2(t))}{\sigma_0^2} \left(\frac{B_s}{f_{D1}(t)} \right)}$$

Equation 7

where $f_{D1}(t)$ is the Doppler shift.

In Tampere trials, the maximum speed of the vehicle is 40km/hour and the carrier frequency of the system is 5.9 GHz, resulting in the maximum Doppler frequency shift of $f_{D1} = 218.5$ Hz. Generally, the received signal to noise ratio (SNR), $\frac{E(p_t \cdot \alpha_1^2(t))}{\sigma_0^2}$, is larger than 0 dB. Normalised by the received SNR, $\frac{E(p_t \cdot \alpha_1^2(t))}{\sigma_0^2}$, the channel estimation error from Doppler shift is no more than 0.002%. Since the channel bandwidth, B_s , is much larger than the Doppler shift, compared to the received SNR, the impact of the estimation error caused by Doppler shift is not significant, and somehow can be ignored.

Based on this analysis, it can explain that in the Tampere trials, when the autonomous vehicle ran at the speeds of 5 km/h, 10 km/h, 15 km/h, 20 km/h, 30 km/h and 40 km/h, the mean delay and jitter are not affected significantly by the variation of the speed, as shown in Figure 55 and Table 21.

B. Impact of Multipath

In the system, multipath could have two kinds of impact. One is to improve the system performance due to multipath diversity, which requires all the paths are resolvable at the receiver. That is, each individual path can be identified at the receiver, which has high requirement on the receiver's circuits design and can impose high cost at the receiver. Generally, current commercial mobile device do not have the capability of exploring multipath diversity. The other impact is to bring in ISI, which can degrade the system performance. Due to the impact of multipath, during the receiving period of a signal, the signal could be combined with signals which were transmitted in the previous symbol periods, and therefore, experience ISIs. In 5G-DRIVE trials, the receiver at the testing vehicle are not capable of exploring the multipath diversity gain, but it experienced ISI caused by multipath. Therefore, in this sub-section, the impact of multipath on ISI is investigated.

Assuming the transmit power, p_t , is the same during all the symbol periods, the total power of the ISIs can be obtained as

$$\sigma_I^2(t) = \sum_{i=1}^{N_I(t)} [p_t \cdot \alpha_{n_i}^2(t)]$$

Equation 8

where $\alpha_{n_i}(t)$ is the amplitude of the fading for the i th ISI from the n_i th path.

Figure 89 illustrates the impact of number of paths on the bit error rate when there is an LOS path. In the trial, with the bandwidth of 10MHz, the symbol duration is 0.1us. As mentioned above, the RMS delay could be larger than 2.5us. Therefore, in the simulation, the maximum number of paths considered is 25. Figure 89 shows the bit error rate (BER), achieved by BPSK modulation scheme, versus the SNR, when the number of paths causing ISIs takes the value of 1, 6, 12, 18 and 24. It can be seen that when the number of interfering paths increases, the BER performance degrades. The degradation is significant when the number of ISI paths changes from a very small value to a relatively large value, e.g., from 1 path to 6 paths. However, when the number of ISI paths is relatively large, further increasing the number of paths will not impact the performance significantly. That also indicates that the impact of the number of paths will be saturated when it is large enough. Furthermore, it can be seen from Figure 89 that when SNR is large enough, the ISI interference floor appeared. The BER performance will not be improved by increasing the transmit power.

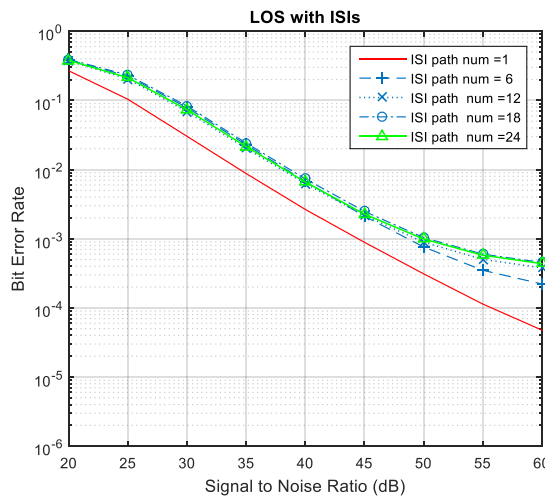


Figure 89: Bit error rate under different number of paths when LOS exists

It can be seen from trial results shown in Table 23 when the antenna height increases, the performance of transmission latency improves, which indicates the received SINR improves, even

though the transmission distance between the BS and vehicle slightly increases due to the increase of the antenna height increases. As explained earlier, due to the impact of multipath, the receiving devices suffer from ISI introduced by multipath, rather than benefiting from multipath diversity gain. Therefore, based on above analyses, an interesting finding can be postulated. That is, the number of ISI paths decreases when the height of the transmitting antenna increases. As the performance improvement is observable, it can be predicted that when the antenna height changes from 1.4 to 3.8, the number of paths in the trials varies from tens of paths to just a few paths. It also can be predicted that when the height of the antenna is large enough, the performance cannot be improved any further, while the increased distance between the BS and vehicle may impact the performance dominantly.

4.1.3.3 On interruption of communication in MEC-based V2X services

V2X services have specific communication requirements. One of the often-cited requirements is low latency. When the mobile networks are used for V2X communication i.e., C-V2X (this section is focused on the aspects of the network communication via Uu interface), the 5G network comes with a promise of low delay and high bitrate. Moreover, the network slicing technology can be used to customize the required network behaviour and deploy V2X specific service functions. One of the technologies that can be used in the context is Multi-access Edge Computing (MEC). The MEC allows for application-level traffic optimization, providing that way reduction of the overall network traffic and shorter communication delays. Moreover, MEC allows receiving contextual information from RAN as well as optimizing the traffic distribution, resources utilization and network performance. The MEC architecture [26] consists of two major parts: MEC system-level comprised of OSS, applications/infrastructure orchestration entities and application life cycle management proxy; and MEC Host level consisting of MEC Platform (MEP) that hosts MEC applications and exposes API to them, MEC Platform Manager (MEPM) responsible for the management of platform itself as well as applications life cycle, Virtualization Infrastructure and its Manager and finally the underlying network (e.g., local, external or 3GPP network). The fundamental mechanisms of MEC are:

- seamless inter-platform application mobility, MEC Platform services APIs for e.g., user's location and radio conditions exposure.
- underlying data network traffic steering for selective applications-related data redirection.
- MEC applications (MEC Apps) orchestration.

The architectural framework allows for MEC implementation with or without NFV. In a mobile network, the MEC application must be installed in a MEC Host serving base stations in the area in which terminals will use the application. There are published numerous papers that describe the optimized deployment of the MEC infrastructure. The most common optimization criteria consider cost, energy consumption and the data plane delay.

One of the MEC problems is MEC applications mobility linked with it the User Context Transfer (UCT) procedure. The operations are triggered when the UE moves from base stations that are handled by one MEC Host (i.e. MEP) to another one. In combination with the handover, the application mobility process, as well UCT, may cause communication breaks longer than acceptable by some services, for example, by V2X. In this section, the problem will be analysed.

Communication requirements of V2X services

The robustness of V2X services and their high diversity result in a wide spectrum of requirements that have to be fulfilled by the communication systems. Without a doubt, the most significant contributor in the area of defining the V2X use cases and the respective technological demands is 5G Automotive Association (5GAA). In the forthcoming parts of this section, the high-level overview of the requirements defined by 5GAA and 3GPP will be presented.

V2X service requirements defined by 5GAA

The V2X ecosystem is expected to enable a diversity of applications and services with stringent requirements in terms of latency and throughput [27], [28]. Typically, the V2X use cases can be grouped into the following categories:

- *Safety* – mechanisms for safety improvement (emergency braking, collision warning, cooperative lane change assistance, etc.),
- *Autonomous Driving* – semi-, fully automated, and remote operation of a vehicle,
- *Vehicle Platooning* – the creation of dynamic groups of vehicles to exchange information and coordinate operations (e.g., maintenance of inter-vehicle distance),
- *Society and Community* – use cases of interest to the society and public (vulnerable road user protection, traffic light priority, crash reporting, etc.),
- *Convenience* – facilitation for drivers (infotainment, assisted and cooperative navigation, autonomous smart parking),
- *Traffic Efficiency and Environmental Friendliness* – enhancements for traffic optimization (e.g., green light optimal speed advisory, traffic jam information, smart routing),
- *Vehicle Operations Management* – operational and management use cases benefiting vehicle manufacturers (sensors monitoring, remote support, software updates, etc.).

The estimated requirements for exemplary use cases belonging to each category are presented in Table 27.

Use case group	Exemplary use case	Throughput	Service Level Latency
Safety	Cross-Traffic Left-Turn Assist	Implementation-dependent (≈1 kB per message)	≤10 ms
Autonomous/Cooperative Driving	Automated Intersection Crossing	≈9 Mbps	≤10 ms
Vehicle Platooning	Vehicles Platooning in Steady State	8-24 kbps (V2V)	≤50 ms
Society and Community	Patient Transport Monitoring	≈10 Mbps	≤150 ms
Convenience	Obstructed View Assist	≈5 Mbps	≤50 ms
Traffic Efficiency	Bus Lane Sharing	<1 Mbps (implementation-dependent)	≤200 ms
Vehicle Operations Management	Software Update	≈80 Mbps	N/A

Table 27: V2X use cases groups with exemplary use cases and associated latency and throughput requirements.

V2X requirements defined by 3GPP

The 3GPP has already defined a set of general service requirements to be addressed by the LTE C-V2X variant in Release 14 [18], mostly oriented towards base use cases, i.e. requiring relatively small bandwidth and having medium latency constraints. The list of the most important in the context of V2X and MEC are presented in Table 28.

System requirement	Maximum value
Latency of messages transfer between two UEs supporting V2V/P application (directly or via an RSU)	100 ms
Latency for particular usage (i.e. pre-crash sensing) only, the E-UTRA(N) should be capable of transferring messages between two UEs supporting V2V application	20 ms
Communication latency for time-critical V2V applications	100 ms

Communication latency between UE supporting V2I and RSU	100 ms
Communication latency between UE and an application server both supporting V2N (end-to-end)	1000 ms
Frequency of transmitted messages per UE	10/s
Periodic broadcast messages payload (UE-UE)	50-300 bytes
Event-triggered messages payload (UE-UE)	1200 bytes

Table 28: General service requirements for C-V2X as stated by the 3GPP [18]

The 3GPP has also identified a set of requirements regarding advanced V2X scenarios [29]. The most stringent in terms of end-to-end latency or bandwidth involves emergency trajectory alignment (3 ms), remote driving (5 ms), sensor information sharing (1 Gbps) or video sharing (700 Mbps).

Some V2X services, namely V2V, can be implemented using direct communication between cars in a close distance. These services will typically use LTE-ProSe (Sidelink) as the basis.

Discussion on 5GAA and 3GPP requirements in the context of MEC

The analysis of the 5GAA and 3GPP requirements allows grouping them into three categories of delay:

- delays longer or equal to 100 ms (most of the TS 22.185 requirements);
- delays in the range of 5-25 ms (some of the 5GAA requirements, RTT/2);
- delays shorter than 10 ms (most of the TS 22.186 requirements).

Most of the applications generate moderate traffic, some in the range of 10-100 kbps, some medium traffic (1-10 Mbps), some has high bitrate requirements (10-100 Mbps) and there are very few that require more than 500 Mbps.

The trials of 5G-DRIVE described in deliverable D3.3 [30] show that the 5G network (eMBB) is capable of delivery of 500 Mbps (TCP traffic) and over 650 Mbps (UDP traffic) in the downlink (similar results have been achieved during outdoor measurements on both Surrey and Orange trial sites) and around 70 Mbps in the uplink. In best cases, the measured RTT was in the range of 9-25 ms with an average equal to 13 ms. The evaluation of the 4G connectivity [31], [32] shows that this technology can deliver data with an average delay in the range of 20-50 ms depending on the load, the configuration of the network and the measurement scenario.

As previously presented, the usage of MEC can contribute to lower delay and more efficient traffic distribution. The latter is important when the traffic intensity is high (>50 Mbps). It must be noted that in such cases, the 4G/5G technology cannot provide low delay as the URLLC traffic intensity is expected to be low. The usage of MEC for high-intensity traffic with a delay of 50 ms or more is straightforward. In fact, ignoring ineffective traffic concentration, such cases can be handled without MEC. The low delay applications become much more interesting as they require fast handovers, and in the case of MEC, a negligible interruption caused by application mobility and user context transfer (UCT). It is worth noting that the RAN part should introduce a delay in the range of 0.5-1 ms; therefore, for the very low delay, there is still a good margin to be filled by operations that are performed out of the RAN domain. Despite a common opinion, the delay of transmission caused by distance is relatively low (typically 6 μ s/km) and its contribution to the overall, end-to-end delay in real deployments is negligible if the distance between a UE and server is smaller than 10 km (this is the case for most cities). In rural areas, the usage of MEC Hosts collocated with base stations brings significant benefits in terms of delay.

Problem Statement

The MEC approach can shorten the data path, which is especially critical in V2X services. In such a case, MEC can be seen as a similar communication mechanism to ProSe (Sidelink). In this case, however, the mobile network base station can be seen as a relay, but in combination with MEC, it can be seen as a low-delay, programmable service platform. Moreover, the RSU can also be

implemented using this technology. Such an approach provides multiple benefits, especially in the context of the management and programmability of services. MEC can be used for C-V2V, C-V2P and C-V2I (RSU case) services that, in general, are characterized by low bitrate and low delay requirements.

Cellular V2X has proved to have several advantages over its non-cellular counterpart, i.e. IEEE 802.11p. First, it provides more reliable and collision free-resource allocation mechanisms even in scenarios where the density of the served UEs is considerably high (CSMA-CA mechanisms for WiFi). The optimized resource scheduling enables meeting latency requirements and limits potential denial of access to the channel. Moreover, the operation within a broad cellular ecosystem also creates the opportunity to extend the number of possible applications, e.g., including V2P or easier integration with systems operating at the edge of the network such as MEC.

The benefits of MEC have their price. One of the primary deficiencies of MEC is a need of support for seamless mobility of users or cars at the MEC level. MEC has support for applications mobility, but this mechanism is not well defined. In MEC documents, it is written explicitly that the implementation of the mechanism can be application dependent. The application mobility problem can be decomposed into two issues. One is the core application mobility that can be understood as a dynamic deployment of applications in MEC Hosts in which the application is needed, and another problem is linked with User Context Transfer (UCT), i.e. transfer of user-specific data linked with the application. In the greedier MEC application deployment, it can be assumed that V2X supporting applications are deployed in advance in all MEC Hosts; however, the problem of the UCT persists. The UCT should be triggered by a handover operation (HO) to the base station that is served by another MEC Host during the transition - it can be seen as a connectivity break. A MEC Host, depending on the deployment scenario, can handle one or more base stations (eNBs or gNBs). More MEC Hosts in the same serving area increase the number of context transfers and cost in terms of OPEX and CAPEX. At the same time, they provide more efficient traffic distribution and lower delay.

In this work, a preliminary analysis of the service continuity problem in the multi-MEC Hosts scenario is analysed. We have used simulated car mobility and analysed the impact of UCT mechanisms defined by 3GPP for a different number of base stations served by a MEC Host and mechanisms proposed by 3GPP for UCT. To analyse the possible service continuity issues, we will start from the handover issue as it may cause data transmission interruptions.

Handover impact on service continuity in 5G networks

In 5G networks, the HO can deal with beam level mobility or cell level mobility. The latter may cause connectivity interruptions. The basic mechanism, i.e. the hard handover, can introduce delays of about 50 ms [33]. More advanced mechanisms can significantly decrease this time even to 6 ms under specific conditions (MBB + RACH-less HO described in detail in [33]).

To reduce the HO-related communication break, several new concepts have been introduced in 5G. One of them is the conditional handover feature standardized in the 3GPP Release 16. In this approach, the UE receives a handover command and stores it without applying it as it would have done in classical handover. Together with the command, the mobile terminal also receives an associated condition to be monitored. When the condition is met, the mobile terminal applies the previously-stored handover command, as if the network would have just sent it. In this approach, the HO is prepared by the network but executed by the terminal. According to [33], the interruption time, in this case, is typically about 50 ms.

Alternatively, to meet the popular “zero interruption time” requirement, relevant primarily to URLLC communication type, the mechanism of PDCP duplication over NR-NR Dual Connection (DC, simultaneous connectivity to two gNBs) has been defined within the 3GPP Release 16. Due to the duplication of packets and their paths, the 1:1 traffic protection is inherently provided. As keeping the continuous redundancy leads to the effect of resources consumption duplication, the mechanism of dynamic activation/deactivation of PDCP duplication via MAC command has also been defined (support of dual-protocol stack needed at the UE side). However, saving the resources consumption

by implementing dynamic DC activation prior to the handover procedure is at the expense of the increased algorithmic and signalling effort.

MEC-caused communication interruptions

The UCT operation must be performed for each UE that is moving from the area served by one MEC Host to the area served by another MEC Host. The MEC system is aware of the network-level mobility management status thanks to the signalling exchange with the mobile network via Mp2 reference point. Hence, the UCT operation can be synchronized with the respective HO trigger. To that end, the MEC RNIS API provides to MEC applications the information about HO progress (CellChangeNotification), which is subscribed on a per-UE basis. It includes the information about source/target base stations and HO status (in preparation, in execution, completed, rejected or cancelled).

Our model assumes that there is no need for application mobility, i.e. all MEC Hosts have the core part of the application already deployed. However, the data record linked with a specific UE must be transferred. The UCT is performed at the UE level. To make the process fast, it must be executed individually rather than in a batch mode, i.e. for several UEs simultaneously.

According to ETSI [34], the UCT can be:

- application self-controlled – UCT, in this case, is performed by the server- or client-side application. It is assumed that the application can detect the need for its context transfer and can execute it without assistance from the MEC system. The MEC role is to provide outting of the application traffic to the new serving MEC App instance;
- device application assisted – in the case of a device, the application associated with the user's MEC App, initiates/triggers the application mobility and keeps the user context in the client during the relocation;
- MEC-assisted UCT – the mobility mechanism and context transfer are triggered and performed by the mechanisms residing in MEC.

MEC-assisted UCT

Now we will describe the MEC-assisted UCT, as we expect that the approach due to standardization should be the most popular one. The application controlled, and device-assisted UCTs approaches will be discussed later.

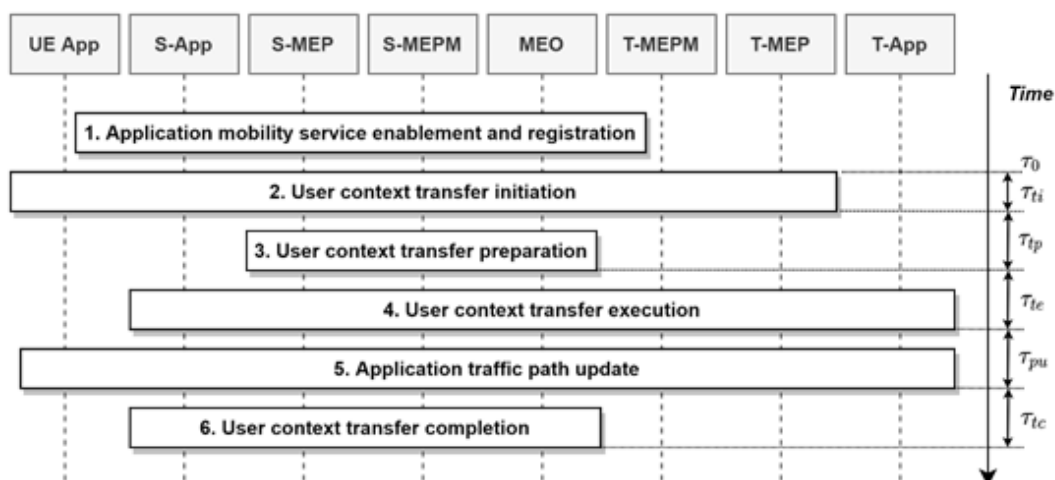


Figure 90: MEC App UTC procedure as described in [34] with the delay induced by each phase of the procedure.

The generic procedure in this case with the involved entities is presented in Figure 90. The context transfer process involves several sub-procedures and message exchanges between serving instances of MEC App (S-App), MEC platform (S-MEP), and MEC platform Manager (S-MEPM), the target

counterparts (T-App, T-MEP, and T-MEPM, respectively) and MEC orchestrator (MEO). These sub-procedures consist of:

- Initiation – detecting and triggering mechanisms for transferring the User Context (UC) to the target application instance,
- Preparation – optional sub-procedure for MEC-assisted UCT, and used for MEC system to prepare for the transfer,
- Execution – context transfer and synchronization of the application instance running on the target MEC host,
- Application traffic path update – data plane reconfiguration operations to redirect the traffic to the application on the target MEC host,
- User context transfer completion – MEC system clean-up of the user context from the source MEC host.

The time duration of the above-mentioned procedures is difficult to estimate since the reactivity (interfaces, message processing etc.) of each entity is implementation dependent. Nonetheless, high-level approximations can be made to assess the impact of context transfer procedure on the V2X service continuity. The time duration of the first phase, i.e. the mobility service (AMS, Application Mobility Service) enablement and registration, is not considered since it is usually performed at the beginning of the application's lifecycle. Therefore, the time duration of the context transfer procedure is measured from the very beginning of initiation phase (marked as).

For the assessment, the following time duration estimations of the UCT subprocesses have been proposed:

- τ_{virt} – latency caused by virtualization technologies, which are used by MEC. The specific value can be different depending on server's configuration, current load and infrastructure virtualization methods (VMs, containers) as described in [24], [25]. In terms of VMs the RTT can vary from 0.4-6 ms (high load) while for containerized environments, induced delays are typically in range of 0.45-0.6 ms (about 144 μ s caused by virtualization layers). The optimistic variant is selected of latency equal to 0.5 ms of 0.45-0.6 ms (about 144 μ s caused by virtualization layers). The optimistic variant is selected of latency equal to 0.5 ms.
- τ_{RTT} – RTT value depending on the physical distance between the UE and the RAN node (gNB/RSU) and between the RAN node and serving MEC host. For the estimations the RTT value of 10 μ s being an equivalent of approximately 1 km of distance between UE and RAN node has been selected.
- τ_{TCP} – latency caused by establishment of TCP session between the two hosts (3-way handshake), usually assessed as 1.5 of RTT.
- τ_{API} – latency caused by a single API call. This value is strongly dependent on the API type and retrieved data. Currently, the best web frameworks can achieve as low as 1.1 ms for a single database query [35]. For the estimations the value equal to 0.2 ms will be chosen to assess more optimistic conditions (API tailored for a specific procedure and no database access).
- τ_{IH} – RTT between two MEC hosts (inter-host RTT). For simplification the distance of 2 km is adopted, i.e. 20 μ s of delay.
- τ_{MEO} – RTT between MEC host and centralized MEO (for simplification, the same distance to both MEC hosts is assumed equal to 2 km, i.e. 20 μ s).
- τ_{ct} – time needed to physically transfer UC data between two applications residing in two MEC hosts. Depending on the context size and MEC hosts interconnection (link bandwidth, latency etc.) the transfer time can vary significantly. For the calculations the context size of 1 kB and bandwidth of 80 Mbps reserved for the transfer of the context have been adopted, resulting in 100 μ s of delay.

The adopted values are presented in Table 29.

Subprocess/technological delay	Duration [μ s]
τ_{virt}	500
τ_{RTT}	10
τ_{TCP}	15
τ_{API}	200
τ_{IH}	20
τ_{MEO}	20
τ_{ct}	100

Table 29: Delay factors present during the UCT procedure with the estimated delay induced by each factor.

To estimate the delay related to UCT execution it is necessary to make some assumptions concerning the context size and the capacity of a link used for context transferring. The user context is generally a record that consists of data related to a specific UE. Its size is MEC application dependent. We have assumed that the context size is in the range of 1 kB-1 MB.

We will calculate the link capacity for a single user context by dividing the link capacity by the number of needed context transfers. To evaluate the number of context transfers, we have made simulations for the worst case that is a dense urban area with high-speed roads. The RAN/MEC configuration is presented in Table 30.

Cell radius	150 m (3.5 GHz, capacity cells)
Number of base stations per MEC Host	1, 4, 9
Antennae radiation pattern	omnidirectional
MEC host virtual resources capacity	able to handle all the incoming traffic
Total number of cells	36 (9×4), situated along the main road
Link capacity for inter-connection of cells (Xn) or MEC Mp3 link	10 Gbps in case of independent Mp3 link 1 Gbps in case of shared Mp3 and Xn link (10% of link capacity)

Table 30: The configuration of RAN and MEC environment considered in the simulations.

The simulations have been performed using SUMO simulator [36]. For the simulation the map of the area located in the north of Warsaw has been used (cf. Figure 91).



Figure 91: The area used for simulations (left) and its representation in SUMO simulator (right).

The main parameters of the performed simulations are listed in Table 31.

Parameter	Value
Simulation time	60 min
Map area size	1500 m × 1400 m
Roads type	Main/motorways
Traffic density	High but fluent
Crossing types	Junctions (ramps)

Table 31: Parameters of simulations performed in SUMO

The main purpose of simulations was to estimate the number of UCT per second. The obtained results are presented in Table 32.

Number of cells per MEC Host	The overall number of UCTs during simulations (60 min)	The average number of UCT/s per MEC Host	Minimum number of UCT/s per MEC Host	Maximum number of UCT/s per MEC Host (the worst case)
1	47848	0.532	0	1.800
4	20603	0.636	0	1.930
9	13719	0.953	0.36	1.528

Table 32: Hosts deployment scenarios

It must be noted that the increased number of base stations per MEC Hosts (i.e. less MEC Hosts) decreases the overall number of UCTs to be handled but less than linearly. It is also worth noting that the nine-fold reduction of the number of MEC Hosts doubles the number of UCTs per MEC Host. Analysis of Table 32 shows that we need to handle no more than 2 UCTs per second. A properly designed system must be designed for the worst case and include a margin. Therefore, we assume that the system should be able to handle 4 UCTs/s. That means that in the case of an isolated Mp3 link of 10 Gbps capacity, if we allocate 10% of the link capacity for UCT, we may have about 250 Mbps per UCT (the TCP mechanisms will split the link capacity in a fair share way) and in case of shared Mp3/Xn link we may have ten times less, i.e. 25 Mbps for single UCT transfer. All the above-presented calculations allow the estimation of the total execution time of UCT. The results are presented in Table 33.

Phase	Remarks	Delay factors	Delay estimation [ms]
2	The UCT initiation lies on a decision process regarding the context mobility actions (internal or external, e.g., caused by Radio Network Information Service events)	τ_{API}	0.4
3	UCT preparation phase	Initial process related to the creation of communication buffers, etc.	0.2

4	UCT execution is dependent on two factors on the footprint of the context and on the bitrate of the link that is used for the context transfer. One may assume that the user context size is in the range of 1 kB - 1 MB. More detailed information about the bitrate allocated for each UE is presented below	User context footprint and capacity link capacity (per UE): 1 kB@ 25 Mbps 1 MB @ 25 Mbps 1 kB@ 250 Mbps 1 MB @ 250 Mbps	0.32 320 0.032 32
5	Application traffic path update procedure as depicted in [MEC018]	$\tau_{API} * 2 + \tau_{MEO} + 1.5 * \tau_{IH} + 4 * \tau_{virt}$	2.450
6	UCT completion lies on notification of the AMS and performing a clean-up on the source MEC Host	$\tau_{RTT} + \tau_{TCP} + \tau_{API} + \tau_{virt}$	0.725
-	Total context transfer time	-	3.775 + (Phase 4: 0,032-320)

Table 33: The estimation of the time duration of the UCT procedure

Table 33 shows that the total UCT time in the best case is 4 ms, while in the worst one, it can be even 324 ms. Keeping in mind optimized UCT size and load-dependent behaviour of the MEC Host Platform, it can be assumed that UCT time should be in the range of 5-10 ms.

Device application-assisted UCT

The device application-assisted UCT is a solution in which the UE has the context information record and sends it to a new MEC Host when the handover is executed. In such a case, the MEC Host will obtain the new information with a delay caused by the following factors:

- handover implementation (in the range of ~0 ms for dual connectivity mode during HO to 50 ms for the basic hard HO [33]).
- network configuration and its influence on the User Plane end-to-end latency (the 5G-DRIVE project deliverable D3.3 [30] estimates it in the range of 20-50 ms for LTE and about 15 ms for 5G); for URLLC, the delay is in the range of few milliseconds, but the amount of data should be relatively small.
- UCT over UE uplink data rate (50-70 Mbps according to the deliverable D3.3); if the context is small (1 kB range) and the URLLC for such transmission is used, the impact on latency is negligible.

This approach simplifies the way of the UCT execution; in some cases (URLLC and dual-link handover), it may provide the time of interruption of communication between the terminal and the MEC Host below 10 ms. However, in most cases, such delay will be no shorter than in the case of MEC based UCT, which may start when the handover is triggered (in the discussed cases, it begins when the handover is already executed). Moreover, the UE radio uplink bit rate is lower than the connection that can use the inter MEC Host interface.

Application self-controlled UCT

The application self-controlled option gives the application programmer freedom how to handle the UCT. In such a case, the UCT procedure described by 3GPP can be ignored. Keeping in mind the need for short interruption of MEC-based operations, we propose a solution that fundamentally changes the approach to UCT. The proposed solution lies in transferring UCT of UEs located close to the “borders” between neighbouring MEC Hosts “areas”. In this approach, the target MEC Host will obtain the context before the handover is triggered. It can, however, only read the context, which is continuously updated by the application located in the source MEC Host. The handover execution for

such UEs reverts the MEC Hosts permissions. In such a case, the application can predict the future position of UE and therefore, the impact of the UE (i.e. car) on other cars served by the target MEC Host is known. The concept is presented in Figure 92.

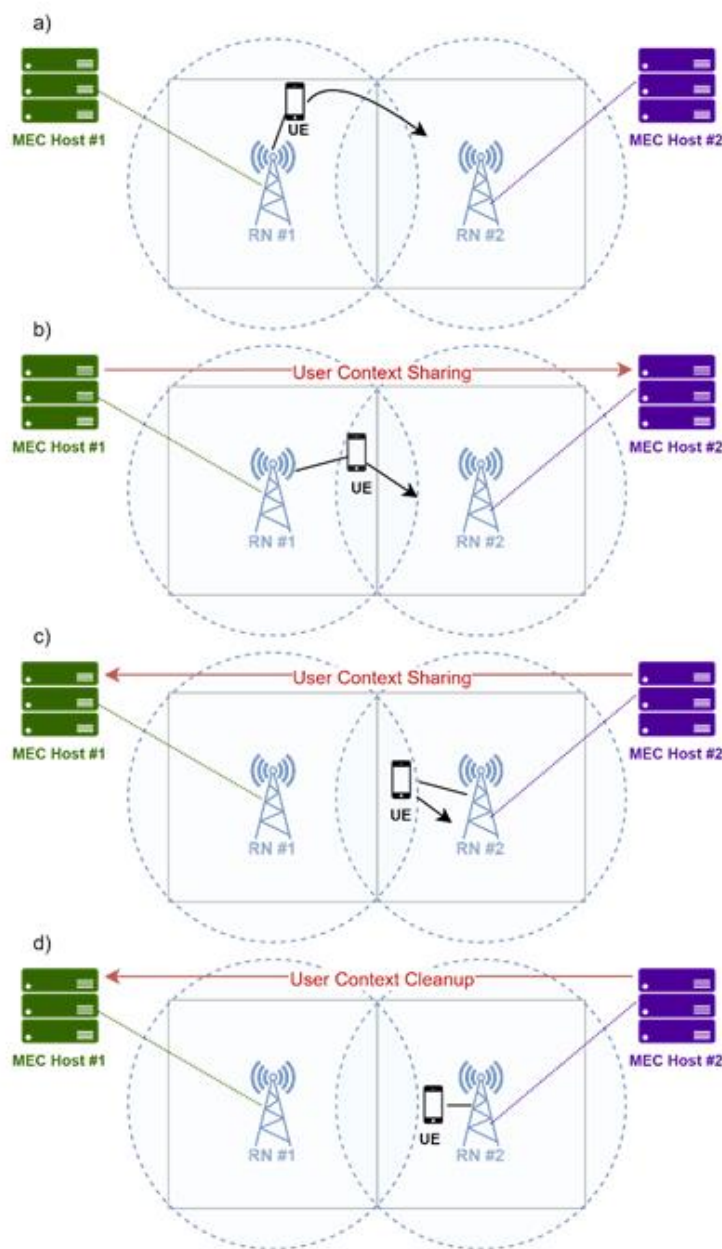


Figure 92: A proposal of sharing UC for application controlled UCT: a) The UE moves towards the area of operation of RAN Node #2 (gNB or RSU), b) The UE is in the vicinity of the area of operation of RN#2, c) The HO has been performed and the UE is served by RN #2, d) after the predefined time after HO, the removal of user context from MEC Host #1 is performed.

Three main phases can be distinguished in the proposed UCT sharing mechanism. First, the UE is served by RN #1 (the context is synchronized with MEC Host #1), as presented in Figure 92a). As the UE moves towards the area of operation of RAN Node #2 (gNB or RSU), the likelihood of HO is increased (cf. Figure 92b). When the possibility of a HO is high (user application can be notified by other applications performing mobility/HO prediction algorithms), MEC Host #1 starts to share the user context information with the MEC Host #2. When the HO is performed, the application context is synchronized between MEC Host #2 and MEC Host #1 as long as the UE stays in the vicinity of RN #1 (to prevent ping-pong behaviour cf. Figure 92c). The clean-up of the application in MEC Host #1 is performed when the UE leaves the “border” area (cf. Figure 92d).

The high-level workflow of the proposed procedure is presented in Figure 93.

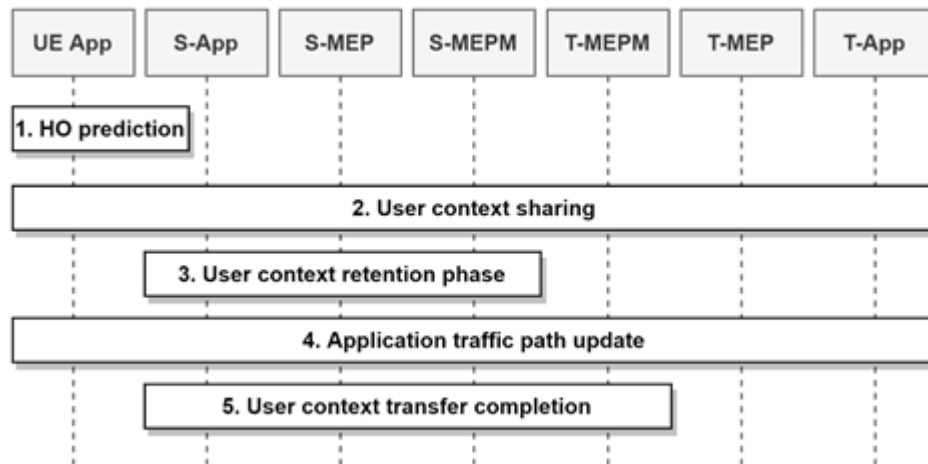


Figure 93: Workflow of the application controlled UCT with UC sharing.

The following phases are distinguished in the procedure:

- HO prediction – the information regarding possible handover with a target for application self-controlled UCT, which can be triggered either by the UE or external application that performs mobility prediction.
- User context sharing phase – the source MEC Host initiates a session to transfer user context data to the possible target MEC Host indicated by mobility predictions and keeps synchronizing the context information in the target MEC Host.
- User context retention phase – occurs after the successful HO. The new serving MEC Host (i.e. target MEC Host) shares the context information with the previously serving MEC Host for a predefined period of time (to prevent the ping-pong behaviour).
- Application traffic update – this phase occurs after the beginning of the retention phase and is the same as in MEC assisted UCT case.
- User context transfer completion – is triggered by the end of the user context retention phase and is composed of procedures needed to perform MEC system clean-up, i.e. removing user context from the source MEC host.

Such proactive UCT solves the problem of interruption of UE with MEC-based application straightforwardly. Moreover, it seems that this approach is a candidate for standardization as many low delay applications can reuse it.

Conclusions

MEC comes with the promise of low delay communication and effective traffic steering. As we have shown in the urban area, the transmission delay is almost negligible (below 0.1 ms for 10 km). Moreover, the time-critical V2X traffic is characterized by a relatively low bitrate. Both observations led us to conclude that sparse MEC Host locations can serve nicely V2X time-critical applications in urban areas. The approach also provides benefits in terms of OPEX and CAPEX over highly distributed MEC infrastructure.

Moreover, in a dense MEC Hosts network, the MEC application mobility and UCT events happen more often, causing potential application-level interruptions. The UCT happens when a UE moves between two areas handled by different MEC Hosts (MEPs). HO usually triggers it. The described three options of handover implementation show that the HO may take from nearly zero milliseconds (in the case of the dual connectivity approach) to about 50 ms.

The UCT procedure can introduce application-level communication interruption that is not acceptable by low-delay based V2X services. Fortunately, two of the three UCT approaches by 3GPP can be triggered when the handover procedure starts.

The defined by 3GPP MEC-based UCT takes several phases and using MEC RNIS API it can be triggered by the handover start procedure. The approach is composed of several phases which execution time cannot be easily predicted as it deals with software-oriented operations. In this section, we have made such an attempt. Our estimations have shown that the delay induced by UCT can be in the range of 5 ms to 10 ms (if UCT size is optimized).

The so-called device application assisted UCT starts when the handover is completed, and it can provide short communication interruption only when the URLLC mode is used, and the context footprint is small (few kilobytes). In such a case, the UCT time can be shorter than 10 ms.

Finally, the problem of UCT can be nicely solved at the application level. In such an approach, it is possible to provide dual access to apps located in both source and target MEPs for UEs (i.e. cars) located in the area where the handover may occur. Moreover, in this case, the target MEP App may use the concerned UE information in advance. Such a simple, proactively triggered UCT combined with dual connectivity-based HO can provide zero interruption time.

In conclusion, for low-delay MEC services in the urban area, we recommend using a relatively sparse MEP network as it will minimize the number of UCTs as well as CAPEX and OPEX. In such a case, we also recommend using dual connectivity based HO and application triggered UCTs as described in the previous subsection.

In this section, we focused on a specific use case. Other use cases that, for example, ignore low delay but generate high-bitrate local traffic may benefit from dense MEP mesh. Such observations led us to conclude that the areas handled by MEP should be defined by each application independently. So far, this is not the case.

4.2 Joint V2X trials in China

The joint EU-China V2X trials in China were performed in Shanghai test site. As mentioned in Section 3.4.2.3, the LTE-V2X test sessions can be divided into three categories:

4.2.1 Interoperability tests among different vendors

The interoperability tests between different terminal (RSUs and OBUs in this case) and different vendors were performed under the GLOSA use case. To test the interoperability of the Signal Phase and Time (SPaT) messages and Basic Safety Messages (BSMs) being transmitted and received among RSUs and OBUs from different vendors, two scenarios were designed: one RSU transmits SPaT messages and multiple OBUs from different vendors receive them; one OBU transmits BSMs and multiple RSUs from different vendors receive them. The results of both scenarios confirmed the successful transmitting and receiving of SPaT messages and BSMs among terminals, and thus confirmed the interoperability of RSUs and OBUs from different vendors.

4.2.2 V2I/V2V (LTE-V2X technology) coverage tests

The V2I/V2V coverage tests were performed with LTE-V2X technology-based OBUs and RSUs.

For the scenario of the V2I (OBU-RSU) coverage test under non-line of sight¹⁹, an OBU in a test vehicle was moving away from an RSU (installed about eight meters above ground level on a light pole). SPaT messages were transmitted from the RSU to the OBU, and the end-to-end Packet Error

¹⁹ NLOS: in the test case, regular/ heavy greenery on the test site.

Rates (PER) were measured.

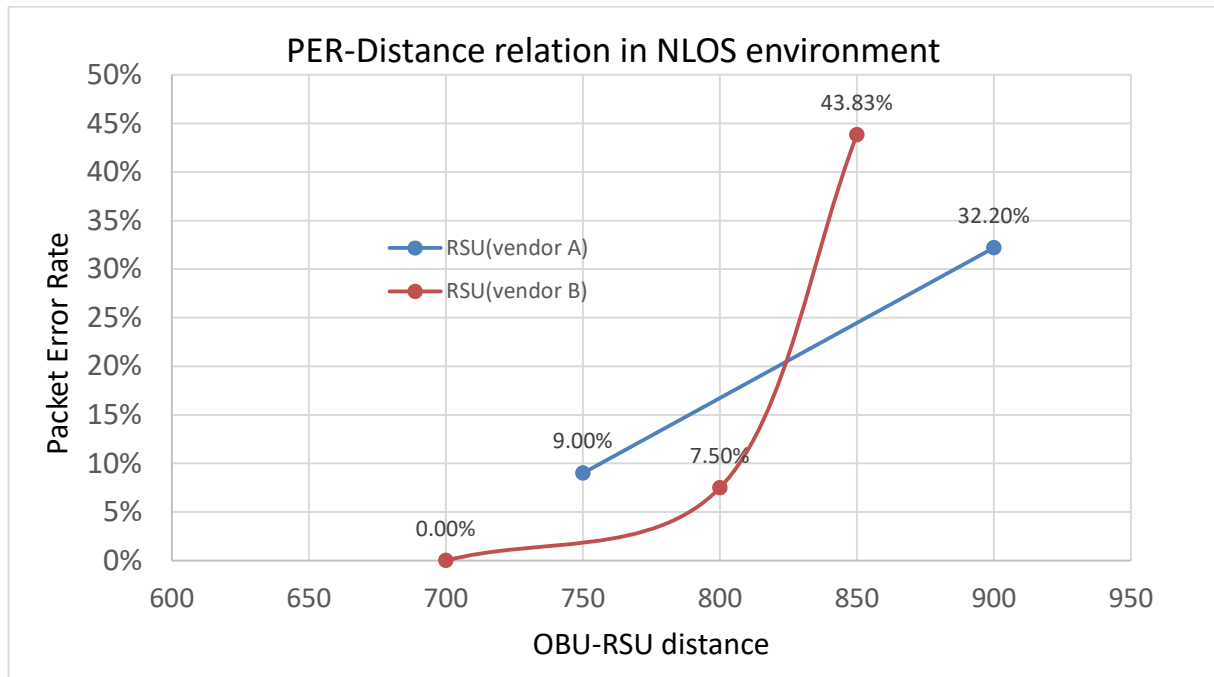


Figure 94: The PER and OBU-RSU distance relationship in an NLOS test environment

Figure 94 showed that the PERs of both RSUs (from two vendors: Vendor A and Vendor B) significantly increase when the distance between the OBU and RSU was further than 800 meters, which indicated that the RSU coverage could be around 800 meters in NLOS conditions, considering the end-to-end reliability KPI of PER. Note that the objective of V2I coverage test in NLOS conditions is to set up RSUs OBUs and to measure the RSUs coverage using performance indicator - PER. Performance comparisons from the result plots is out of joint EU-China V2X trial objectives and not applicable since they are set with factory default configurations. Using factory default configurations for RSU/OBU devices, the trial findings show these devices complied and conform to the preliminary targeted KPIs set for the joint EU-China V2X use cases in China, see section 3.4.3.2.

For the scenario of the V2V (OBU-OBU) coverage test under line of sight (LOS) and NLOS conditions, two sub-scenarios were performed: two vehicles (OBUs) in driving mode under LOS/NLOS conditions and two vehicles (OBUs) in fixed positions under NLOS conditions.

Driving mode: LOS/NLOS	OBU-OBU distance [m]	Latency (Mean) [ms]	PER
Near point (LOS)	0	16.29	0%
Far point (NLOS)	400	15.5	0%

Table 34: The mean latency of varying OBU-OBU distance

Table 34 showed the end-to-end latency and PER between two OBUs in driving mode in both LOS/NLOS environments. The measurements showed that the average latency is around 16 ms. When the distances of two OBUs were within communication range, the latencies were not affected. The PER was stable at 0% when the two OBUs were within a communication range of 400 meters.

Table 35 showed the end-to-end latency and PER between two OBUs, measured at fixed positions in an NLOS environment. Some degradation on the average latency can be observed when the two OBUs were placed from 400 meters apart to 450 meters apart in the NLOS environment. The PER increased from 0% to 17%, which indicated the communication range in this case is around 450 meters. To calculate the average latency and PER, the data sample retrieving period was around 15

minutes once the connections were established and functioning. BSM messages were sent from one OBU to the other with an interval of 100 ms, which equivalent to 10 messages per second. The data sample size was around 9000 data points to acquire statistically meaningful latency and PER calculation.

Fixed position: NLOS		
OBU–OBU distance [m]	Mean latency [ms]	PER
400	15.32	0%
450	18.81	17%

Table 35: The mean latency of fixed OBU–OBU distances

4.2.3 LTE-V2X (PC5) performance tests

The LTE-V2X performance tests included latency and PER tests under single and multiple transmitting stations. To illustrate, the joint EU-China V2X trial use case - Intersection safety (intersection collision warning) was tested here by sending BSMs. In this test category, two scenarios were tested: a single terminal transmits, and four terminals receive (transmission between one OBU and four RSUs); multiple terminals transmitted, and multiple terminals received (transmission among twenty OBU/RSU stations: six RSUs and fourteen OBUs). In these two scenarios, the performance of LTE-V2X was evaluated with the end-to-end latency and PER, see section 3 for the assessment KPI definition.

For the first scenario, where a single OBU transmitted and multiple terminals received, the end-to-end latency (mean) was within 25ms and the differentiation of the measurements were low when the distances between the OBU and multiple RSUs were at far, middle, and near points (all within a communication range of 800 meters). This latency of less than 25ms proved that the performance of LTE-V2X devices met the preliminary targeted KPI in Table 16. The PERs of all receivers were all less than 10%, which also confirmed the performance reliability of the LTE-V2X and devices and again, within the targeted KPI in Table 16.

For the second scenario of multiple terminals transmitting and multiple terminals receiving, a large-scale feasibility test, focusing on the intersection collision warning use case, was carried out using twenty physical LTE-V2X technology-based RSU/OBU stations. Then, the end-to-end latency (mean) were measured among all transmissions. The results analysis showed that the average latency was less than 38ms and the PER was less than 10%. With the number of physical terminals increasing from five terminals to twenty terminals, the end-to-end latency (mean) was increased from less than 25ms to less than 38ms. Please note these findings were subjective to the deployment of terminals and their configurations (factory default), which conformed with the preliminary targeted KPIs set for joint EU-China V2X trials but not applicable for LTE-V2X terminals' performance comparison among different vendors.

5 Conclusions

Section 2.2 presented the results of the preparatory tests carried out in the JRC Radio Spectrum Laboratory. The goal of these tests was twofold: on the one hand, they aimed at building technical competences in the operation and testing of commercial ITS-G5/LTE-V2X devices. On the other hand, they laid the ground for the co-channel coexistence tests described in section 2.2.2. Whilst conducting the preparatory tests, 5G-DRIVE submitted 7 technical contributions to ETSI EN 302 571 – the Harmonised European Standard for radio communications equipment of Intelligent Transport Systems operating in the 5.9 GHz band [2]. These technical contributions to EN 302 571 are described in more detail in Deliverable D6.4 (Final Report on Standardisation).

As to the issue of co-channel coexistence of C-ITS technologies, section 2.2.2 presented an experimental evaluation of co-channel coexistence method C in ETSI TR 103 766 [3] using commercial ITS-G5 and LTE-V2X devices. Results showed that ETSI method C contributed to reducing PER in the commercial ITS-G5 receiver compared to PER values observed under an LTE-V2X interfering signal, although not completely. This was due to LTE-V2X signals with ITS-G5 PHY header insertion causing some performance degradation of the channel sensing function in the PHY layer of the ITS-G5 transmitter. In addition, section 2.2.2 also studied the impact of ITS-G5 signals on the performance of the Semi-Persistent Scheduling algorithm featured in the MAC layer of commercial LTE-V2X devices. Experiments results showed that SPS achieved a PER in the LTE-V2X receiver close to 0% and a stable Inter-Packet Gap distribution for all interfering signals whilst keeping end-to-end packet latency within a user-configurable Packet Delay Budget.

Sections 2.3.1 presented laboratory experiments of frequency jamming on ITS-G5 using OpenC2X. Experiment results show the impact of the jamming source power and its placement on performance while considering the distance between communicating devices. Section 2.3.2 presented laboratory experiments using OpenC2X of an MDS to detect grey hole attacks. Experiments helped not only to evaluate the impact of radio interferences on the accuracy of MDS but also to enhance its resilience. The results of these experiments, although by all means not definitive in their results, give us a good indication of the phenomena.

Section 4.1.2 presents an operational deployment of a suite of day-1 C-ITS services in the JRC Ispra campus using commercial ITS-G5 and LTE-V2X devices. The goal of the Ispra field trial is to illustrate the different trade-offs between key performance metrics (PER and end-to-end packet latency) of commercial ITS-G5 and LTE-V2X devices. Overall, field tests results suggest a robust performance of the LTE-V2X PHY and MAC layers in terms of Packet Error Rate. As to end-to-end packet latency, ITS-G5 devices attained lower packet latency than LTE-V2X devices under clean channel and low load conditions. This is due to (a) the opportunistic nature of the CSMA/CA channel access mechanism of ITS-G5 and (b) the Packet Delay Budget of C-ITS messages being set to 100 ms in the factory-default configuration of the commercial LTE-V2X devices used in the Ispra field trial (packet latencies of up to 100 ms are in line with the service requirements for day-1 C-ITS services).

The experimental results of the joint EU–China trials performed in Tampere, Finland, and in Shanghai, China, under the collaboration that was part of the 5G-DRIVE and 5G Large-scale trial presented in section 4.1.1 and 4.2, followed the guidance of joint EU-China V2X trial harmonised framework. As a result, the designs and results gained through joint EU–China trials under the 5G-DRIVE and 5G Large-scale trial projects open the possibility for parallel findings comparison in many ways. Section 4.1.1 and 4.2 examined the measurement results of both trial sites in terms of important aspects of joint EU-China use cases (GLOSA and the intersection safety): trial specifications, message type comparison, end-to-end average latency, and end-to-end packet error rate.

For the trial specification in a broader sense, on the one hand, the European 5G-DRIVE trial in Finland was based on implementing a C-V2X and LTE/5G network in order to support automated driving. The performance of LTE/5G commercial cellular network was illustrated in section 4.1.1 and the measurement results of several KPI metrics—such as mean latency, jitter, and the PER—are shown as well. On the other hand, the Chinese 5G Large-scale trial project in Shanghai did not take

measurements using the 5G cellular network alone and focused on LTE-V2X PC5 trial results only. As for the trial configuration parameters considering LTE-V2X only, the LTE-V2X devices at both sites were configured according to factory default, which conformed to the joint-use-case-driven preliminary targeted KPIs. In addition, OBUs and RSUs from different vendors were used in the Chinese trials, which not only showed the interoperability of LTE-V2X terminals from different vendors at the Shanghai test sites, but also the measured results of the different terminal devices conformed to our preliminary targeted KPIs.

For the message types, it has been identified in [37] and [38] that the message types used in the GLOSA use case and the intersection safety use case in Europe and in China differ. For the GLOSA use case, SPaT and CAM messages are used at the Finnish trial site while SPaT messages and Basic Safety Messages (BSM) are used at the Shanghai trial site. For the intersection warning use case, Decentralized Environmental Notification Message (DENM) and cooperative awareness messages (CAM) are used in Finland while BSMs are used in Shanghai. The similar usage of SPaT messages is intuitive to understand. Considering that the PC5 radios are the same but the software stack is modified across the regions and considering that the BSM in China is likely to be a combination of a DENM and CAM message types in Europe regarding the functionalities in different use cases, these make the harmonisation of joint EU-China V2X trials possible by designing the joint EU-China V2X trial framework. The messages (GLOSA: SPaT and MAP) for supporting automated driving when approaching urban intersections are not time-critical (requires millisecond reaction time) but need to be received 10 - 200 m before the intersection area. The test message sizes were 200 - 800 kB which is realistic for ASN.1 coded message.

The preliminary targeted KPIs for MAP, SPaT was to reach less than 10% packet error rate. The findings reported in section 4.1.1 showed that this can be reached when distance between LTE-V2X units is less than 800 m. The range observed in this trial is highly dependent on the given RF morphology and obstructions. It should be noted that while the factory default configurations of LTE-V2X devices complied with our targeted KPI, other use cases in the future may have different range requirements, which can be met through some RF and capacity optimization (e.g. through more RSUs, better antennas, antenna direction/tilts/heights etc.). For LTE/5G network connection in urban areas, the quality of connection is also highly dependent on the distance to the closest base station and the surrounding environment. If there are no stationary or dynamic obstacles within the urban space such as buildings, greenery, hills, trucks etc., then in LOS conditions the communication range can be few kilometres with PER remaining less than 5%. The antenna height is another significant factor. For RSUs, the position of the antenna should be chosen to maximize the height, positively impacting the range. In vehicles with one antenna installation, roof is preferred for the same reason. Of course, a diversity system with different antenna positions could benefit from NLOS reflections. This aspect is left for future research. The LTE/5G latencies observed in the tests were mainly around 30 - 80 ms depending on antenna height and packet size. However, the outlier results showed that when cellular connection was low quality due to NLOS, the 5G from IP network to Connected Vehicle latencies increased to more 1000 ms and also PER started to increase, while the latency requirements for automated driving were estimated to be less than 100 ms.

For the mean end-to-end latency, it is shown that the driving speed of the automated vehicle (ranging from 10 to 40 km/h) and message packet size differences did not affect the latency of LTE-V2X at the Finnish trial site. But the message transmission interval, for example, 50 ms (20 messages/s, emulating 20 LTE-V2X device stations) and 5 ms (200 messages/s, emulating 200 LTE-V2X device stations), has a noticeable effect on the mean latency. The latency in the joint EU-China V2X trials in Tampere, Finland in Europe is increased from within 25 ms to within 30 ms when the number of emulated stations is increased from 20 to 200. This is as expected as the latency of LTE-V2X is expected to increase when the channel load increases, and the bandwidth occupation worsens. The LTE-V2X PC5 performance test with physical LTE-V2X device stations in the Shanghai trial site showed that the latency mean is around 15 ms when there are around five devices that did not congest the communication channel. Moreover, the large-scale use cases' feasibility tests in Shanghai also showed that the latency mean is increased to within 38 ms when the number of

physical device participants (e.g., multiple RSUs and multiple OBUs in multiple vehicles) increases to twenty in a multiple-use case overlay scenario across the site. Since the vehicle is approaching the area with about 25 kph, it means messages need to be received within the 1.5 s latency tolerance for keeping a sufficient safety margin. And the latency results were well under the tolerance.

Please note these findings were observations of phenomena that are subjective to the deployment of equipment and their configurations (factory default), which conformed with the preliminary targeted KPIs set for joint EU-China V2X trials but not applicable for LTE-V2X devices' performance comparison among different manufacturers, and also not applicable for performance comparison across different technologies.

For SME and commercial use aspects in the 5G-Drive project, the importance of accurate and reliable hybrid positioning messaging for C-V2X, particularly in challenging satellite visibility environments, is high. Hybrid navigation tests showed the benefits of multi-sensor positioning systems using C-V2X communication to complement the positioning quality. Testing also verified the requirement of the navigation-based timing signal for the functionality of C-V2X.

Also, the need for synchronization with GNSS information to secure basic functionalities of commercial RSU and OBU has been validated in section 4.1.3.1. Communication tests with commercially available V2X-vehicles proved that the plug and play approach is still missing. During test preparation, one OEM provided commercial test vehicles in EU markets with US radiofrequency, which pointed out interoperability problems. In addition, the testing and opportunities exploring of road owners, authorities, and municipalities should in the future focus on practical cross-border and extensive scale utilisation. And at the end of the chain, interactive communication with road users happens. However, before communication links between infrastructure and road users need to be established, the back-end systems must collect and share precise and valuable information. Nonetheless, more work needs to be conducted in this field. Assessment and large-scale demonstrations in Europe and beyond, will enhance data-based evidence and will provide the industry and stakeholders with the opportunity to attain a better understanding on the comparison and benchmarking of the 5G benefits in the various regions around the globe.

The LTE-V2X performance impact regarding important factors, such as the vehicle speed and antenna height of the RSU, are theoretically validated in section 4.1.3.2 based on the V2X link budget model. Moreover, through the theoretical analyses based on the measurement results from the trial, we could verify the findings from the trials and drew better understanding that for when the antenna height changes from 1.4 to 3.8 meters, the number of paths in the trials varies from tens of paths to just a few paths. These trends of observations could be used to instruct the future modelling of V2X links.

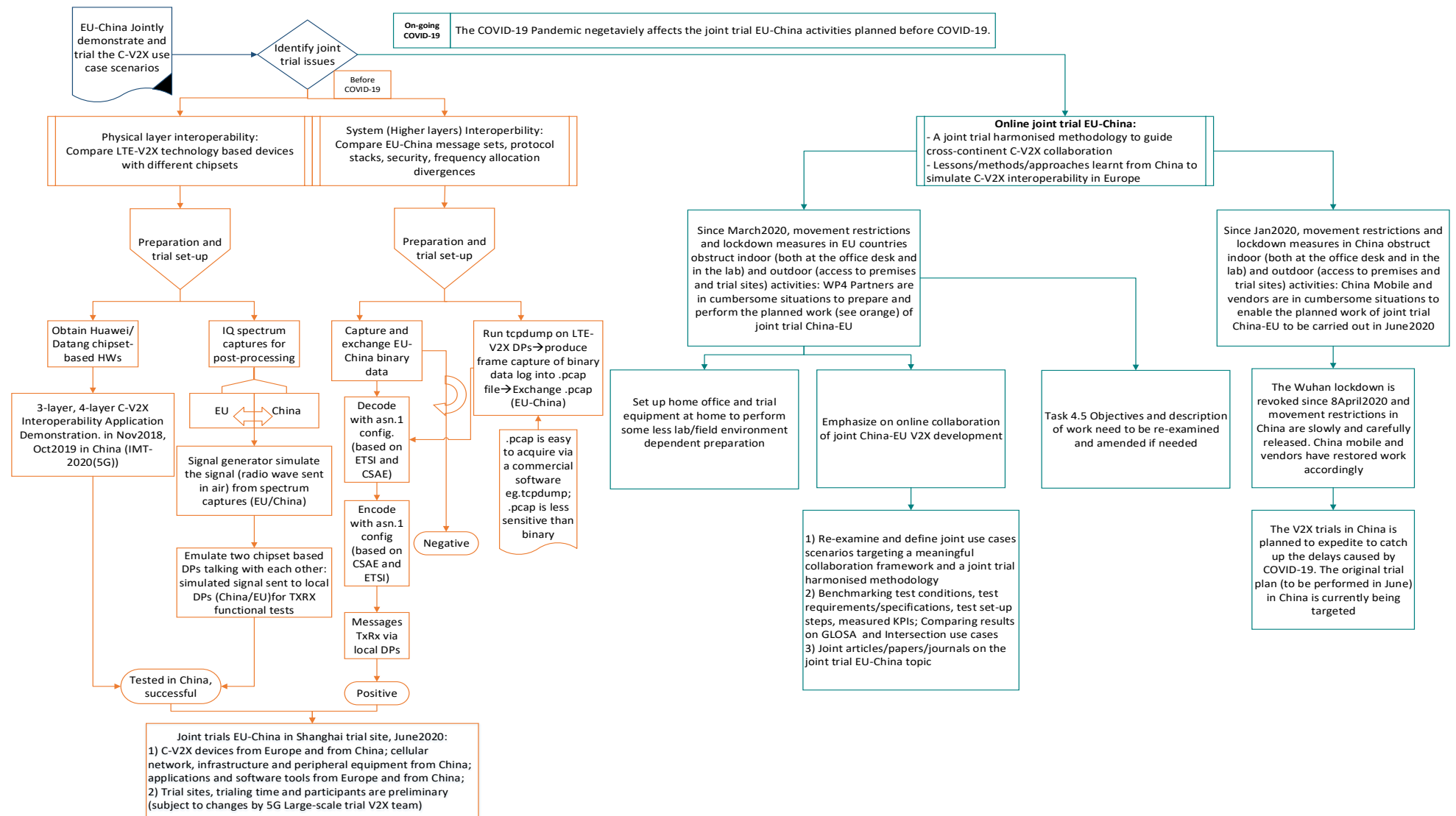
MEC comes with the promise of low delay communication and effective traffic steering. As we have shown in the urban area, the transmission delay is almost negligible (below 0.1 ms for 10 km). and the time-critical V2X traffic is characterized by a relatively low bitrate. Both observations led us to conclude that sparse MEC Host locations can serve nicely V2X time-critical applications in urban areas. The approach also provides benefits in terms of OPEX and CAPEX over highly distributed MEC infrastructure. In section 4.1.3.3, we have described a connection interruption problem that can be caused by the User Context Transfer (UCT) procedure of MEC. The procedure is typically triggered by a handover. Our estimations have shown that the delay induced by UCT implemented according to ETSI MEC specifications can be in the range of 5 ms to 10 ms. The problem can be nicely solved at the application level. In such an approach, it is proposed to make a UCT copy in target MEC-MEPs for all UEs (i.e. cars) located close to cell border. Such a simple, proactively triggered UCT combined with dual connectivity-based handover can provide zero interruption time.

References

- [1] Commission Implementing Decision (EU) 2020/1426 of 7 October 2020 on the harmonised use of radio spectrum in the 5875-5935 MHz frequency band for safety-related applications of intelligent transport systems (ITS) and repealing Decision 2008/671/EC.
- [2] European Telecommunications Standards Institute (ETSI), EN 302 571 V2.1.1: Intelligent Transport Systems (ITS); Radio communications equipment operating in the 5 855 MHz to 5 925 MHz frequency band; Harmonised Standard covering the essential requirements of article 3.2 of Directive 2014/53/EU.
- [3] European Telecommunications Standards Institute (ETSI), TR 103 766: Intelligent Transport Systems (ITS); Pre-standardization study on co-channel co-existence between IEEE- and 3GPP-based ITS technologies in the 5855 MHz-5925 MHz band; TR on co-channel co-existence between ITS-G5 and LTE-V2X.
- [4] European Telecommunications Standards Institute (ETSI), TR 103 667: Intelligent Transport Systems (ITS); Study on Spectrum Sharing between ITS-G5 and LTE-V2X technologies in the 5 855 MHz-5 925 MHz band.
- [5] Wang, Jian, et al. "A survey of vehicle to everything (V2X) testing." *Sensors* 19.2 (2019): 334.
- [6] C. A. Kerrache, C. T. Calafate, J.-C. Cano, N. Lagraa et P. Manzoni, «Trust management for vehicular networks: An adversary-oriented overview», *IEEE access*, vol. 4, pp. 9293--9307, 2016.
- [7] Tobin, J., Thorpe, C., Magoni, D., & Murphy, L. (2017, June). An Approach to Mitigate Multiple Malicious Node Black Hole Attacks on VANETs.
- [8] 5G-DRIVE consortium, Deliverable D5.3: Final Report of Security and Data Protection in Future 5G Vehicular Networks (Subsection 3.4.3.1 and 3.4.3.3)
- [9] Car-2-Car Communications Consortium (C2C-CC), White paper on ITS-G5 and Sidelink LTE-V2X Co-Channel Coexistence Mitigation Methods, [Available online]: https://www.car-2-car.org/fileadmin/documents/General Documents/C2CCC_WP_2091_Co-ChannelCoexistence_MitigationMethods_V1.0.pdf
- [10] Molina-Masegosa, R.; Gozalvez, J.; "LTE-V for Sidelink 5G V2X Vehicular Communications: A New 5G Technology for Short-Range Vehicle-to-Everything Communications"; *IEEE Vehicular Technology Magazine*, vol. 12, issue 4 (2017).
- [11] Laux, S., Pannu, G. S., Schneider, S., Tiemann, J., Klingler, F., Sommer, C., & Dressler, F. (2016, December). OpenC2X—An open source experimental and prototyping platform supporting ETSI ITS-G5. In *2016 IEEE Vehicular Networking Conference (VNC)* (pp. 1-2). IEEE.
- [12] Lindberg et.al, 5GCAR Deliverable D2.2 Intermediate Report on V2X Business Models and Spectrum (version 2.0, public), Fifth Generation Communication Automotive Research and innovation, 2019-02-28.
- [13] CEPT/ECC. 2020. The harmonised use of Safety-Related Intelligent Transport Systems (ITS) in the 5875-5935 MHz frequency band. ECC Decision (08)01. available in [<https://docdb.cept.org/download/1583>]. cited on 8 June 2021.]
- [14] IoT news. <https://www.iottechnews.com/news/2019/jul/05/europe-votes-eu-wifi-5g-connected-cars/> Web site cited on [12 August 2019]
- [15] Chen et. al, EU-China research and trial cooperation on V2X, ZTE communication magazine
- [16] European commission portal: Spectrum needs for Intelligent Transport Systems/ Web site cited on [24 April 2020]
- [17] 5G-MOBIX consortium, Deliverable D2.5 Initial evaluation KPIs and metrics V1.4, 31 October 2019

- [18] 3GPP TS 22.185 V16.0.0: 3rd Generation Partnership Project; Technical Specification Group Services and System Aspects; Service requirements for V2X services; Stage 1 (Release 16).
- [19] 5G-DRIVE consortium, Deliverable D4.1 V2X development and test plan V1.0, April 2019
- [20] Vediafi, 2021, Clean Vehicles Wizard, <https://www.vedia.fi/cvw-clean-vehicles-wizard/>
- [21] Andrea Goldsmith, *Wireless Communications*, Cambridge University Press, 2012.
- [22] M. A. R. Baissas and A. M. Sayeed, "Pilot-based channel estimation for time-varying multipath channels for coherent CDMA receivers," *IEEE Transactions on Signal Processing*, vol. 50, no. 8, pp. 2037-2049, Aug. 2002.
- [23] D. Piazza and L. B. Milstein, "Analysis of multiuser diversity in time-varying channels," *IEEE Transactions on Wireless Communications*, vol. 6, no. 12, pp. 4412-4419, Dec. 2007.
- [24] Oljira, D. B., Brunstrom, A., Taheri, J., Grinnemo, K.: Analysis of Network Latency in Virtualized Environments. 2016 IEEE Global Communications Conference (GLOBECOM), pp. 1--6. DOI: 10.1109/GLOCOM.2016.7841603
- [25] Sollfrank, M., Loch, F., Denteneer, S. Vogel-Heuser, B.: Evaluating Docker for Lightweight Virtualization of Distributed and Time-Sensitive Applications in Industrial Automation. *IEEE Transactions on Industrial Informatics* **17**(5), 3566-3576 (2021). DOI: 10.1109/TII.2020.3022843
- [26] ETSI, Multi-access Edge Computing (MEC); Framework and Reference Architecture, GS MEC 003 V2.2.1, Dec. 2020.
- [27] 5GAA, Use Cases Volume I: Methodology, Examples and Service Level Requirements, v1.0, White Paper, Jun. 2019.
- [28] 5GAA, C-V2X Use Cases Volume II: Examples and Service Level Requirements v1.0, White Paper, Dec. 2020.
- [29] 3GPP, Service requirements for enhanced V2X scenarios, 3GPP TS 22.186 v16.2.0, Jun. 2019.
- [30] 5G-DRIVE Consortium, Deliverable D3.3 "Final Report of eMBB Trials", v3.0, May 2021
- [31] Wylie-Green, M. P., Svensson, T., "Throughput, Capacity, Handover and Latency Performance in a 3GPP LTE FDD Field Trial", 2010 IEEE Global Telecommunications Conference GLOBECOM 2010, 1--6 (2010). doi:10.1109/GLOCOM.2010.5683398
- [32] Irmer, R. et al. "Multisite field trial for LTE and advanced concepts.", 47(2), 0-98 (2009). doi: 10.1109/mcom.2009.4785385
- [33] Tayyab, M., Gelabert, X., Jäntti, R., "A Survey on Handover Management: From LTE to NR", in *IEEE Access*, vol. 7, pp. 118907-118930, 2019, doi: 10.1109/ACCESS.2019.2937405.
- [34] ETSI, Multi-access Edge Computing (MEC); Application Mobility Service API, GS MEC 021 V2.1.1, Jan. 2020.
- [35] TechEmpower, Web Framework Benchmarks [Online]. Available: <https://www.techempower.com/benchmarks/#section=data-r20&hw=ph&test=db&l=zijzen-7&a=2>, (Accessed 17/06/2021)
- [36] Simulation of Urban Mobility, [Online]. Available: <https://www.eclipse.org/sumo/contact/>
[S3.4.2.1] 5G-DRIVE Consortium, Deliverable D4.2 "5GD-D4.2_Joint specification for V2X trials_v1.5", August 2020
- [37] Matti Kutila, Kimmo Kauvo, Pasi Pyykönen, Xiaoyun Zhang, Victor Garrido Martinez, Yinxiang Zheng, Shen Xu, A C-V2X/5G Field Study for Supporting Automated Driving, *IEEE IV*, May 2021
- [38] Xiaoyun Zhang, Matti Kutila, Kimmo Kauvo, Victor Garrido Martinez, Juha Karppinen and Lasse Nykänen, Influence of infrastructure antenna location and positioning system availability to open-road C-V2X supported Automated Driving, *IEEE 5G for CAM*, May 2021

Appendix A Joint EU-China V2X trial campaign schematic



Appendix B EU (CAM) and China (BSM) message comparison

Message Type	EU	China
CAM – BSM binary	<pre> 07 84 32 33 34 35 36 37 38 33 10 B1 B2 B3 B4 B6 B0 0C A0 76 FF 4A C2 AC 23 0F FF FF FF 0F A1 C2 00 0F F6 00 00 00 00 00 01 FE FF F7 FF FF FF F8 01 E0 01 37 FF FF D2 CF E3 CF FF F0 F1 00 00 00 00 00 00 00 01 FF FF C2 03 FF FF FF 3F FF FF FF 81 F8 00 00 00 00 00 00 00 06 FF FF FF FE FF FF FF C0 00 01 90 FF 80 </pre>	<pre> 07 84 32 33 34 35 36 37 38 33 10 B1 B2 B3 B4 B6 B0 0C A0 76 FF 4A C2 AC 23 0F FF FF FF 0F A1 C2 00 0F F6 00 00 00 00 01 FE FF F7 FF FF FF F8 01 E0 01 37 FF FF D2 CF E3 CF FF F0 F1 00 00 00 00 00 00 00 01 FF FF C2 03 FF FF FF 3F FF FF FF 81 F8 00 00 00 00 00 00 06 FF FF FF FE FF FF FF C0 00 01 90 FF 80 </pre>
CAM – BSM ASN.1	<pre> DEFINITIONS AUTOMATIC TAGS ::= BEGIN IMPORTS ItsPduHeader, CauseCode, ReferencePosition, AccelerationControl, Curvature, CurvatureCalculationMode, Heading, LanePosition, EmergencyPriority, EmbarkationStatus, Speed, DriveDirection, LongitudinalAcceleration, LateralAcceleration, VerticalAcceleration, StationType, ExteriorLights, DangerousGoodsBasic, SpecialTransportType, LightBarSirenInUse, VehicleRole, VehicleLength, VehicleWidth, PathHistory, RoadworksSubCauseCode, ClosedLanes, TrafficRule, SpeedLimit, SteeringWheelAngle, PerformanceClass, YawRate, ProtectedCommunicationZone, PtActivation, Latitude, Longitude, ProtectedCommunicationZonesRSU, </pre>	<pre> BSM DEFINITIONS AUTOMATIC TAGS ::= BEGIN -- imports and exports EXPORTS BasicSafetyMessage; IMPORTS AccelerationSet4Way FROM DefAcceleration BrakeSystemStatus FROM VehBrake VehicleSize FROM VehSize Position3D, PositionConfidenceSet FROM DefPosition DSecond FROM DefTime TransmissionState FROM VehStatus Speed, Heading, SteeringWheelAngle, MotionConfidenceSet FROM DefMotion MsgCount FROM MsgFrame VehicleClassification FROM VehClass VehicleSafetyExtensions FROM VehSafetyExt; BasicSafetyMessage ::= SEQUENCE { </pre>

<pre> CenDsrcTollingZone FROM ITS-Container {itu-t(0) identified-organization(4) etsi(0) itsDomain(5) wgl(1) ts(102894) cdd(2) version(1)}; CAM ::= SEQUENCE { header ItsPduHeader, cam CoopAwareness } CoopAwareness ::= SEQUENCE { generationDeltaTime GenerationDeltaTime, camParameters CamParameters } CamParameters ::= SEQUENCE { basicContainer BasicContainer, highFrequencyContainer HighFrequencyContainer, lowFrequencyContainer LowFrequencyContainer OPTIONAL, specialVehicleContainer SpecialVehicleContainer OPTIONAL, ... } HighFrequencyContainer ::= CHOICE { basicVehicleContainerHighFrequency BasicVehicleContainerHighFrequency, </pre>	<pre> msgCnt MsgCount, id OCTET STRING (SIZE(8)), -- vehicle ID plateNo OCTET STRING (SIZE(4..16)) OPTIONAL, -- Reserved for Electronic Vehicle Identification secMark DSecond, pos Position3D, accuracy PositionConfidenceSet, transmission TransmissionState, speed Speed, heading Heading, angle SteeringWheelAngle OPTIONAL, motionCfd MotionConfidenceSet OPTIONAL, accelSet AccelerationSet4Way, brakes BrakeSystemStatus, size VehicleSize, vehicleClass VehicleClassification, -- VehicleClassification includes BasicVehicleClass and other extendible type safetyExt VehicleSafetyExtensions OPTIONAL, ... } END </pre>
---	---

```
        rsuContainerHighFrequency
    RSUContainerHighFrequency,

        ...

    }

    LowFrequencyContainer ::= CHOICE {
        basicVehicleContainerLowFrequency
    BasicVehicleContainerLowFrequency,

        ...

    }

    SpecialVehicleContainer ::= CHOICE {
        publicTransportContainer
    PublicTransportContainer,

        specialTransportContainer
    SpecialTransportContainer,

        dangerousGoodsContainer
    DangerousGoodsContainer,

        roadWorksContainerBasic
    RoadWorksContainerBasic,

        rescueContainer
    RescueContainer,

        emergencyContainer
    EmergencyContainer,

        safetyCarContainer
    SafetyCarContainer,

        ...

    }

    BasicContainer ::= SEQUENCE {
        stationType      StationType,
        referencePosition ReferencePosition,
```

```

...

}

    BasicVehicleContainerHighFrequency ::=
SEQUENCE {
        heading                Heading,
        speed                   Speed,
        driveDirection
DriveDirection,
        vehicleLength
VehicleLength,
        vehicleWidth           VehicleWidth,
        longitudinalAcceleration
LongitudinalAcceleration,
        curvature               Curvature,
        curvatureCalculationMode
CurvatureCalculationMode,
        yawRate                 YawRate,
        accelerationControl
AccelerationControl OPTIONAL,
        lanePosition            LanePosition
OPTIONAL,
        steeringWheelAngle
SteeringWheelAngle OPTIONAL,
        lateralAcceleration
LateralAcceleration OPTIONAL,
        verticalAcceleration
VerticalAcceleration OPTIONAL,
        performanceClass
PerformanceClass OPTIONAL,
        cenDsrcTollingZone
CenDsrcTollingZone OPTIONAL
    }

```



```
BasicVehicleContainerLowFrequency ::=
SEQUENCE {
    vehicleRole      VehicleRole,
    exteriorLights    ExteriorLights,
    pathHistory       PathHistory
}

PublicTransportContainer ::= SEQUENCE {
    embarkationStatus EmbarkationStatus,
    ptActivation       PtActivation
OPTIONAL
}

SpecialTransportContainer ::= SEQUENCE {
    specialTransportType
SpecialTransportType,
    lightBarSirenInUse
LightBarSirenInUse
}

DangerousGoodsContainer ::= SEQUENCE {
    dangerousGoodsBasic
DangerousGoodsBasic
}

RoadWorksContainerBasic ::= SEQUENCE {
    roadworksSubCauseCode
RoadworksSubCauseCode OPTIONAL,
    lightBarSirenInUse
LightBarSirenInUse,
    closedLanes        ClosedLanes
OPTIONAL
```

```
}

RescueContainer ::= SEQUENCE {
    lightBarSirenInUse LightBarSirenInUse
}

EmergencyContainer ::= SEQUENCE {
    lightBarSirenInUse LightBarSirenInUse,
    incidentIndication CauseCode OPTIONAL,
    emergencyPriority EmergencyPriority
OPTIONAL
}

SafetyCarContainer ::= SEQUENCE {
    lightBarSirenInUse LightBarSirenInUse,
    incidentIndication CauseCode OPTIONAL,
    trafficRule          TrafficRule
OPTIONAL,
    speedLimit           SpeedLimit OPTIONAL
}

RSUContainerHighFrequency ::= SEQUENCE {
    protectedCommunicationZonesRSU
ProtectedCommunicationZonesRSU OPTIONAL,
    ...
}

GenerationDeltaTime ::= INTEGER {
    oneMilliSec(1)
} (0..65535)
```

END

Appendix C Examples of test reports from the preparatory tests conducted in the JRC Radio Spectrum Laboratory

This appendix presents a selection of three test reports for the preparatory tests carried out at the JRC Radio Spectrum Laboratory following the technical requirements and procedures in ETSI EN 302 571 (Harmonised European Standard for radio communications equipment of Intelligent Transport Systems in the 5.9 GHz band). In particular, the following test reports using commercial ITS-G5 and LTE-V2X Roadside Units (RSUs) have been included for illustrative purposes:

- **Transmit Power Control** (section 5.3.3 in ETSI EN 302 571, device under test: ITS-G5 RSU)
- **Transmitter spectrum mask within the 5 GHz ITS frequency band for 10 MHz channels** (section 5.3.5 in ETSI EN 302 571, device under test: LTE-V2X RSU)
- **Power spectral density** (section 5.3.3 in ETSI EN 302 571 V2.1.1, device under test: LTE-V2X RSU)

Test reports for all preparatory tests in section 2.2.1.2 are available upon request.

C.1 Transmit Power Control test

C.1.1 Test information

- Date of test: 01/03/2019
- Normative reference: ETSI 302 571 V2.1.1, section 5.3.3.2.3
- Device under test: ITS-G5 roadside unit, device manufacturer and model name [REDACTED]
- Firmware version: [REDACTED]

C.1.2 Test setup

For transmit power control measurement, test setup #002 in Figure 95 is used. A fast power sensor RPR3006W from DARE Instruments is connected to antenna port 1 of the DUT through a test cable assembly. The test cable assembly consists of a coaxial cable, a 10 dB attenuator, a 20 dB attenuator and two N-SMA adaptors. Measurement data of the cable assembly is saved locally.

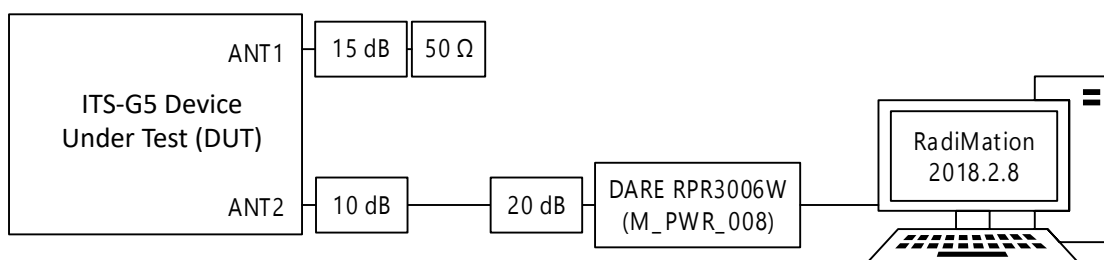


Figure 95: Test setup #002

C.1.3 DUT configuration and operation

The basic 802.11p application test-tx together with chconfig are used for generating and transmitting test packets.

Test is performed for only one carrier frequency (5.86 GHz) and only one antenna port. Transmit power is varied from -4 dBm to +23 dBm by 1 dB increment by running test-tx with parameter -p from -8 to 46.

Configuration example for channel 172 and -4 dBm output power:

- `chconfig -s -c 172`
- `test-tx -n 10000 -r 100-a 1 -c 172 -p -8`

Configuration example for channel 172 and 23 dBm output power:

- `chconfig -s -c 172`
- `test-tx -n 10000 -r 100-a 1 -c 172 -p 46`

C.1.4 Test procedure

The test procedure implements ETSI EN 302 571 clause 5.3.3.2.3 for conducted measurement of transmit power control. A modified version adds a description specific to the current DUT and instrumentation.

C.1.4.1 Original test procedure

The test procedure shall be as follows:

Step 1:

- Connect the DUT transmitter output to the test setup and activate normal operation at its minimum TPC output power PM , with $PM \leq 3$ dBm EIRP according to clause 4.2.4.2.

Step 2:

- Measure the duty cycle x of the DUT transmitter.
- The observed duty cycle of the transmitter ($\frac{t_{ON}}{t_{ON}+t_{OFF}}$) shall be noted as x ($0 < x \leq 1$) and shall be recorded in the test report.

Step 3:

- Measure DUT transmitter output power.

Step 4:

- The observed value shall be noted as A (in dBm).
- The EIRP shall be calculated from the measured output power A (in dBm), the observed duty cycle x , with the stated antenna gain G in dBi and the cable and connector losses L in dB, according to $P_{(e.i.r.p)} = A + L + G + 10 \times \log\left(\frac{1}{x}\right)$ (dBm).
- If more than one antenna assembly is intended for this power setting, the gain of the antenna assembly with the highest gain shall be used.

Step 5:

- $P_{(e.i.r.p)}$ shall be recorded in the test report as lowest output power level P_L .

Step 6:

- Increase the current DUT transmit power P_T by 1 dB.
- If $P_T < P_H$ repeat Step 2 to Step 4, else the test is completed.

Step 7:

- $P_{(e.i.r.p)}$ shall be recorded in the test report as TPC output power level.
- Continue with Step 6.

C.1.4.2 Modified test procedure

The test procedure shall be as follows:

Step 1:

- Connect the DUT transmitter output 1 (ANT1) to the test setup and activate normal operation at the highest output power level as described in section DUT configuration and operation.

Step 2:

- Measure the duty cycle x of the DUT transmitter using the power sensor RPR3006W from DARE Instruments. The accompanied software RadiMation 2018.2.8 is used with the following parameters:
 - Carrier frequency: 5.86 GHz
 - Trigger: Manual
 - Trigger level: -40 dBm
 - Measurement time: 1s
 - Sample rate: 1000000
 - Gap time: 5 ms

- Threshold level: -20 dBc

Step 3:

- Measure DUT transmitter output power (A). This step is accomplished by recording the value P displayed as RMS in the Measurement Values window of software RadiMation (see Figure 96). The output power A shall be calculated from the measured value P and the test cable assembly losses L_t , according to $A1(dBm) = P1(dBm) + L_t(dB)$.

Step 4:

- The EIRP shall be calculated from the measured output power A (in dBm), the observed duty cycle x , with the stated antenna gain G in dBi and the cable and connector losses L in dB, according to $P_{(e.i.r.p)} = A + L + G + 10 \times \log\left(\frac{1}{x}\right) (dBm)$.

Step 5:

- $P_{(e.i.r.p)}$ shall be recorded in the test report as lowest output power level P_L .

Step 6:

- Increase the current DUT transmit power P_T by 1 dB.
- If $P_T < P_H$ repeat Step 2 to Step 4, else the test is completed.

Step 7:

- $P_{(e.i.r.p)}$ shall be recorded in the test report as TPC output power level.
- Continue with Step 6.

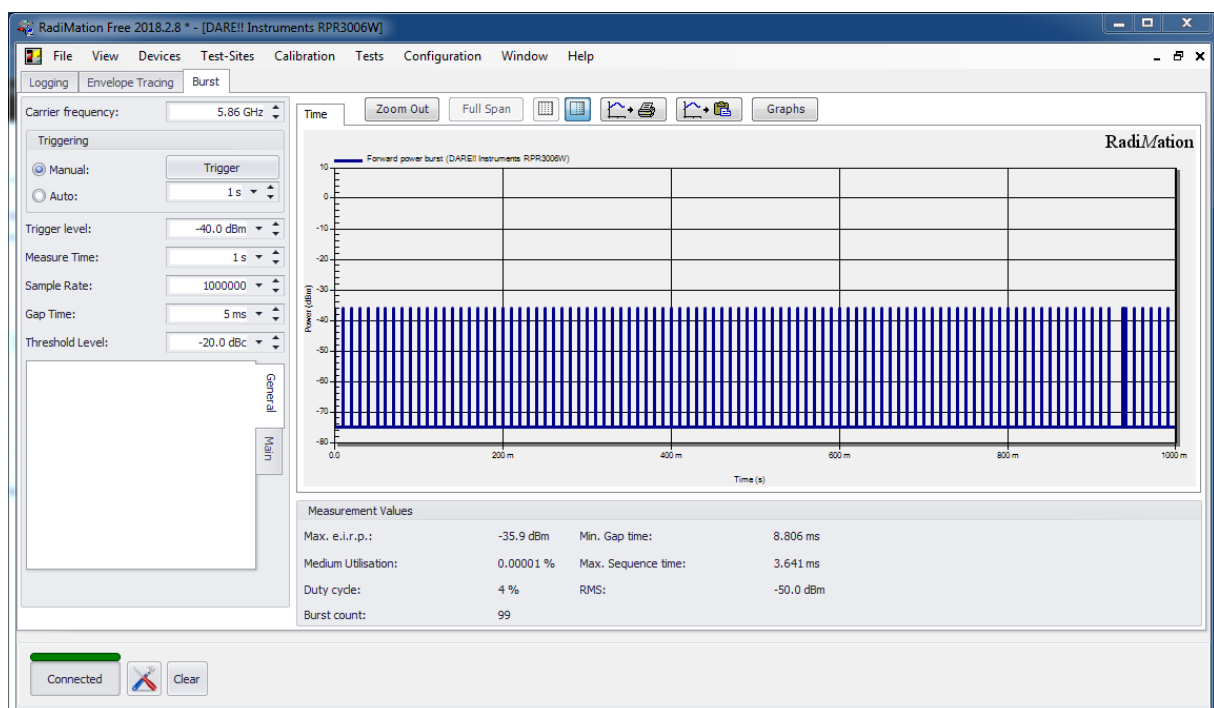


Figure 96: Power sensor software used to measure duty cycle and output power

C.1.4.3 Results

The result of the transmit power control measurement is summarized in Table 36.

The transmit power control test passes because the minimum TPC output is less than 0 dBm e.i.r.p on a single antenna and can be varied up to the maximum specified RF output power e.i.r.p of the DUT. This maximum power is achieved when the device output power P_T is set to 23 dBm.

P_T (dBm)	P (dBm)	A (dBm)	x (%)	G (dBi)	L (dB)	TPC (dBm)
-4	-50.0	-19.5	4.0	4.0	0.0	-1.5
-3	-49.0	-18.5	4.0	4.0	0.0	-0.5
-2	-47.8	-17.3	4.0	4.0	0.0	0.7
-1	-46.8	-16.3	3.9	4.0	0.0	1.8
0	-45.7	-15.2	4.0	4.0	0.0	2.8
1	-44.6	-14.1	4.0	4.0	0.0	3.9
2	-43.6	-13.1	4.0	4.0	0.0	4.9
3	-42.6	-12.1	4.0	4.0	0.0	5.9
4	-41.5	-11.0	4.0	4.0	0.0	7.0
5	-40.7	-10.2	4.0	4.0	0.0	7.8
6	-39.6	-9.1	4.0	4.0	0.0	8.9
7	-38.6	-8.1	4.0	4.0	0.0	9.9
8	-37.6	-7.1	4.0	4.0	0.0	10.9
9	-36.7	-6.2	4.0	4.0	0.0	11.8
10	-35.7	-5.2	4.0	4.0	0.0	12.8
11	-34.6	-4.1	4.0	4.0	0.0	13.9
12	-33.6	-3.1	4.0	4.0	0.0	14.9
13	-32.6	-2.1	4.0	4.0	0.0	15.9
14	-31.6	-1.1	4.0	4.0	0.0	16.9
15	-30.6	-0.1	4.0	4.0	0.0	17.9
16	-29.6	0.9	4.0	4.0	0.0	18.9
17	-28.5	2.0	4.0	4.0	0.0	20.0
18	-27.6	2.9	4.0	4.0	0.0	20.9
19	-26.6	3.9	4.0	4.0	0.0	21.9
20	-25.4	5.1	4.0	4.0	0.0	23.1
21	-24.6	5.9	4.0	4.0	0.0	23.9
22	-23.5	7.0	4.0	4.0	0.0	25.0
23	-22.3	8.2	4.0	4.0	0.0	26.2

Table 36: Results transmit power control measurement

Definition of table fields:

- L_t : Test cable assembly losses;
- P : Measured mean power;
- A : Transmitter output power;

- ***L***: Cable and connector losses;
- ***G***: Stated antenna gain;
- ***x***: Observed duty cycle;
- ***TPC***: Transmit power control output power level.

C.2 Spectrum mask test

C.2.1 Test information

- Date of test: 20/10/2020
- Normative reference: draft ETSI EN 302 571 V2.1.12, section 5.4.5
- Device under test: LTE-V2X roadside unit, device manufacturer and model name [REDACTED]
- Firmware version: [REDACTED]

C.2.2 Test setup

For RF output power measurement, test setup #001 shown in Figure 97 is used. A spectrum analyser Rohde&Schwarz FSP7 is connected to antenna port 1 of the DUT through a test cable assembly. The test cable assembly consists of a coaxial cable, a 10 dB attenuator, a 20 dB attenuator and two N-SMA adaptors. Measurement data of the cable assembly is saved locally.

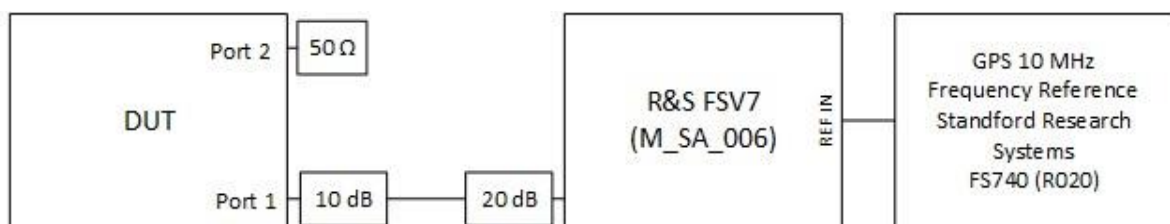


Figure 97: Test setup #001

C.2.3 DUT configuration and operation

“Activate normal operation” is understood as making the DUT transmitting in normal mode as opposed to the coexistence mode defined in ETSI TS 102 792.

The test is performed for each nominal carrier frequency of XXX using the corresponding configuration file and running the command `acme -l 1000 -l 100`. This configuration forces the allocation of 50 RBs thus transmission in full frequency band.

Configuration files for the LTE-V2X radio chipset are available upon request.

Carrier frequency (MHz)	EARFCN (3GPP Channel Number)	IEEE 802.11 Channel Number	Configuration file
5860	54590	172	172_50RBs_no_cr_limit_all_mcs.xml
5870	54690	174	174_50RBs_no_cr_limit_all_mcs.xml
2880	54790	176	176_50RBs_no_cr_limit_all_mcs.xml
5890	54890	178	178_50RBs_no_cr_limit_all_mcs.xml
5900	54990	180	180_50RBs_no_cr_limit_all_mcs.xml
5910	55090	182	182_50RBs_no_cr_limit_all_mcs.xml
5920	55190	184	184_50RBs_no_cr_limit_all_mcs.xml

Table 37: Configuration files used for each nominal carrier frequency

C.2.4 Test description

The test procedure implements clause 5.4.5.3.2 of draft ETSI EN 302 571 v2.1.12 for the measurement of the spectrum mask in conducted mode. The difference between this draft version and the current version (V2.1.1) is that emissions limits are not anymore defined relative to in-band power but as absolute e.i.r.p power in dBm in a measurement bandwidth of 100 kHz. The previous version was problematic because it did not allow a device to respect unwanted emission limits by lowering its transmit power.

As the DUT does not transmit simultaneously on two antenna ports (and assuming that it transmits with the same power spectral density on both ports) measurement is performed only on port 1.

C.2.5 Test procedure

The test procedure shall be as follow:

Step 1:

- Connect the DUT port 1 to the test setup and activate normal operation at the highest output power level as described in section DUT configuration and operation. Use the following spectrum analyser settings:
 - Centre Frequency: 5.86 GHz
 - Frequency Span: 50 MHz
 - RBW: 100 kHz
 - VBW: 1 MHz
 - Sweep Time: 10 ms
 - Spectrum mode: FFT
 - Detector Mode: RMS
 - Trace Mode: Average
 - Trigger: Gated IF power

Step 2:

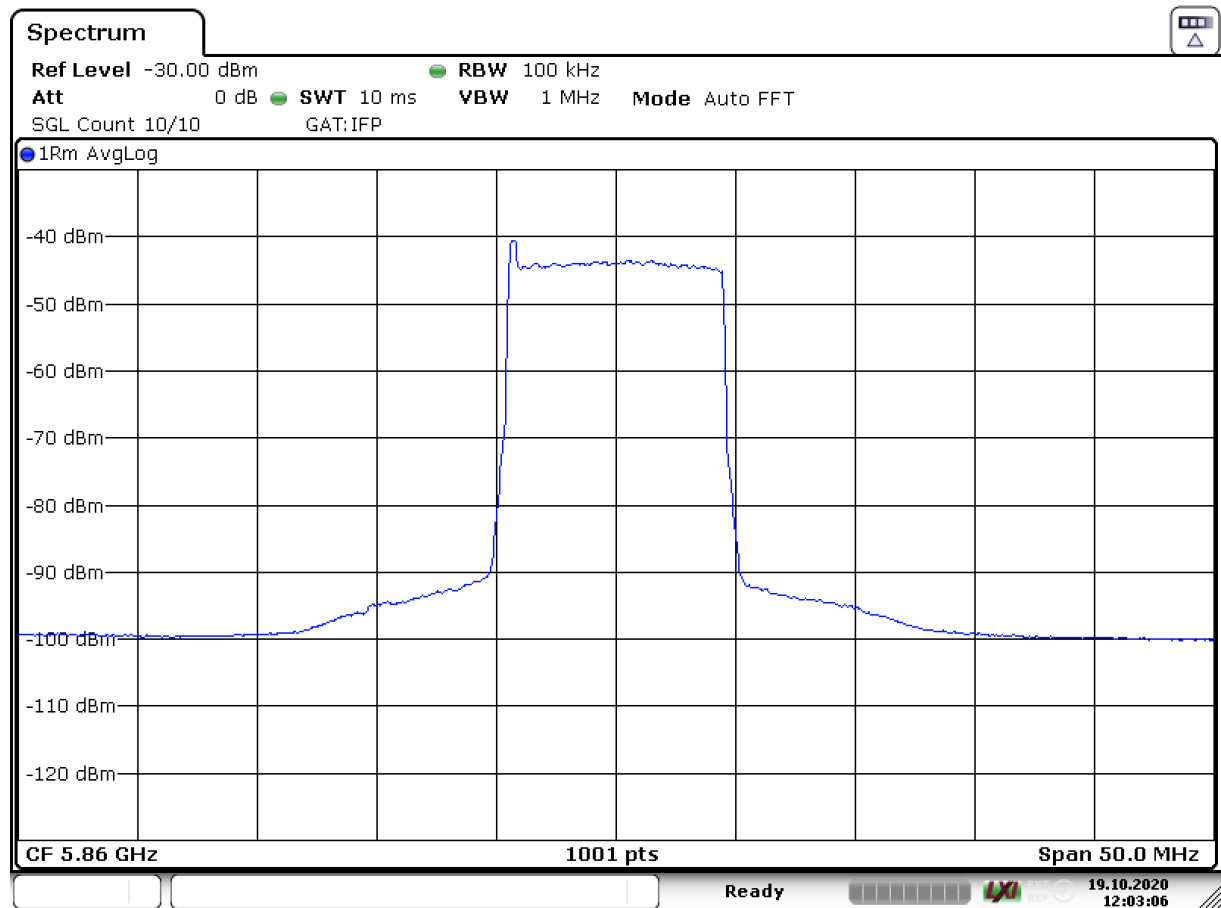
- Record the trace in an ASCII file.

Step 3:

- Use the Matlab script AddSpectrumMask.m (available upon request) to add the cable assembly loss and antenna gain to the recorded trace and plot the emission spectrum together with the frequency mask.

Step 4:

- Repeat steps 1 to 4 for carrier frequencies 5.87, 5.88, 5.89, 5.90, 5.91 and 5.92 GHz.



Date: 19.OCT.2020 12:03:06

Figure 98: Spectrum trace measured with 100 kHz RBW

C.2.6 Results

Graphical results of the spectrum mask test are shown in the following figures. Red traces are the absolute frequency mask. The blue trace represents the transmitter power spectral density measured in 100kHz bandwidth but expressed in unit of dBm/10 MHz.

The spectrum mask test passes because the power spectral density is below the frequency mask for all nominal carrier frequencies.

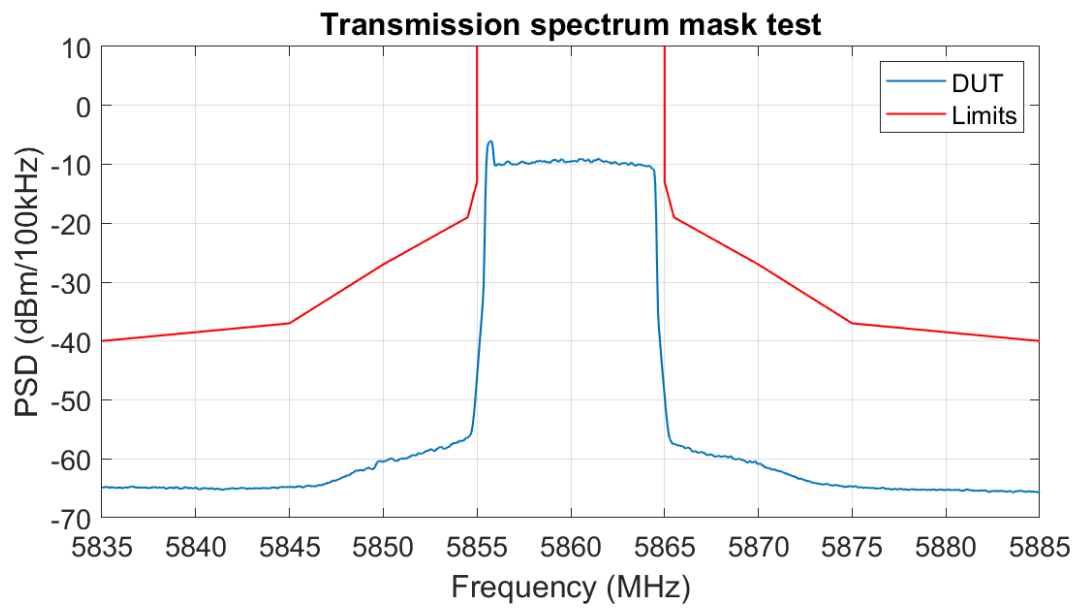


Figure 99: Transmission spectrum mask for nominal carrier frequency $f_c=5860$ MHz

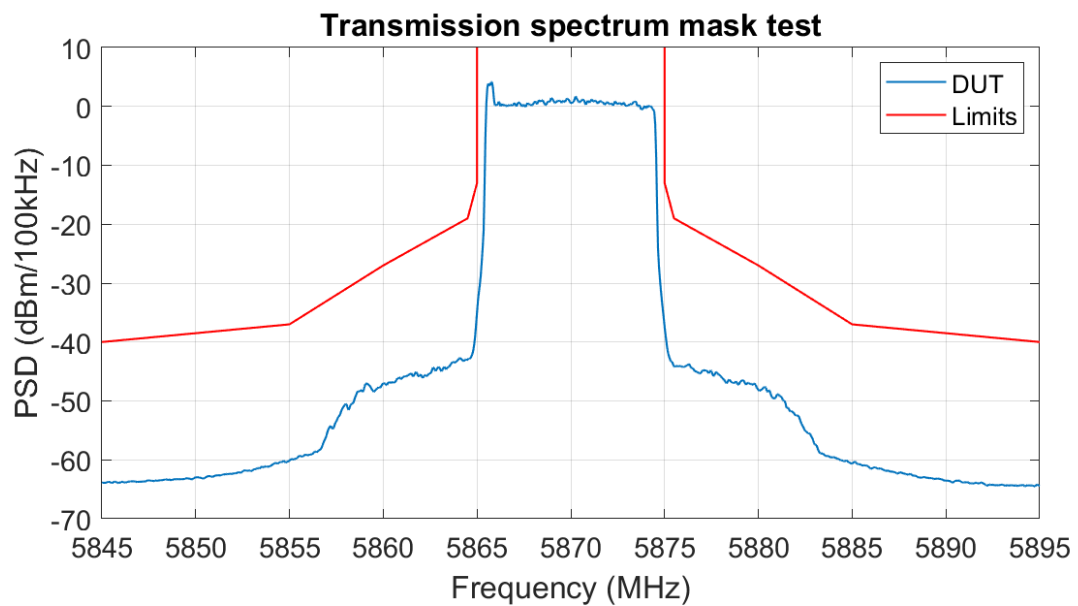


Figure 100: Transmission spectrum mask for nominal carrier frequency $f_c=5870$ MHz

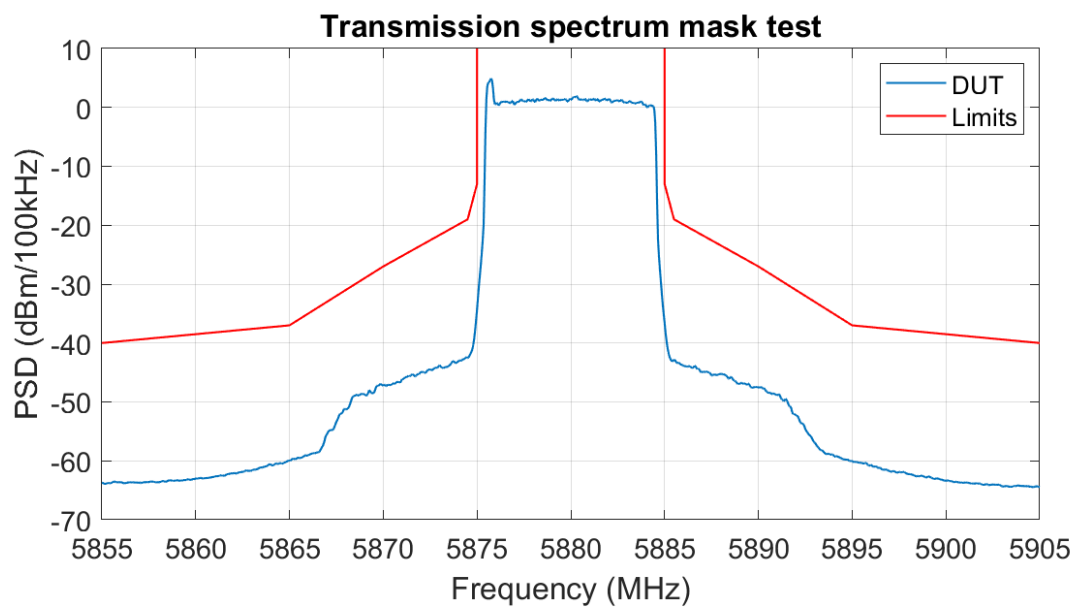


Figure 101: Transmission spectrum mask for nominal carrier frequency $f_c=5880$ MHz

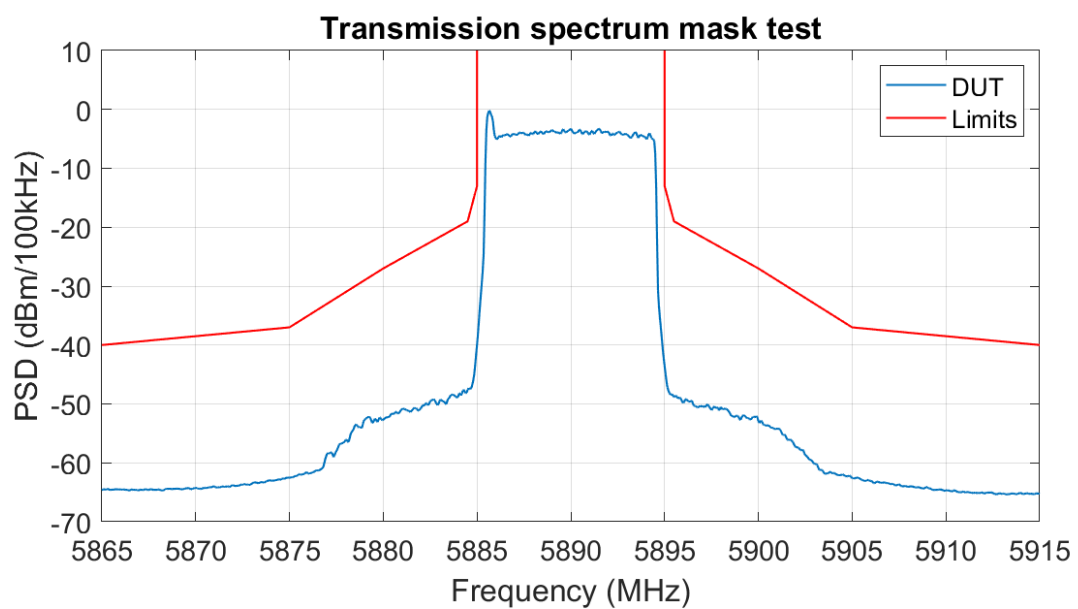


Figure 102: Transmission spectrum mask for nominal carrier frequency $f_c=5890$ MHz

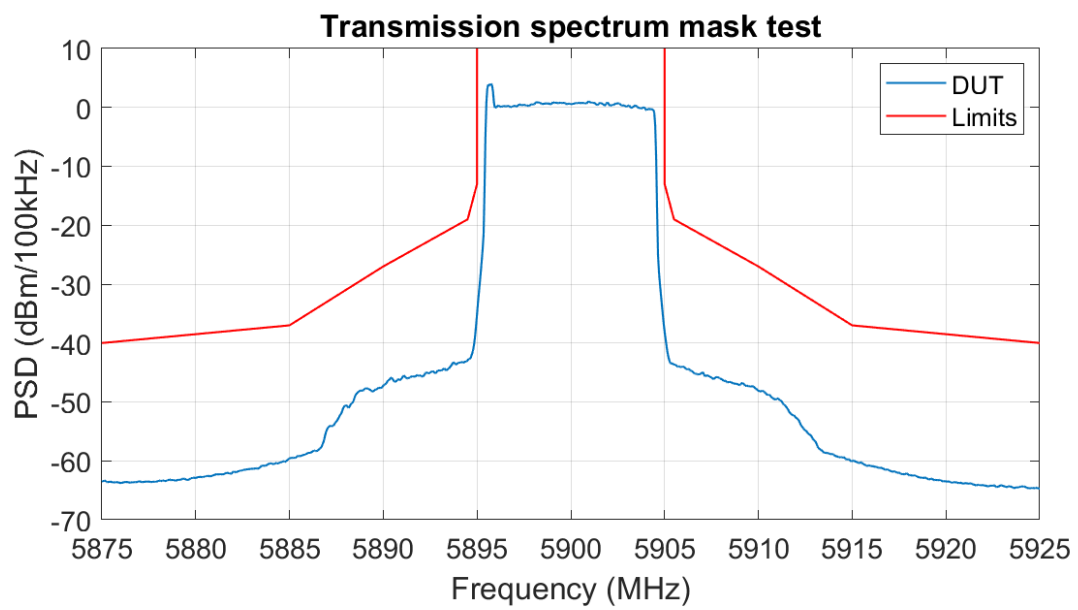


Figure 103: Transmission spectrum mask for nominal carrier frequency $f_c=5900$ MHz

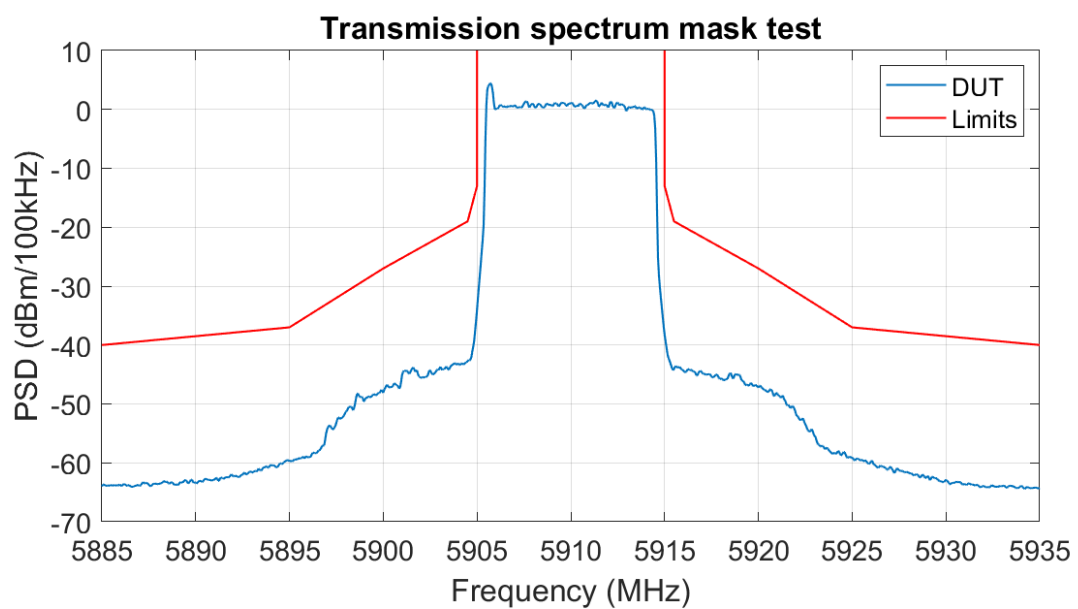


Figure 104: Transmission spectrum mask for nominal carrier frequency $f_c=5910$ MHz

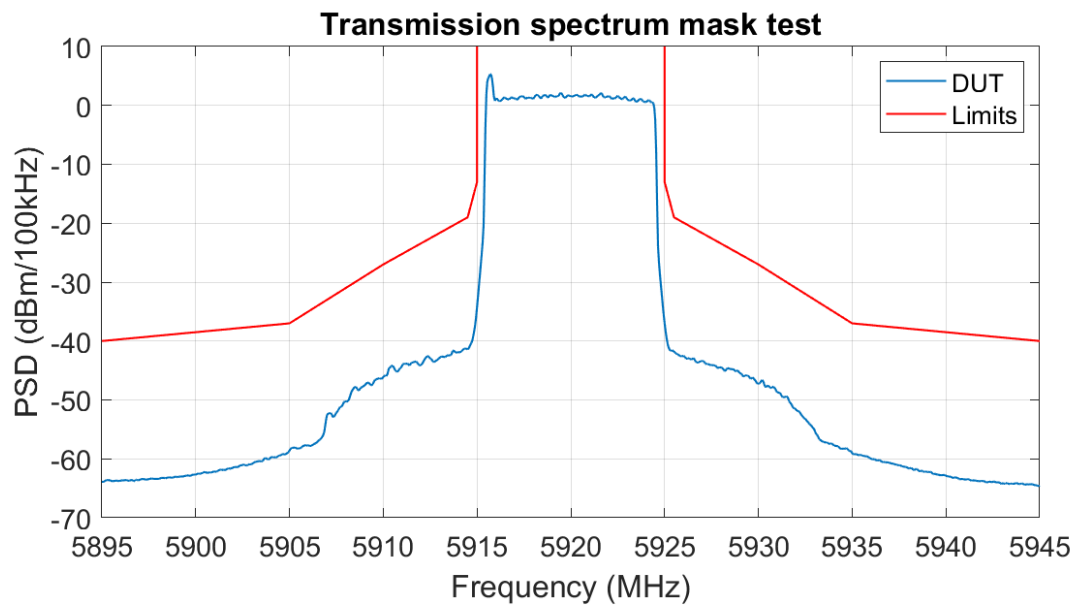


Figure 105: Transmission spectrum mask for nominal carrier frequency $f_c=5920$ MHz

C.3 Power spectral density test

C.3.1 Test information

- Date of test: 23/11/2020
- Normative reference: ETSI EN 302 571 V2.1.1 section 5.3.3.3.2.2
- Device under test: LTE-V2X roadside unit, device manufacturer and model name [REDACTED]
- Firmware version: [REDACTED]

C.3.2 Test setup

Figure 106 shows the test setup used for the implementation of the power density test. A spectrum analyser Rohde&Schwarz FSP7 is connected to antenna port 1 of the DUT through a test cable assembly. The test cable assembly consists of a coaxial cable, a 10 dB attenuator, a 20 dB attenuator and two N-SMA adaptors. Measurement data of the cable assembly is saved locally.

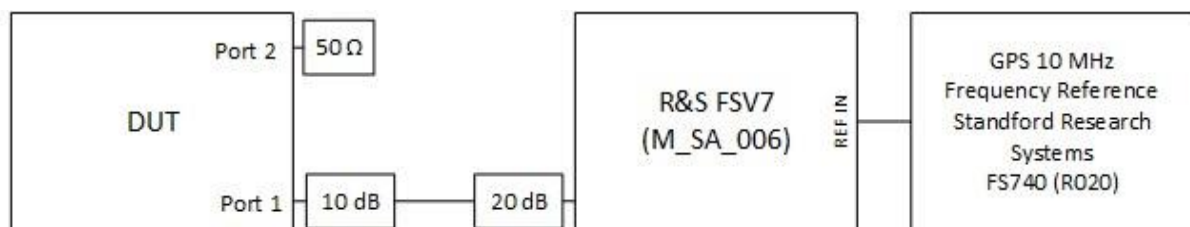


Figure 106: Test setup #001

C.3.3 DUT configuration and operation

“Activate normal operation” is understood as making the DUT transmitting in normal mode as oppose to the coexistence mode defined in ETSI TS 102 792.

The test is performed for each nominal carrier frequency in Table 38 using the corresponding configuration file and running the command `acme -l 1000 -l 100`. This configuration forces the allocation of 50 RBs thus transmission in full frequency band.

Configuration files for the LTE-V2X radio chipset are available upon request.

Carrier frequency (MHz)	EARFCN (3GPP Channel Number)	IEEE 802.11 Channel Number	Configuration file
5860	54590	172	172_50RBs_no_cr_limit_all_mcs.xml
5870	54690	174	174_50RBs_no_cr_limit_all_mcs.xml
2880	54790	176	176_50RBs_no_cr_limit_all_mcs.xml
5890	54890	178	178_50RBs_no_cr_limit_all_mcs.xml
5900	54990	180	180_50RBs_no_cr_limit_all_mcs.xml
5910	55090	182	182_50RBs_no_cr_limit_all_mcs.xml
5920	55190	184	184_50RBs_no_cr_limit_all_mcs.xml

Table 38: Configuration files used for each nominal carrier frequency

C.3.4 Test description

The test procedure implements ETSI EN 302 571 clause 5.3.3.2.2 for conducted measurement of power spectral density with some modifications. The modifications consist in measuring the power spectral density during transmission using the FFT mode of the spectrum analyser. By doing so, there is no need to measure and correct for the duty cycle x .

As the DUT does not transmit simultaneously on two antenna ports (and assuming that it transmits with the same power spectral density on both ports) measurement was performed only on port 1.

C.3.4.1 Original test procedure (section 5.3.3.3.2.2 of ETSI 302 571)

The test procedure shall be as follows:

Step 1:

- Connect the DUT transmitter output to the test setup and activate normal operation at highest output power level. The minimum transmitter on-time shall be 10 μ s.

Step 2:

- Measure the power spectral density D . The mean power density EIRP is calculated from the measured power density (D), the observed duty cycle x (see clause 5.3.3.3.2.1, Step 2), and the applicable antenna assembly gain G (expressed in dBi) according to the formula below. If more than one antenna assembly is intended for this power setting, the gain of the antenna assembly with the highest gain shall be used:

- $PD = D + G + 10 \times \log \left(\frac{1}{x} \right)$;
- PD (dBm/MHz) shall be recorded in the test report.

C.3.4.2 Modified test procedure

The test procedure shall be as follow:

Step 1:

- Connect the DUT port 1 to the test setup and activate normal operation at the highest output power level as described in section DUT configuration and operation. Use the following spectrum analyser settings:
 - Centre Frequency: 5.86 GHz
 - Frequency Span: 20 MHz
 - RBW: 1 MHz
 - VBW: 10 MHz
 - Sweep Time: 800 μ s
 - Detector Mode: RMS
 - Trace Mode: Average
 - Trigger: Gated IF power, Gate offset 20 μ s, gate length 800 μ s.

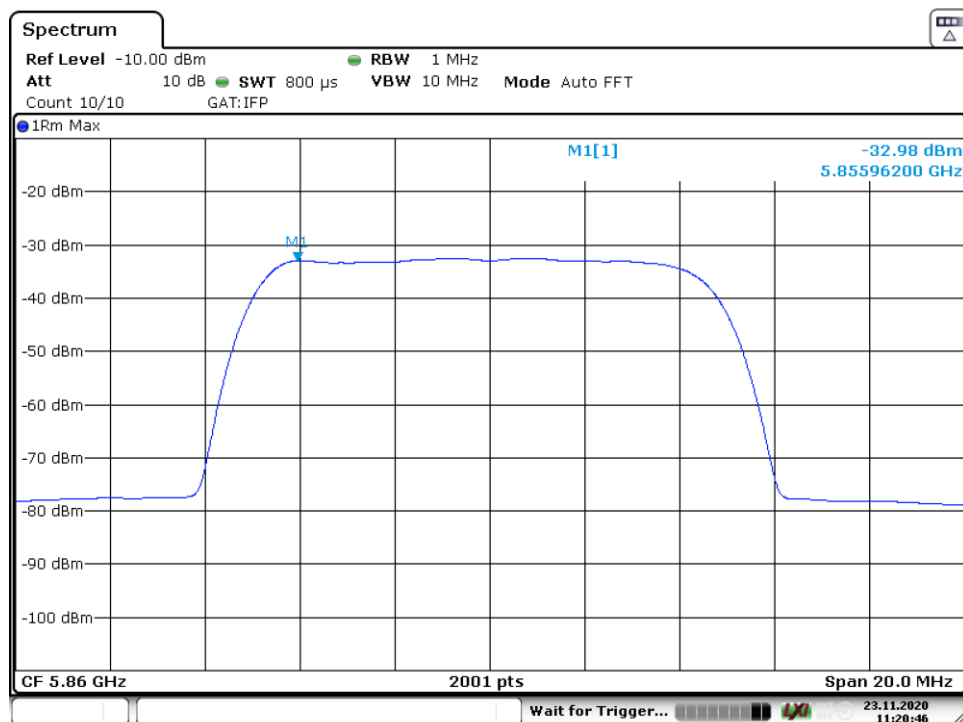
Step 2:

- Find the peak value using the marker peak function. This level is recorded as measured power density P . the highest mean power (Power Density) D in a 1 MHz band shall be calculated from the measured value P and the test cable assembly losses L_t , according to $D(\text{dBm/MHz}) = P(\text{dBm/MHz}) + L_t(\text{dB})$.
- The maximum spectral Power Density EIRP is calculated from the above measured Power Density D , the applicable antenna assembly gain G in dBi, according to the formula below. This value shall be recorded in the test report:

$$PD = D + G (\text{dBm/MHz})$$

Step 3:

- Repeat steps 1 to 2 for carrier frequencies 5.87, 5.88, 5.89, 5.90, 5.91 and 5.92 GHz.



Date: 23.NOV.2020 11:20:47

Figure 107: Power spectral density measurement with R&S FSV7 spectrum analyser

C.3.5 Results

The result of the power spectral density measurement is summarized in Table 39.

Power spectral density test passes because the maximum power spectral density (PD) does not exceed 23 dBm/MHz EIRP.

F_c (MHz)	P (dBm)	D (dBm)	G (dBi)	PD (dBm/MHz)
5860	-32.98	-2.48	4	1.5
5870	-22.61	7.89	4	11.9
5880	-21.82	8.68	4	12.7
5890	-21.82	8.68	4	12.7
5900	-22.07	8.43	4	12.4
5910	-22.28	8.22	4	12.2
5920	-22.37	8.13	4	12.1

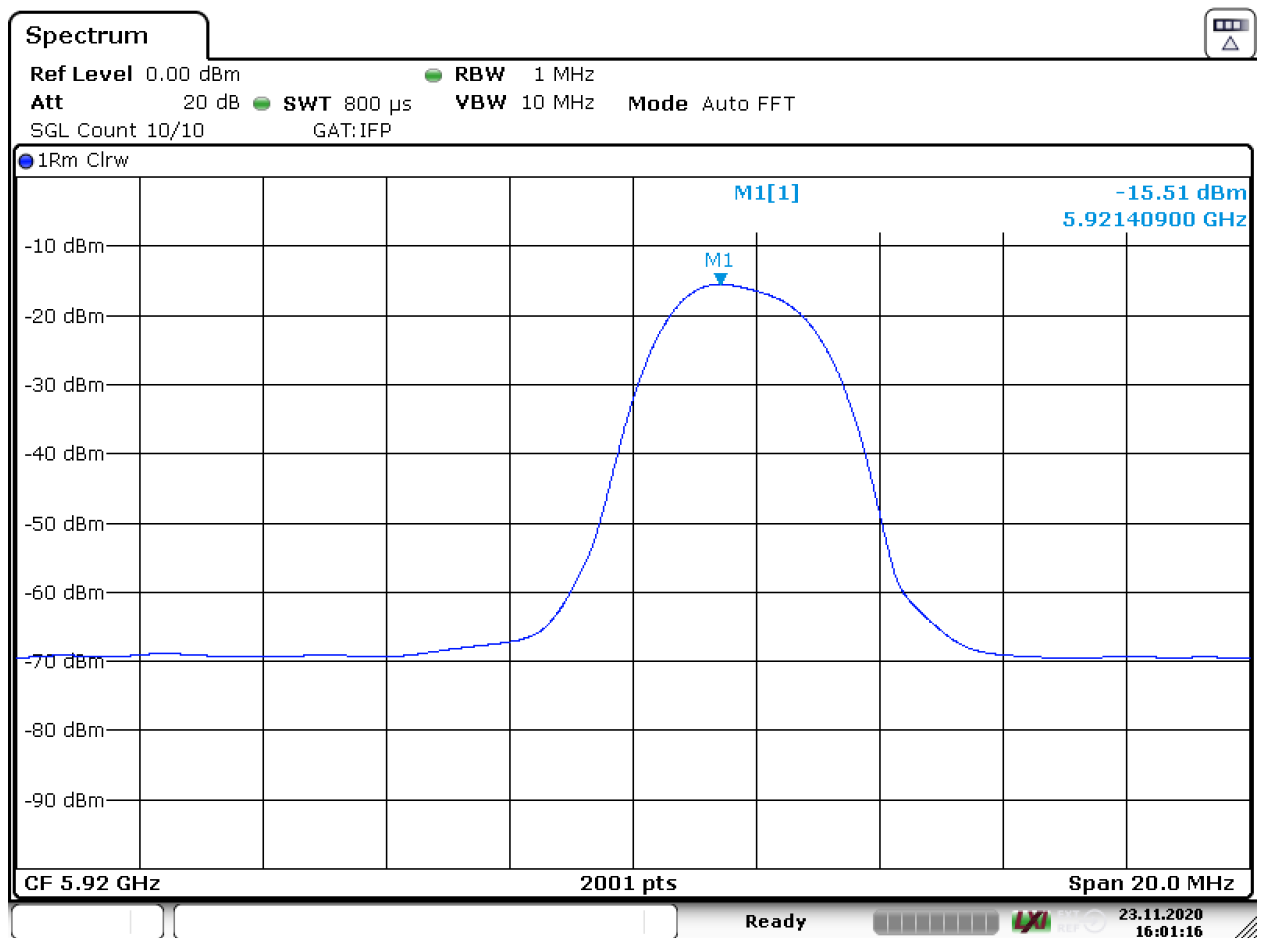
Table 39: Results of RF output power measurement for all nominal carrier frequencies

C.3.6 Some remarks about transmission bandwidth

The DUT was configured to transmit in 50 RBs. With 50 RBs, the RF power is spread over a 9 MHz bandwidth and therefore the power spectral density is 7 dB lower than it would be with a 10-RB allocation and with the same transmit power. To test the worst-case scenario, a configuration with 10 RBs should be used instead.

Neither the current version of EN 302 571 (v2.1.1) nor the last draft (v2.1.12) specifies a transmit bandwidth. This is because the standard was originally aimed at testing ITS-G5 technology that uses a fixed 10 MHz channel.

Additional measurements with 10 RBs were performed using the command `acme -l 50 -l 100`. Results are shown in Figure 108. The power spectral density increases to 19 dBm/MHz, but it is still 4 dB below the limit of 23 dBm/MHz.



Date: 23.NOV.2020 16:01:16

Figure 108: Power spectral density measurement with 10 RBs allocated

Appendix D Laboratory setups for experimental evaluation of co-channel coexistence method C in ETSI TR 103 766

This annex describes the different laboratory setups for the experimental evaluation of co-channel coexistence method C in ETSI Technical Report 103 766. The results from these co-channel coexistence experiments have been presented in section 2.2.2.

Table 40 summarises all laboratory configurations for the co-channel coexistence experiments. All experiments were carried out in conducted mode to have full control over all test conditions (e.g., received power, signal attenuation, etc.).

Test ID	C-ITS Transmitter	C-ITS Receiver	Interfering signal	Observations
1.1	ITS-G5	ITS-G5	ITS-G5	Interferer is a commercial device
1.2	ITS-G5	ITS-G5	LTE-V2X	Interferer is a commercial device
1.3	ITS-G5	ITS-G5	LTE-V2X (with ITS-G5 header)	Interferer is a VST replaying LTE-V2X synthetic signal
2.1	LTE-V2X	LTE-V2X	ITS-G5	Interferer is a commercial device
2.2	LTE-V2X	LTE-V2X	LTE-V2X	Interferer is a commercial device
2.3	LTE-V2X	LTE-V2X	LTE-V2X (with ITS-G5 header)	Interferer is a VST replaying LTE-V2X synthetic signal

Table 40: Laboratory setups for experimental evaluation of co-channel coexistence method C

D.1 Experiment 1.1: ITS-G5 is victim technology, ITS-G5 is interfering signal

D.1.1 Laboratory setup

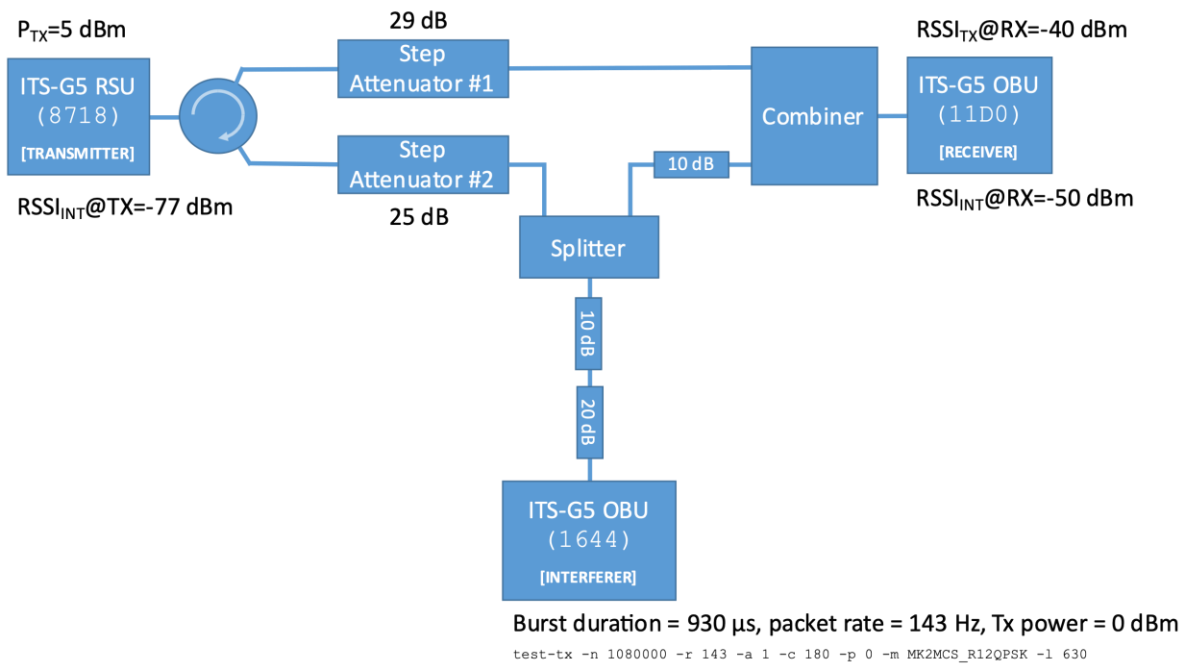


Figure 109: Laboratory setup for experiment 1.1

D.1.2 Additional notes

- The transmitter, receiver and interferer devices are commercial ITS-G5 units;
- The Signal-to-Interference Ratio (SIR) at the receiver is set to 10 dB (fixed) using the programmable step attenuator #1;
- This experiment scans the interferer power at the transmitter from -100 to -50 dBm in 1-dB steps using the programmable step attenuator #2;
- The wanted signal (transmitter to receiver) features an application-layer packet rate of 100 packets/s, a packet length of 350 bytes and uses a QPSK ½ Modulation and Coding Scheme (MCS);
- The interfering signal (interferer to transmitter and receiver) features an application-layer packet rate of 143 packets/s and a packet length of 630 bytes. At the RF level, this configuration translates into a $duty\ cycle = \frac{t_{ON}}{t_{ON} + t_{OFF}} = 13.3\%$

D.2 Experiment 1.2: ITS-G5 is victim technology, LTE-V2X is interfering signal

D.2.1 Laboratory setup

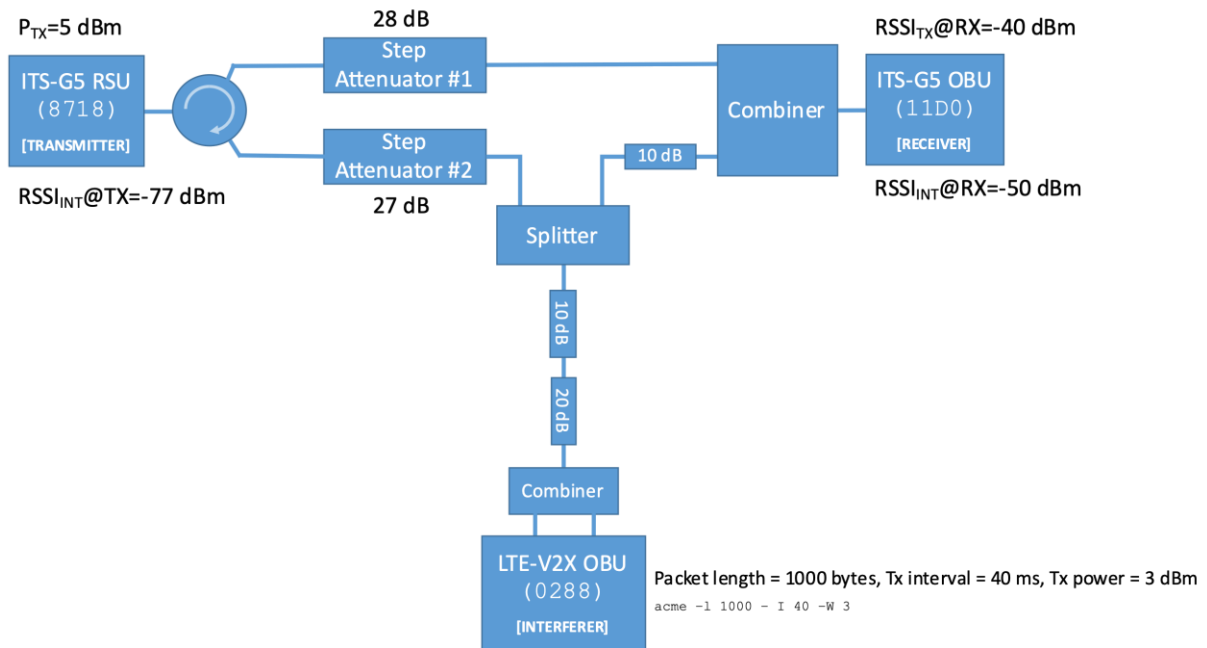


Figure 110: Laboratory setup for experiment 1.2

D.2.2 Additional notes

- The transmitter and receiver devices are commercial ITS-G5 units. The interferer device is a commercial LTE-V2X device;
- The Signal-to-Interference Ratio (SIR) at the receiver is set to 10 dB (fixed) using the programmable step attenuator #1;
- This experiment scans the interferer power at the transmitter from -100 to -50 dBm in 1-dB steps using the programmable step attenuator #2;
- The wanted signal (transmitter to receiver) features an application-layer packet rate of 100 packets/s, a packet length of 350 bytes and uses a QPSK ½ Modulation and Coding Scheme (MCS);
- The interfering signal (interferer to transmitter and receiver) features an application-layer packet rate of 25 packets/s and a packet length of 100 bytes. At the RF level, this configuration translates into a $duty\ cycle = \frac{t_{ON}}{t_{ON} + t_{OFF}} = 13.3\%$

D.3 Experiment 1.3: ITS-G5 is victim technology, LTE-V2X (with header) is interfering signal

D.3.1 Laboratory setup

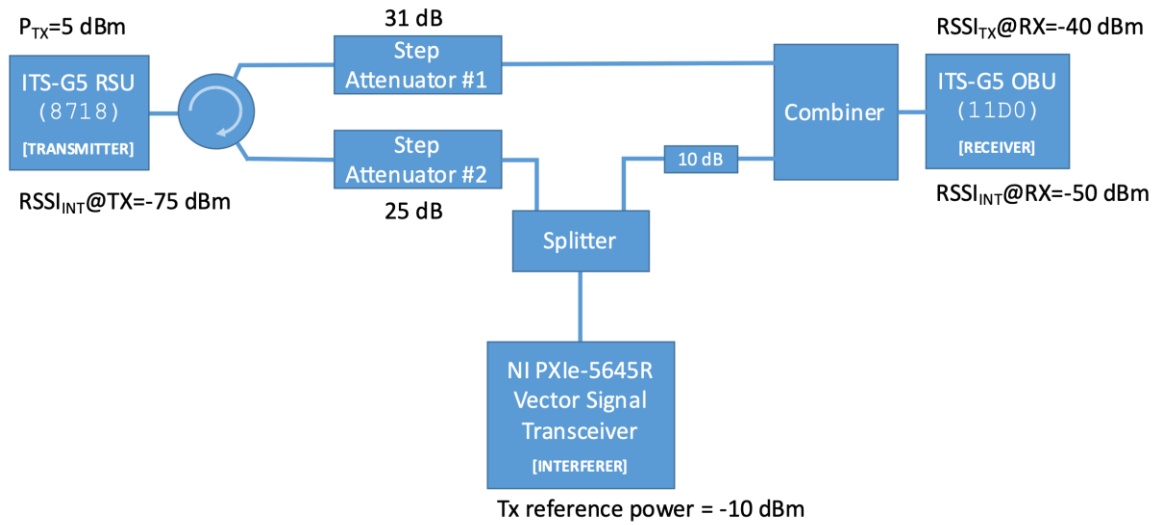


Figure 111: Laboratory setup for experiment 1.3

D.3.2 Additional notes

- The transmitter and receiver devices are commercial ITS-G5 units. The interferer device is a Vector Signal Transceiver replaying the LTE-V2X synthetic signal (i.e., LTE-V2X with ITS-G5 PHY header insertion) in infinite loop;
- The Signal-to-Interference Ratio (SIR) at the receiver is set to 10 dB (fixed) using the programmable step attenuator #1;
- This experiment scans the interferer power at the transmitter from -100 to -50 dBm in 1-dB steps using the programmable step attenuator #2;
- The wanted signal (transmitter to receiver) features an application-layer packet rate of 100 packets/s, a packet length of 350 bytes and uses a QPSK $\frac{1}{2}$ Modulation and Coding Scheme (MCS);
- The interfering signal (interferer to transmitter and receiver) features an application-layer packet rate of 25 packets/s and a packet length of 100 bytes. At the RF level, this configuration translates into a $duty\ cycle = \frac{t_{ON}}{t_{ON} + t_{OFF}} = 13.3\%$

D.4 Experiment 2.1: LTE-V2X is victim technology, ITS-G5 is interfering signal

D.4.1 Laboratory setup

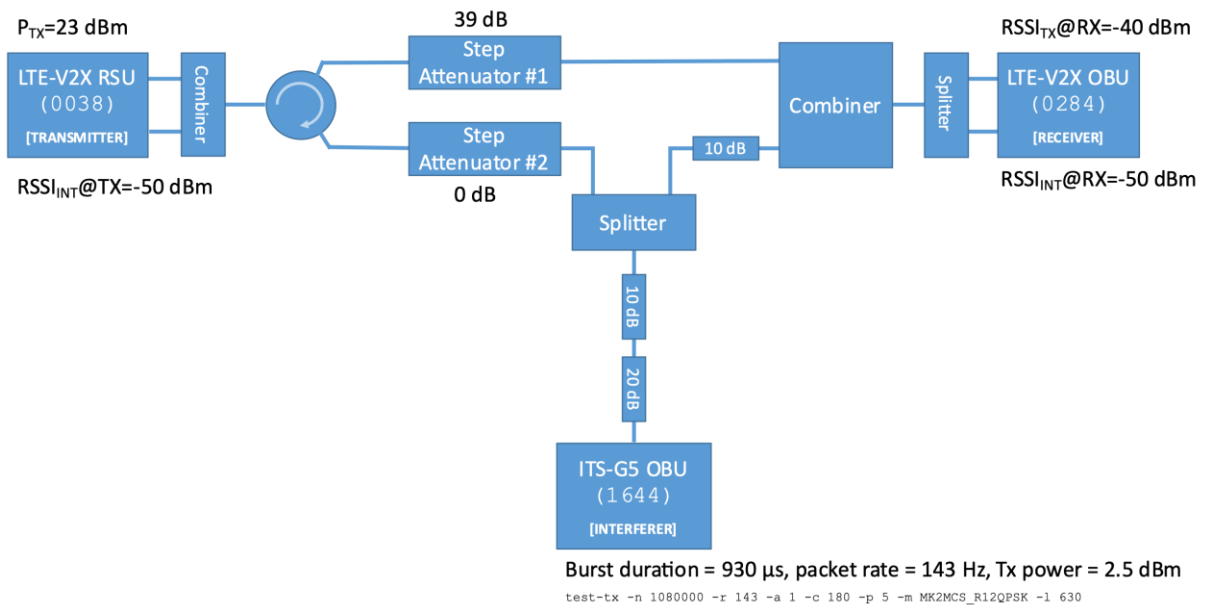


Figure 112: Laboratory setup for experiment 2.1

D.4.2 Additional notes

- The transmitter and receiver devices are commercial LTE-V2X units. The interferer device is a commercial ITS-G5 unit;
- The Signal-to-Interference Ratio (SIR) at the receiver is set to 10 dB (fixed) using the programmable step attenuator #1;
- This experiment scans the interferer power at the transmitter from -100 to -50 dBm in 1-dB steps using the programmable step attenuator #2;
- The wanted signal (transmitter to receiver) features an application-layer packet rate of 100 packets/s and a packet length of 350 bytes. The MCS is dynamically selected by the Semi-Persistent Scheduling (SPS) algorithm in the LTE-V2X MAC layer;
- The interfering signal (interferer to transmitter and receiver) features an application-layer packet rate of 143 packets/s and a packet length of 630 bytes. At the RF level, this configuration translates into a $duty\ cycle = \frac{t_{ON}}{t_{ON}+t_{OFF}} = 13.3\%$

D.5 Experiment 2.2: LTE-V2X is victim technology, LTE-V2X is interfering signal

D.5.1 Laboratory setup

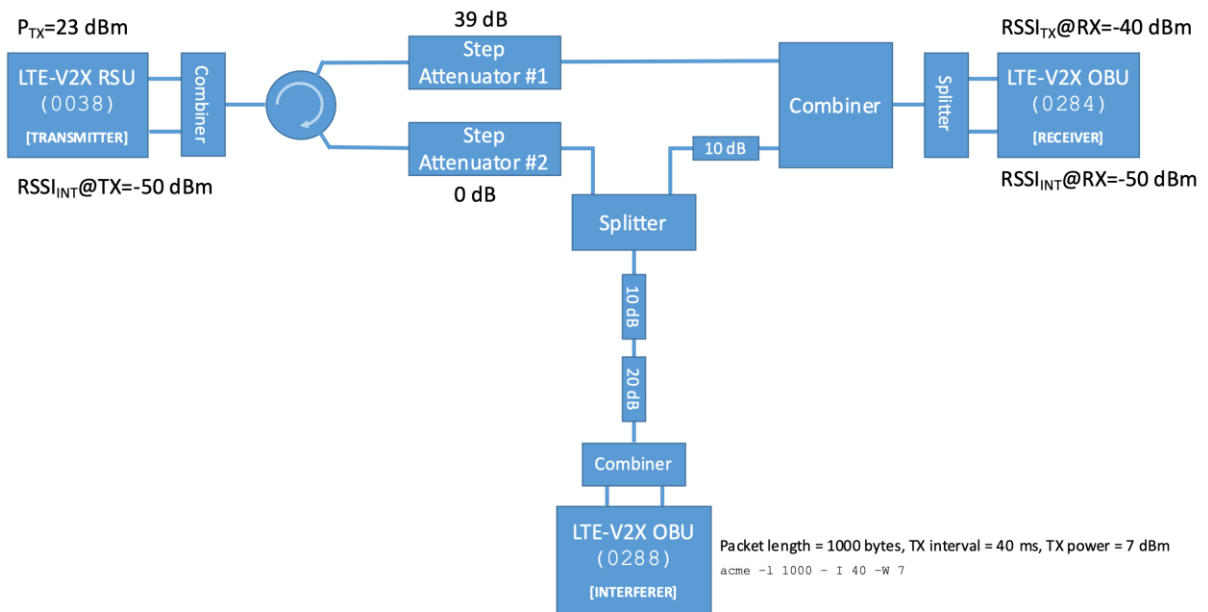


Figure 113: Laboratory setup for experiment 2.2

D.5.2 Additional notes

- The transmitter, receiver and interferer devices are commercial LTE-V2X units;
- The Signal-to-Interference Ratio (SIR) at the receiver is set to 10 dB (fixed) using the programmable step attenuator #1;
- This experiment scans the interferer power at the transmitter from -100 to -50 dBm in 1-dB steps using the programmable step attenuator #2;
- The wanted signal (transmitter to receiver) features an application-layer packet rate of 100 packets/s and a packet length of 350 bytes. The MCS is dynamically selected by the Semi-Persistent Scheduling (SPS) algorithm in the LTE-V2X MAC layer;
- The interfering signal (interferer to transmitter and receiver) features an application-layer packet rate of 25 packets/s and a packet length of 100 bytes. At the RF level, this configuration translates into a $duty\ cycle = \frac{t_{ON}}{t_{ON} + t_{OFF}} = 13.3\%$

D.6 Experiment 2.3: LTE-V2X is victim technology, LTE-V2X (with header) is interfering signal

D.6.1 Laboratory setup

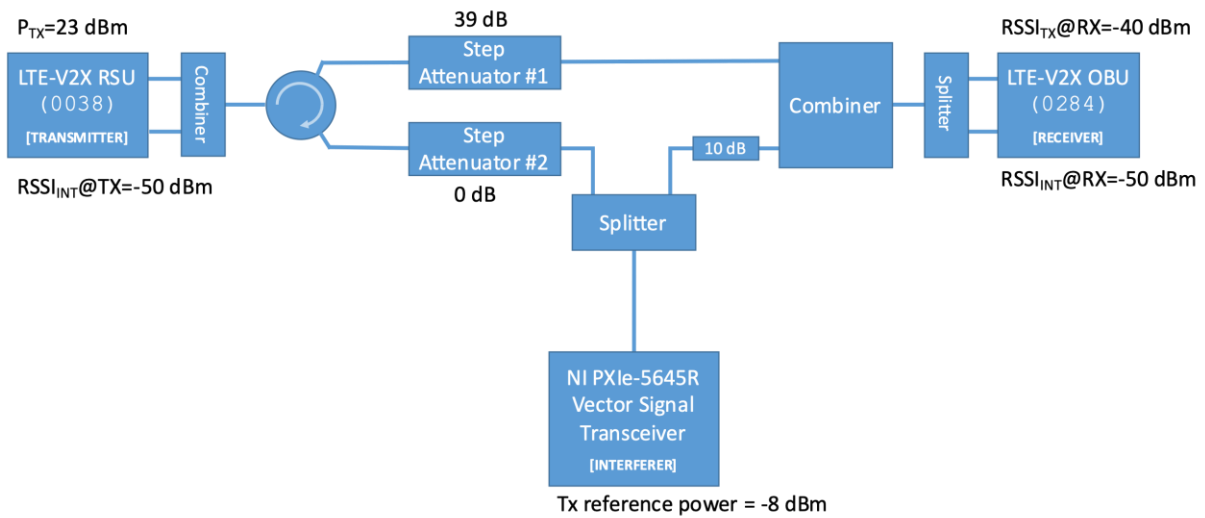


Figure 114: Laboratory setup for experiment 2.3

D.6.2 Additional notes

- The transmitter and receiver devices are commercial LTE-V2X units. The interferer device is a Vector Signal Transceiver replaying the LTE-V2X synthetic signal (i.e., LTE-V2X with ITS-G5 PHY header insertion) in infinite loop;
- The Signal-to-Interference Ratio (SIR) at the receiver is set to 10 dB (fixed) using the programmable step attenuator #1;
- This experiment scans the interferer power at the transmitter from -100 to -50 dBm in 1-dB steps using the programmable step attenuator #2;
- The wanted signal (transmitter to receiver) features an application-layer packet rate of 100 packets/s and a packet length of 350 bytes. The MCS is dynamically selected by the Semi-Persistent Scheduling (SPS) algorithm in the LTE-V2X MAC layer;

The interfering signal (interferer to transmitter and receiver) features an application-layer packet rate of 25 packets/s and a packet length of 100 bytes. At the RF level, this configuration translates into a *duty cycle* $= \frac{t_{ON}}{t_{ON}+t_{OFF}} = 13.3\%$